

1528

**Österreichische
Beiträge
zu
Meteorologie
und Geophysik**

1528

Heft 1

1989

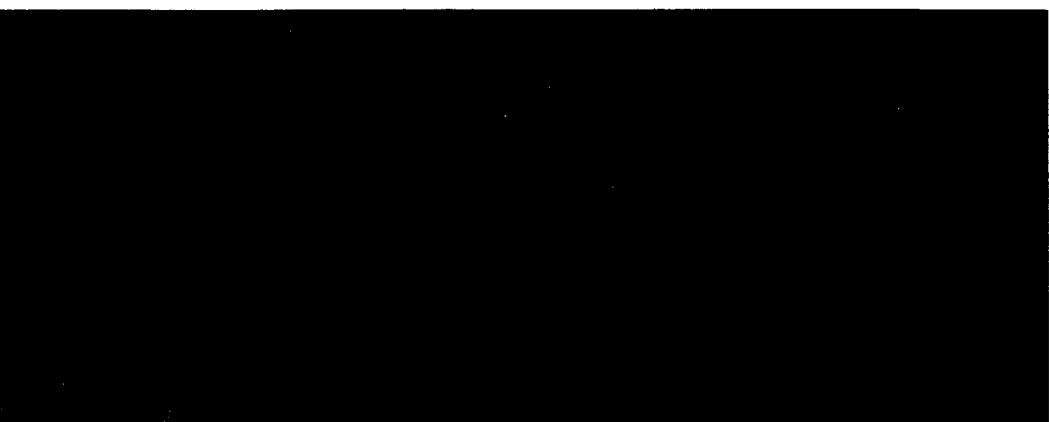
19.5.

**EVALUATION OF
ATMOSPHERIC DISPERSION MODELS
APPLIED TO
THE RELEASE FROM CHERNOBYL**

**International Meeting
of the European Association
for the Science of Air Pollution**

**EURASAP
Vienna, November 14-16, 1988**

Wien 1989



HSZ

**Österreichische Beiträge zu Meteorologie
und Geophysik**

Heft 1

**EVALUATION OF
ATMOSPHERIC DISPERSION MODELS
APPLIED TO
THE RELEASE FROM CHERNOBYL**

International Meeting
of the European Association
for the Science of Air Pollution

Vienna, November 14-16, 1988

Wien 1989



Zentralanstalt für Meteorologie und Geodynamik, Wien

Publ. Nr. 329

I M P R E S S U M

Herausgeber: Peter Steinhauser
Zentralanstalt für Meteorologie und Geodynamik
Hohe Warte 38, A-1190 Wien
Austria (Österreich)

Redaktion: Veronika Zwatz-Meise

Graphik und Layout: Eva Untersteiner
Verlag: Zentralanstalt für Meteorologie und Geodynamik, Wien
Druck: Rabl, Schrems

Redaktioneller Beirat:

Siegfried J. Bauer: Institut für Meteorologie und Geophysik, Universität Graz
Inge Dirmhirn: Institut für Meteorologie, Klimatologie und Grundlagen der
Physik, Universität für Bodenkultur, Wien

Rudolf Gutdeutsch: Institut für Meteorologie und Geophysik, Universität Wien
Michael Hantel: Institut für Meteorologie und Geophysik, Universität Wien
Volker Höck: Institut für Geowissenschaften, Universität Salzburg
Michael Kuhn: Institut für Meteorologie und Geophysik,
Universität Innsbruck

Hermann Mauritsch: Institut für Geophysik, Montanuniversität Leoben
Franz Nobilis: Hydrographisches Zentralbüro, Wien
Helmut Pichler: Institut für Meteorologie und Geophysik,
Universität Innsbruck

Karl Rinner: Institut für Weltraumforschung,
Österreichische Akademie der Wissenschaften

Adrian Scheidegger: Institut für Theoretische Geodäsie und Geophysik,
Technische Universität Wien

Wolfgang Seiberl: Institut für Meteorologie und Geophysik, Universität Wien
Franz Weber: Institut für Geophysik, Montanuniversität Leoben

Das Werk ist urheberrechtlich geschützt.
Die dadurch begründeten Rechte bleiben vorbehalten.
Auszugsweiser Abdruck des Textes mit Quellenangabe gestattet.

V O R W O R T

Mit dem Tagungsbericht von der EURASAP-Tagung über "Evaluation of Atmospheric Dispersion Models Applied to the Release from Chernobyl" eröffnet die Zentralanstalt für Meteorologie und Geodynamik ihre neue Serie "Österreichische Beiträge zu Meteorologie und Geodynamik".

Diese Reihe soll der Veröffentlichung von Originalbeiträgen, insbesondere solchen größeren Umfangs, sowie von Berichten über Tagungen und Forschungsprogramme dienen. Diese Reihe steht allen Kolleginnen und Kollegen als Publikationsorgan zur Verfügung.

Herausgeber und die Geschäftsführung der Redaktion werden von der Zentralanstalt gestellt, während ein Redaktionsbeirat, dem die Professoren der Meteorologie und Geophysik der österreichischen Universitäten sowie Vertreter benachbarter Disziplinen angehören, über die wissenschaftliche Qualität der Beiträge wachen wird.

Diese Serie löst die bisherige Reihe der "Arbeiten aus der Zentralanstalt für Meteorologie und Geodynamik" - vielfach als "Blaue Hefte" bekannt - und die Reihe der "Berichte über den Tiefbau der Ostalpen" ab. Die in diesen Serien ebenfalls veröffentlichten speziellen Datensammlungen, wie sie im Zuge von Forschungsprogrammen und der Landesaufnahme gewonnen werden, werden in Zukunft ebenso wie Untersuchungen mit dominierendem Datencharakter als "Beihefte zu den Jahrbüchern der Zentralanstalt für Meteorologie und Geodynamik" herausgegeben werden, wobei nach Sachgebieten getrennte Reihen vorgesehen sind.

Der Herausgeber

T A B L E O F C O N T E N T S

	P A G E
<i>I INTRODUCTION SESSION.....</i>	<i>7</i>
The Effect of the Chernobyl Accident of the CEC Research on the Environmental Consequences of Nuclear Accidents G. Graziani	9
Qualitative Evaluation of Atmospheric Transport Models Using Anatex Data M.M. Pendergast and W.W. Bowman.....	13
Numerical Modelling in the Event of a Nuclear Accident H.M. ApSimon and J. Wilson.....	15
Physico-Mathematical Modelling of Regional Transport in the Atmosphere of Radioactive Substances Following the Chernobyl Accident Y.S. Sedunov, V.A. Borzilov, N.V. Klepikova, N.I. Troyanova, E.V. Chernokozhin.....	23
<i>II NORTHERN HEMISPHERE STUDIES.....</i>	<i>31</i>
Evaluation of a Long Range Particle-In-Cell Transport and Diffusion Model Based on an Analysis of the Chernobyl Reactor Accident M.H. Dickerson and R. Lange.....	33
Simulation of Atmospheric Dispersion of Chernobyl Radioactivity by SPEEDI H. Ishikawa, M. Chino, H. Yamazawa and S. Moriuchi.....	41
Continental and Hemispheric Scale Dispersion of Nuclear Debris from the Chernobyl Accident J. Pudykiewicz.....	49

III LAGRANGIAN MODELS AND TRAJECTORY ANALYSIS..... 59

Comparison of Trajectories Calculated During and
After the Chernobyl Accident

H. Kolb, P. Seibert, V. Zwatz-Meise and G. Mahringer..... 61

The ZAMG/BKA - Trajectory Project

H. Kolb and W. Steinmann..... 71

The Finnish TRADOS Model as applied to the
Chernobyl Release

G. Nordlund..... 75

The Development of an Operational Puff Dispersion Model

G.H.L. Verver and H.J. Van Rheineck Leyssius..... 83

Chernobyl Accident: Modelling of Dispersion over
Europe of the Radioactive Plume and Comparison with
Air Activity Measurements

A. Albergel, D. Martin and J.M. Gros..... 93

Assessment of Source Terms in a Nuclear
Accident Situation

J.J.N. Wilson and H.M. ApSimon..... 107

IV EULERIAN/MONTE CARLO MODELS..... 117

Transport and Deposition of Radionuclides in Europe
after the Chernobyl accident studied with the European
Deposition Model (EURAD)

A. Ebel, H. Geiß, H. Hass, H.J. Jacobs, M. Laube
M. Memmesheimer..... 119

The Use of Numerical Prediction Models of the
Deutscher Wetterdienst in Air Pollution Modelling

I. Jacobsen and U. Pflüger..... 129

The Development of the U.K. Operational Multi-Particle Transport and Dispersion Model
R.H. Maryon and F.B. Smith..... 137

Media: A French Eulerian Operational Model of Pollutant Dispersion in the Atmosphere: Application to the Case of Chernobyl release and further Developments
J.P. Piedelievre, L. Musson-Genon and F. Bompay..... 147

V MESOSCALE ASSESSMENTS WITHIN A COUNTRY AND DEPOSITION.. 157

A Model for Radioactive Ground Contamination Analysis
J. Urbancic and Z. Jeran..... 159

Dose Rate Patterns in Austria after the Chernobyl Accident and their Relations to Precipitation
P. Seibert and H. Kolb..... 167

Assessing the Wet Deposition of Radionuclides
H.M. ApSimon and P.A. Stott..... 179

VI FINAL DISCUSSION..... 191

VII APPENDIX..... 195

Protocol of the WMO/IAEA/CEC Atmospheric Transport Model Evaluation Study (ATMES) - Draft..... 197

A U T H O R I N D E X

N A M E	P A G E
Albergel A.	93, 179
ApSimon H.M.	15, 107, 179
Bowman W.W.	13
Bompay F.	147
Borzilov V.	23
Chernokozhin E.	23
Dickerson M.H.	33
Ebel A.	119
Geiß H.	119
Graziani G.	9
Gros J.M.	93
Hass H.	119
Ishikawa H.	41
Jacobs H.J.	119
Jacobsen I.	129
Jeran Z.	159
Klepikova N.V.	23
Kolb H.	61, 71, 167
Lange R.	33
Laube M.	119
Mahringer G.	61
Martin D.	93
Maryon R.H.	137
Memmesheimer M.	119
Moriuchi S.	41
Musson-Genon L.	147
Nordlund G.	75
Pendergast M.M.	13
Pflüger U.	129
Piedelievre J.P.	147
Pudykiewicz	49
Sedunov Y.S.	23
Seibert P.	61, 167
Smith F.B.	137
Steinmann W.	71
Stott P.A.	179
Trojanova N.I.	23
Urbancic J.	159
Van Rheineck Leyssius H.J.	83
Verver G.H.L.	83
Wilson J.	15, 107
Yamazawa H.	41
Zwatz-Meise V.	61

I

INTRODUCTION

SESSION

THE EFFECT OF THE CHERNOBYL ACCIDENT ON THE CEC RESEARCH ON THE ENVIRONMENTAL CONSEQUENCES OF NUCLEAR ACCIDENTS

G. GRAZIANI

COMMISSIONE DELLE COMUNITA EUROPEE

CENTRO COMUNE DI RICERCA

21020 ISPRA (VARESE), ITALIA

The Chernobyl accident has given a new impact to the actions of the Commission of the European Communities on Radiation Protection, whose legal frame is established by Chapter III of the EURATOM TREATY.

During the last year, the Council of Ministers has adopted the following features:

- a decision on early information exchange between Member States and the Commission in the event of a radiological emergency;
- a decision on the adhesion of the Community to the International Convention on early notification of nuclear accidents;
- a regulation on a first set of maximum permissible levels of radioactivity in foodstuffs following a nuclear accident;
- a special regulation on radioactivity levels of imported agricultural products.

Several other decisions are in preparation and will be supported by the Scientific Research Programmes of the Commission, which will provide the SCIENTIFIC BACKGROUND and rationale for decisions and recommendations.

The shared-cost 1985-1989 Radiation Protection Programme was under way at the time of the Chernobyl accident, and several running actions were modified to account for the new situation.

2. THE MARIA PROJECT

The Commission of the European Communities, in the framework of its Radiation Protection Programme, initiated in 1983 the project on "METHODS FOR ASSESSING THE RADIOLOGICAL IMPACT OF ACCIDENTS - M A R I A".

The priorities of the MARIA programme were re-evaluated after the Chernobyl accident, and additional projects were started.

Among those of more direct relevance to the subject of the Conference, it is worth mentioning the

Long-distance atmospheric transfer programme

Its objective is to develop a long-distance atmospheric transfer model using forecast meteorological data to display where and when countries are likely to be affected during

the course of and following a protracted release.

Research will concentrate on some key issues, such as source term estimation, complex terrain modelling, analysis and quality assurance of radiological data, and emergency response.

3. ACTIVITIES AT THE JOINT RESEARCH CENTRE

Following the Chernobyl accident, a Task Force was created by the competent Directorates of the Commission of the European Communities (CEC) with the goal of re-examining all the aspects of nuclear safety, from the reactor design to the off-site radiological consequences, and emergency plans.

Since the very beginning, many of the groups into which the Task Force was divided, evidenced the necessity of having the large number of environmental radioactivity measurements (that were performed in the different countries which were reached by the polluted air plume) stored in an easily accessible form.

The measurements were executed both in the frame of the standard system created to monitor the operational radioactivity releases from national nuclear plants, and by a number of other laboratories which were especially entrusted for this occurrence.

The necessity of storing such a large set of Community data

into an adequate frame, which is able to permit an easy handling and retrieval of the information, has led the JRC to create the REM Bank (REM standing for Radioactivity Environmental Monitoring).

It will be accessible for scientific application such as studies on the atmospheric dispersion of the various radioelements, and verification of relevant physical and mathematical models.

The Bank has grown up to a size of about 300,000 radioactivity measurements, mainly from Member Countries.

Particular care has been put in the MENU-driven enquiry procedure, which is fully transparent and user-friendly.

The measurements were obtained both from national offices as well as from universities, small laboratories, etc...

They have been introduced into the bank, starting from different supports, such as magnetic tapes, floppy disks or simply copying data from official papers.

Complementary to the radiological data, other information concerning meteorological and rainfall data was also gathered for the period of interest (26th of April - 15th of May).

Presently, the bank is being extended to cover the period prior to the Chernobyl accident, back in 1984, utilizing information obtained by D.G. XI, Health and Safety, in compliance to ART.35-36 of the EURATOM TREATY. These data will be used to prepare the EC periodical reports on radioactivity levels in the EC.

QUALITATIVE EVALUATION OF ATMOSPHERIC
TRANSPORT MODELS USING ANATEX DATA

M. M. Pendergast and W. W. Bowman

The Savannah River Laboratory (SRL) has assisted the National Oceanic and Atmospheric Administration (NOAA) and the United States Air Force in the planning of the Across North America Tracer Experiment (ANATEX), which was conducted during the winter of 1987. The SRL Adjusted Geostrophic Model was run in order to help decide sampler locations, the number of samplers required and the quantity of tracer released in order to help decide sampler locations, the number of samplers required and the quantity of tracer released in order to assure a successful experiment. Following the ANATEX experiment, SRL image processing capabilities were used to create color graphical displays of model and observed tracer distributions. These visual aids have been used for the qualitative evaluation of the SRL model.

The ANATEX model evaluation study, being conducted by the U. S. Environmental Protection Agency and NOAA is evaluating several models in "blind" tests using the ANATEX data base. A "blind" test is one in which modelers do not have access to the observed concentration data before submitting their results for evaluation. SRL was asked to supplement these quantitative evaluations with the qualitative evaluations using color graphical displays. The participants of the ANATEX model evaluation study have provided SRL calculated tracer concentration at the 77 ANATEX sampler locations covering most of Central and Eastern U. S. and Southern Canada. Daily model and observed concentrations were used to construct film loops. The film loops are recorded on VCR tape for ease of study.

Status of the SRL Adjusted Geostrophic Model, its quantitative comparisons with the Chernobyl data base and the status of the qualitative model evaluation of the ANATEX models will be discussed.

The information contained in this article was developed during the course of work under Contract No. DE-AC09-76SR00001 with the U.S. Department of Energy.

DISCUSSION

QUESTION: Fraser: Dr. Nordlund previously raised the potential difficulty posed by releases over extended periods (even from a given source point) being widely diffused and thus making it difficult to relate concentrations at individual measuring points to releases originating at specific times or over specific sub-periods. To what extent have such difficulties appeared in the ANATEX analysis?

ANSWER: Of the 84 releases from GGW about 20 were made during meteorological conditions that transported the tracer fast enough through the sampler array such that the 24 hr average concentration differentiated individual plumes.

QUESTION: Labrousse: What analyses did you use and how were the interpolations calculated?

ANSWER: The calculated and observed tracer concentrations were analysed using a nearest neighbour technique; no attempt was made to smooth the data. The meteorological variables were analysed using a variable scan radius and a 1/R weighting scheme. Time continuity was assured by using the previous analysis as first guess.

QUESTION: Seibert: What is the residence time of the tracer materials in the atmosphere? Will it be possible to conduct another experiment with the same tracer material?

ANSWER: The tracer is non depositing and I would expect the residence time to be years. The US Air Resources Laboratory of N.O.A.A. suggests that modelers study their calculations with the results of ANATEX for many years before doing another experiment. However if funding is available they might want to do another one.

QUESTION: Vergeiner: Referring to airplane sampling near the source: are there data on (horizontal) minimum dispersion in very stable conditions near the source (scale = 100 km)?

ANSWER: Almost every one of the ANATEX tracer releases had benefit of airplane sampling to define initial movement and tracer spread. I am sure that one will be able to find cases which are stable.

NUMERICAL MODELLING IN THE EVENT OF A NUCLEAR ACCIDENT

Helen M ApSimon, Julian Wilson

Air Pollution Group, Imperial College, London SW7 2AZ

Abstract:

Numerical models have been widely used in risk studies to estimate how hypothetical releases of radionuclides will disperse and lead to exposure of the population. In this context large numbers of possible scenarios are treated; absolute accuracy in simulating each situation is not necessary as long as there is no systematic bias, and the errors balance out statistically to give the overall distribution of possible consequences. Since the Chernobyl accident there has been more interest in the use of numerical models as tools to assist in real-time in emergency procedures if and when a nuclear accident occurs. However the use of models in a real situation is distrusted by many people, who feel that the only way to assess an emergency situation is by making radiological measurements. This paper addresses uncertainties involved in modelling and argues that a combination of both approaches should be employed, using numerical modelling as an aid in intelligent interpretation of measurements, and suggesting priorities for international exchange of radiological data.

1 Introduction

The Chernobyl accident on 26 April 1986 has generated interest in the use of numerical models to assist in emergency procedures by predicting the dispersal and deposition of atmospheric releases of radionuclides, and the subsequent contamination. This paper addresses the capabilities and limitations of such models, and suggests how they may best be used in conjunction with monitoring resources in an emergency situation following a major nuclear accident.

Requirements during different phases of a nuclear accident.

Traditionally three phases of a nuclear accident have been defined within the context of emergency procedures to protect the public in the vicinity. The first normally lasts up to a few hours, and may or may not include a warning phase before any actual atmospheric release occurs. During this first phase rapid decisions may be required on control measures such as evacuation and sheltering, and issue of iodine tablets, to protect the public from direct exposure within the plume. In the next phase monitoring data and resources are less restricted and decisions are required on contamination of agricultural produce and food. Efficient direction of monitoring facilities to the areas most contaminated is required. This phase may last several days or even longer. Finally the third phase is the recovery phase when conditions are gradually returned to normal. Decisions are required on decontamination and withdrawal of control measures.

In the event of a major accident leading to contamination at longer distances and across frontiers in other countries, three slightly different phases may be defined for each national authority. The first question for each country is whether radioactive material from the accident is likely to reach it, and if so when. In such a situation the first phase corresponds to the period up to the time of arrival, and is effectively a warning phase. The requirement for long-range models is accurate prediction of where material will travel to and which areas will be affected. Once material arrives national monitoring facilities provide direct observations of the passage of the radioactivity and resulting deposition. The concerns are similar to those in the vicinity during the second phase - identification of the areas most affected and controls on foodstuffs and agricultural produce if necessary. Here more detailed spatial analysis of the situation within the country, using available precipitation or other data in the event of significant deposition, is appropriate. This involves a different type of modelling from the long-range modelling, (see ApSimon and Stott 1988, and ApSimon, Wilson and Simms 1988) Finally in the aftermath of the accident there is usually a review of the events leading to the

accident and its subsequent release characteristics. In this third and final phase models are again useful in conjunction with measurements, to deduce the quantities released and their variation in time (Wilson and ApSimon 1988).

At the time of Chernobyl little was known initially about the release, although a full account of the accident was given later in August 1986 by Soviet scientists. It should be appreciated that when a major accident occurs knowledge about the release is likely to be very limited. If a release takes place through a monitored stack then there may be good indications of the variation of the release over time and its radionuclide composition. If however there is a major explosion as at Chernobyl, then it is very difficult to assess what is released, and also other information relevant to its subsequent dispersal - such as the height to which material is ejected, which is important because wind varies with altitude. The composition of the release is very significant for the accident consequences. In some cases, such as the accident at Three Mile Island for example, only noble gases escaped; these are very inert and do not deposit on the ground so that exposure is limited to the periods when contaminated air is overhead, and doses from inhalation and submersion. In other situations volatile nuclides such as I-131 will be the priority concern, as in the case of the Windscale accident in 1957. In the case of Chernobyl a wider range of nuclides was released including coarse fuel fragments which settled out in the vicinity, and the long-lived caesium isotopes (Cs-137 and Cs-134 with half-lives of 28 years and 2 years respectively) which have caused the longer-term problems in Europe, mainly in relation to contamination of vegetable and animal produce.

Modelling

Since the Chernobyl accident attempts have been made in several countries to simulate dispersal of the release using modelling techniques of different types and sophistication. These include plume models, simulating a plume along an estimated trajectory; Lagrangian puff models based on following the histories of puffs of material released across the map area; Eulerian grid models in which the advection-diffusion equations are integrated; and particle models following large numbers of discrete particles representing the release.

Our own early results with a Lagrangian model, MESOS, were presented on 21 May 1986 at the UK Nuclear Installations Inspectorate, and have been reported elsewhere (ApSimon et al 1987). It was perhaps surprising that so much could be deduced about the accident before the full description of the accident given by the Soviet scientists in August 1986. Although this model is relatively simple and was developed to study hypothetical accidents for probabilistic risk assessment purposes, it makes direct use of meteorological observations from synoptic stations and ships. It does not use detailed 3-dimensional analysed wind-fields, and can not be used in forecasting mode with forecast wind-fields. Nevertheless the results can be used to illustrate the uncertainties and difficulties in assessments during an emergency situation.

First question - where will the material travel to, and which areas will be affected?

A powerful tool in deciding where material will travel to is trajectory analysis. For example when Chernobyl occurred such analysis was used in back-trajectory mode from Scandinavia to establish the likely source. Our own trajectory analysis with MESOS indicated that the release had continued from Chernobyl into the early days of May because of the areas affected in the first week of May 1986. However comparison of trajectories calculated by different organizations differ widely.

Table 1: Comparison of trajectories produced by different models

Trajectory Start 12.00 26/4/1986	Model							
	TRANCO 950 mb		TRANCO 850 mb		TRANCO 700 mb		MESOS	
Traveltime	Long.	Lat.	Long.	Lat.	Long.	Lat.	Long.	Lat.
1 day	24.3	52.9	21.7	55.5	22.3	55.3	24.6	56.6
2 days	20.2	56.3	17.0	61.3	22.0	60.0	17.5	58.0
3 days	20.0	55.0	14.7	63.1	26.1	61.2	14.1	55.3
5 days	13.3	45.0	-1.9	69.7	39.3	53.4	0.7	48.6

(NB All trajectories originated at Chernobyl, Longitude 30.15, Latitude 51.16)

This is illustrated in table 1 where the estimated positions on a trajectory originating from Chernobyl at noon on 26 April are compared after various travel times using different techniques. The MESOS trajectories are based on observed surface pressure fields, with adjustments to the geostrophic winds for the estimated wind-profile in the atmospheric boundary layer over the depth of the material. The TRANCO trajectories are based on analysed windfields of the UK Meteorological Office (fine mesh model for Europe) at different levels in the atmosphere, 950mbar (500 m altitude), 850mbar (1500 m) and 700 mbar (3000 m). Transport over continental distances such as occurred from Chernobyl is largely within this altitude range except where material is carried aloft in for example precipitation systems and fronts. Note that the forecast windfields, up to 24 or say 72 hours ahead would give different results again from the analysed windfields. The differences in table 1 are typical though of the sort of differences that can occur, and obviously they increase in time.

The differences in table 1 are not all due to the differences in the data used. The numerical techniques for integrating forward (or backward) in time differ, and the method of interpolation between times for which the data is prescribed (step-wise changes every 3 hours for MESOS, linearly interpolated between 6 hour analysed wind-fields for the Tranco model). There are also different techniques from those illustrated in table 1. Geostrophic winds can be calculated using 6 hourly 850 mb pressures instead of surface pressures, although the data is sparser, especially over the sea, and does not reveal small scale features as well (which can be important). Analysed windfields from different meteorological services will also differ. The examples in table 1 are all 2-dimensional trajectories calculated at constant levels. Other methods employ 3-dimensional isentropic treatments, where material moves vertically to maintain a constant potential temperature, or vertical wind components computed by forecasting model analysis. Vertical motion is certainly important, and such techniques might be valid in frontal situations with large scale ascent for example; but are debatable where sub-grid scale transfer occurs as in convective storms, or within the mixed boundary layer or complex orographic terrain. On the other hand the capability of 2-dimensional models such as MESOS to simulate the transport of material from Chernobyl through the 3-dimensional frontal situation over Scandinavia is definitely limited (and it is for this reason that our current model development is towards a 3-dimensional Monte-Carlo particle model).

With the differences manifest between trajectories, when can we have any confidence in them?

Traditionally trajectory analysis is not usually considered valid beyond 72 hours of travel, but after Chernobyl various workers calculated trajectories up to 12 days or more over Europe, and beyond over the northern hemisphere. The answer to the problem of validity is probably to compute more than just one trajectory for each starting time. Thus for example perturbation analysis on the MESOS trajectories was quite revealing. Applying a small perturbation in the form of a backing angle (say

10 degrees) indicated where trajectories became unstable because of the meteorological situation encountered, effectively areas with large divergence in the windfield such as occurs in the centre of a depression. Some examples are shown in figure 1, in this case indicating how large mountain barriers can induce uncertainty for example whether material flows north or south round the Alps, and how the Carpathian mountains divert flow over Turkey and Greece. These were two areas where we considered our own MESOS model results to be weak.

Lateral spreading

Trajectories, although interesting to compare between different models, are not directly verifiable or comparable with observations from monitoring of a release. The areas affected depend not only on trajectories, which can be defined in physical terms as the path of the centre of mass (for a release over a short period); these areas depend also on the spread about the trajectories. Over long travel distances however this spread is largely dependent on synoptic scale wind shear. A big divergence or sensitivity of a trajectory is often an indication of large lateral spreading and dilution. However there will be additional spreading due to turbulence and boundary layer processes. These are often included empirically. For example many plume models assume a formula for the cross-wind spread such as

$$\sigma_y = 0.5 t \quad (\sigma_y \text{ in metres, } t \text{ in seconds}) \quad (1)$$

based on a range of experimental tracer data, bomb testing releases etc. (Doury 1980).

The sensitivity to such assumptions has been investigated with the MESOS model assuming 2 different treatments of the smaller scale boundary layer processes. To understand this it is necessary to explain a little more about the way lateral spreading is represented in the MESOS model. In MESOS a prolonged release such as occurred at Chernobyl is treated as a sequence of 3 hour releases. Trajectories are calculated for puffs released at the beginning and end of each 3 hour release, and material in between is assumed to fan out between the trajectories as a sequence of intermediate puffs. The area exposed by each 3 hour release thus depends on the individual spreading of each puff as well as the divergence of trajectories. Spreading based on equation 1 was first assumed, increasing individual puffs linearly with time, and in the comparison case this was altered to give a gradually diminishing puff growth levelling off after 4 days travel. The analysis showed (ApSimon, Wilson and Simms 1988) that results based on the greater puff spread frequently led to estimated times of arrival a day or so earlier, and in some cases made the difference between indicated exposure or non-exposure. In considering the importance of this the spread of a puff (amounting to 1000 km width after 10 days travel with the linear law) has to be compared with the uncertainty in the trajectory. Another factor which should be taken into account is the along-wind spread, which would tend to advance the estimated time of arrival. This is one explanation for the tendency of the observed arrival times to be slightly ahead of the estimated values in MESOS.

Vertical spreading

The treatment of vertical spreading is also significant, and varies according to the overall treatment of advection and dispersion. MESOS is a Lagrangian model, following the history of material across the map area and simulating vertical dispersion according to the changes in the estimated depth and nature of the mixing layer. An increasing mixing layer depth leads to dilution; onset of a low-level inversion isolates material above it, which can not then be depleted by dry deposition. Other Lagrangian models superimpose an assembly of plumes along estimated trajectories, and often assume a constant mixing layer depth of the order of 1000 metres.

More complex Eulerian models integrate the equations of diffusion over a 3-dimensional grid of cells spanning the region of interest. Although these models do not calculate trajectories, many of the same uncertainties are still inherent, and there can be problems of numerical diffusion in the calculations. Their resolution in the vertical depends on the number and spacing of levels, but

it is doubtful whether such effects as nocturnal jets would be represented, even if meteorological data such as sodar wind profiles indicated their presence.

Other models, especially those on a northern hemisphere scale simulate the release as an assembly of particles using Monte - Carlo techniques to simulate deviation from trajectories for advection in the assumed wind - fields. There are new developments in conjunction with meteorological forecasting services currently under way in this category. In these sub - grid scale phenomena, such as the vertical redistribution within storm systems, taking material aloft as well as leading to deposition, can be represented to some extent. The capabilities of such models to allow for complex 3 - dimensional transport through frontal systems requires investigation.

Air concentrations - checking model results.

After predicted time of arrival and overall areas exposed have been addressed, the next question is how large the air concentrations are likely to be on arrival in a target country. This requires fairly accurate quantitative information on the source terms for these individual nuclides. A good visual presentation of calculated air concentrations can be provided by a sequence of maps giving "snap - shots" of the estimated situation at different times, or averaged over sequential periods (eg ApSimon, Wilson and Simms 1988). This can also be very helpful in comparing results from different models (but is not so simple with the continuous plume models for example).

Meteorological charts at corresponding times are useful supporting information to explain the patterns obtained, and indicate where the results are likely to be more uncertain. For example in presenting our own early results from the MESOS model, we stated that the initial movement indicated towards Sweden in the frontal system would in reality also have extended towards Finland. Similarly orographic features are difficult to incorporate in models. Thus we recognised that transport of material round the Alps, and blocking effects of the Pyrenees were likely to be poorly represented in our MESOS estimates. Nevertheless from the simulation we gained a general indication of how air was circulating over Europe and the magnitude of the concentrations involved, which was very useful in interpreting measurements.

Wet deposition

Since the accident consequences and the control measures necessary may well be dominated by the deposition of nuclides like Cs - 137 it is also important to give the best possible indications of what regions are most likely to be significantly affected by precipitation intercepting the airborne material. Forecasting data only give very broad indications of precipitation fields and it is not possible to indicate the detailed patchiness of the distribution in advance.

Even in the intermediate phase after the material has reached a target country and is passing overhead, detailed precipitation data is not readily accessible in many countries unfortunately. This is the subject of a separate paper (ApSimon and Stott 1988).

Most models use a simple wash - out model to estimate deposition. This does not allow for export of material to higher levels in the free troposphere in precipitation systems. Nor does it reflect features such as orographic enhancement over higher terrain. In any case the uncertainties in transport are much larger once material has reached a frontal system or region of unstable convective storm activity. The modelling of transport through precipitation systems is an area on which we are now concentrating.

International exchange of radiological measurement

The need to check model results against observations emphasizes the need for immediate international exchange of selected radiological measurements. When extrapolating forwards in time over extended periods of several days, such data may also be used to revise and improve model predictions during the further spread of the release. They are also required to refine source term estimates

in post-facto analysis.

From the above discussion and experience gained from Chernobyl, a high priority is measurements of atmospheric concentrations over sequential periods at reliable monitoring stations. The measurement periods and units used should be clearly stated as well as the nuclides and the observed concentrations. There is also need for standardisation in measurement of I-131, or at least an indication of whether measurements apply just to the particulate fraction or the total gaseous and particulate forms. In some instances the chemical form could also be very significant.

Gross beta measurements, although more qualitative, can also be very useful in giving good time resolution of the advance and passage of the cloud. Thus the gross beta data from the FRG network were very useful after Chernobyl in indicating to us that the MESOS model results were slightly in advance of the actual passage of the material westwards across Europe, and could with greater sophistication have been used to revise the simulated time of arrival in the UK. Aircraft measurements and observations aloft are also very valuable to show differential movement.

Standard gamma detector networks tend to become dominated by deposition, which is highly variable on a local scale. Such measurements are of little use in the present international context apart from indicating time of arrival. They do not provide guidance on when air concentrations peak, or when clean air is overhead again. The main use of such gamma detectors is to indicate the pattern of deposition within a country after passage of the release; the network needs to be very dense to avoid confusion due to failure to resolve precipitation features. Such data is probably too extensive to transmit rapidly over the GTS system of the World Meteorological Organisation in any case.

Likewise direct measurements of deposition on soil or grass are also of limited use in model evaluation, and the sampling techniques used after Chernobyl were also widely varied and non-comparable. Data on contamination of food-stuffs may be important in the context of food-import controls, but again introduce too many additional factors to help in checking model results.

However with respect to deposition, measurements of concentrations in precipitation (together with precipitation amounts and collection periods) are more directly comparable with model results.

It is therefore suggested that measured concentrations in air and rainwater of selected nuclides, plus selected gross-beta measurements, and measurements aloft, are the most valuable data to exchange internationally as soon as they are available, in the context of forecasting and model simulations.

Conclusion

This paper has examined the role of numerical model simulations during different phases of a nuclear emergency, and suggested how they may be usefully combined with radiological measurements to optimise emergency procedures. It has briefly reviewed some of the different techniques available, and illustrated some of the uncertainties and difficulties. It has also indicated which data is most valuable for rapid international exchange. Given such data it is felt that numerical modelling is a very valuable tool in the event of a nuclear accident with transfrontier implications, and development of such facilities is also of great value in analysis of other types of pollution episode.

References:

ApSimon HM and Stott PA (1988) Assessing the wet deposition of radionuclides. Proc. EURA-SAP meeting Vienna 14-16 November 1988.

ApSimon HM, Wilson and Simms KL Analysis of the Dispersal and Deposition of Radionuclides from Chernobyl across Europe. Submitted to Proc Royal Soc.

ApSimon HM Wilson JN Guirguis S and Stott PA (1987) Assessment of the Chernobyl release in the immediate aftermath of the accident. Nuclear Energy 25, 5.

Doury A (1980) Pratiques française en matière de prévision quantitative de la pollution atmosphérique potentielle liée aux activités nucléaires. Proc CEC seminar "Radioactive releases and their dispersion in the atmosphere following a hypothetical reactor accident" Riso, Denmark 1980.

Wilson JJN and ApSimon HM (1988) Assessment of source terms in a nuclear accident situation. Proc EURASAP meeting Vienna 14-16 November 1988.

DISCUSSION

COMMENT: Fraser: Dr. ApSimon mentioned in her presentation that the longterm aim is to allow forecasting of the passage of plumes and subsequently illustrated major differences generated by a small change in input when extrapolating over up to 5 day periods based on measured meteorological data. Bearing in mind the additional uncertainties in forecast meteorological data, what is the point of the ATMES exercise looking at more than 24 - 48 hour diffusion periods? Personally, I feel, that if models using a given approach can, on the basis of measured data reproduce actual effects out to longer periods, I will always have more confidence in such an approach for short periods also. The accuracy of forecast meteorological data I see as a separate problem, although inevitably it will contribute to the degree of ultimate confidence we can have in forecasting the passage of accidental releases of radioactive or other pollutants.

COMMENT: Pendergast: One of the members at the audience mentioned that since long range meteorological forecasts are not good, why use any longer than 14 hours. The issue of the requirement of long range predictions of meteorology is very important especially with regards to aircraft sampling where 36 hrs - 48 hrs forecasts are necessary for sample deployment.

ANSWER: Yes, I think this emphasizes the need for international collaboration in exchange of information to optimise updating of forecasts 24 to 48 hours ahead.

QUESTION: Urbancic: You found trajectories are inherent instable and the instability can be enlarged by introduction of more sophisticated models. Do you mean it is not the consequence of the inherent instability of the problem which cannot be dependent on the model.

ANSWER: I did not mean to imply that the complex models were worse. I meant to say that even though Eulerian and other sophisticated models do not directly calculate trajectories necessarily (i.e. the loci of the centre of mass), this does not mean that they do not have the same uncertainties as the simpler models in treating advection.

QUESTION: Vychytil: Did you use different modeling approaches for the transport of aerosols (like Caesium) and for the transport of rare gases like Xenon?

ANSWER: Since we were not considering coarse aerosol deposited locally, we assumed that the Cs on fine aerosols and the rare gases were advected and mixed in the same way. However the rare gases are assumed not to deposit, whereas dry and wet deposition are included for caesium.

PHYSICO-MATHEMATICAL MODELLING OF REGIONAL TRANSPORT
IN THE ATMOSPHERE OF RADIOACTIVE SUBSTANCES FOLLOWING
THE CHERNOBYL ACCIDENT

Yu.S.Sedunov, V.A.Borzilov, N.V.Klepikova,
N.I.Troyanova, E.V.Chernokozhin

Institute of Experimental Meteorology
Obninsk, USSR, 249020

Summary: Regional and transboundary models for transport, diffusion and deposition of radioactive materials at a range of 2000-4000 km are presented. Restoration of the source parameters was performed through solving an inverse problem from available experimental data on the density of contamination by radionuclides. The source intensity was evaluated and the fields of ^{131}I deposition were simulated. Estimates were made for transport of ^{131}I .

1. INTRODUCTION

In the wake of the Chernobyl accident and especially after signing in Vienna the Convention on Early Notification on Nuclear Accidents new efforts were made to improve physico-mathematical modelling of propagation of radioactive substances in the atmosphere and their deposition on the underlying surface. It should be noted that a limitation of the modelling lies in the shortage of input data on the source parameters and it demands that, along with a direct problem of contaminant propagation in the atmosphere, an inverse one - that of restoration of the source parameters should be solved.

The objectives of modelling of an accidental nuclear release are as follows:

- to describe spatial-temporal characteristics of contamination and compile fall-out maps,
- to locate potential zones of increased contamination calling for special investigation,
- to evaluate quantitatively the radionuclide transport across the national border,
- to restore (specify) source parameters.

To meet these goals the following models were developed in the Institute of Experimental Meteorology:

- a trajectory model of transport of airborne particles which is needed for preliminary assessments,
 - a mesoscale Eulerian model for transport (~ 200 km),
 - a regional Eulerian-Lagrangian model of transport (~ 2000 km),
 - a transboundary model based on the Monte-Carlo method (~ 4000 km).
- The models include two submodels: a model of the atmospheric boundary

layer and a model of transport, diffusion and deposition of radionuclides. The models account for the following processes:

- spatial-temporal variations in meteorological conditions: wind, temperature and eddy diffusivity,
- advection, diffusion and deposition of polydisperse aerosols,
- roughness of land and contaminant interaction with the underlying surface.

The models were applied to the Chernobyl accident problems. The Chernobyl accident resulted in the release into the atmosphere of a wide range of radionuclides some of which being on a particulate and in gaseous phase were responsible for regional transport of decay products.

The paper reports on the results of modelling of regional transport of ^{131}I and parameter restoration of its source which was performed with the use of regional and transboundary models.

2. THE MATHEMATICAL MODEL

The model is based on a semiempirical approach of eddy diffusivity which can be presented either as an equation of eddy diffusivity or as a set of stochastic equations of movement of aerosol particles carrying radionuclides. The first approach was employed in developing the regional model:

$$\frac{\partial q}{\partial t} + (u_i - v_R \delta_{i3}) \frac{\partial q}{\partial x_i} = \frac{\partial}{\partial x_i} (\kappa_i \frac{\partial q}{\partial x_i}) - \lambda q + I, \quad i=1,2,3, \quad (1)$$

where q is the concentration of radionuclides in the atmosphere; v_R is the sedimentation velocity of particles with the radius R ; I is the source intensity per unit volume; λ is the constant of radionuclide removal process (their wash-out and decay); u_i is the mean velocity components; κ_i is the eddy diffusivity coefficients of the contaminant along the axes x_1 , x_2 , and x_3 , respectively. At the lower boundary of the domain at the roughness level Z_0 the requirement of partial absorption is met

$$\kappa_3 \frac{\partial q}{\partial x_3} + (v_R - u_3) q = \beta q, \quad (2)$$

where β is the velocity of the contaminant deposition.

Equation (1) was solved by the numerical scheme with splitting procedure at the upper temporal level combined with the hybrid scheme for approximation of advective terms. To attain reasonable spatial resolution over the period from formation of the contaminant cloud to its deposition on the underlying surface we used a moving Eulerian grid with the horizontal scale determined by the current sizes of the contaminant cloud ¹. The deposition density on the underlying surface is

$$P(x_1, x_2, t) = \int_{t_0}^t \beta q(x_1, x_2, z_0, t) dt, \quad (3)$$

where t_0 is the starting of emission.

Equation (1) is written for a monodisperse radionuclide contaminant but the pollutant flux on the underlying surface is the superposition of

particles with variable sizes.

The second approach is applied to the model of transboundary transport and implies investigation of movement of individual particles which are transported in the wind velocity field and subjected to random walk:

$$\frac{dx_i}{dt} = u_i(\vec{x}, t) - V_R \delta_{i3} + u'_i(\vec{x}, t), \quad i=1, 2, 3, \quad (4)$$

where u'_i are the fluctuating components of velocity. Random deviations $\Delta x'_i$ of particles over a time interval Δt is $\Delta x'_i = \sqrt{2K_i(\vec{x}, t)} \cdot \Delta t \cdot \alpha_i$, where α_i is the normal random variable. At the lower boundary we set the condition of partial absorption (2). The source is simulated by prescribing the initial position of particles.

The study of movement of an ensemble of particles allows one to draw conclusions on some characteristics of the contaminant propagation. Simulating the behaviour of not many particles one can obtain integral characteristics, among them an approximate contaminant amount transported across the border, while examination of a numerous particle ensemble makes it possible to determine the contaminant concentration in the atmosphere. The deposition density is

$$P(x_1, x_2, t) = \frac{\mu n}{S}, \quad (5)$$

where μ is the activity of a single particle; n is the number of particles deposited on the area S .

The solution of (1) and (4) requires the data on meteorological fields $u_i(\vec{x}, t)$ and $K_i(\vec{x}, t)$ which are restored from the standard network with the use of parametrization of the atmospheric boundary layer (ABL). The ABL vertical structure for a particular meteorological situation is determined through the use of the similarity theory along with the results obtained by Wipperman's model ² and semiempirical laws of resistance and heat exchange as well. The latter relate large scale processes to the ABL internal parameters. The model involve spatial and temporal interpolation of the ABL calculated parameters.

As input meteorological information we used standard data, which were objectively analyzed by the USSR Hydrometeorological Centre, on surface pressure and temperature, geopotential altitudes, real wind velocities and temperature at standard pressure surfaces (925, 850 and 700 hPa) in the grid points 150x150 km. The use of this information enabled us to render meteorological data input automatic and to provide users with operational computations. The distribution of the roughness parameter $Z_0(x_1, x_2)$ was obtained by the technique described by F.B. Smith and D.F. Carson ³. To estimate propagation of radionuclides in the atmosphere and their deposition, in addition to meteorological information and data on location and time of the accidental release, the following characteristics of the emission are needed: particle sizes, radionuclide composition, initial distribution with height and emission intensity. It is unlikely that such data on the source parameters can

be readily available. Hence, restoration and elucidation of dynamics of the source parameters become essential for the problem solution.

Restoration of the source parameters was performed by solving the inverse problem from the available experimental data on the density of radionuclide contamination with the use of a priori information on the most likely particle sizes in the contaminant and possible vertical source distribution with height. The method is the following. The source is found as the sum L of elementary sources with time of action $(t_m, t_m + \Delta t_m)$ over which we know the emission distribution with height and particle sizes for each source, but do not know its intensity $(\alpha_1, \alpha_2, \dots, \alpha_L)$ with $\alpha_\ell \geq 0$ ($\ell = 1, \dots, L$). The intensity of elementary sources is found from the condition of minimal discrepancy between the values of deposition density calculated as $\sum_{\ell=1}^L \alpha_\ell P_\ell(\vec{x}_j)$ and measured $P(\vec{x}_j)$ ($P_\ell(\vec{x}_j)$ is the deposition field of the ℓ -th elementary source of unit intensity calculated by the regional model). The technique is based on a version of the regularization method ⁴.

3. ESTIMATION OF THE SOURCE INTENSITY AND MODELLING OF ¹³¹I DEPOSITION FIELDS

The involvement of many parameters and complexity of physical processes responsible for radionuclide deposition as a result of the nuclear accident make it difficult to handle the inverse problem. For the problem to be correct contributions of elementary sources in the contamination should be separable. In the case of the Chernobyl accident this requirement was met due to the fact that during the serious stage of the accident (from April 26 to May 6, 1986) meteorological fields underwent significant changes. The results of calculations by the regional model of the weightless contaminant deposition ($\beta = 1 \text{ cm s}^{-1}$) for an impulse-like source of unit intensity are presented on Fig.1. It is seen that during the serious stage of the accident the direction of transport varied (it nearly turned by 360°) which made it possible to solve the inverse problem.

Restoration of ¹³¹I source was carried out with the use of the data on cumulative density of deposition on the underlying surface (the monitoring network of the USSR Committee for Hydrometeorology). The calculated deposition field presented in Fig.2 was also obtained without regard to decay when $V_R = 0$, $\beta = 1 \text{ cm s}^{-1}$. Thus transport of ¹³¹I on aerosols was ignored and the activity of this fraction is estimated to be 10-20% of its gaseous phase activity. Therefore the results of ¹³¹I calculations presented do not claim to describe the deposition at a short range. The calculated deposition field agrees with the time dependent changes in the intensity of ¹³¹I emission (Fig.3) and the height of the emission which mounted to 1300 m in the first three days and dropped down to 300 m in the following days. The time dependent variations of the source were restored up to May 2, 1986. The total intensity of the emission from April 26 to May 5, 1986 (on the assumption

THE STAGES OF THE TRACE FORMATION DUE TO CHANGES OF METEOROLOGICAL SITUATION

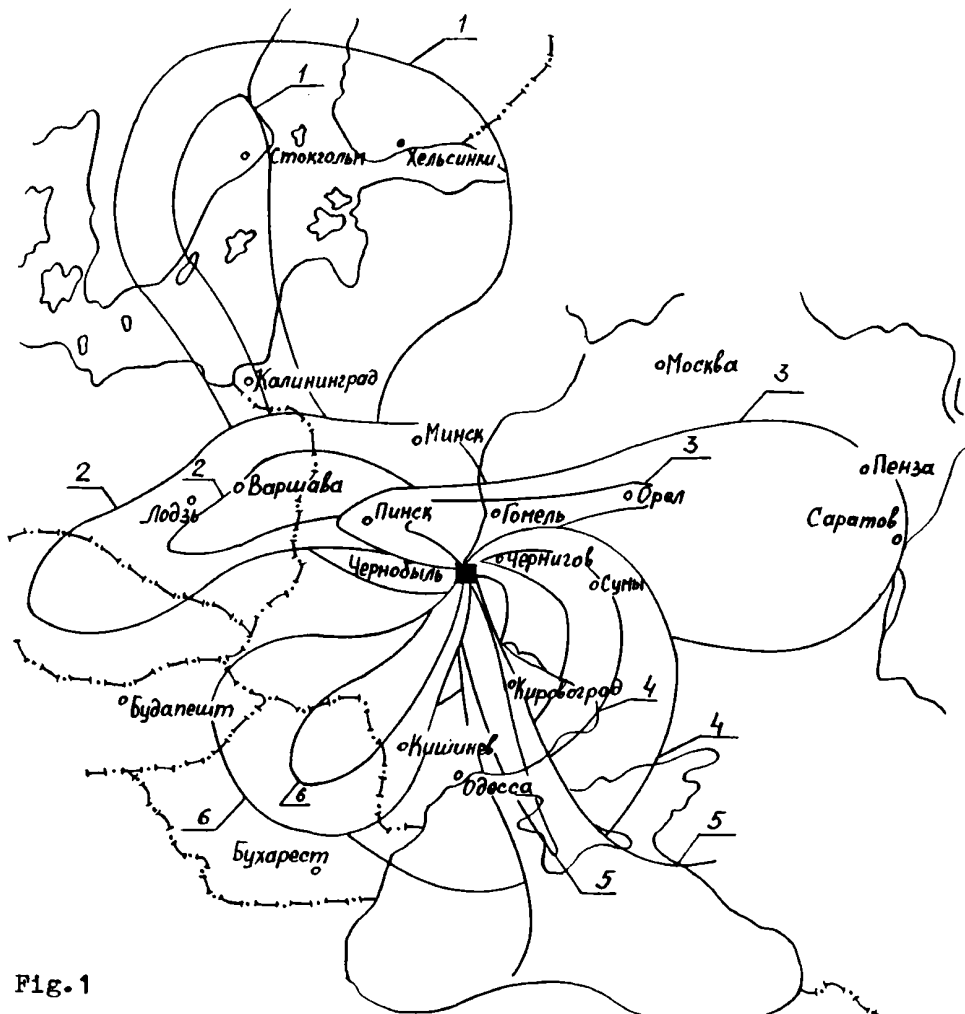


Fig.1

Each trace corresponds to an emission at a given time (GMT)

- | | |
|----------------------------|----------------------------|
| trace 1 - 00.00 GMT 26.04; | trace 2 - 00.00 GMT 27.04; |
| trace 3 - 12.00 GMT 27.04; | trace 4 - 00.00 GMT 29.04; |
| trace 5 - 00.00 GMT 02.05; | trace 6 - 12.00 GMT 04.05. |

that the source intensity remained constant from May 1 to May 6, 1986) amounted to 1.3×10^7 Ci which is close to the data reported to IAEA without regard to decay (10^7 Ci). About 50% of ^{131}I release has deposited on the territory shown in Fig.2 and the rest of it was carried off at greater distances.

4. TRANSBOUNDARY TRANSPORT

The model of transboundary transport was used for assessing ^{131}I transport across the USSR border. The total activity of ^{131}I transported across the border is estimated to be 5.6×10^6 Ci.

THE CALCULATED FIELD OF ^{131}I FALL-OUT FOR THE 10-th DAY FOLLOWING THE ACCIDENT (WITHOUT REGARD TO DECAY)

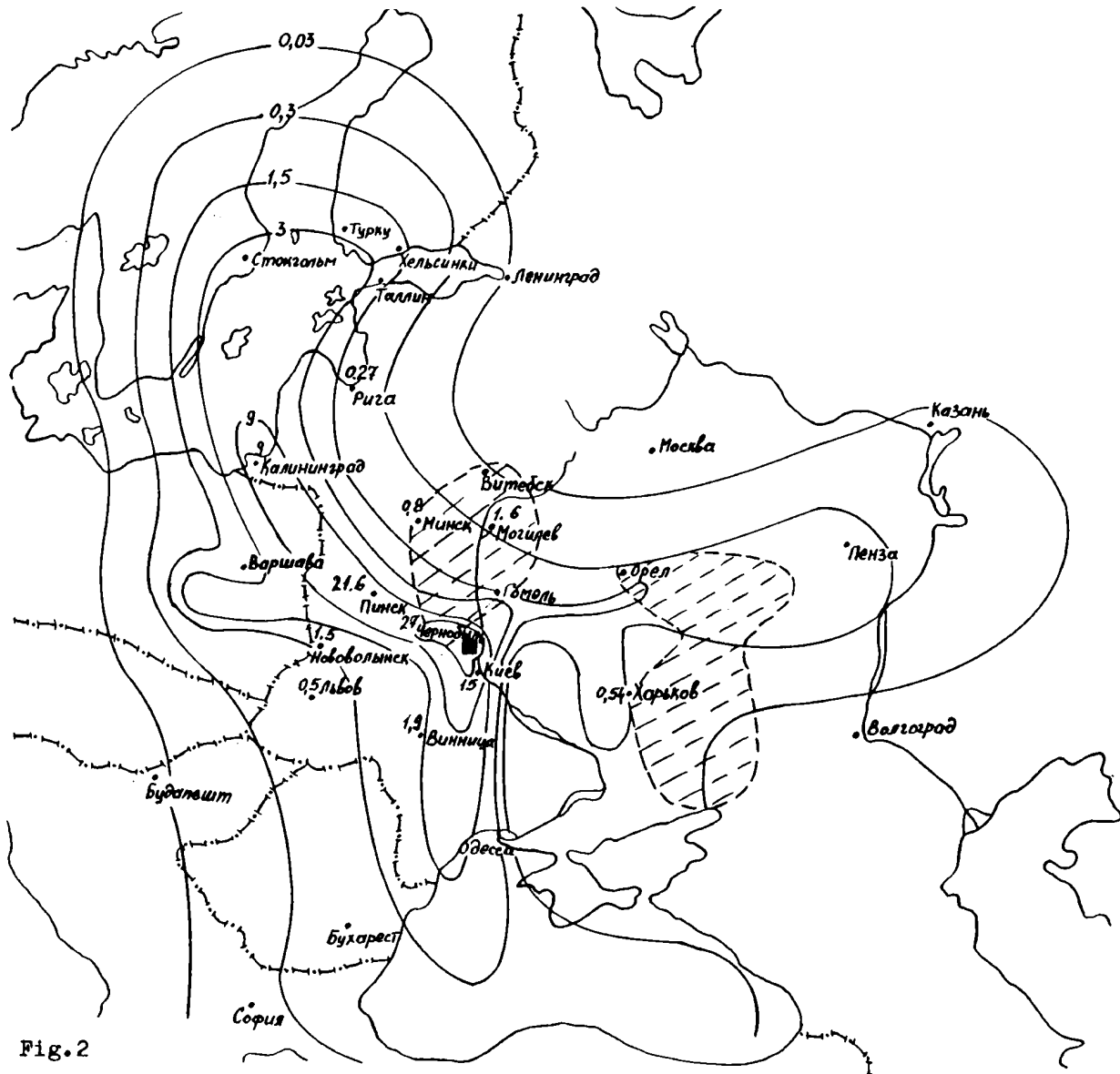


Fig.2

-3- the intensity of ^{131}I on the underlying surface is equal to 3 Ci km^{-2} . Isolated figures show the measured values of activity. The areas of heavy rainfall are hatched.

The transport across the border was basically due to radionuclides which entered the atmosphere in the first 36 hours following the accident and the countries affected were Poland, Sweden and Finland. The total emission transported across the border amounted to $3.9 \times 10^6 \text{ Ci}$ which made up approximately one half of the entire ^{131}I release over this period but a part of it came back to the USSR (the Baltic republics and Karelia). The radionuclides released in the atmosphere from April 27 to April 29 actually were not

transported across the border. But later a part of the emission which occurred from April 29 to May 6 was transported across the border.

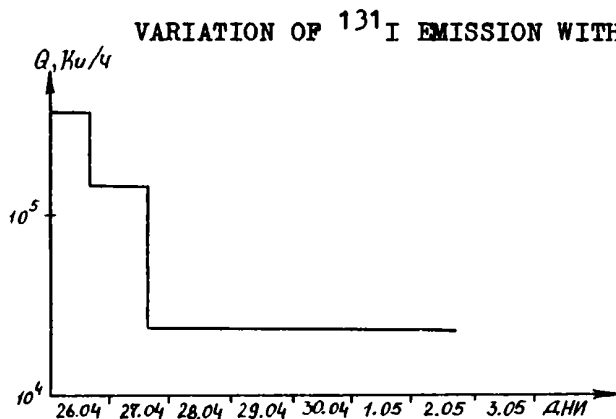


Fig. 3

The contamination affected Rumania, Bulgaria, Turkey, Czechoslovakia and Hungary. The contaminants which reached these countries were not all deposited there, a part of them was transported farther. The Table contains the estimates of ^{131}I emissions transported to the countries adjacent to the USSR. Quantitative estimates were made only for the transport across the USSR border while the transport between other countries was evaluated qualitatively.

State	Total emission, ^{131}I , Ci	Time of emission
Poland	2.0×10^6	26.04.86-27.04.86
Sweden and Finland	1.9×10^6	26.04.86-27.04.86
Rumania	1.0×10^6	29.04.86-06.05.86
Bulgaria	0.3×10^6	01.05.86-04.05.86
Turkey	0.3×10^6	29.04.86-04.05.86
Hungary and Czechoslovakia	0.1×10^6	04.05.86-06.05.86

Similar calculations were made for transport of ^{137}Cs radionuclides. They fully agree with the data submitted to IAEA on the total ^{137}Cs emissions ($\sim 10^6$ Ci).

REFERENCES

1. Борзилов В.А. и др. Метеорология и гидрология, 1988, № 4, с.57-65.
2. Wippermann F. Beitr. Phys. Atmos., 1975, Vol. 48, p. 30-48.
3. Smith F.B., Carson D.F. Bound. Layer Meteorol., 1977, Vol. 12, p. 307-330.
4. Тихонов А.Н., Арсенин В.Я. Методы решения некорректных задач. - М: Наука, 1986, 287 с.

II

NORTHERN HEMISPHERE
STUDIES

Evaluation of a Long Range Particle-In-Cell Transport and Diffusion Model Based on an Analysis of the Chernobyl Reactor Accident

Marvin H. Dickerson

Rolf Lange

Lawrence Livermore National Laboratory
P.O. Box 808, L-262
Livermore, CA 94550

Summary of Past Work

Work described in this presentation was accomplished over an eighteen month period after the Chernobyl accident, during which time model calculations were compared to environmental measurements supplied by the WHO as well as several individual countries. Results of these calculations and comparisons to measurements have been published in several reports with the most complete description of these studies provided by Lange, 1988. Using the source term data shown in Table 1, the spatial distribution of material released from the Chernobyl reactor is shown by Figure 1. After four days (Figure 1.b) material is moving in three major directions: (1) the lowest layer, within the first 1500m, is dispersed over Eastern Europe and Scandinavia, (2) another large collection of particles located above about 4 km are moving toward the Middle East, and (3) the third group of particles are moving east toward Japan. By day 10 (Figure 1.d) material has reached the western United States and is spreading over most of the Northern Hemisphere with the exception of eastern North America.

Figure 2 shows the 24 hour averaged ^{131}I surface air concentrations (Bq/m^3) over Europe for four daily time periods out to May 3, 1986. It should be noted that rainout was not included in these calculations. Also, due to the coarse resolution of the mesh used for these calculations, local concentration estimates can be up to two orders of magnitude low as pointed out by Lange, 1988. Table 2 lists a comparison between measured and

calculated surface air concentrations (Bq/m^3) and cloud arrival times. Comparisons for ^{131}I appear to be very reasonable, i.e., approximately 60% are within a factor of two while comparisons for ^{137}Cs did not reach this level of accuracy. It is not clear at this time why the difference is this large between the two radionuclides. Arrival times agree well with many of the observations, leaving Austria, Hungary, France, Southern Italy, United Kingdom, and Kuwait as the exceptions. Again it is difficult to determine why these differences occur; however, some possibilities are discussed below.

Model Improvement

Below are listed the model improvements we have made since the work discussed in this presentation was completed and other improvements we hope to complete in the future. As part of this process we plan to use the ANATEX data set that is described by another participant in this meeting.

1. Implemented

- a. The PATRIC model (Lange, 1978a) was merged with ADPIC (Lange, 1978b) to generate HADPIC providing a tool for evaluation of transport and diffusion of pollutants from the local to the hemispheric scale. The HADPIC model is interfaced directly to hemispheric forecast and analysis wind field data bases provided by the U.S. Air Force Global Weather Central.
- b. Based on Chernobyl modeling results preliminary adjustments were made to the diffusion parameters in ADPIC to simulate dispersion on the hemispheric scale.

2. Future

- a. Monte Carlo Diffusion. Particle-in-cell models like ADPIC or HADPIC lend themselves well to a random walk type of diffusion calculation. This method has the advantage that it needs no computational grid for the diffusion calculation, and hence is free from grid resolution problems. It is proposed to implement this method into HADPIC and compare the results with the gradient diffusion theory

now used in the code. It will be particularly useful when HADPIC is used on scales from the mesoscale on upward to hemispheric scales, where grid cells become very large, and the code might essentially always run in the source particle (Gaussian) mode because plume concentration gradients are not resolved. This method will replace, or compliment, the gradient diffusion module and will replace the limited Gaussian source particle prescription in the present HADPIC.

- b. Mesoscale Hydrodynamic Model. The development of a mesoscale forecasting model to be used as an alternative wind field driver to MATHEW to compute pollutant dispersal with HADPIC requires several adaptations of HADPIC. These include, transformation to terrain following coordinates if a finite difference forecast model is adopted, or some interpolative process of the wind field or both. Monte Carlo type diffusion appears preferable in either case. This development should include variable vertical cell spacing to improve resolution near the surface.
- c. Diffusion Parameterization. K profiles for a double boundary layer separated by an inversion are needed for HADPIC, as well as K profiles for the troposphere above the boundary layer. This would include space and time varying energy dissipation rates on a hemispherical scale.
- d. Surface Types. Lower boundary surface types (e.g., sea versus land surfaces) need to be included in HADPIC, particularly as they relate to the vertical diffusion parameterization.
- e. Wet Precipitation. Implementation of the wet deposition formulation in HADPIC needs to be addressed with an eye on being able to merge time and space dependent precipitation deposition from both measurements and forecast models.
- f. Topography. Topography needs to be introduced into HADPIC.

Acknowledgements

This work was performed under the auspices of the U.S. Department of Energy by the Lawrence Livermore National Laboratory under contract W-7405-Eng-48.

References

- Lange, R., 1978a, PATRIC, A Three-Dimensional Particle-In-Cell Sequential Puff Code for Modeling the Transport and Diffusion of Atmospheric Pollutants, Lawrence Livermore National Laboratory Report, UCID-17701.
- Lange, R., 1978b, ADPIC—A Three-Dimensional Particle-In-Cell Model for the Dispersal of Atmospheric Pollutants and its Comparison to Regional Tracer Studies, *J. Appl. Meteor.*, 17, 320–329.
- Lange, R., 1988, Dose Estimates from the Chernobyl Accident, *Nuclear Technology*, Vol. 82, No. 3.

Appendix A: Tables and Figures

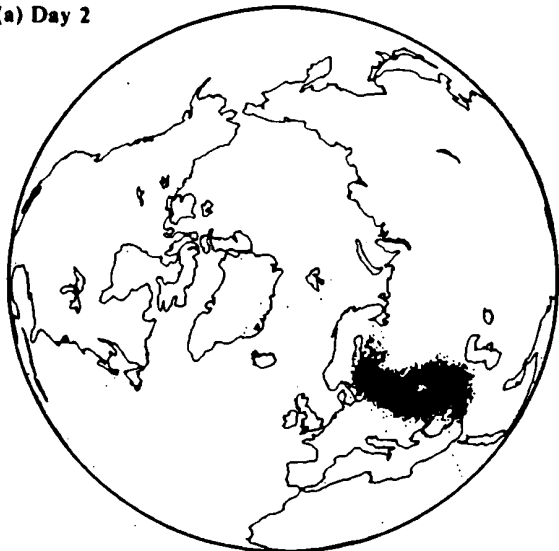
Nuclide	Fraction	Activity Released (Bq)
¹³⁷ Cs	1.0	8.9×10^{16}
¹³⁶ Cs	0.2	2.0×10^{16}
¹³⁴ Cs	0.5	4.8×10^{16}
¹³¹ I	20.	1.7×10^{18}
¹³³ I	42.	3.7×10^{18}
¹⁴¹ Ce	0.1	8.9×10^{15}
¹⁴⁴ Ce	0.06	5.2×10^{15}
¹⁴⁰ Ba	0.5	4.4×10^{16}
¹⁴⁰ La	0.5	4.4×10^{16}
⁹⁵ Zr	0.1	8.9×10^{15}
⁹⁵ Nb	0.1	8.9×10^{15}
¹³² Te	4.2	3.7×10^{17}
¹⁰³ Ru	0.3	3.0×10^{16}
¹⁰⁶ Ru	0.06	5.2×10^{15}
¹³³ Xe	—	6.5×10^{18}

Table 1. Activity fraction relative to ¹³⁷Cs and estimated activity released, decay corrected to 26 April 1986 (Lange, 1988).

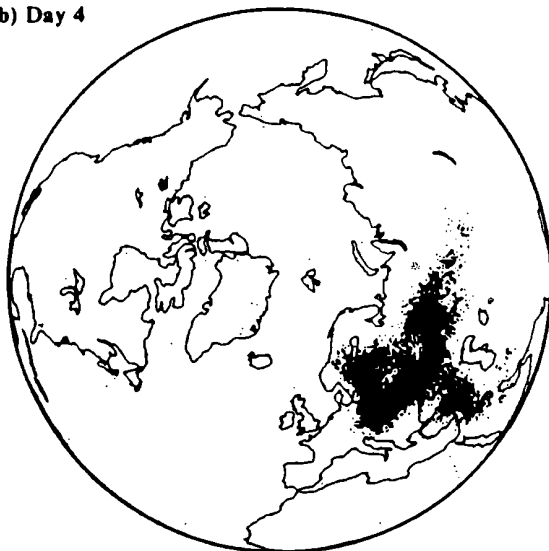
Location	Dates	¹³¹ I		¹³⁷ Cs		Cloud Arrival Time	
		Meas.	Calc.	Meas.	Calc.	Calc.	Meas.
Nurmijarvi (Finland)	4/29-5/3	3.7	3.8	0.08	0.6	4/27	4/27
Stockholm	4/28-5/6	3.6	8.0	0.2	1.1	4/27	4/27
Kjeller (Norway)	4/28-5/5	6.2	9.5	0.2	1.3	4/27	4/27
Munich	4/30-5/6	7.0	6.5	1.7	0.9	4/30	4/30
Austria	4/29-5/5	3.5	4.2	-	-	4/30	4/29
Budapest	5/1-5/5	3.0	4.2	0.6	0.5	4/30	4/29
N. Italy	4/30-5/6	17	6.6	0.7	0.4	4/30	4/30
S.E. France	5/1-5/6	9.8	6.6	0.4	0.7	4/30	4/29
Paris	5/1-5/7	0.7	3.7	0.2	0.5	5/1	4/29
S. Italy	5/1-5/6	8.0	1.9	0.6	0.2	5/2	5/1
Netherlands	5/1-5/5	7.1	9.3	-	-	5/2	5/2
Berkeley (U.K.)	5/1-5/3	0.3	0.5	0.05	0.02	5/3	5/2
Chilton (U.K.)	5/2-5/3	5.4	4.5	0.9	0.2	5/3	5/2
Athens	5/3-5/5	29	18	-	-	5/3	5/3
Kuwait	5/4-5/9	0.3	0.1	0.06	0.03	5/7	5/5

Table 2. A comparison between measured and calculated surface air concentrations (Bq/m³) and cloud arrival times. (Lange, 1988)

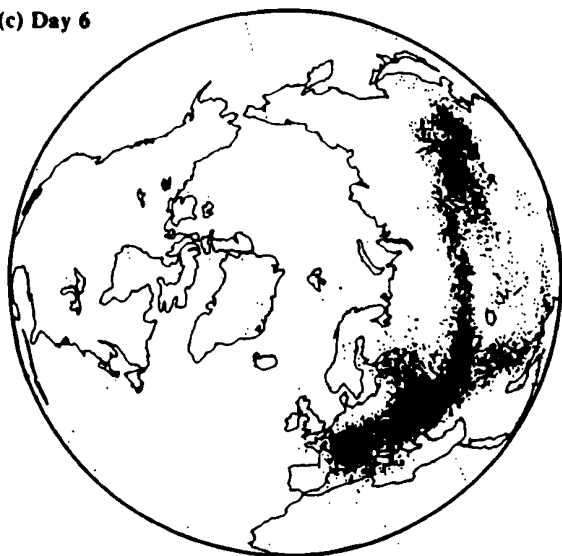
(a) Day 2



(b) Day 4



(c) Day 6



(d) Day 10

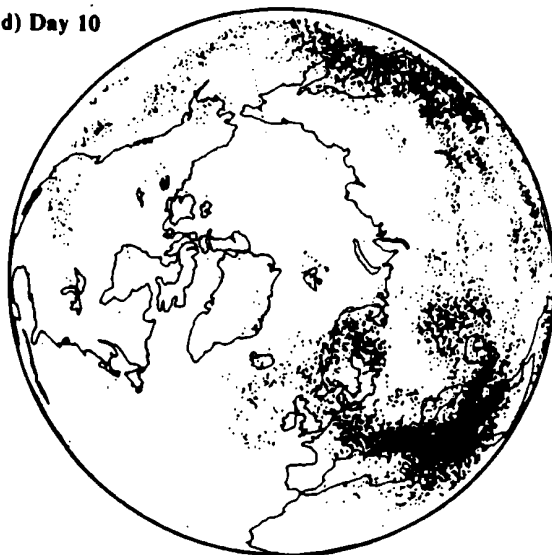


Figure 1. ARAC plots showing how the clouds of radioactive material spread around the Northern Hemisphere at (a)2, (b)4, (c)6, and (d)10 days after the initial explosion (Lange, 1988).

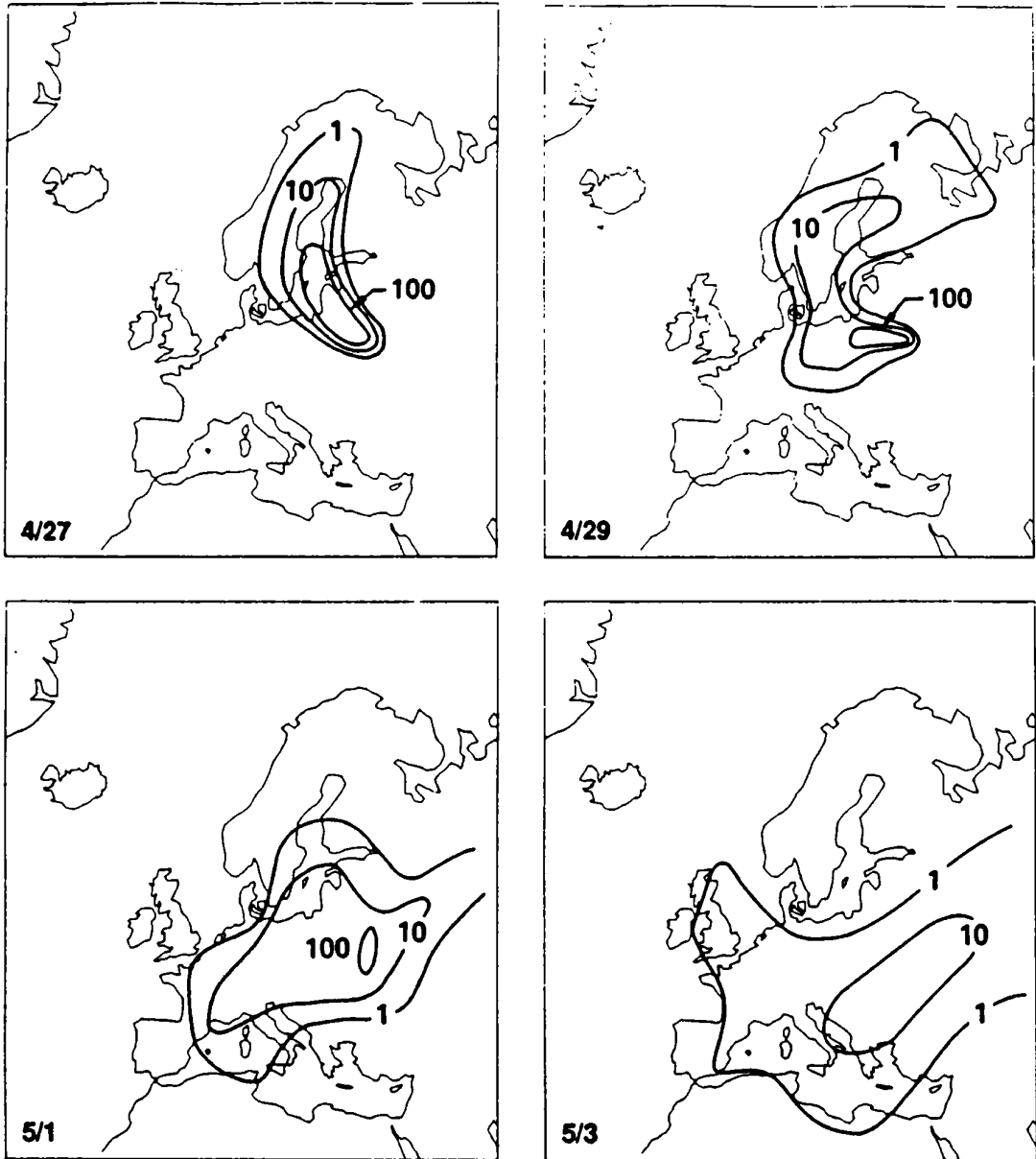


Figure 2. ^{131}I 24 hour averaged surface air concentration patterns over Europe (Bq/m^3) based on the PATRIC model for dates listed (Lange, 1988).

DISCUSSION

QUESTION: ApSimon: I agree that underlying surface of land or sea has an influence on dispersion. How do you include this with respect to both mesoscale effects on windfields and effects on turbulence?

ANSWER: First, we plan to use the identification land/sea surfaces to define temperature differences that can effect the vertical diffusion.

QUESTION: Geiss: 1. How did you calculate the vertical distribution of the emissions (plume rise). 2. How did you estimate the time dependence of the emissions?

ANSWER: 1. We initially estimated, based on the boundary layer depth determined from a nearby vertical sounding, that the emissions were contained with the first 1500 m above the surface. Later this assumption was verified by a cumulus cloud model and an assumption about the heat source. Later, after measurements of activity were made by aircraft over Japan we established an upper level cloud centered at 5000 m. The upper level cloud lasted for the first 24 hrs. The lower level emissions were constant for 6 days.

QUESTION: Hehn: For model validation, in which time intervalls and local meshes should the experimental results be evaluated? In Germany we presently evaluate the Iodine-131 activity in air near ground in two hour averages.

ANSWER: Your 2 hour average data would be ideal for testing models at distances grater than 1000 km. This is true, because it allows for defining time of arrival/departure and by averaging allows comparisons to measurements over various times from 2 to 24 hrs.

QUESTION: Nordlund: Was precipitation scavenging taken into account in the calculations you have made?

ANSWER: No, we have not yet included precipitation scavenging in our calculations.

Simulation of Atmospheric Dispersion of Chernobyl Radioactivity
by SPEEDI

Hirohiko ISHIKAWA, Masamichi CHINO, Hiromi YAMAZAWA and Shigeru MORIUCHI

*Department of Environmental Safety Research
Japan Atomic Energy Research Institute,
Tokai-mura, Ibaraki-ken, 319-11, Japan*

Summary : The dispersion of $Cs-137$ released from Chernobyl was diagnostically simulated by a three dimensional mass-consistent wind field model and a particle dispersion model. The calculations clarified the transport paths of the radioactive clouds over Europe from April 26 to May 11, 1986. The calculated concentration of airborne radioactivity agreed with the monitoring data qualitatively, although there were some differences between them. The surface deposition was also calculated by using precipitation data from the 171 meteorological stations. For many locations, there was reasonable correlation between them.

1. INTRODUCTION

To better understand the long-range transport of airborne radioactivity, the Japan Atomic Energy Research Institute started a research program to improve the capability of SPEEDI (System for Prediction of Environmental Emergency Dose Information)⁽¹⁾. The goal of this program is to estimate the dose of a severe nuclear accident in a synoptic region. Both the physical models and the code system are to be refined.

This program included the simulation of atmospheric dispersion of Chernobyl radioactivity. This was diagnostically simulated by the refined mass-consistent wind field model and the particle dispersion model of SPEEDI. The dispersion and deposition of $Cs-137$ released each day during the accident were calculated and compared with data from monitors. This paper describes the models, assumptions and results.

2. MODELS

2.1 Wind field Model

A three dimensional mass-consistent wind field model was used to compute the wind field. This model is equivalent to MATHEW⁽²⁾ used in the ARAC system. First, the observed wind data are interpolated/extrapolated to produce an initial guess of the wind field. Next, this wind field is adjusted to satisfy mass conservation using a variational technique.

For application to a synoptic wind field, following points of this model were refined.

- The map factor associated with a projection of the earth's surface to a computational 'flat' plane was considered.
- The interpolation/extrapolation method to produce the initial guess of the wind field was refined.
- The proper value of parameter $K = a_1/a_2$ was determined.

Based on a parametric study, $K = 0.01$ was used.

2.2 Dispersion and Dose Model

A Lagrangian particle dispersion model was used to solve the transport-diffusion equation. The radioactive plume is expressed by a mass of particles where each particle is transported by the wind provided by the wind field model. The wind at each time step is temporally interpolated using the four daily wind fields. The diffusion is expressed by the random-walk motion of each particle. The strength of the random-walk motion is adjusted to yield a Gaussian concentration distribution with Pasquill-Gifford $\sigma_i (i=x, y)$ in a homogeneous wind field.

The dry deposition is calculated by the surface depression model. Particles in the lowest grid cell give a portion of their radioactivity to the ground. The deposition velocity for $Cs-137$ is assumed to be 0.1 cm/sec. The wet deposition is also computed. The wash-out coefficient is assumed to be $10^{-4} \cdot R (\text{sec}^{-1})$, where R is the rainfall intensity

(mm/h).

A dose calculation module is added to the dispersion model. This module calculates the exposure rate and the external gamma dose due to cloud-shine and ground-shine. It also calculates internal dose due to inhalation.

3. DATA AND ASSUMPTIONS

3.1 Meteorological Data

The four daily surface wind data (00Z, 06Z, 12Z and 18Z) from 171 WMO surface meteorological observatories and upper wind data (00Z and 12Z) at pressure levels of 850 and 700 millibars (mb) from 101 WMO aerological observatories were used in the wind field calculation. The upper wind data were temporally interpolated to produce upper wind 'observation' at 06Z and 18Z of each day.

The precipitation data at surface stations were used in the dispersion model to calculate wet deposition.

3.2 Computational Area and the Topography

The computational area is 3600 km by 3600 km in the projected map. The vertical height is 3000 m. The computational mesh is 51 x 51 units horizontally and 20 units vertically. so that the mesh interval is horizontally 72 km and vertically 150 m. The topography can be introduced in the models, but is not included in this study.

3.3 Dispersion Condition

The height of the atmospheric boundary layer was assumed to be 2000 m. In this layer the diffusion coefficient which corresponds to atmospheric stability class *C* was used. In the layer above 2000 m, a value which corresponds to atmospheric stability class *F* was applied. These assumptions allow fast vertical diffusion to 2000m. Above this layer the diffusion is weak.

3.4 Source Term

Although the initial distribution of source materials should be considered, a point release was assumed. The release height was assumed 1000 m during the first 9 hours of the accident and 200 m after that. However, the release height did not have significant effects on the calculation except in the vicinity of the release-site because of the assumed fast vertical diffusion up to 2000 m. A continuous unit release rate was assumed.

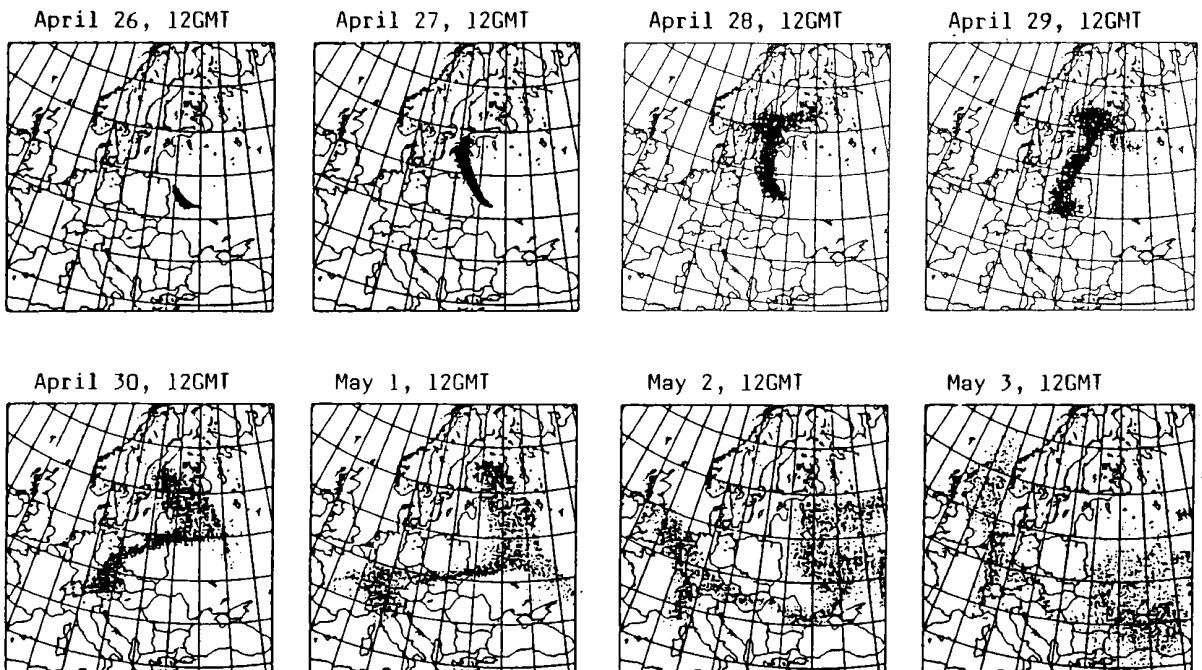


Fig.1 Transport of marker particles released in the first 24 hours (The first plume).

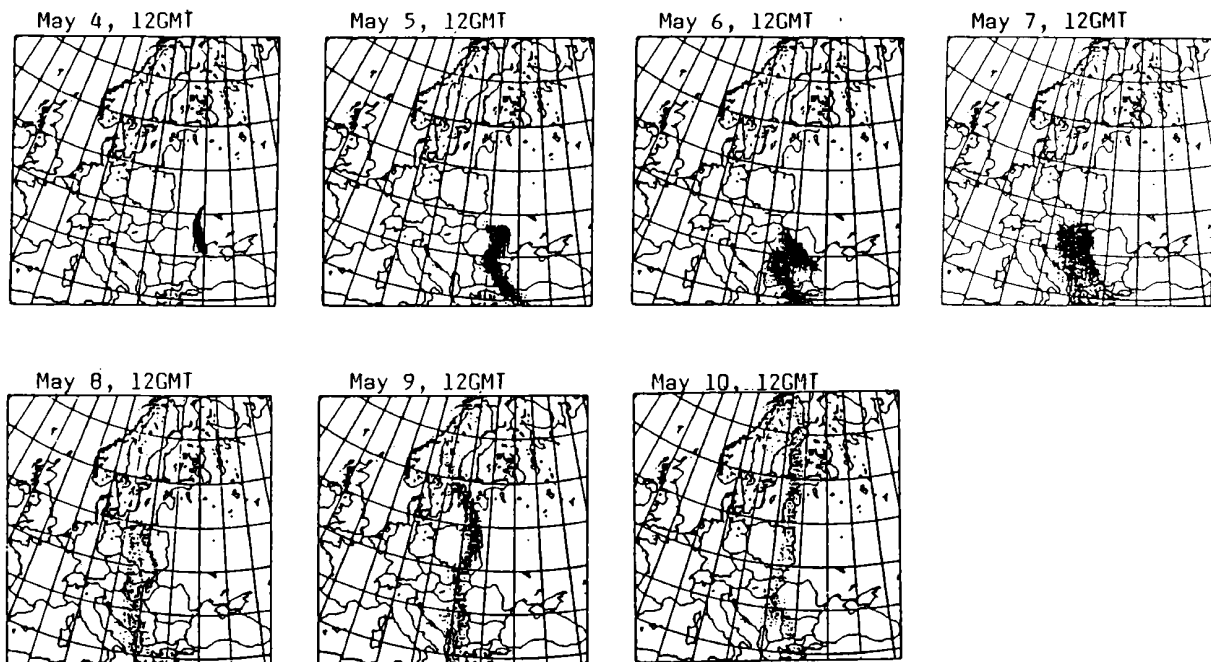


Fig.2 Transport of marker particles released in the May 4 (The ninth plume).

4. RESULTS

4.1 Qualitative Feature of the Movement of Plumes

The movement of radioactive clouds of $Cs-137$ released in every 24-hour period from the first to the tenth day was calculated individually for each cloud. The radioactive cloud released during the n-th day of the accident is referred as the n-th plume in this paper. For instance, the first plume is the radioactive cloud released during April 25, 21Z to April 26, 21Z and the tenth plume is that released during May 4, 21Z to May 5, 21Z.

The movement of marker particles released in the first 24 hours (First plume) is shown in Fig. 1. Each dot is the projection of a marker particle to the earth's surface. This figure indicates that the radioactive cloud moved to the northwest initially and reached Sweden and Finland in the afternoon of April 27. In Sweden⁽³⁾, the first increase of gamma radiation was detected at several monitoring posts facing the Baltic Sea in the afternoon of April 27. In Finland⁽⁴⁾, an increase of radioactivity was detected at some aerosol monitoring stations in the evening of the same day. The calculations agree with these monitoring data. During the next day, April 28, the northern part of the plume migrated into mid-Sweden. A branch extended to the east and reached to the U.S.S.R. The southern part of the plume began to move to the southwest and covered Poland. In Poland the radioactivity began to increase in the early morning of the April 28 at stations in the northeast part of the country⁽⁵⁾. During the period from April 29 to May 1, the southern part of the plume was transported to the west and progressively covered Czechoslovakia, Austria, Switzerland, southern Germany, Italy and France. On May 2, the western edge of the plume moved to the north and covered Belgium, Holland and the United Kingdom. It reached the west coast of Norway on May 3. These movements correspond to the increase in the concentration of airborne radioactivity in these areas. The observed arrival times of radioactive clouds in central and western Europe corresponds to the movement of the first plume.

The second plume, released on April 27, first moved to the west. On April 28, it was stretched in an east-west direction. After April 28, the western part of this plume showed movements similar to the later part of the first plume. The eastern part of the second plume moved eastward until April 30. It then moved southward and by May 3 it had swept over the southern Ukraine, Romania, Bulgaria, Yugoslavia, Greece and Turkey. The movements of plumes released on April 28 through May 3 (the third to the eighth plumes) were similar to the eastern part of the second plume. Until April 30, the radioactive clouds were transported to the east. After that they moved southward.

They finally went out of the computational region, mainly at the southern and partly at the eastern boundaries.

The ninth plume (released in May 4) and the tenth plume (released in May 5) showed different movements from the previous plumes. The movement of the ninth plume is shown in Fig.2. It moved southward initially and then it moved to the west where it covered Rumania, Bulgaria and Yugoslavia. It then gradually moved northward and covered Hungary on May 7. It reached Poland on May 8 and Sweden on May 9. The tenth plume showed similar movement, but it reached Poland on May 7 and Sweden on May 8. The increase in concentration of airborne radioactivity was observed in Stockholm on May 8 and 9. In Budapest (8) the second increase began on May 7. These monitoring data correlate with calculations.

Generally speaking, the calculations qualitatively agreed with the monitoring data in most European countries. However, the calculations were unable to predict the arrival of radioactive clouds at several locations. According to reports (7),(8), Chernobyl radioactivity was detected at sites in Denmark in the afternoon of April 27. In Turkey (7), the first detection was reported on April 30. Increases of radioactivity were detected on April 28 (9) at several Norwegian stations, increases of radioactivity were These observations cannot be explained by the calculation.

The detection of each plume in selected cities is summarized in Fig.3. For instance, Stockholm experienced only the first plume in April and both the ninth and the tenth plumes on May 8 and 9. Vienna was significantly affected by both the first and the second plumes for several days and to a lesser degree by the ninth plume. Bucharest was affected by all plumes but the seventh plume.

4.2 Quantitative Comparisons

If the release rate R_i of each day is given, the concentration of airborne radioactivity at a certain site can be computed by

$$C(t) = \sum_{i=1}^N R_i \cdot x_i(t) \tag{1}$$

where x_i is the concentration of the airborne radioactivity of the i -th plume assuming continuous unit release and N is the number of plumes released until time t . The release rate of Cs-137 in the days from April 26 to May 5 were derived from Table 4.12 and 4.13 of the Soviet Report to IAEA (10) as $R_i = 0.3, 0.1, 0.085, 0.063, 0.05, 0.05, 0.1, 0.125, 0.175, 0.2$ MCi/day.

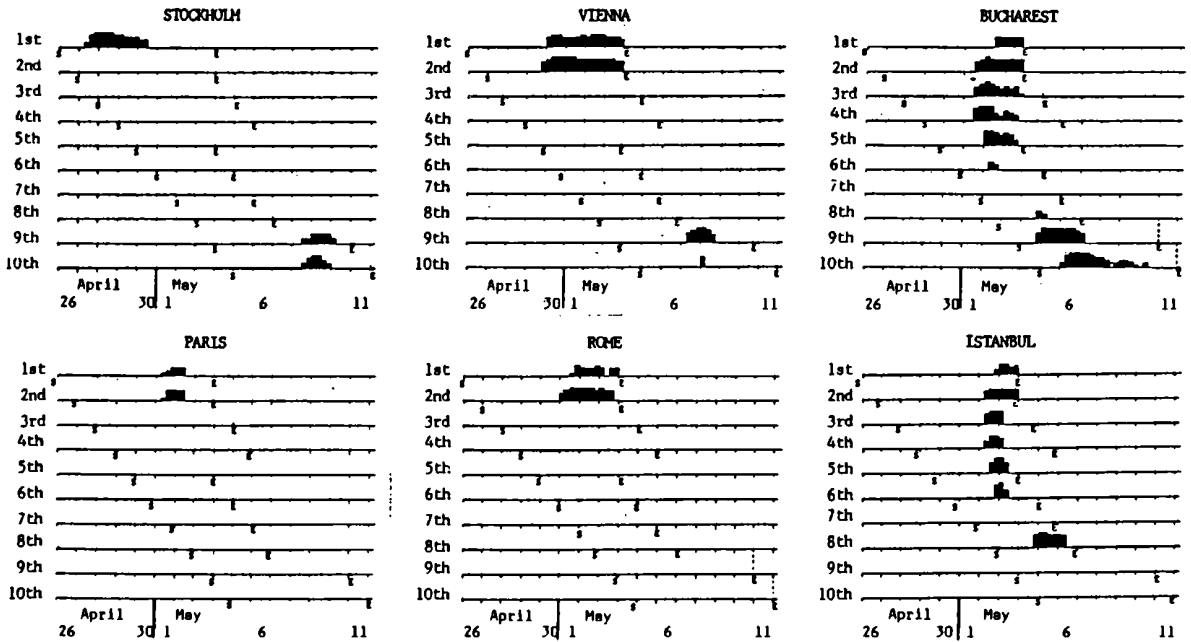


Fig.3 Detection of calculated plumes at selected cities. Each bar represents relative concentration of airborne radioactivity. The symbols S and E in the figures represent the calculation start and end times, respectively.

The resulting calculations are compared with measurements (11,12,13,14,15,16) in Fig.4. In Stockholm and Helsinki the calculated concentrations of airborne radioactivity are higher than measured. The measurement in Helsinki shows large temporal variation. In central and western Europe, the observed values are generally higher than calculated. In Warsaw the correspondence is fairly good.

4.3 Deposition

The deposition accumulated until May 3 caused by the first plume is shown in Fig.5a. The release rate is again assumed to be unity. Significant deposition was calculated around Chernobyl. This was caused by dry deposition. Other high value islands in mid-Sweden, central Europe and the northern part of the United Kingdom were due to precipitation. An example of temporal variation of accumulated deposition is shown in Fig.5b. Significant deposition was occurred in Gavle due to wet deposition, because of heavy rain from April 29, 00Z to 06Z. During this period the increase of surface deposition was only moderate at Stockholm which is about 150 km south of Gavle.

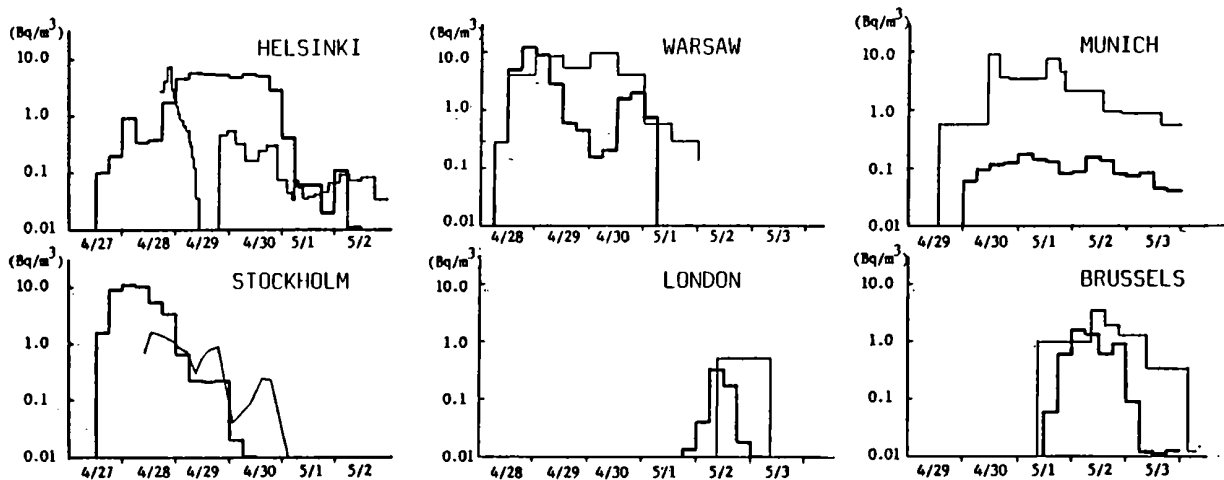


Fig.4 Comparisons of calculated concentrations (thick line) with measurements (thin line).

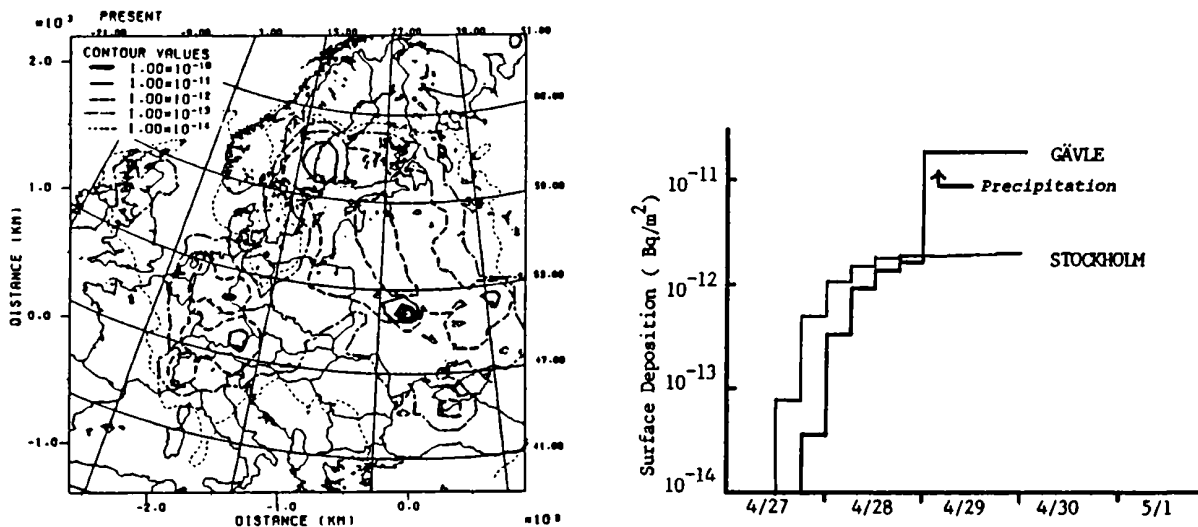


Fig.5 (a) Surface deposition accumulated until May 3 due to the first plume and (b) temporal variations of accumulated depositions in Stockholm and Gavle. The release rate is assumed as 1Bq/h.

As mentioned by many researchers, the surface deposition pattern strongly depends on the distribution of precipitation. However, for the real-time simulation the available precipitation data are limited to those provided through the WMO GTS network. Considering the poor spatial correlation of precipitation, the spatial distribution data from surface observatories included in GTS is too sparse. Therefore some assumptions are needed to produce grid-by-grid precipitation data used in the calculation of wet deposition. This situation makes it difficult to get reliable results for wet deposition.

5. CONCLUDING REMARKS

The dispersion and the deposition of radioactivity from Chernobyl were diagnostically calculated. The transport of radioactivity from Chernobyl over Europe was, except for some locations, qualitatively explained by the calculation. The quantitative agreement was satisfactory considering uncertainties involved in both the calculations and the measurements. The deposition calculations would be improved if more detailed precipitation data were given.

The results of these calculations are supported by data from the dense network of meteorological observations in Europe. The application of these models to dispersion around Japan will be confronted by the problem of sparse data over the Pacific Ocean. Additional information will be needed to construct the initial guess of the wind fields.

REFERENCES

- (1) Imai, K. *et al.* : SPEEDI - A Computer Code System for Real-Time Prediction of Radiation Dose to the Public due to an Accidental Release, JAERI 1297, 1985.
- (2) Sherman, C.A. : A Mass-Consistent Model for Wind Field over Complex Terrain, *J. Appl. Meteor.*, Vol.17, No.3, 1978.
- (3) Kjelle, P.E. : Fallout in Sweden from Chernobyl Part 1, *SSI-report 86-20*, 1986.
- (4) Alvela, H. *et al.* : Environmental Gamma Radiation in Finland and the influence of meteorological conditions after the Chernobyl Accident in 1986, *STUK-A65*, 1987.
- (5) Javrowski, : National reports (Poland), *IAEA Bull.*, Vol.28, No.3, 1986.
- (6) Andras, A. *et al.* : Monitoring the Radiation Consequences due to the Disaster at the Chernobyl Nuclear Facility, *KFKI-1986-49/K*, 1986.
- (7) Salo, A. : Information exchange after Chernobyl, *IAEA Bull.*, Vol.28, No.3, 1986.
- (8) National Agency of Environmental Protection : The reactor accident at Chernobyl, U.S.S.R. - Radiation Measurement in Denmark, *DK-8600332*, 1986.
- (9) Pacyna, J. *et al.* : Air Radioactivity at Selected Stations in Norway after the Chernobyl Reactor Accident, *NILU-TR-7/86*, 1986.
- (10) INSAG, 1986 : International Nuclear Safety Advisory Group, "Summary Report on the Post-Accident Review Meeting on the Chernobyl Accident", August 30 - September 5, 1986, IAEA, Vienna, 1986.
- (11) Sinkko, K. *et al.* : Airborne Radioactivity in Finland after the Chernobyl Accident in 1986, *STUK-A56*, 1987.
- (12) Jagielak, J. *et al.* : Effective Dose Equivalent to average individuals in Warsaw after the Chernobyl accident, *Radiation Protection Dosimetry*, Vol.20, No.4, 1987.
- (13) Winkelmann, I. *et al.* : Ergebnisse von Radioaktivitätsmessungen nach dem Reaktorunfall in Tschernobyl, *ISH-Heft 99*, 1986.
- (14) Jensen, M. *et al.* : National reports (Sweden), *IAEA Bull.*, Vol.28, NO.3, 1986.
- (15) Cambray, R.S. *et al.* : Observation on Radioactivity from the Chernobyl Accident, *Nuclear Energy*, Vol.26, No.2, 1987.
- (16) Deworm, J.P. *ed.* : A Comparison of the Measurements Released to the Chernobyl Nuclear Accident, *BLG-595*, 1987.

DISCUSSION

QUESTION: ApSimon: Can I confirm how vertical winds are deduced. Am I right that these are based on the conservation of mass equation?

ANSWER: Basically, the vertical components are computed from mass continuity. But the strength of them depends on a parameter. A parametric study was done and the proper values were searched. In the present case, the vertical winds are not strong. The strength of the vertical wind is less than 1 m/s at most of the computational area.

QUESTION: Dickerson: Did you have terrain in your model?

ANSWER: No. But now a world topographical data base is completed. Therefore, we will use topography in the next series of calculation.

QUESTION: Underwood: Could you explain what type of dispersion model you used. You said it was "random walk" but not Markov chain.

ANSWER: We solve the transport-diffusion equation. The diffusion is expressed by the random-walk-motion. But the magnitude of the random-walk motion is adjusted to fit Pasquill-Gifford σ_x , σ_z in the homogenous wind field. In the Markov-chain model, the movement of a particle is related with its previous movement. But we don't do that. One of the advantages of our method is that the time step Δt can be larger than that of Markov-chain.

CONTINENTAL AND HEMISPHERIC SCALE DISPERSION
OF NUCLEAR DEBRIS FROM THE
CHERNOBYL ACCIDENT

J. Pudykiewicz Atmospheric Environment Service of Canada
2121 Trans Canada Highway, suite 534, Dorval, Quebec Canada H9P 1J3

Summary: A 3-dimensional hemispheric tracer model is employed for the simulation of the dispersion of the nuclear debris from the Chernobyl accident. The tracer model is driven by a series of meteorological fields derived from the hemispheric objective analysis scheme of the Canadian Meteorological Center (CMC). Verification of the model indicates good accuracy and substantial improvement compared to the preliminary experiments with a very simple 2-dimensional hemispheric tracer model.

1. INTRODUCTION

The meteorological aspects of the Chernobyl accident have been analysed by numerous researchers interested in the problem of atmospheric dispersion (ApSimon¹). The initial Canadian simulation was performed on a hemispheric grid in a pressure coordinate system using a very simple 2-D model (Pudykiewicz²).

Following the emergency simulation, extensive development work with the tracer model was conducted. The current version of the system is fully three - Dimensional (3 - D) and could be executed on a grid with horizontal resolution of 50 km over the Northern Hemisphere. The tracer model is driven by a series of meteorological fields derived from the Hemispheric Objective Analysis scheme of the Canadian Meteorological Center (CMC) or from the hemispheric or global spectral model. The accident scenario employed in the simulation was derived from the data presented at the post-accident meeting of the International Atomic Energy Agency (IAEA) in Vienna in August 1986. The model results were verified against measurements from a network covering most of the Northern Hemisphere and indicate substantial improvement when compared to the simple models used immediately after the Chernobyl accident. We expect that the test against "Chernobyl data" will become very useful for the intercomparison of the different models used for atmospheric tracer studies. The current work with the model is related mostly to the incorporation of a cloud water scheme in the hemispheric version and testing of the Global predictive version of the system.

2. THE TRACER MODEL.

The 3 - Dimensional tracer model employed in this study is based on the mass conservation equation (in specific activity form) written in the terrain following coordinate system σ :

$$\frac{\partial \bar{A}^{-1}}{\partial t} = -V_H^\sigma \nabla_H^\sigma \bar{A}^{-1} - \sigma \frac{\partial \bar{A}^{-1}}{\partial \sigma} + v_g^1 (\partial \Gamma \bar{A}^{-1} / \partial \sigma) + \partial / \partial \sigma \Gamma^2 K_z \frac{\partial \bar{A}^{-1}}{\partial \sigma} + \bar{S}_A^{-1} \quad (1)$$

where :

$i = 1, M$; M - number of species, σ - vertical coordinate, $\sigma = p / \pi$
 p , π -pressure and surface pressure, \bar{A}^i - grid cell average specific activity
 \bar{V}_H^σ - grid cell average horizontal wind vector, ∇_H^σ - horizontal nabla
operator in the σ system, $\dot{\sigma}$ - vertical motion field in the σ system,
 v_g^i - gravitational settling velocity, $\Gamma = g \sigma / R T$, g - acceleration
due to gravity, R - gas constant, T - temperature, K_z - vertical diffusion
coefficient, $\langle \rangle$ - averaging operator, \bar{S}_A^i - sum of the external sources and
sinks

Numerical solution of the transport equation.

The model equations were transformed to the polar stereographic projection system true at 60° N. The corresponding equations may be written as follows:

$$\frac{\partial \bar{A}^i}{\partial t} = (L_1 + L_2 + L_3 + L_4 + L_5) \bar{A}^i \quad (2)$$

where:

$$L_1 := -m^2 \tilde{V}_H^\sigma \nabla_H^\sigma, \quad L_2 := -\dot{\sigma} \partial / \partial \sigma, \quad L_3 := v_g^i \partial / \partial \sigma \Gamma, \quad L_4 := \partial / \partial \sigma \Gamma^2 K_z \partial / \partial \sigma + Q^i$$

$$L_5 := S^i, \quad \tilde{V}_H^\sigma = (1/m) \nabla_H^\sigma, \quad m - \text{map scale factor}$$

The time discretization of (2) is performed by successively applying the operators $L_1 - L_5$ to advance a time step Δt and then successively applying the operators in reverse order to advance a further time step.

The horizontal and vertical advection and gravitational settling are performed using the semi-Lagrangian algorithm developed by Robert and subsequently used for pollution problems by Pudykiewicz and Staniforth⁴. The vertical diffusion is solved using the implicit iterative method. The last substep related to scavenging and radioactive decay is accomplished using the analytic solution of the radioactive decay equation.

The hemispheric grid of the model is uniform with a resolution of 150 km on the Polar Stereographic Projection. The corresponding grid domain is 180 * 180 points centered on the North Pole. Eleven levels were employed to numerically solve Eq. 1.

The meteorological input.

The transport model was driven by the data stored in the archiving system of the Objective Analysis (OA) of the Canadian Meteorological Center (CMC). The analysis system is executed in a 6 hr cycle and uses optimum interpolation of the forecast errors in order to provide analysed wind components, geopotential, temperature and dew point depression. The driving model of the OA system is a hemispheric primitive equation spectral model described originally by Daley et al.⁵. The function of the spectral model is to provide the 6 hr. forecasts required in the assimilation cycle. The forecast model is initialized using Nonlinear Normal Mode Initialization and uses a more extensive parameterization of the physical processes compared to the initial version.

The target grid of the analysis at the moment of the accident was a gaussian latitude-longitude grid with a resolution of 128*32 points over the Northern Hemisphere. The temporal resolution of the meteorological fields from the OA system was 6 hrs. The meteorological fields for intermediate time levels were obtained by time interpolation.

The profile of the vertical diffusion coefficient required to solve eq. (1) was computed externally using the analytical theory of the surface layer and the O'Brien profile above the constant flux layer. The value of the diffusivity in the free atmosphere was assumed to be constant and equal to K_H . This approximation is sufficiently accurate for the simulation of atmospheric tracers on a hemispheric scale. The deposition velocity appearing in the boundary condition was computed as the inverse of the sum of the resistances of the turbulent and laminar deposition layers and the resistance of the surface.

The source term.

We approximated Q^1 , the source term in our experiments with the 3-D hemispheric tracer model, by the following expression:

$$Q^1(\eta_x, \eta_y, \sigma, t) = (E^1(t) F(\sigma) / (2\pi\sigma_H^2)) \text{Exp} \left[- r^2 / 2 \sigma_H^2 \right] \quad (8)$$

where:

- $E^1(t)$ - amount of the radioactivity released
- $F(\sigma)$ - function describing vertical distribution of the release
- r - distance from the accident site
- σ_H - standard deviation of the horizontal mass distribution

The function $E^1(t)$ was obtained from the data presented at the meeting of the International Atomic Energy Agency (IAEA) in August 1986. The effective height of the release was between 1500 and 4000 m.

3. RESULTS OF THE SIMULATION.

The hemispheric tracer model was executed for a time period of 4 weeks starting on April 25 1986. During the first two days after the Chernobyl accident, the radioactive cloud was transported mostly towards Scandinavia. A second southern segment of the cloud had spread south-east over the Black Sea in the direction of the Middle - East (Fig. 1a). The initial stage of the transport occurred in a synoptic situation dominated by a high pressure system east of the accident site and a low located in the vicinity of Iceland.

On April 28 the synoptic situation changed and the northern part of the radioactive cloud moved southward, crossing Poland, Germany and Austria. Subsequently on April 29, after the dissipation of the blocking high pressure system centered north-east of Chernobyl, a well developed westerly flow began to transport radioactive material across the USSR. The surface values of the activity of I-131 on April 29 are depicted in Fig.1b. It is important to note that the cyclonic circulation system related to the deep low centered in the region of Iceland began to move radioactive material from Scandinavia and the eastern part of the North Sea towards Greenland. The most important conclusion to be drawn from the analysis of the initial stage of the transport is that the two major directions of transport to the Western Hemisphere were established at the end of April, 1986 (Fig1b).

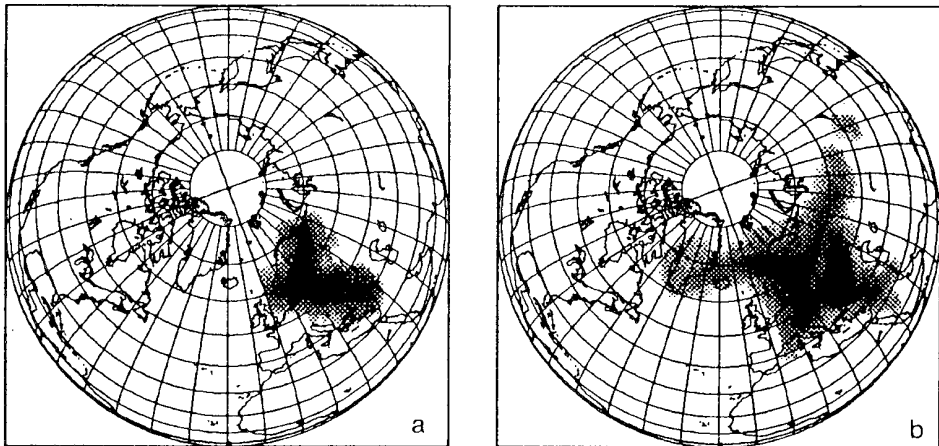


Fig.1 Activity fields [bq kg^{-1}] for I_{131} at $\sigma = 1$ (a) April 27 1986 and (b) April 29 1986

During the following days, the radioactive cloud was transported along these two major routes towards North America. On May 1, the radioactive cloud spread over Greenland and the region of small activities approached the northern part of Quebec (Fig.2a). The part of the cloud travelling along the westerlies was separated from the arctic part of the cloud by the high pressure system which had developed over the North Pole (fig.2b). It is important to note that at this time the amount of radioactive material transferred to Greenland was still quite large despite the fact that the Icelandic low so critical to the transfer of radioactivity across the Atlantic became weaker and moved north-eastward.

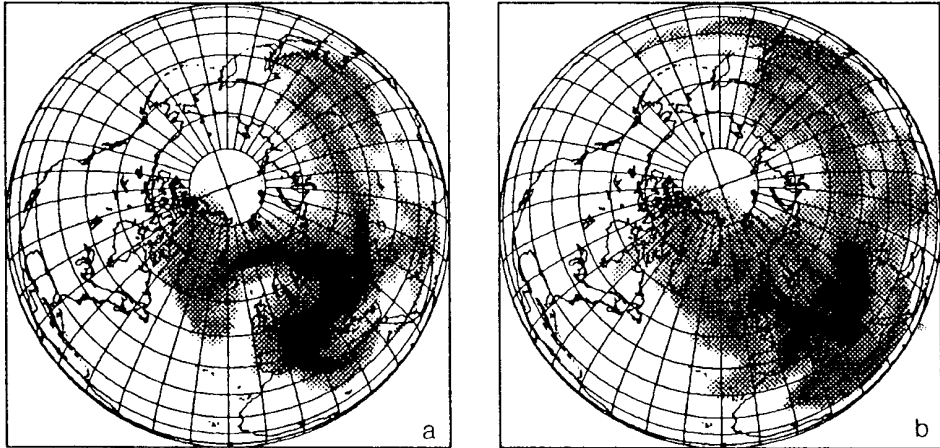


Fig.2 Activity fields [bq kg⁻¹] for I₁₃₁ at $\sigma = 1$ (a) May 1 1986 and (b) May 3 1986.

On May 5 the eastern part of the cloud at the anemometer level ($\sigma = 1$.) had spread across Asia and the Pacific Ocean (Fig.3a). Note the two "spots" separated from the main body of the cloud; these are related to the descending large scale motions in high pressure system located over the eastern part of the Pacific.

The situation depicted in Fig.3a is thus an example of an effect related to the 3-D character of the transport. The material travelling much faster at high levels was brought down by descending large scale motion and appeared at the surface in the region of southern California as early as May 5, 1986. In the region of the Canadian arctic, the flow associated with the low pressure system centered over northern Quebec and the high pressure system over the North Pole transported the radioactive material westward. This transport feature is an interesting example of easterly flow in the polar region.

On May 6, after the dissipation of the low over Northern Quebec, the radioactive material which had originally spread over the arctic region moved rapidly southeastwards passing through Ontario, Quebec and the Atlantic provinces of Canada (Fig.3b). The Atlantic part of Canada was thus affected initially by radioactive material injected from the arctic regions on May 6. The main part of the cloud to affect the Atlantic region arrived later, namely around May 8 (Fig. 3d). The descending motions on the western side of the radioactive cloud brought down a small amount of the material from the higher levels. The radioactive material appeared along the west coast from Vancouver to Alaska and over the southwestern states of the USA.

On May 8, the scale of the radioactive cloud became comparable to the scale of the Northern Hemisphere because eddy-like mixing by the synoptic scale low pressure systems superposed with the average zonal flow spread radioactive material towards equatorial regions (Fig.3d). The cloud viewed on the hemispheric scale shows essentially a pattern analogous to turbulent diffusion, with low pressure systems acting as mixing eddies. The transport over Asia and the Pacific was actually a superposition of the zonal flow and eddy mixing whereas transfer of the radioactive material across the Atlantic ocean had a purely eddy-like character.

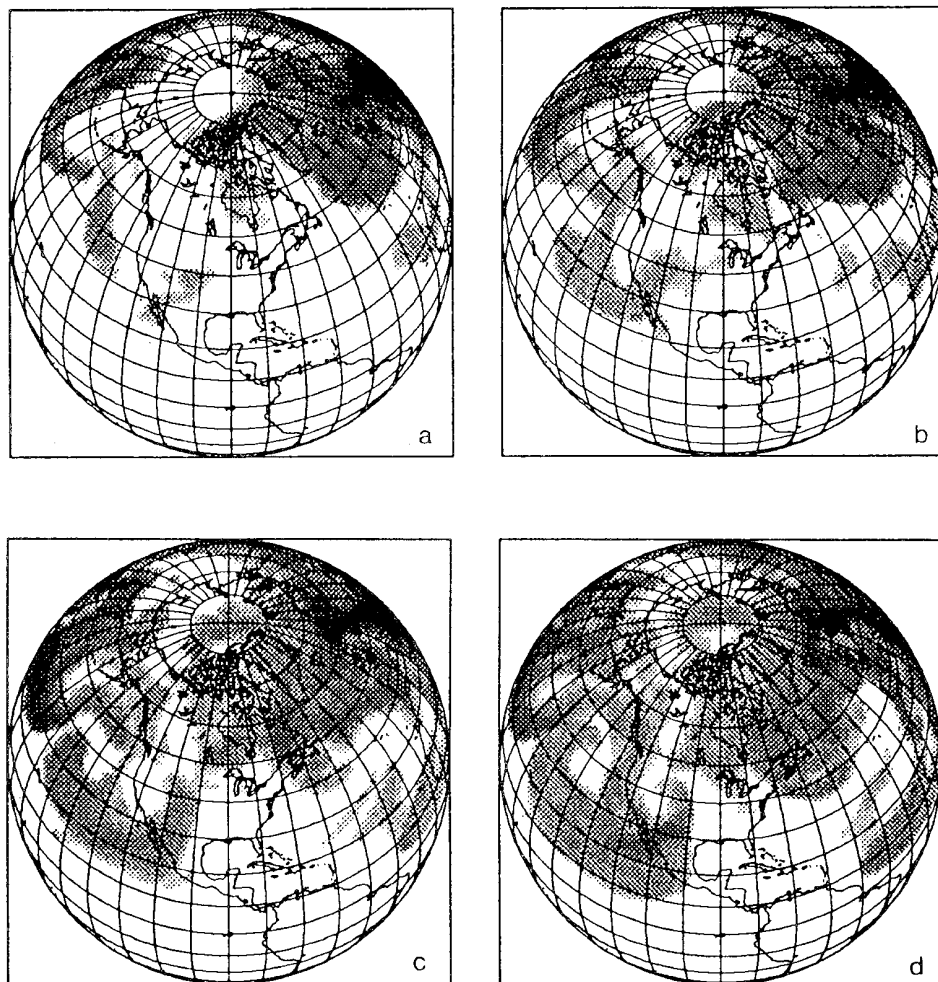


Fig.3 Activity fields [bq kg^{-1}] for I_{131} at $\sigma = 1$ (a) May 5 1986, (b) May 6 1986. (c) May 7 1986, (d) May 8 1986.

4. VERIFICATION OF THE MODEL.

Verification of the model results was performed in this study only for the surface activities of I-131. Data for the American receptors was derived from Larsen et al ⁶ whereas the Canadian measurements were provided by Tracy (private communication). The network considered in this verification study consisted of 17 stations. Experimental results to be discussed in this paper were selected to verify the most characteristic stages of the hemispheric scale transport of radionuclides from the Chernobyl nuclear accident.

Debris from Chernobyl was first detected in Finland and Sweden. The comparison of the activities of I-131 predicted by the model at the anemometer level ($\sigma=1$)⁷ to the values obtained from the measurements in Stockholm (Jensen and Lindhe⁷) is shown in Fig.4a.

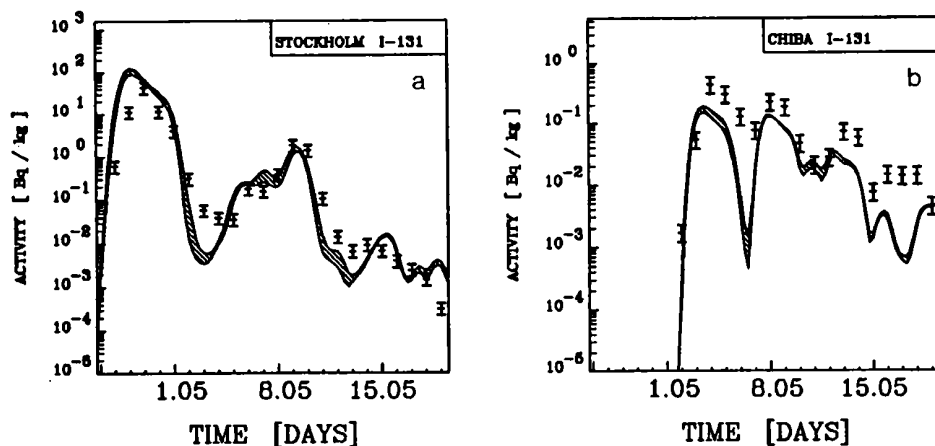


Fig. 4 Comparison of the observed and simulated time series of I-131 activity in: a) Stockholm, b) Chiba (Honshu Island-Japan). The measured values are represented by vertical bars, the model results correspond to the dashed area between the two lines, representing the uncertainty of the sampling process.

The measured values of the activity are represented by the vertical error bars. For the purpose of display, we assumed that the error is 30% , as was done in the paper describing the 2-D model results (Pudykiewicz²). The analysis of Fig.4a indicates a very good coherence between specific activities observed at the surface and simulated values at the anemometer level. The time variations of the specific activity are reproduced very well throughout the simulation. Analysis of the model results indicates that the radionuclides from the Chernobyl accident transported by a steady westerly flow reached Japan on May 3. This conclusion drawn from the numerical simulation corresponds very well to the abrupt increase of the radioactivity of the surface air at Honshu Island, as reported by Higuchi et al⁸. The quantitative model verification for Japan is depicted in Fig.4b where measurements at Chiba are compared with the model results. The correspondence between the simulated and the observed times of arrival of the radionuclides is quite good. The simulation of the general trend of radioactivity at Honshu Island is also correct.

The verification of the 3-D model for Canadian and American stations (Pudykiewicz³) clearly indicates the good accuracy of the numerical results. It is shown that the predicted times of arrival and the times of arrival of maximum activity agree quite well with the observed values. The ratio of the calculated and observed values varies between 0.21 and 2.80 with an average value of 1.05.

Statistical verification of the model is presented by the correlation coefficient in the table 1. The activities considered in the hemispheric scale

simulation are of the order of millions of Bequerell / kg close to the source and fractions of mBq/kg in the remote locations. Because of this extreme variability of activities the correlation coefficient was computed also for the logarithms of the activities. The correlation coefficient for the logarithmic case ρ_{\log} is displayed in Table 1. The fact that the ρ_{\log} is so large shows that the order of magnitude of the activity field predicted by the model agrees very well with observation. The agreement between the simulated and observed values is perhaps less evident, however in view of the parameters of Table 2 (Pudykiewicz³), we can conclude that the overall performance of the model is quite satisfactory.

Table 1 Correlation coefficient computed for logarithms of the activity versus linear correlation coefficient

STATION	ρ_{\log}	ρ
HELSINKI	0.73	0.70
STOCKHOLM	0.80	0.78
CHIBA	0.96	0.85
MOOSONEE	0.95	0.80
GREENWOOD	0.94	0.81
VANCOUVER	0.90	0.63
BARROW	0.84	0.38
WINDSOR	0.86	0.72
OTTAWA	0.88	0.77
CHESTER	0.95	0.94
CALGARY	0.89	0.80
REGINA	0.87	0.78

5. CONCLUSIONS.

The simulation described here is a good indication that with the computing power currently available and with high resolution numerical models, it is possible to treat advection dominated processes with good accuracy. We do not suggest that the model described here will perform under other circumstances as well as it has performed on the Chernobyl case. More research related to the parameterization of mesoscale processes is needed in order to further refine the technique. The good verification of the present tracer model should increase confidence in the possibility of accurately simulating atmospheric tracers.

6. ACKNOWLEDGEMENTS.

The author wish to express his gratitude to Dr P. Merilees for his continued interest shown in the problems related to the simulation of the Chernobyl accident over past two years. Thanks are also due to Mr. Bruce Brasnett of CMC who read a draft of this paper.

7. REFERENCES.

- 1 ApSimon H. and J.J. Wilson (1986): Tracking the Cloud from Chernobyl. *New Scientist* 17, 42-45.
- 2 Pudykiewicz J. (1988): Numerical Simulation of the transport of Radioactive Cloud from the Chernobyl Nuclear Accident, 40 B, 241-259.
- 3 Pudykiewicz J. (1989): Simulation of the Chernobyl dispersion with a 3 - D hemispheric tracer model. (to appear in *Tellus*).
- 4 Pudykiewicz J. and A. Staniforth (1984): Some properties and comparative performance of the semi-Lagrangian method of Robert in the solution of the Advection-Diffusion Equation. *Atmosphere-Ocean*, 22, 283 - 308.
- 5 Daley R., C.Girard, J.Henderson and I.Simmonds (1976): Short-Term Forecasting with a Multi-Level Spectral Primitive Equation model. *Atmosphere* 14, 98-134.
- 6 Larsen R., C.G.Sanderson, W.Riviera and M.Zamichielli (1986): The characterization of radionuclides in North American and Hawaiian surface air and deposition following the Chernobyl accident. Department of Energy Report EML-460, 331 pp.
- 7 Jensen M. and Lindhe J.C. (1986): Activities of the Swedish authorities following the fallout from the Soviet reactor accident. Report of the National Institute of Radiation Protection, Stockholm, Sweden.
- 8 Higuchi H., H.Fukatsu, T.Hashimoto, N.Nonaka, K.Yoshimizu, M.Omine, N.Takano and T.Abe (1988): Radioactivity in surface air and precipitation in Japan after the Chernobyl accident. *Journal of Environmental Radioactivity* 6, pp 131-144 .

DISCUSSION

QUESTION: Dickerson: What additional Chernobyl data would help in your model evaluation studies?

ANSWER: A more consistent and quality controlled data set where time of arrivals and concentrations can be better explained.

QUESTION: Ishikawa: How did you deduce the vertical distribution of the source?

ANSWER: The sub-grid-scale problem of estimating the vertical distribution of the release was solved with a nonhydrostatic model of the thermal convection on a very fine grid. Our estimates are very close to the values reported in the other studies related to the simulation of the Chernobyl accident.

QUESTION: Maryon: How do you account for material at 300 MB?

ANSWER: The vertical transport of the radioactive material was accomplished in the model by large scale vertical motion and eddy mixing.

QUESTION: Nordlund: You obtained many good results for I-131, do you have tested your calculation results on CS-137? CS-137 has generally appeared to be more difficult to calculate accurately than I-131.

ANSWER: The model verification was performed also for CS-137 and CS-134. Some results are reported in Davidson et al (Nature Vol. 237, 7 Aug. 1987)

QUESTION: Seibert: Did you make verifications with stations in the tropics?

ANSWER: Verification of the model results was performed only for the receptors located in Europe, Japan and North America.

III

LAGRANGIAN MODELS AND
TRAJECTORY ANALYSIS



COMPARISON OF TRAJECTORIES CALCULATED DURING AND AFTER
THE CHERNOBYL ACCIDENT

H. Kolb , P. Seibert

Institute of Meteorology and Geophysics, University of Vienna
A-1010 Vienna, Austria

V. Zwatz-Meise

Central Institute for Meteorology and Geodynamics
A-1190 Vienna, Austria

G. Mahringer

Federal Office of Civil Aviation
A-1040 Vienna, Austria

Summary: During the Chernobyl accident two trajectory models based on gridpoint values of the ECMWF model were used for forecasts by the Austrian weather service. A retrospective analysis proved the two dimensional model to be superior to the three dimensional one. Differences between trajectories calculated from forecasts and those calculated later from analysed fields were small.

Though satisfactory on the whole, neither the Austrian trajectories nor any other trajectories available at real time came within ten hours of the observed time of arrival of the radioactive cloud in Austria.

1. Introduction

Before and during the time of the Chernobyl accident, 48-hour backward trajectories were calculated routinely for the major Austrian cities. When the accident first became known in Vienna, early in the morning of April 28th, the trajectories already indicated the arrival of contaminated air masses in Austria within the next two days.

2. Trajectory models

At the time of the Chernobyl accident, two trajectory models were installed at the Central Institute for Meteorology and Geodynamics (Austrian weather service). Both models use grid point values supplied by ECMWF. One is a two-dimensional model with trajectories following isobaric surfaces (Huber-Pock et al., 1980), the other one is three-dimensional with isentropic trajectories (Mahringer, 1986).

2.1. 2-d model

The 2-d model makes use of the 6-hourly horizontal wind components supplied by the ECMWF model. A polynomial interpolation procedure based on 3x3x3 grid points for x, y and t is used, which does not change the values at the grid points.

The Petterssen (1956) procedure is used to calculate the trajectories. The iteration is terminated when the improvement by a new step is less than 10% of the grid distance (15 km).

2.2. 3-d model

The second model available uses geostrophic approximation to calculate trajectories from the geopotential values on the levels 1000 hPa, 850 hPa, 700 hPa and 500 hPa, supplied by the ECMWF model every 12 hours.

The initial fields are smoothed by a nine-point filter to enhance the convergence of the iterative process. Some details of the wind field are lost in this procedure. Interpolation of the geopotential to the starting point of the trajectory is linear in space and quasi-linear in time.

The horizontal displacement is evaluated in steps of three hours using geostrophic wind components calculated from 4 grid points and a 3-step iterative procedure similar to Petterssen's (1956), but assigning a stronger weight to the end point of the first approximation than to the starting point. The model thus reacts very fast to changes in wind direction.

After 12 hours of isobaric computation the vertical displacement is determined by the assumption of (dry) adiabatic motion, i.e. the end point is shifted vertically to the level with the potential temperature of the starting point. This displacement is neglected if the potential temperature change is less than 1 K / 12 h or if the difference of potential temperatures between two neighbouring pressure surfaces is less than 1.5 K. The vertical motion is limited to 80 hPa / 12 h.

This vertical displacement is divided into 3 equal parts, which are added to the horizontal displacement after 3, 6 and 9 hours. New calculations for the horizontal displacement are made from the third hour onward. There is no further iteration of this procedure.

This process is repeated for every 12 hours of calculation.

2.3. Validation of the models

The error in trajectory calculations (fig. 1) is a sum of the errors of

- original data (measurements, codes, transmission,..)

gl. November 11, 1999

Errors in trajectory calculations

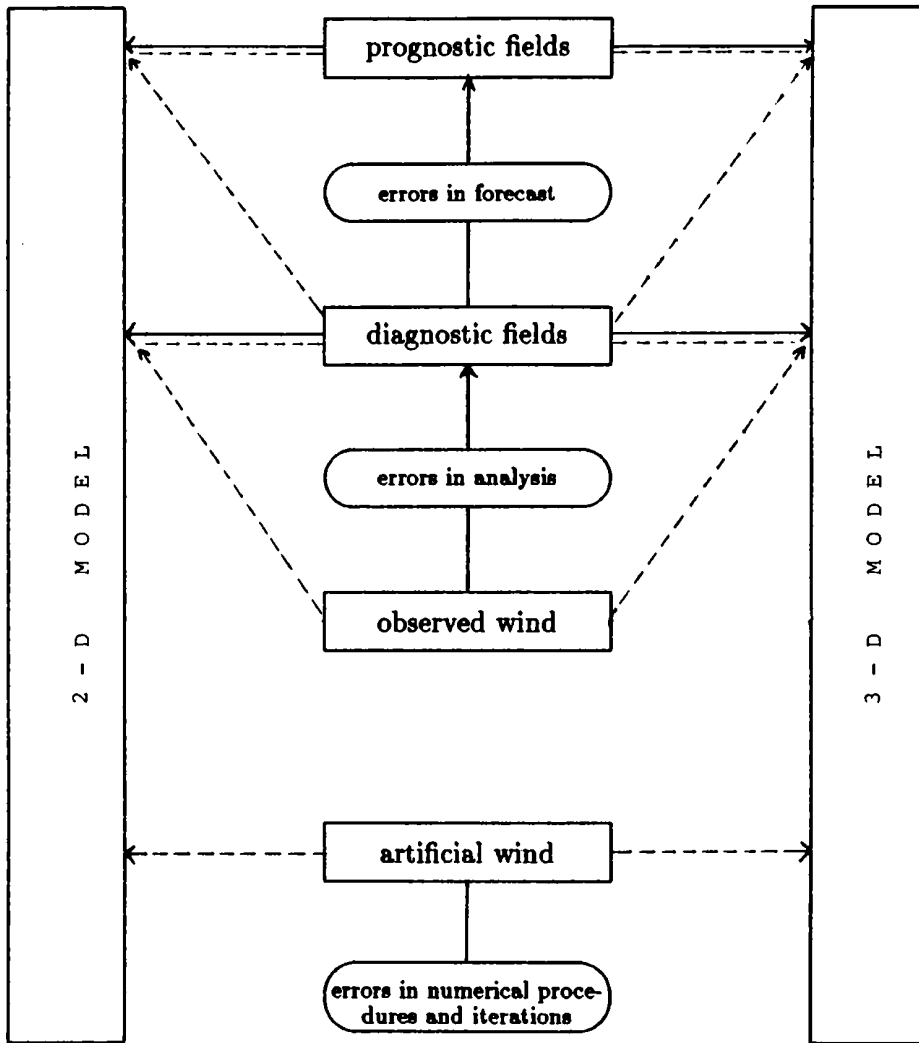


Fig. 1: Errors in trajectory calculations.

- ECMWF analysis procedure
- ECMWF prognostic fields
- temporal and spatial interpolation between grid points
- numerical procedures
- iteration procedures
- model assumptions (2-d, geostrophic approximation, stepwise vertical displacement,...).

The relative importance of the different errors can be checked by different validation methods (Mahringer, 1986).

The mere numerical process including iteration was tested in a circular wind field or geopotential field with constant velocities. Trajectories showed a small tendency to spiral, with a 2% displacement for the 2-d model, and 4% for the 3-d model.

For comparisons between original radiosonde wind data and analysed and forecasted ECMWF grid point values, 24-hour-trajectories starting at 12 GMT from 10 different locations in Europe at the 850 hPa level were calculated with each of the models for 205 days in 1985/86.

Comparisons of radiosonde wind speeds at the starting point show that, on the average, trajectories move about 10% slower than the wind indicates. The difference is smaller if the trajectories are compared with analysed wind fields instead of observed ones. The difference is larger for the 3-d model, probably due to the additional smoothing and due to the geostrophic approximation.

Trajectories tend to move to the right of the wind direction at the starting point (10° on the average). The smaller the speed of the wind, the larger is the deviation of direction. Much of this disappears if comparisons are made against the analysed wind field. Again, the differences are larger for the 3-d model.

Small scale effects and variances of wind speed and direction are lost in the trajectory calculations due to the smoothing of the ECMWF model analysis and - in the case of the 3-d model - the additional smoothing in the trajectory model.

Comparisons of analysed and forecasted grid point values of wind speed and direction show that there is a similar tendency of reduced speeds and an additional bias toward right-turning winds.

A comparison of the vertical displacement calculated by the 3-d model with the ECMWF vertical velocities yielded unsatisfactory results. It is, however, difficult to identify the source of the errors. In any case, neglecting vertical displacement becomes the more problematic the longer a trajectory is followed.

3. Application during the Chernobyl accident

For validation purposes, two aspects of the Chernobyl event were chosen: the first reported rise in radioactivity in Kajaani, Finland, in the evening of April 27th, 1986, and the first arrival of contaminated air in Austria in the morning of April 29th, 1988.

The trajectories to Finland are especially suitable for validation because there is good reason to believe that the air bringing the first increase in radioactivity left Chernobyl at the onset of the accident.

The time of emission of the contaminants which reached Austria is not known a priori, but, due to the very dense network of monitoring stations in Austria, the time of arrival is well known.

The two trajectory models were immediately applied during the event, based on the forecasted fields (Kolb et al., 1986). From the beginning, the 3-d model seemed to perform less well; so, all the forecasts were based on the 2-d model. After the event, comparisons of the performance of both models using forecasted and analysed fields have been made.

The 2-d trajectories were calculated for 850 hPa because this level best reproduced the observed transport during the first days. For 3-d trajectories a source height of about 600 m (950 hPa) was chosen, but due to vertical transport and mixing near the source, the main level of transport was between 800 hPa and 900 hPa for these as well.

The 2-d trajectories starting on the April 26th at 00 UT reach Kajaani 48 hours later (28th, 00 UT), a few hours after the rise was recorded there. There are some differences between the trajectories from forecasted and from analysed fields, but in the important region they are very small. The 3-d trajectory is much slower, and responds to the shift in wind direction over the Baltic Sea, which affects the 2-d trajectory only 12 hours later (fig. 2).

The same tendency holds true for the following trajectories (26th 12 UT, 27th 00 UT and 27th 12 UT): 3-d trajectories are slower and resemble 2-d trajectories started about 12 to 18 hours later.

The arrival of contaminated air in Austria is best reproduced by the trajectories leaving Chernobyl the 27th at 06 UT for the 2-d case and on the 26th at 12 UT or the 27th at 00 UT for the 3-d case. In the 3-d case, the trajectories pass some 500 km to the north of Austria. In the later trajectories, the shift in wind direction toward Austria is recognizable. Due to low wind speed over Poland, one of the trajectories (analysed field) does not reach Austria within 96 hours of its departure from Chernobyl.

The 2-d trajectories reach Austria at about 18 UT on the 29th (analysed field) or the morning of the 30th (forecasted field), and cross Austria during the next day or two (fig. 3). The first rise in radioactivity in Austria was recorded at two stations in the northeast of the country on the 29th at 07 UT; from there the cloud advanced slowly, reaching Vienna at about 12 UT. As can be shown, the first rise was a very local effect (P. Seibert et al., 1988) which cannot be expected to reproduced by the trajectories. Nevertheless, they were late by at least 6 hours.

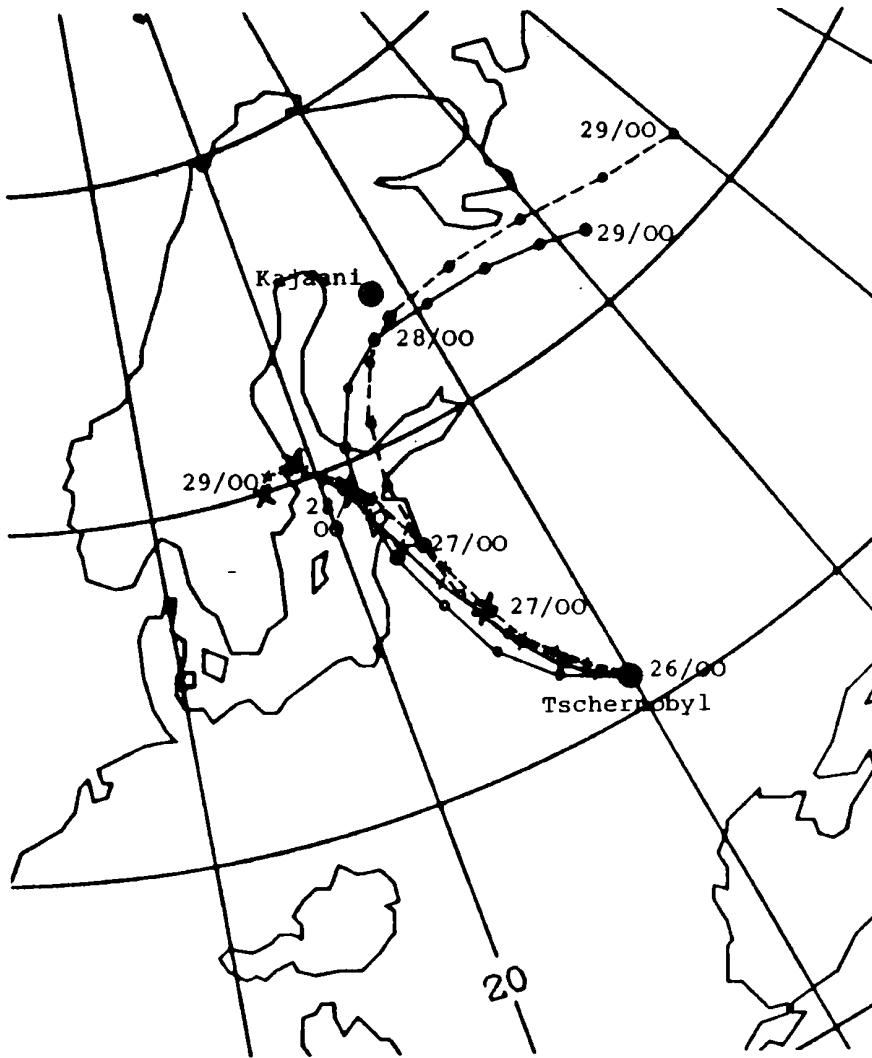


Fig. 2: Trajectories starting from Chernobyl on April 26th, 1986 at 00 UT.

- | | | | |
|---|-----------|-----|-------------------|
| o | 2-d model | --- | forecasted fields |
| x | 3-d model | — | analysed fields |

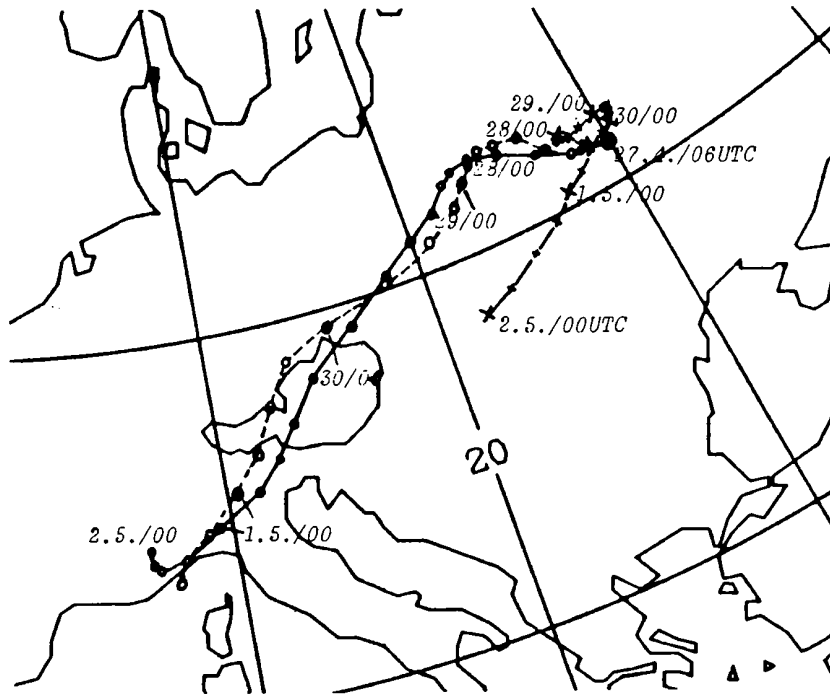


Fig. 3: Trajectories starting from Chernobyl on April 27th, 1986 at 06 UT.
Symbols as in figure 2.

4. Conclusion

Of the two trajectory models available at the Central Institute for Meteorology and Geodynamics in Vienna, the 2-dimensional isobaric model yields better results in spite of the simpler physics involved, compared to the 3-dimensional isentropic model. Modifications of smoothing, interpolation and iteration procedures could considerably improve this model. All trajectories have a tendency to move too slowly, partly due to the smoothing of the ECMWF fields. These conclusions, drawn from other methods of validation, are born out by the Chernobyl "experiment".

As a result of the experience gained by the Chernobyl event,

- the 2-d model is used as standard model at present;
- the 3-d model will be modified;
- the range of the trajectory calculations has been increased from two days to five days backward and forward;
- trajectory calculations are being made available to non-meteorologists involved in decision-making during nuclear accidents.

There are also plans to attach a simple diffusion-deposition model to the trajectory calculations.

5. References

- Huber-Pock, F., Ch. Kress, V. Zwatz-Meise (1980): A method for numerical computation of trajectories including approximated ageostrophic wind components. Arch. Met. Geoph. Biokl., Ser. A., 29, 205-217.
- Kolb, H., G. Mahringer, P. Seibert, W. Sobitschka, P. Steinhauser, V. Zwatz-Meise (1986): Diskussion meteorologischer Aspekte der radioaktiven Belastung in Österreich durch den Reaktorunfall in Tschernobyl. Arbeiten aus der Zentralanstalt für Meteorologie und Geodynamik, Heft 69, Wien.
- Mahringer, G. (1986): Trajektorien und ihre Anwendung in der Umweltmeteorologie. Diplomarbeit, Universität Wien.
- Petterssen, S. (1956): Weather Analysis and Forecasting, Vol. 1, 2. Ed., McGraw-Hill, New York.
- Seibert, P. et al. (1988): Dose rate patterns in Austria after the Chernobyl accident and their relation to precipitation. (In this volume.)

DISCUSSION

QUESTION: ApSimon: Have you considered using the movement of some types of cloud to validate trajectories? For example a ring of cloud at a higher altitude moved across Chernobyl close to the time of the accident and could be tracked.

ANSWER: The 2-d model was originally developed to forecast cloud movement for synoptic forecasts - but no quantitative validation has been done. Experience shows that you have to be very careful in the choice of clouds, especially when approaching the Alps.

QUESTION: Ishikawa: Does your trajectory come back to Chernobyl if you compute it reversary?

ANSWER: We have not checked that yet.

COMMENT: Vergeiner: This comment, of course, applies to the other contributions as well. We should insist on calling Chernobyl a "CATASTROPHY", since a single reactor managed to contaminate the whole of Europe seriously with radioactive poisons. This is an unbelievable action and MUST NOT BE REPEATED. P.S. As people and, therefore, technical facilities are not perfect, this means that all nuclear installations must be shut down.

The ZAMG/BKA - Trajectory Project

Helga Kolb and Werner Steinmann
Institute for Meteorology and Geophysics, University of Vienna
A-1190 Vienna, Austria

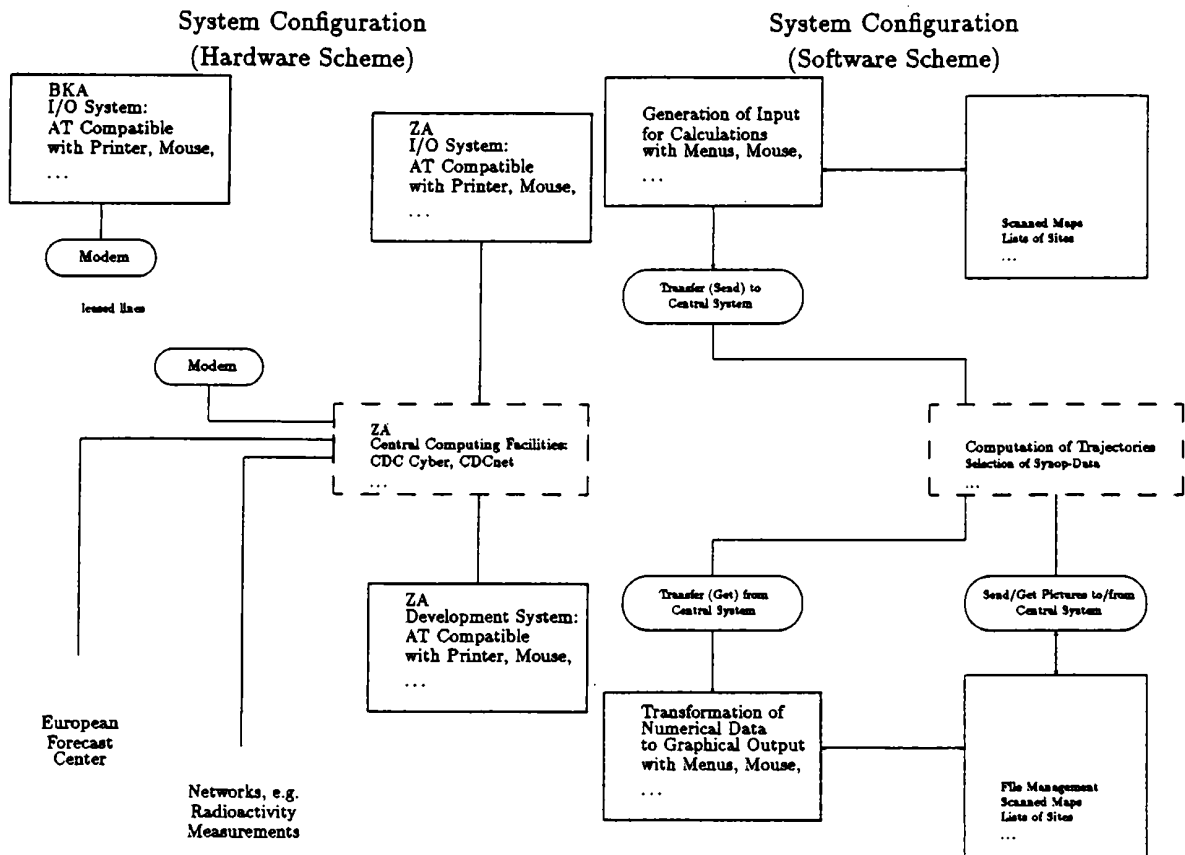
Summary: In consequence of the Chernobyl accident a system has been devised to make trajectories based on the ECMWF-gridpoint values available to decision makers on a real time basis.

Introduction

The goal of the trajectory project was to make real time trajectories available at the emergency center of the Chancellery (Bundeskanzleramt) through a user-friendly environment and easily readable graphical display. For additional information synoptic data were to be available as overlay.

System Configuration

Three I/O-devices (IBM-AT-Compatibles) are connected to the central computing facilities at the Central Institute for Meteorology and Geodynamics (ZAMG), Vienna, where the up-to-date data bases for ECMWF gridpoint values and synoptic data are available, and where trajectory calculations are made (fig. 1).

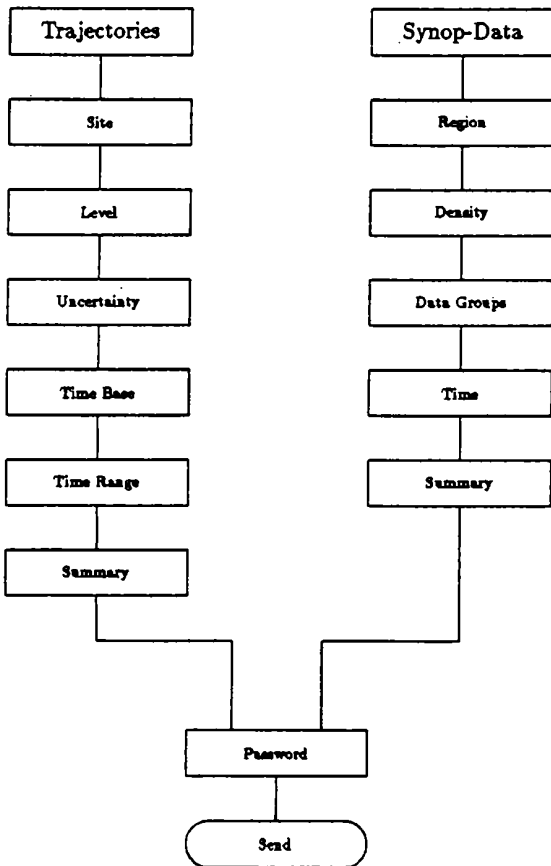


Features

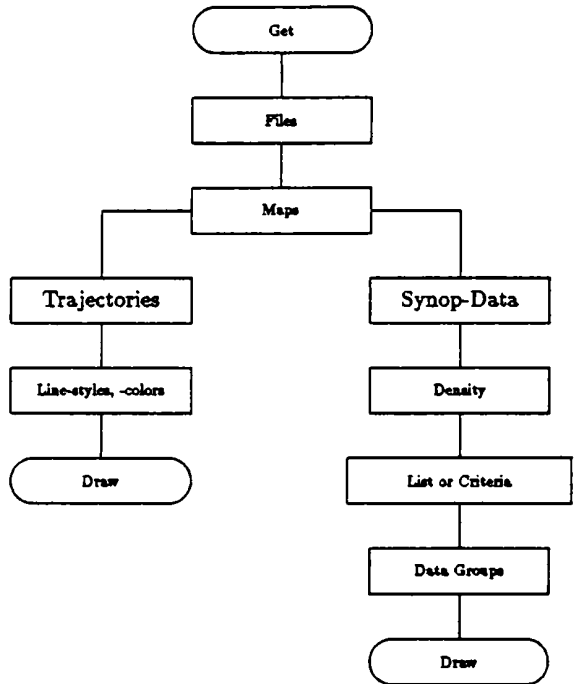
Menus to create input and output attempt a combination of high flexibility and easy handling. Backward and forward trajectories can be calculated for freely chosen sites, levels and time ranges within the availability of ECMWF gridpoint data, i.e. 5 days back and 5 days ahead for an area from about 20° W to 40° E and from 70° N to 20° S (fig. 2). To indicate reliability of trajectories, neighboring trajectories can be automatically calculated ("uncertainty").

Whereas calculation and transfer time for trajectories is negligible, transferring large amounts of synoptic data can be time consuming. The input menu therefore offers efficient methods of choosing only relevant data for transfer.

Input



Output Selections



Default values permit a rapid view of results in graphical form, but menus are available to improve readability and interpretation by appropriate choice of background maps, synoptic data, colors and line-styles of trajectories etc. (fig. 3). Additional features like zooming, splitting the picture, storing or replaying the session, editing the picture, identifying stations, transferring a picture from one I/O-device to another, etc. facilitate work with the system and communication between users.

Figure 4 offers an example of graphical output.

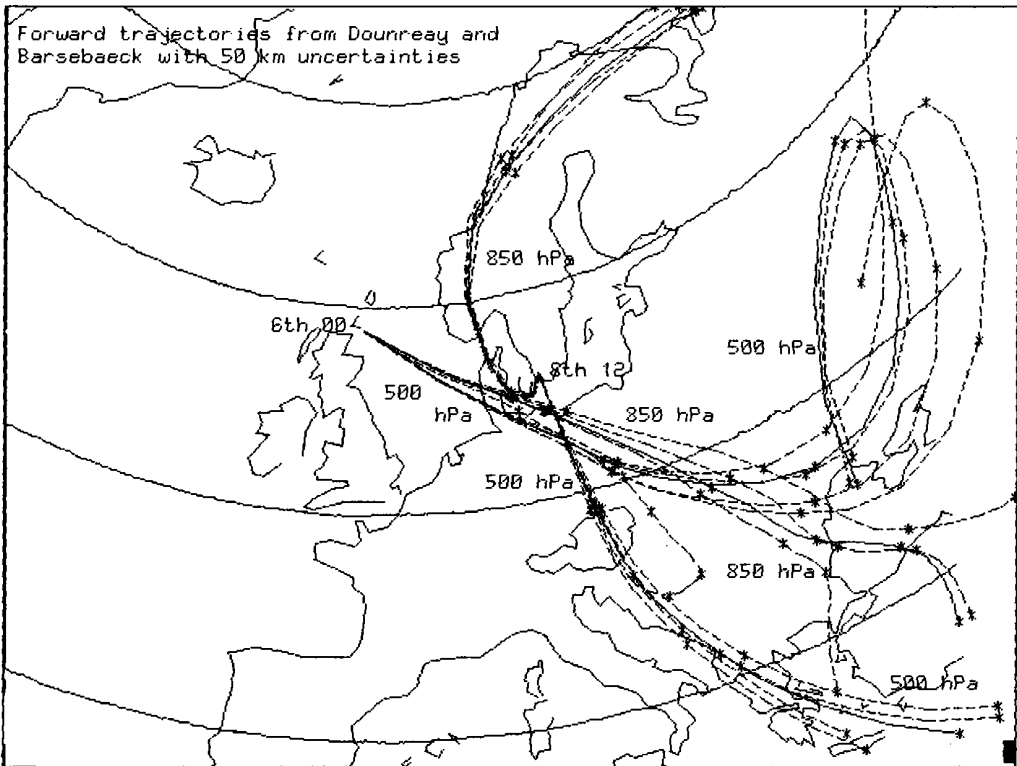


Fig. 4: Forward trajectories from Dounreay and Barsebaeck with 50 km uncertainties

THE FINNISH TRADOS MODEL AS APPLIED TO THE CHERNOBYL RELEASE

Göran Nordlund
Finnish Meteorological Institute
Sahaajankatu 22 E
SF-00810 Helsinki, Finland

Summary: The TRADOS trajectory-dose calculation system had already been developed some years before the Chernobyl accident. In applying the system to the Chernobyl case, the calculation routines required no major changes. Some calculation procedures are, however, very crude, especially those describing the diffusion on the basis of synoptic scale data. It was therefore somewhat surprising that the calculated data and observed fall-out values in Finland agreed fairly well. The reason for this is linked to the fact that the two most important parameters, i.e. the trajectory paths and deposition by scavenging, were comparatively easy to estimate for the first phase of the Chernobyl accident.

1. INTRODUCTION

The Finnish TRADOS trajectory-dose calculation system was developed in the early 1980s. In contrast to most other systems, it uses non-gaussian approaches in estimating diffusion (Nordlund et al. 1979; OECD/NEA, 1984).

The main application of the TRADOS system has been risk-assessment studies on remote NPPs (Nordlund et al., 1985). In the first phase following the Chernobyl accident, the TRADOS system was applied to estimate the source term. After this, TRADOS was used to estimate long-term doses to be expected in Finland. In both applications TRADOS was used in its basic form, i.e. without modifications specifically for the Chernobyl event.

2. THE TRADOS CALCULATION SYSTEM

2.1. Mathematical formalism

By defining an undepletion factor f_{ri} for the mass standing in the plume, and a relative normalized concentration C_{zi} in a vertical direction, we can construct the following equation,

$$\frac{df_{ri}}{dt} = -\lambda_i - v_d C_{zi}(1m) - k,$$

where v_d is the dry deposition velocity, λ_i the precipitation scavenging coefficient, k the radioactive decay factor, and i refers to the time step. For C_{zi} the following equation is valid:

$$\int_0^{\infty} C_{zi}(z) dz \equiv 1.$$

Relative concentration, deposition and cloudshine dose values may now be expressed as:

relative concentration

$$\chi_i = 1/u_i \cdot C_{yi} \cdot C_{zi} \cdot f_{ri}$$

where u_i is the wind velocity and C_{yi} the relative crosswind concentration;

relative deposition

$$\omega_i = 1/u_i \cdot C_{yi} \cdot f_{ri}(C_{zi}(1m)v_d + \lambda_i)$$

relative cloudshine dose

$$\Gamma_i = 1/u_i \cdot C_{yi} \cdot f_{ri} \cdot f_r$$

where f_r is calculated using a separate code applying steady state profiles and gaussian distribution in the horizontal direction (Vuori, 1978).

Finally, the doses are calculated by:

Cloudshine dose

$$D_{i,j} = \sum Q_{k,i} \cdot DC_{k,j} \cdot \Gamma_j$$

where Q is the release of activity and DC the dose factor; k refers to nuclide, i to time step number and j to exposure pathway.

Inhalation dose

$$E_{i,j} = \sum Q_{k,i} \cdot DC_{k,j} \cdot \chi_i(1m)$$

and, further, the

Groundshine and ingestion dose

$$F_{i,j} = \sum Q_{k,i} \cdot DC_{k,j} \cdot \omega_i$$

In the following we describe in more detail the calculation of dispersion and fallout. Concerning the calculation of dose values, see Vuori (1978) and Korhonen et al. (1987).

2.2 Parameter values

For dry deposition v_d and precipitation scavenging the following values have been used:

- v_d 0.01 m/s, except for noble gases
and organic iodine 0.0
- λ 0.0 in dry weather and for noble gases
 $10^{-4} s^{-1}$ by rain
 $5 \cdot 10^{-5} s^{-1}$ by snow

These above values are not necessarily the best ones. v_d should at least be a function of atmospheric stability and λ of precipitation intensity. However, in applying TRADOS to the Chernobyl event, the above values were employed.

The vertical distribution of dispersing material is calculated in TRADOS by using a gradient transfer approach, i.e. by solving numerically the diffusion equation:

$$u(z) \frac{\partial C(x,z)}{\partial x} = \frac{\partial}{\partial z} [K_z(z) \frac{\partial C(x,z)}{\partial z}],$$

with the following boundary conditions:

at $z = z_i$ $K_z(z) \equiv 0$ z_i = height of the boundary layer

at $z = 1m$ $[K_z(z) \frac{\partial C(x,z)}{\partial z}] = -v_d C(x,1m)$.

For the vertical diffusion coefficient K_z , the stability dependent profiles shown in Figure 1 were applied. These profiles are adapted from Pasquill (1974), except for $z \leq 10$ m, where K_z is set equal to K_z at 10 m.

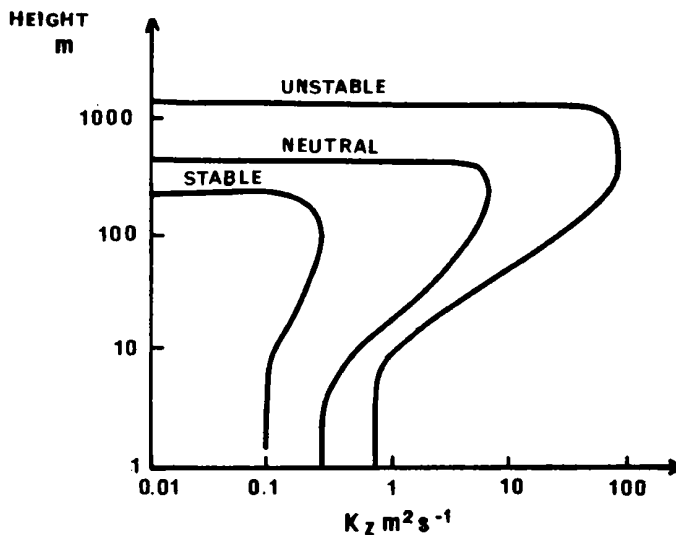


Figure 1. Profiles of the eddy diffusion coefficient K_z for different atmospheric stability types, applied in the TRADOS-system.

Horizontal diffusion is simulated in TRADOS in the following way: A basic turbulent scale diffusion is estimated using a horizontal spread corresponding to specific standard deviations in the different stability classes

$$\delta_y(x) = a \cdot x^b .$$

where a and b are determined as follows:

stability type	a	b
stable	0.0653	0.9023
neutral	0.1277	0.9050
unstable	0.3710	0.8664

behind transport distances of 100 km

$$\delta_y(x) = \delta_y(100\text{km}) \sqrt{\frac{x(\text{km})}{100}} .$$

For horizontal diffusion due to plume meandering and wind veering, the following approach is used: The area covered by the plume is assumed to correspond to the area between preceding and subsequent trajectory, as shown in Figure 2.

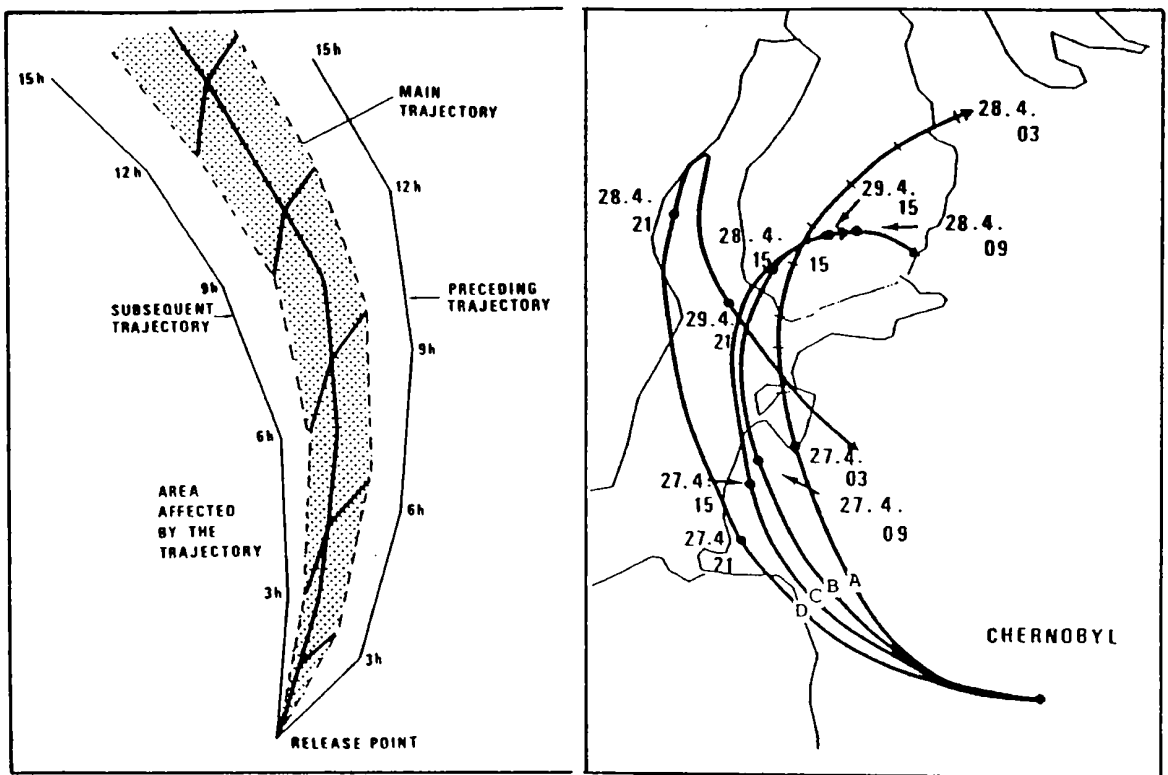


Figure 2. The approach used in TRADOS for determining the area affected by the radioactive cloud. A minimum horizontal width is applied to correspond to the estimated effect of small-scale turbulent diffusion.

Figure 3. Trajectories from Chernobyl 26.4.1986, 18 UTC (A), and 27.4.1986, 00 UTC (B), 06 UTC (C) and 12 UTC (D).

2.3. Stability and precipitation classification

In TRADOS stability and precipitation are determined from information given in numerical weather forecasts, according to the following schemes (Tables 1 and 2).

These very simple schemes are acceptable for statistical risk-assessment studies, but are definitely not sufficiently reliable for episode-studies. Therefore, in using TRADOS for the Chernobyl event, stability and precipitation were determined from the actual weather maps.

Table 1. Scheme for determining turbulence types(stability).

Velocity of surface wind (m / s)	NET RADIATION CLASS					
	N1	N2	N3	N4	N5	N6
$0 \leq v < 2$	UNSTABLE		NEUTRAL		STABLE	
$2 \leq v < 4$	UNSTABLE		NEUTRAL		STABLE	
$4 \leq v < 5$	UNSTABLE		NEUTRAL		STABLE	
$5 \leq v < 7$	UNSTABLE		NEUTRAL		STABLE	
$7 \leq v$	UNSTABLE		NEUTRAL		STABLE	

Table 2. Scheme for determining net-radiation class (N1-N6), cloud cover and precipitation in northern Europe (north of 55°N), according to the mean vertical wind (W) in the layer 1000 - 500 mb.

SEASON	WINTER		SPRING		SUMMER		AUTUMN	
	day	night	day	night	day	night	day	night
clear $W \leq 0$ cm/s	N4	N6	N4	N5	N1	N6	N1	N6
cloud cover $0 < W \leq 1$ cm/s	N4	N5	N3	N5	N2	N5	N2	N5
precipitation $W > 1$ cm/s	N4	N4	N4	N4	N4	N4	N4	N4

2.4. Calculation of trajectories

In TRADOS, the trajectories are calculated on a two-dimensional grid, with 150 x 150 km grid size, according to numerically analyzed winds at 850 mb or some other constant pressure level. The wind values for points within a grid square are computed by means of linear interpolation. Wind field analyses are made every 6th hour. Each analysis is assumed to be valid + 3 hours. The trajectories are then calculated in 1 hour time increments with two 0.5 hour iteration periods. Trajectories are started at 3 hour intervals. Each trajectory is followed for six days, if it is not abandoned earlier, because it leaves the calculation area. Along the trajectories, stability and type of precipitation are determined according to the schemes in Tables 1 and 2. Further, topography, sea-land distribution and mountains are taken into

account in determining the stability. The calculation techniques used in allowing for changes in dispersion conditions, during transport, e.g. stability, are described in Nordlund et al. (1985).

3. APPLICATION OF TRADOS TO THE CHERNOBYL ACCIDENT

In the first phase after Chernobyl, TRADOS was used to estimate the source term, by calculating backwards from fallout data. The source term calculation gave release values which agree fairly well with information obtained later. This calculation is described briefly in Korhonen et al. (1978).

After receiving reliable information on the source term, TRADOS was applied to estimate radiation doses to be expected in Finland. In these estimations the following release values were used (Table 3).

Nuclide	Activity of discharge, PBq 26.04.1986
Xe-133	180
Kr-85m	5.6
Kr-85	-
I-131	170
Te-132	150
Cs-134	5.6
Cs-137	11
Mo-99	17
Zr-95	17
Ru-103	22
Ru-106	7.4
Ba-140	18
Ce-141	15
Ce-144	17
Sr-89	9.2
Sr-90	0.56
Np-239	100
Pu-238	3.7E-3
Pu-239	3.7E-3
Pu-240	7.4E-3
Pu-241	0.74
Pu-242	1.1E-5
Cm-242	0.11

Table 3.
Activity of Chernobyl discharge at first day after accident

The release values in Table 3 correspond to the following release fractions:

Table 4. Release fractions of the isotopes in the Chernobyl accident leakage of first 24 hours.

ISOTOPE						
Xe-Kr	Cs-Rb	I	Te-Sb	Ba-Sr	Ru #a	La #b
0.03	0.04	0.06	0.04	0.003	0.006	0.003

#a) includes Ru,Rh,Co,Mo,Tc #b) includes Y,La,Zn,Nb,Ce,Pr,Nd,Np,Pu,Am,Cm

Tables 3 and 4 give the release values for the first day only, this is because direct transport to Finland occurred only during the first 24 hours of the accident. The calculated air trajectories for these first 18 hours are shown in Figure 3. In the figure trajectories have been drawn every 6 hours; the trajectories starting \pm 3 hours lie approximately between these 6-hour trajectories.

Table 5 shows the main result, i.e. the estimated external gamma dose over a period of 30 years from fall-out. The dose values are given for each trajectory separately. The total dose of 5500 manSv agrees relatively well with the corresponding dose of 3200 manSv estimated later on the basis of observed fall-out data.

Table 5. External gamma-dose from fallout in Finland during 30 years. (shielding factor 0.25)

Trajectory #	Gamma-dose (weighted by population distribution)
1	2140 manSv
2	160 manSv
3	135 manSv
4	1170 manSv
5	1740 manSv
6	160 manSv
7	0 manSv

total dose in Finland 5500 manSv

#)trajectories have been started at 3 hour intervals;
first trajectory starts on 25 April 1986, 21:00 hours UTC.

4. DISCUSSION

In its present form the TRADOS system is a fast and easy way of evaluating radioactive doses caused by remote radioactive releases. However, the system includes some very rough assumptions concerning the connection between diffusion and meteorological parameters. Also the treatment of dry and wet deposition must be regarded as fairly simple. Taking these weaknesses into account, the agreement between observed fall-out values and model calculation was surprisingly good in the Chernobyl applications. This is obviously due to the fact that the most important factors, the paths of the trajectories and precipitation scavenging were accurately simulated. The precipitation distribution could be observed from weather maps, and the calculation of dispersion trajectories for the first day of the Chernobyl release was relatively easy.

REFERENCES

1. KORHONEN, R., ROSSI, J. AND VUORI, S., 1987. Evaluation of long-range transport of radioactive releases from the Chernobyl accident and radiological consequences in Finland. Technical Research Centre of Finland, Technical report, ROSA-2/87, 29 p.
2. NORDLUND, G., SAVOLAINEN, I. AND VUORI, S., 1979. Effect of application of surface depletion model on estimated reactor accident consequences, Health Phys. 37, 337 - 345.
3. NORDLUND, G., PARTANEN, J. P., ROSSI, J., SAVOLAINEN, I. AND VALKAMA, I., 1985. Radiation doses due to long range transport of airborne radionuclides released by a reactor accident; effects of changing dispersion conditions during transport. Health Phys. 49, p. 1239 - 1249.
4. OECD/NEA, 1984. International comparison study on factor accident consequence modeling OECD, 2 rue André-Pascal, 75775 Paris Cedex 16, France.
5. PASQUILL, F., 1974. Atmospheric Diffusion. New York:Wiley.
6. VUORI, S., 1978. Fast correction of cloud dose data files due to changes in dispersion parameters. Health Phys. 34, 727 - 728.

DISCUSSION

QUESTION: Serrano: What is the way for the calculations of U_w ? Do you take into account the decoupling of the wind field during night time?

ANSWER: In the present version of the TRADOS-model we don't apply friction velocity (U_w) values at all. We have constant eddy diffusion coefficient profiles for different stability classes and fixed v_d , i.e. dry deposition values. We don't take vertical wind shear into account.

QUESTION: Vergeiner: What was the actual Chernobyl-caused deposition (say Cs^{137}) across Finland in kBq/m^2 , and what variance? Is it true, that the people up north ("Samen") had to (partly) leave because of high contamination? A chart of kBq/m^2 is shown and interpreted. Little contamination in the north of Finland problems high background due to previous nuclear tests.

THE DEVELOPMENT OF AN OPERATIONAL PUFF DISPERSION MODEL

G.H.L. Verver,
Royal Netherlands Meteorological Institute (KNMI)
De Bilt, The Netherlands

and H.J. Van Rheineck Leyssius
National Institute of Public Health and
Environmental Protection (RIVM)
Bilthoven, The Netherlands

Summary: In the Netherlands, a puff dispersion model for operational use is being developed, for the simulation of dispersion over Europe. The model is linked closely to a meteorological model, the KNMI Fine Mesh-LAM or the ECMWF-GCM. A brief outline of this system is given. As a test, the Chernobyl episode is simulated and the results are compared with previous model runs, as well as with measurements. It is shown that arrival times are simulated well, and that the model skill has improved slightly after the introduction of detailed mixing height fields.

1. INTRODUCTION

In the Netherlands, after the Chernobyl accident, activities have been initiated to improve the availability of dispersion models during a similar emergency situation. In order to react accurately, dispersion models are used as tools to estimate the situation as it is, and to predict the situations hours or days ahead.

KNMI and RIVM work together to develop an operational model that describes transport of accidentally released material. Also a framework is designed to make all the necessary meteorological data available.

Requirements for the system were: -1- a suitable dispersion model for dispersion over Europe, and -2- input data for the model must be operationally available, and -3-, computer time needed for the calculations must be less than the reaction time allowed to the proper authorities to take precautionary measures.

In the first part of this paper a very brief description of the system and its elements is given. In the second part results are shown of some experiments with the puff dispersion model applied to the Chernobyl accident.

2. SYSTEM ARCHITECTURE

In figure 1 the sources and flow of meteorological information in connection with the dispersion models are drawn.

Weather observations are the starting point of the avalanche of meteorological information. Numerical models, like the ECMWF-GCM and the KNMI FM-LAM process these data, and generate prognostic fields hours or days ahead. Therefore these data (like wind and rain data) are well suited for use in operational dispersion models that have the same dimensions.

In the next sections, the function of each part of the system is explained.

2.1 THE ECMWF GLOBAL CIRCULATION MODEL

The European Centre for Medium Range Weather Forecasts runs a global circulation model (GCM) and sends daily meteorological data to the member states. From this coarse mesh model analysed and prognostic windfields are obtained at two heights ($z \approx 200\text{m}$ and $z \approx 1500\text{m}$). The analysed data, when they become available to KNMI and RIVM, are 36 hours back in time at most.

The ECMWF generates meteorological data that is used by the puff dispersion model to calculate concentrations and depositions up to at least 3 days ahead.

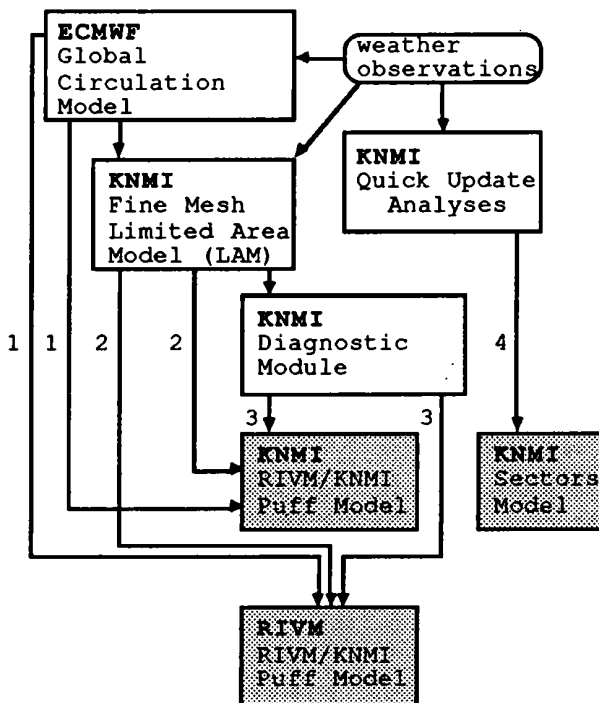


Figure 1. Flow scheme of meteorological data for operational dispersion models (numbers 1 to 4 refer to table 1).

To calculate the situation as it was in the past, up to only one day ahead, extensive use will be made of the KNMI FM-LAM.

2.2 THE KNMI FINE MESH LIMITED AREA MODEL (FM-LAM)

At KNMI a fine mesh version of the ECMWF global model is implemented. This model generates analyses and predictions effectively 24 hours ahead. The vertical resolution is lower than the ECMWF model.

The FM-LAM serves directly as a fast source of detailed wind- and rainfields for the puff-dispersion model. Every 3 hours prognoses are updated and an analyses of the meteorological situation is added to the meteorological database. The Diagnostic Module (next section) uses a large amount of data from the FM-LAM.

2.3 THE DIAGNOSTIC MODULE

The KNMI FM-LAM has a rather coarse vertical resolution. The diagnostic module is designed to analyse meteorological fields of the lower part of the atmosphere, generated by the FM-LAM, to get boundary layer parameters like u^* , mixing height and Obukhov length. These boundary layer parameters are used by the puff dispersion model to calculate deposition velocities, windshear, vertical and horizontal turbulent diffusion.

The module runs whenever a new series of data is produced by the FM-LAM (every 3 hours).

2.5 THE QUICK UPDATE ANALYSES

This module analyses hourly observations of wind and pressure, and generates a grid of horizontal windvectors at $z=10m$ for the Netherlands and direct surroundings. The most recent data that become available this way are 90 minutes delayed at most.

2.6 THE SECTORS MODEL

This model calculates the sector outside of which no contamination occurs (with an 80% confidence level) (Lablans,1974).

Table 1. Description of the sources of meteorological information.

<u>SOURCES</u>				
	<i>ECMWF-GCM</i>	<i>FM-LAM</i>	<i>DIAGNOSTIC MODULE</i>	<i>QUICK UPDATE ANALYSES</i>
<i>Meteorological Information</i>	wind ($z=200m$, $z=1500m$)	rain wind ($z=65m$, $z=500m$, $z=1500m$)	1/L u^* z_i	wind ($z=10m$)
<i>Area</i>	Europe	Europe	Europe	The Netherlands
<i>Spatial Resolution</i>	135*170Km	60*60Km	60*60Km	20*20Km
<i>Time Resolution</i>	6 Hours	3 Hours	3 Hours	1 Hour
<i>Data Update Time</i>	24 Hours	3 Hours	3 Hours	1 Hour
<i>Minimum Effective Prediction Period</i>	72 Hours	24 Hours	24 Hours	-
<i>Input for:</i>	puff model	puff model	puff model	sectors model
<i>References (Fig. 1)</i>	1	2	3	4

The sector is a function of the 10m windvector, and a distinction is made between a daytime and a nighttime situation.

This simple model is based on the statistics of the persistence of the wind in the Netherlands. The module generates the endangered sector in a number of points (imaginary sites of accidental releases) in the Netherlands beforehand, and uses the results from the Quick Update Analyses.

2.7 THE PUFF DISPERSION MODEL

This section only gives a brief outline of the model. We refer to De Leeuw et al. (1985) and Van Egmond et al. (1983) for a full description.

In the puff model, a continuous or instantaneous emission is divided into a number of gaussian shaped puffs. The mass of a puff is distributed over two layers, the mixing layer and the reservoir layer (fig.2).

- definition of layers-

The mixing height shows a diurnal cycle caused by insolation. Local differences in surface characteristics and differences in insolation caused by cloud cover, make the mixing height also a function of position. These differences will be most apparent near a land/sea transition.

There is no rigid upper limit to the height of the reservoir layer. It is determined by the maximum height to which material of a single puff is dispersed. Therefore, the upper boundary of the reservoir layer depends on the vertical diffusion coefficient for material in the reservoir layer, the maximum height of the mixing layer the previous day and, when the emission takes place above the mixing layer, the effective emission height.

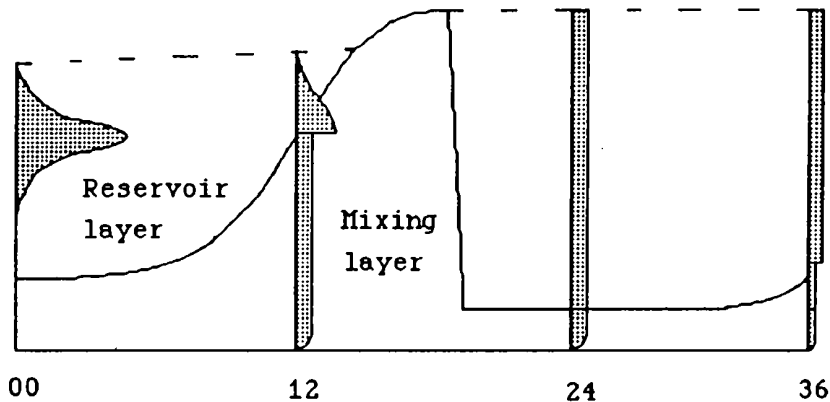


Figure 2 An example of layers and concentration profiles as a function of time of the puff dispersion model

-Horizontal diffusion of gaussian puffs-

The horizontal dispersion is assumed to be a linear superposition of contributions of the horizontal turbulence and vertical shear, according to:

$$\frac{d(\frac{1}{2}\sigma_{x,y}^2)}{dt} = K_T + K_S, \text{ where } K_S \text{ is given by } S^2 \bar{u} \frac{\sigma^2}{2} t \text{ (v. Egmond et al, 1982)}$$

$$\text{and } K_T \text{ by } \bar{u}_p^2 \int_0^t R_L(\tau) d\tau \text{ (eg. Csanada, 1973)}$$

S is the shear in radians/m, which is a function of stability, \bar{u} is the mean windspeed at the mass centre of the puff, t is time, R_L is the autocorrelation function, for which we used $\exp(-\tau/T_L)$, where T_L is the Lagrangian timescale. The variance of the relative windspeed u_p is obtained by: $\overline{u_p^2} = c \cdot \bar{u}^2$. For the constant c we used .09 in the reservoir layer, and .17 in the mixing layer (De Leeuw et al., 1985).

-Vertical dispersion of gaussian puffs

The vertical growth is estimated by the empirical formula $\sigma_z = ax^b$, where a and b are stability dependent quantities. However, when $\sigma_z \gg h$ (h=mixing height), we assume uniform mixing in the mixing layer.

In the reservoir layer, turbulence will be near to zero. The vertical puff growth is set to: $\sigma_z^2 = 2K_z t$ with $K_z = .5 \text{ m/s}$.

-Vertical fluxes between both layers-

The presence of two layers in this model allows a description of the process of fumigation and the transport of pollutants at higher altitudes, decoupled from the surface. The material flux between the mixing layer and the reservoir layer can be written as:

$$\text{Mass Flux} = w_e \cdot c(h) \quad (\text{kgs}^{-1}\text{m}^{-2}),$$

where the entrainment velocity w_e is defined as:

$$w_e \equiv \frac{dh}{dt} - \bar{w}_h = \frac{\partial h}{\partial t} + u \frac{\partial h}{\partial x} + v \frac{\partial h}{\partial y} - \bar{w}_h$$

In the model, the mean vertical velocity \bar{w}_h is neglected.

-Advection of puffs-

The puffs are advected by the horizontal windvectors, obtained from the meteorological model. Vertical interpolation or extrapolation takes place of the wind at the nearest two levels on which they are available. Interpolation to the mass-centre of the puff (including mass in the mixing layer and mass in the reservoir layer) is done using the power law, were we derive the power from the windspeed at the two levels. Horizontally, the windvector of the nearest gridpoint is used.

To account for the effects of windshear on the advection of puffs, a procedure is designed for splitting puffs into two puffs, one in each layer, that will be advected seperately.

-Dry and wet deposition-

The dry deposition flux is estimated using the resistance model:

$$\text{Dry deposition flux} = V_g(z) \cdot c(z) = c(z) / (r_a + r_b + r_s) ,$$

where r_a is the aerodynamic resistance, r_b is the sublayer resistance and r_s is the surface resistance. For the calculation of r_a , we made use of the integrated stability functions from Businger et al. (1971).

To estimate the removal of material by below-cloud scavenging, we use: $dc/dt = c \cdot \Lambda$, where the scavenging coefficient Λ (s^{-1}) is a function of precipitation intensity and mixing height h .

3. SOME TEST RESULTS OF THE PUFF DISPERSION MODEL

The puffmodel has been used to simulate the dispersion of material released near Chernobyl. At that time the system as described in the previous section was not available completely. Only a number of weeks after the accident model results became available.

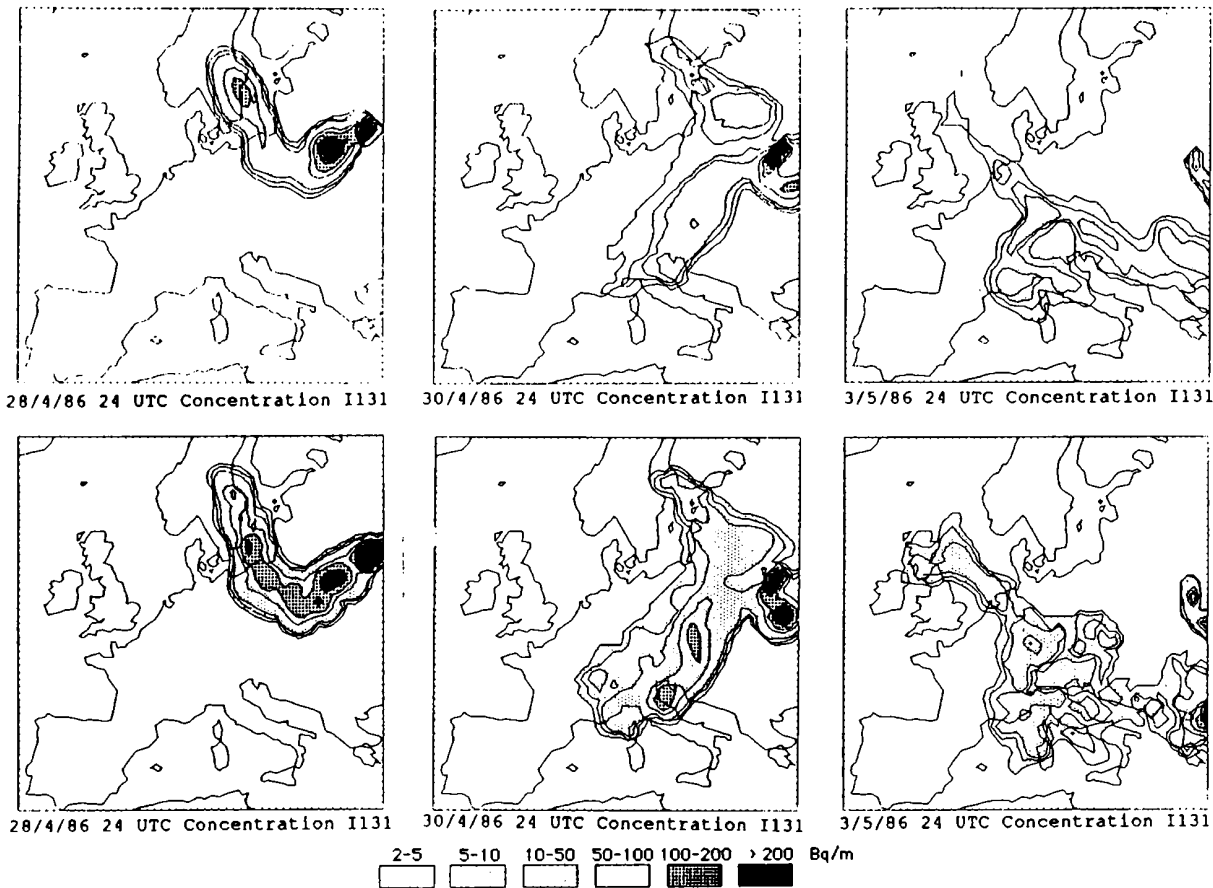


Figure 3 Calculated concentrations I-131 at z=4m. (RIVM/KNMI Puff-model)
 Upper row: run 1 using uniform mixing heights,
 Lower row: run 2 using non-uniform mixing heights.

Source of meteorological information for the test runs was the FM-LAM for rainfields and analyses of wind at 1000mb and 850mb. In a first run we used a uniform mixing height based on radiosonde measurements near Chernobyl. In a second run we used non-uniform mixing heights based on equations derived by Tennekes (1973), Driedonks (1981) and Van Dop (1982) for unstable situations; for stable situations we used a formula derived by Nieuwstadt (1981).

In figure 3 the results are shown of a run that uses the uniform mixing heights (upper row) and a run that uses non-uniform mixing heights (lower row). It can be seen that the overall transport of material differs slightly. However, locally there may be large deviations due to differences in mixing height.

Figure 4 shows measured values of I-131 concentration and the results of both model runs (6-hours average). In all cases the arrival time is estimated with an accuracy of 6 hours. The model overestimates measured concentrations in Stockholm and Budapest. The introduction of non-uniform mixing heights improves the resemblance between calculated concentrations and observed values at all sites except Budapest. For a more extensive discussion is referred to Van Rheineck-Leyssius et al. (1988) and Verver and Scheele (1988).

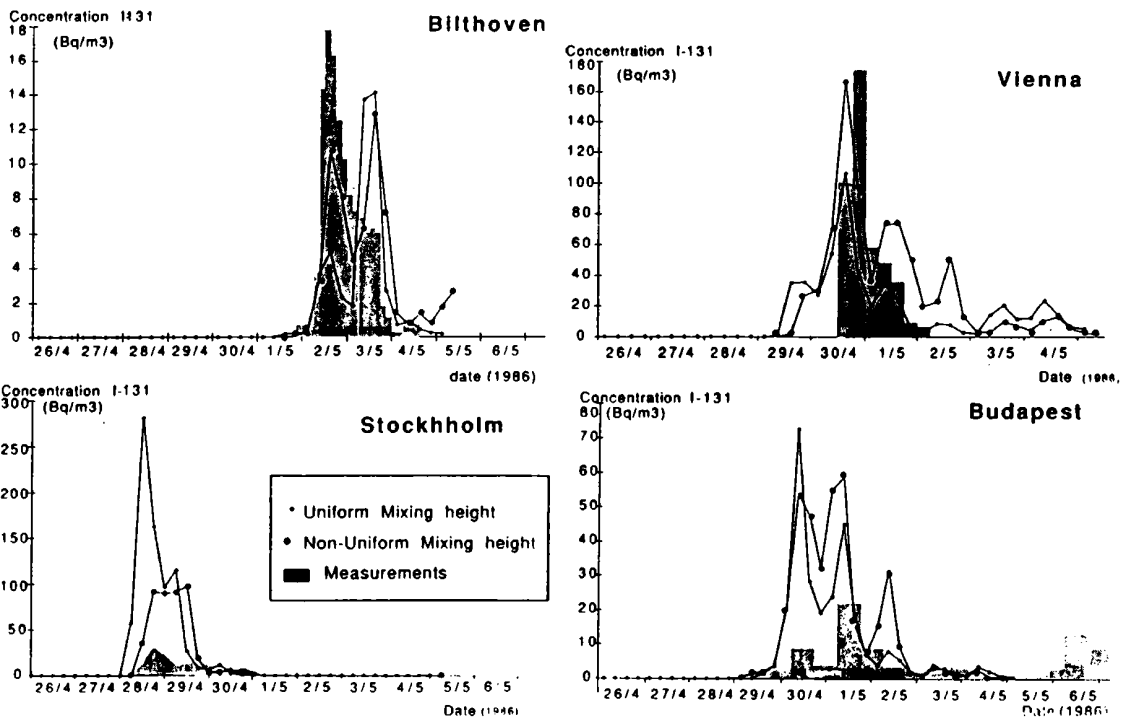


figure 4 Measured and calculated concentrations of I-131 at z=4m, as a function of time for four locations (RIVM/KNMI Puff-model).

4. CURRENT STATE OF DEVELOPMENT

All modules of the system described above are in a testing phase (except of course the ECMWF-GCM). The system is planned to become operational in spring, 1989.

The modules will run on a Convex XL mini super computer. To provide for an extra backup, KNMI and RIVM will both run the same puff dispersion models

5. CONCLUSIONS

The combination of a dispersion model and an atmospheric model in operational use for weather forecasting, makes the system described above a valuable tool in emergency situations. The relatively simple formulation and its modest use of computer resources suits the RIVM-KNMI puff dispersion model for real-time application.

The dispersion model is applied to the Chernobyl release. Arrival times are estimated very well; concentrations show some improvement after the introduction of a more realistic, non-uniform mixing height.

REFERENCES

- Businger, J.A., Wyngaard, J.C., Izumi, I., and Bradley, E.F. (1971), Flux-Profile Relationships in the Atmospheric Surface Layer, *J. Atmospheric Sci.* 28, 181-189.
- Csanada G.T., (1973), *Turbulent diffusion in the environment.* Reidel publ.comp. Dordrecht, Holland
- Dop, H. van, B.J.de Haan, C. Engeldal, (1982). The KNMI mesoscale air pollution model. Scientific Report. W.R. 82-2, KNMI, De Bilt
- Driedonks, A.G.M. (1981). Dynamics of the well-mixed atmospheric boundary layer. Thesis, Royal Netherlands Meteorological Institute, 3730 AE De Bilt, pp. 189.
- Egmond, N.D. Van, H. Kesseboom, (1983). Mesoscale air pollution dispersion models II; Lagrangian PUFF-model, and comparison with Eulerian GRID-model. *Atmospheric Environment* 17, 265-274.
- Egmond, N.D. Van, D.Onderdelinden, H.Kesseboom (1982). Correlation spectrometry as a tool for mesoscale air pollution modelling. Paper presented at the 13th ITM on air pollution modelling and its application. Iles des Embiez, 14-17 september 1982
- Lablans, W.N., P.J. Rijkoort, (1974). De betekenis van de veranderlijkheid van de windrichting voor schattingen van de ligging van het besmette gebied na ongevallen met schadelijke stoffen. KNMI Scientific Report W.R. 74-4 (Dutch)
- Leeuw, F.A.A.M. De, H. Kesseboom, n.d. van Egmond, (1985). Numerieke verspreidingsmodellen voor de interpretatie van meetresultaten van het Nationaal Meetnet voor Luchtverontreiniging; ontwikkeling 1982-1985 (RIVM rapport) (Dutch)
- Nieuwstadt, F.T.M., (1981). The steady-state and resistance laws of the nocturnal boundary layer: theory compared with observations. *Bound. Layer Meteo.* 20, 003-017.
- Rheineck Leyssius, H.J. van, H.J.A van Jaarsveld, F.A.A.M de Leeuw, (1988), A lagrangian model for the real-time simulation of atmospheric transport and dispersion of accidentally released materials. Paper presented at the 17th ITM on Air Pollution Modelling and its Application, Cambridge
- Tennekes, H., (1973). A model for the dynamics of the inversion above a convective boundary layer. *J. Atmos. Sci.* 30, 558-567
- Verver, G.H.L., M.P.Scheele, (1988), Influence of non-uniform mixing heights on dispersion simulations following the Chernobyl accident. Paper presented at the 17th ITM on Air Pollution Modelling and its Application, Cambridge

DISCUSSION

QUESTION: ApSimon: How do you decide when to subdivide a puff, and treat the material above and within the mixing layer separately?

ANSWER: We split a puff when there is a substantial part of the mass in each layer, or when the mixing height changes rapidly (eg. at the end of the day).

QUESTION: Beniston: Concerning applicability of puff model for releases occuring near a receptor area i.e. to what extent can a short-time warning be made possible with such a model.

ANSWER: The meteorological input has a spatial resolution of 60 km, so it is not detailed enough for application in local scale dispersion problems. The reponse time would be small enough (some minutes) for local application.

QUESTION: Ishikawa: 1. Did you compute your mixing height from ECMWF data or from synoptic station data? 2. Did you compare you calculated mixing heights with some observation such as acoustic soundes?

ANSWER: The test I've shown you are done with field of mixing heights based on synoptical data. In the future mixing heights will be based on data from the meteorological LAM. We did not compare the calculated mixing height with acoustic sounder data but with radiosonde data from 12.00 GMT. Subjectif analyses of the radiosonde data showed a correlation of approximately 0.70 with our calculated mixing heights.

QUESTION: Musson-Genon: Do you introduce the large scale vertical velocity in the computation of the height of the boundary layer. Do you think that this effects could be important?

ANSWER: The height of the boundary layer is derived from data computed by the meteorological limited area model. This model includes large scale vertical velocities. But to calculate the

entrainment velocity within the puffmodel, the vertical velocity might be important. Up to now we have not included this in the dispersion model.

QUESTION: Nordlund: Your estimate of the convective mixing height over Stockholm was about 1500 m. Aircraft measurements show mixing up to about 2500 m. Do you think that your model estimates too low mixing height values?

ANSWER: We think that the material was mixed to a high level in the USSR. Then the materials was transported over the cold Baltic sea and a shallow mixed layer was established. When the material in the upper air reached Sweden, only a part of it was fumigated into the boundary layer. This mechanism is supported by the fact that a smaller mixing height in Sweden moved calculated concentrations down to more realistic values.

QUESTION: Seibert: 1. You are using 2 σ -layers for the wind data. What is the real transport velocity? 2. What were the actual values of the plume centre height?

ANSWER: 1. The real transport velocity is calculated by an interpolation to the mass-centre of the puff, using the power law. 2. The height of the mass-centre of the puff can have any value between 0 and \pm 2500 m. It is a function of the vertical distribution of the mass of the puff.

CHERNOBYL ACCIDENT: MODELLING OF DISPERSION OVER EUROPE OF THE RADIOACTIVE PLUME AND COMPARISON WITH AIR ACTIVITY MEASUREMENTS

A. ALBERGEL

Electricité De France Direction des Etudes et Recherches
Département Environnement Atmosphérique et Aquatique
6, Quai Watier F-78401 FRANCE

D. MARTIN (1), J. M. GROS (2)

Météorologie Nationale

(1) Etablissement d'Etudes et de Recherches Météorologiques
Centre de Recherches en Physique de l'Atmosphère F-78470
(2) Etudes Spéciales 2, Avenue Rapp F-75007 FRANCE

Summary: Following the release of radionuclides from the Chernobyl power plant accident, a long-range transport and deposition model is used to describe the plume dispersion over Europe. The aim of this study is the validation of a fast Lagrangian model and a better understanding of relative impact of some mechanisms, such as the initial plume rise. Comparisons between results and ^{137}Cs measurement activity are discussed according to spatial and temporal variations. It is shown that many measurements can be explained only if different initial plume rises taken are considered.

1-INTRODUCTION

Despite the dramatic consequences of the Chernobyl reactor accident, the atmospheric releases of radionuclides provided a challenge for the modellers to test their long-range dispersion models. For many years, operational codes have been developed to quantify the transfrontier fluxes of chemical pollutants (Elliassen, 1978; Elliassen *et al.*, 1983). At the same time, some authors proposed the use of Lagrangian codes to analyse atmospheric transfer of radioisotopes (ApSimon *et al.*, 1985; ApSimon *et al.*, 1986). It was well established that such Lagrangian models provide a good description of climatological long-range transport (typically one month). However, because of the uncertainty in source terms evaluation, the simulation of the pollution episodes could not be validated.

After Chernobyl releases, both source term and measurements data are available and allow the validation of the long-range pollutant transport and deposition model developed by Electricité de France (Aquatic and Atmospheric Environment Département) and Météorologie Nationale (French Weather Service).

This model is used to analyse the Chernobyl radioactive plume dispersion over the European continent. Model predictions are compared with field measurements of ^{137}Cs activity in the air from 26 April to 5 May 1986.

Such studies are also used to provide an evaluation of the reliability of future operational computer codes which deal with the radionuclides atmospheric transfer (Biscay and Moussafir, 1987).

2- THE MEASUREMENTS DATA BASE

The treatment of the radiological data set, which is used in this study, was accomplished by the French Atomic Energy Agency. The data mainly concern Western Europe, including Scandinavian countries. All these data and their uncertainties are described in Robeau *et al.* (1987). ^{137}Cs is chosen as a tracer to compare model output with measured data; this pollutant can be trapped by both paper and charcoal filters. Due to the efficiency of the filters for this element, no filter correction is required. ^{137}Cs is also one of the most frequently measured radionuclides (W.H.O. 1986, Thomas *et al.*, 1986; Savolainen *et al.*, 1986).

The uncertainty in the measurement of low activity ($< 10^{-2} \text{ Bq.m}^{-3}$) can reach 40%.

3- NUMERICAL SIMULATION

The code is a classical segmented plume Lagrangian trajectory model. It has already been used to describe the behaviour of ETNA plumes with diffusion, chemical transformations, dry and wet deposition (see MARTIN *et al.*, 1984).

The model is divided into two parts:

- air mass trajectory computation,
- pollutant diffusion, physical transformation (such as radioactive decay), dry and wet deposition.

3-1 Air mass trajectories

The computation of three-dimensional trajectories was accomplished using the synoptic wind field and vertical velocities obtained from the analyses of the E.C.M.W.F. (European Centre for Meteorological Weather Forecast, Reading, U.K.).

The use of vertical velocity eliminates constraints associated with the level of the trajectory (isobaric for instance). Only the exact location and altitude at the starting point are required. General studies have been made to evaluate this trajectory computation (Martin *et al.*, 1987). It is shown that the kinematic and geographical localization of air masses is improved when vertical velocity is considered.

The computed trajectories for the Chernobyl accident (origin point: 31°15'E, 51°15'N) starting at 850 mb provide interesting qualitative information (Strauss and Gros, 1987), but are not sufficient to explain all the measured data. In consideration of mean plume rise, three sets of trajectories beginning respectively at 925, 850 and 700 mb have been computed. These values characterize the diurnal evolution of the mixing height over the emission area.

To simulate the measurement taken 10 days after the Chernobyl accident (26 April, 00 GMT), height trajectories (i.e. a new trajectory every three hours) for the three plume rise levels have been determined.

Figure 1 illustrates the strong vertical variations of the trajectories occurring during the 10 day period.

Figure 2 gives the geographical localization of air masses leaving the Chernobyl site during the first day. The gap between two symbols plotted on a trajectory provides the distance covered by the trajectory in 24 hours.

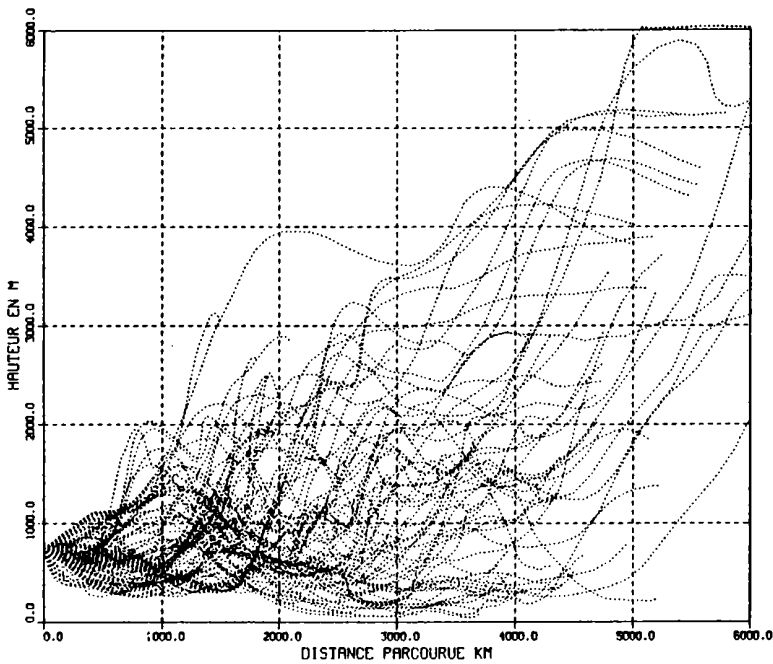


Fig.1 Vertical evolution of all trajectories starting at 925 mb

3-2 Dispersion and deposition

Assuming the plume centreline follows a trajectory defined by straight line segments, a Gaussian concentration field is generated, at a given time, around each segment. A plume segment is characterized by its initial pollutant content and its total distance of travel. The effects of material removal and plume processes are taken into account to ensure pollutant balance at each segment.

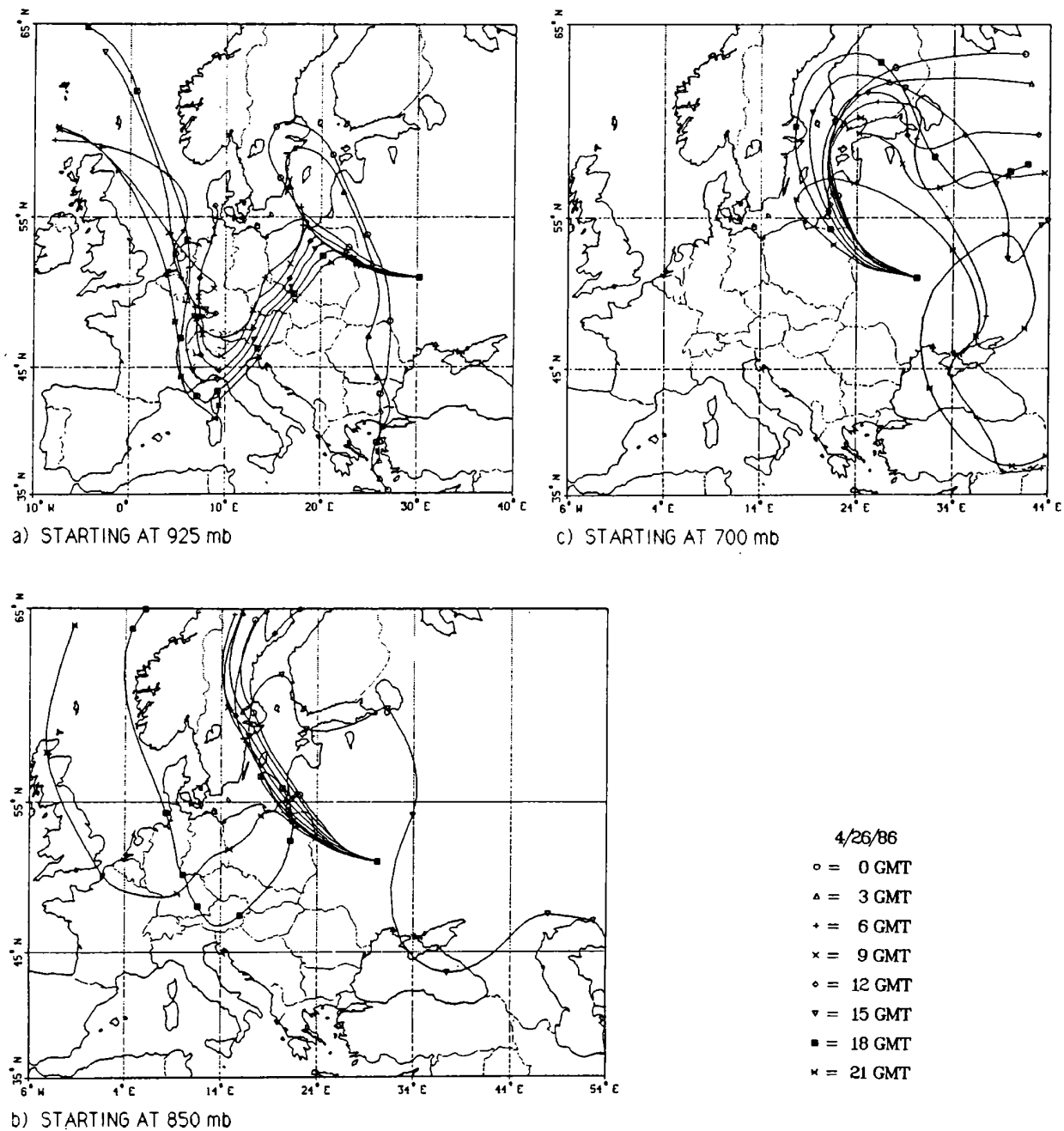


FIGURE 2: CHERNOBYL TRAJECTORIES STARTING EVERY 3 HOURS
APRIL 26th

For the following Chernobyl simulations, some additional assumptions have been made:

- homogeneous vertical concentration between ground and the upper limit of a fictitious mixing height (fixed at 3000 m),
- thickness of precipitation layer also arbitrarily fixed to 3000 m (this assumption is quietly justified since the precipitation fields are not well known: the rainfall values used are short-term predicted by the E.C.M.W.F. (Reading, U.K.) on grid points $1,5^\circ \times 1,5^\circ$),
- radioactive decay for caesium = 30 years^{-1} ,
- dry deposition velocity = 0.0015 m.s^{-1} ,
- scavenging ratio = 10^4 defined as the ratio of air activity (Bq.m^{-3}) by the water of rain activity (Bq.m^{-3} of water).

3-3 ^{137}Cs Source term

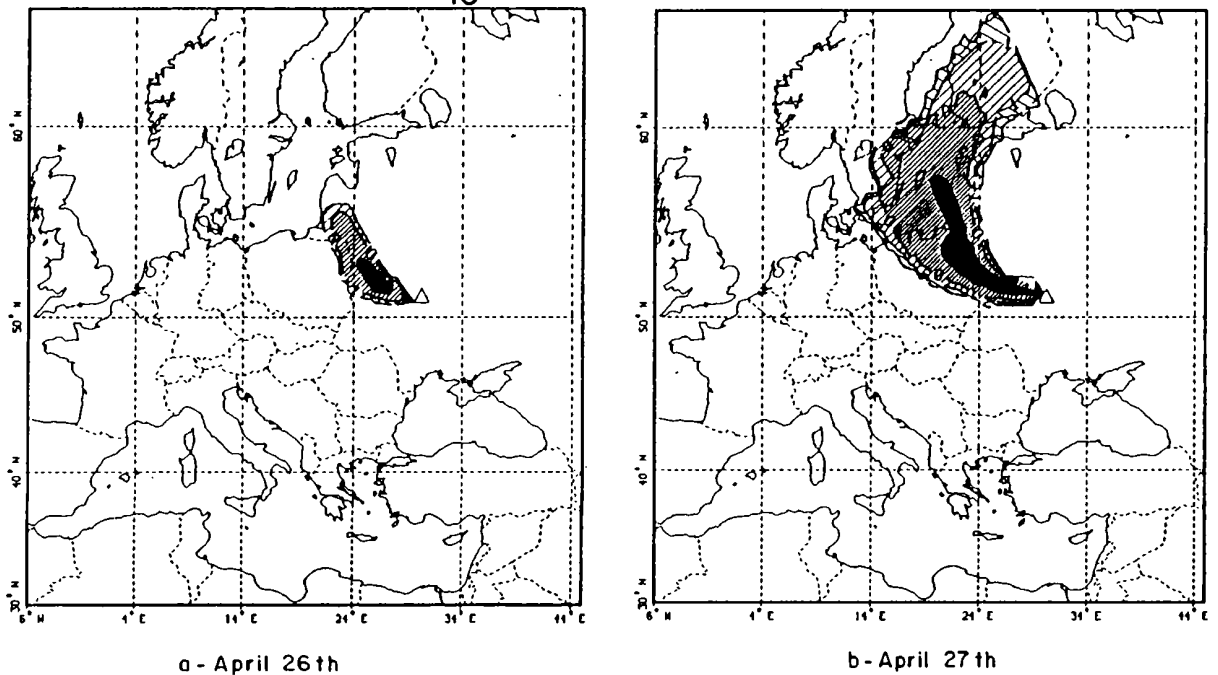
The total source term was evaluated by the USSR authorities and published at the Vienna Conference in August 1986. For the ^{137}Cs , the value is $3.7 \cdot 10^{16} \text{ Bq}$.

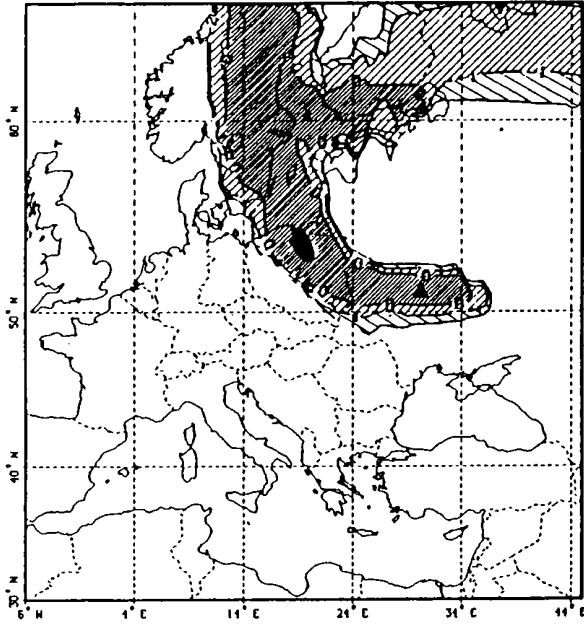
The daily emission percentages were confirmed by the French Atomic Energy Agency assessment:

- 26 April	24.0 %
- 27 April	08.0 %
- 28 April	06.8 %
- 29 April	05.2 %
- 30 April	04.0 %
- 1 May	04.0 %
- 2 May	08.0 %
- 3 May	10.0 %
- 4 May	14.0 %
- 5 May	16.0 %

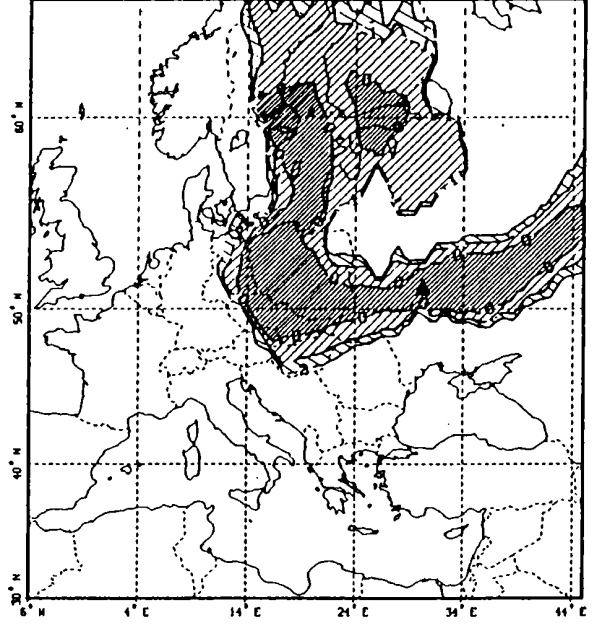
A link was established between pollutant emissions at different initial heights (925 mb, 850 mb, 700 mb) and the mixing layer evolution. This evolution was determined using radiosoundings data given over Kiev at midday and midnight. It was possible to estimate a chronology of the initial emission at each height.

Figure 3 : ISO-LOG₁₀ AIR ACTIVITY OF ^{137}CS (Bq.m^{-3}).

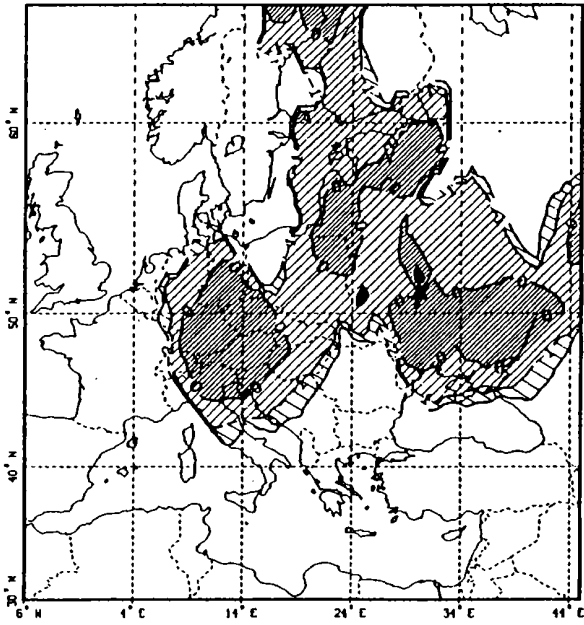




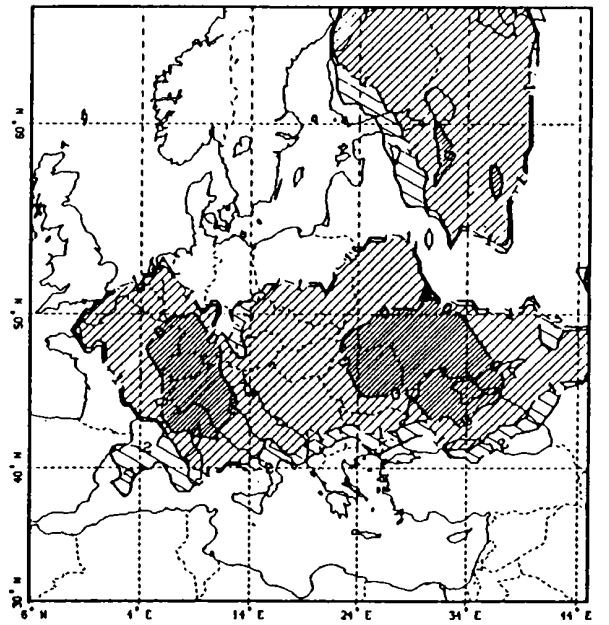
c - April 28th



d - April 29th


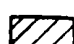




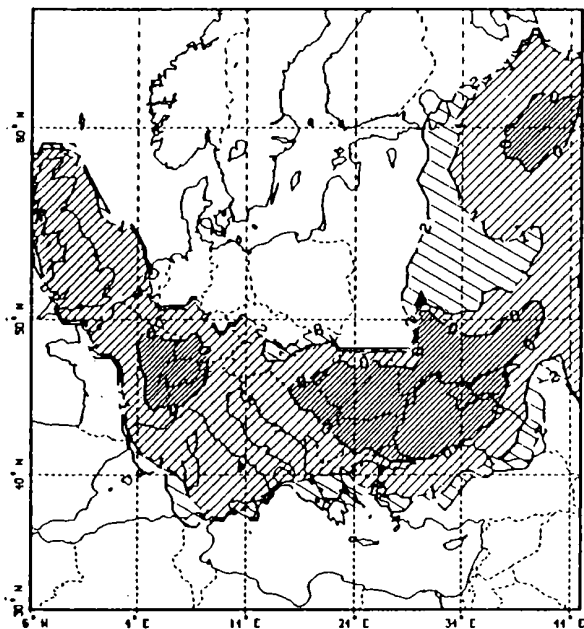
e - April 30th



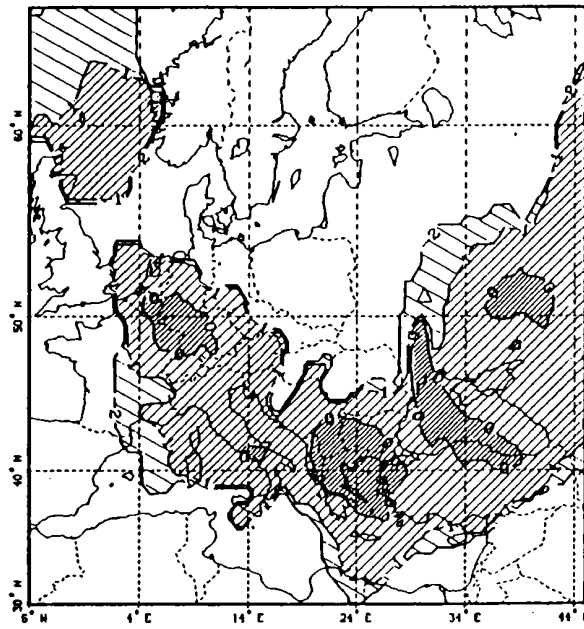
f - May 1st

LEGENDE :

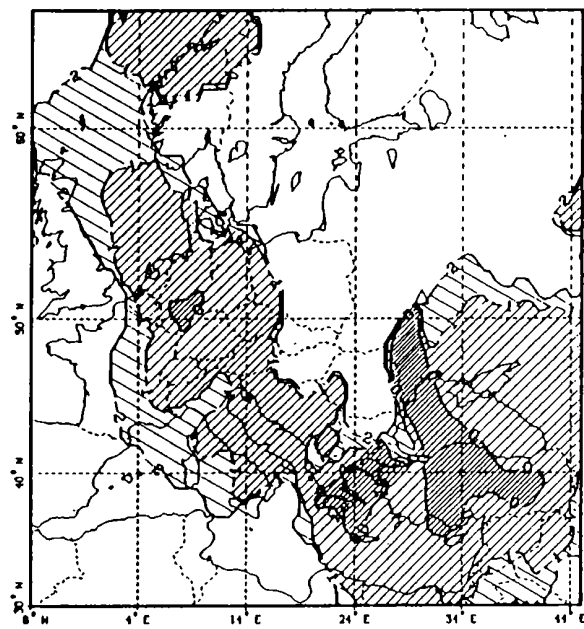
- | | | |
|---|--------------------------|-----------------|
|  | $0.1 \leq A_c \leq 0.01$ | Bq/m^3 |
|  | $1 \leq A_c \leq 0.1$ | |
|  | $10 \leq A_c \leq 1$ | |
|  | $100 \leq A_c \leq 10$ | |



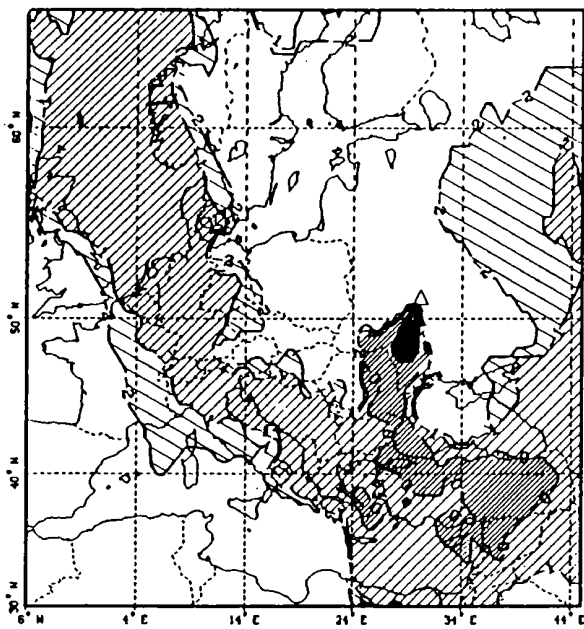
g - May 2nd



h - May 3rd



i - May 4th



j - May 5th

LEGENDE :

- $0.1 \leq A_c \leq 0.01$
 - $1 \leq A_c \leq 0.1$
 - $10 \leq A_c \leq 1$
 - $100 \leq A_c \leq 10$
- Bq/m^3

Figure 3 : ISO-LOG₁₀ AIR ACTIVITY OF ¹³⁷CS (Bq.m⁻³).

3-4 Results

After computation, maps of air activity, dry and wet deposition could be drawn. The use of E.C.M.W.F's predicted precipitation fields leads to a very smooth wet deposition maps. However, the plume depletion due to rainout seems to be correctly evaluated. Figure 3 shows the radioactive cloud progression which is in good agreement with previous studies (De Leeuw *et al.*, 1987).

4- COMPARISON WITH MEASUREMENTS

4-1 Global estimation

As not enough dry and wet deposition measurements were available to compare with computed results, only the actual daily air activity averages are compared.

To quantify the correlation between measured data and computation results, the order of magnitude (i.e. \log_{10} of the ^{137}Cs activity) is considered. In figure 4, measured points are plotted against computed values. Three linear regressions are drawn: $y(x)$ where $\sum(x-x_i)^2$, $\sum(y-y_i)^2$, $\sum((x-x_i)^2+(y-y_i)^2)$ are minimized respectively. The correlation coefficient is 0.57. The total number of plotted values is 402.

The number of times the model results agree, over or underestimate measurements are presented in 'contingency tables'. The first line and the first column are reserved for values lower than $10^{-3} \text{ Bq.m}^{-3}$.

Table I shows that:

- the order of magnitude of ^{137}Cs activity average is computed in 54% of all cases and 70% if only the values greater than 1 Bq.m^{-3} are considered,
- the model underestimates the measured data in 11% of cases,

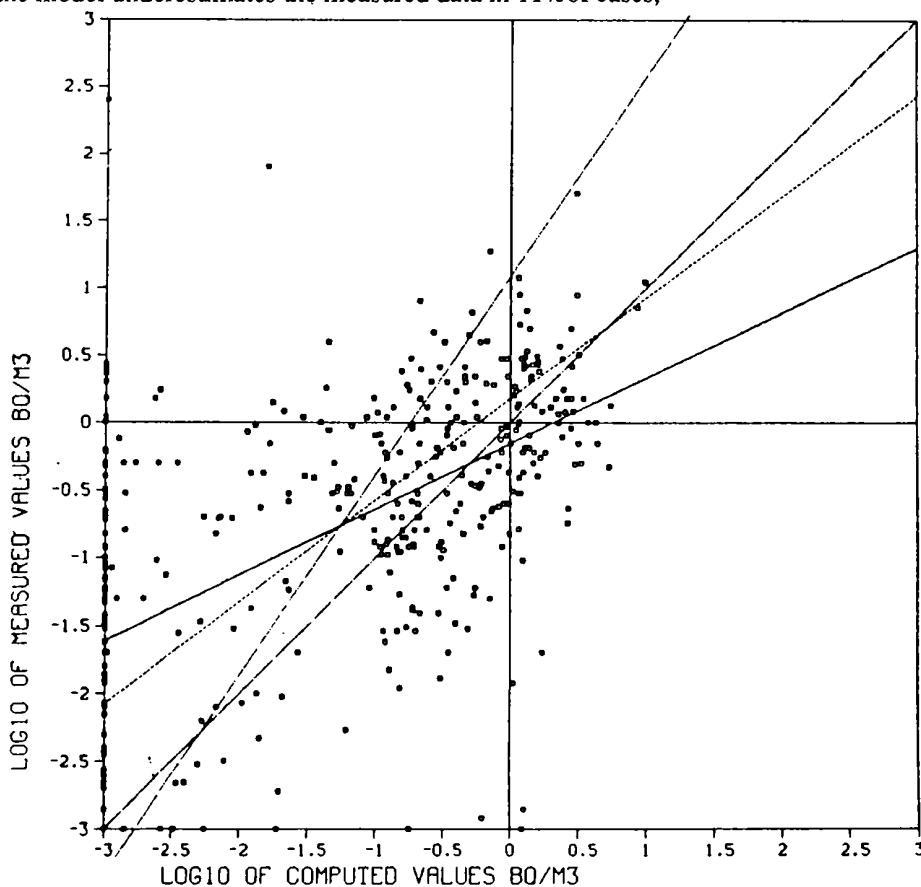


FIGURE 4: COMPARISON MODEL VS MEASUREMENTS OVER EUROPE DURING 10 DAYS PERIOD

- the model overestimates the measured data in 35% of cases,
- the model predicts no pollution where significant activity was measured in 19% of cases and the model predicts pollution where no activity was measured in 2%.

4-2 Regional estimation

- *Italy and Greece* Table II shows a comparison of measured data and computed results for a more limited geographical area including Italy and Greece (35°N, 47°N, 7°E, 30°E). The coefficient of correlation is $r=0.44$ with 101 measured values. We observe on table II that the computed order of magnitude is correct for 80% of the measured activity values.

- *Scandinavian countries* (55°N, 65°N, 7°E, 40°E) Since the correlation coefficient ($r=0.52$ for 77 values) is better than in the previous area, table III shows some disagreements between measured and computed values. Only 25% of the values are in diagonal terms (table III), and near 51% of values are not explained by the model. This result is discussed in section 4-3.

- *France* For the France area (43°N, 51°N, 6°W, 7°E), the results of comparison are given in table IV. The correlation coefficient is better and equal to 0.64 (104 values) and the diagonal terms of table IV produce 53% of considered cases. The model overestimates the measurements in 28% (but only 11% of the computed values exceed measured data by less than one log₁₀ module).

CONTINGENCY TABLES COMPARISON MODEL/MEASUREMENT

TABLE I: EUROPE (10°W,40°E,35°N,65°N)

	Am<-3	-3≤Am<-2	-2≤Am<-1	-1≤Am<0	0≤Am<1	1≤Am<2	2≤Am<3	
Ac<-3	17	3	18	33	22	0	1	94
-3≤Ac<-2	2	0	0	1	3	0	0	6
-2≤Ac<-1	4	0	6	9	14	0	0	33
-1≤Ac<0	1	0	6	5	35	1	0	48
0≤Ac<1	1	1	2	25	188	4	0	221
1≤Ac<2	0	0	0	0	0	0	0	0
2≤Ac<3	0	0	0	0	0	0	0	0
	25	4	32	73	262	5	1	402

Table I: Comparison between model results and measurements of daily 137 cs air activity averages (log₁₀ Bqm⁻³ Am measured activity, Ac computed activity) for Europe

TABLE II: ITALY AND GREECE (7°E,30°E,35°N,47°N)

	Am<-3	-3≤Am<-2	-2≤Am<-1	-1≤Am<0	0≤Am<1	1≤Am<2	2≤Am<3	
Ac<-3	1	0	1	2	1	0	0	5
-3≤Ac<-2	0	0	0	0	1	0	0	1
-2≤Ac<-1	0	0	0	1	2	0	0	3
-1≤Ac<0	0	0	0	0	12	0	0	12
0≤Ac<1	0	0	0	1	79	0	0	80
1≤Ac<2	0	0	0	0	0	0	0	0
2≤Ac<3	0	0	0	0	0	0	0	0
	1	0	1	4	95	0	0	101

Table II: Comparison between model results and measurements of daily 137 cs air activity averages (log₁₀ Bq.m⁻³. Am measured activity, Ac computed activity) for Italy and Greece

TABLE III: NORTHERN EUROPE (7°E,40°E,55°N,65°N)								
	Am<-3	-3≤Am<-2	-2≤Am<-1	-1≤Am<0	0≤Am<1	1≤Am<2	2≤Am<3	
Ac<-3	6	3	9	16	12	0	0	46
-3≤Ac<-2	0	0	0	0	0	0	0	0
-2≤Ac<-1	0	0	1	1	1	0	0	3
-1≤Ac<0	0	0	0	1	0	3	0	4
0≤Ac<1	0	0	0	13	11	0	0	24
1≤Ac<2	0	0	0	0	0	0	0	0
2≤Ac<3	0	0	0	0	0	0	0	0
	6	3	10	31	24	3	0	77

Table III: Comparison between model results and measurements of daily ¹³⁷Cs air activity averages (log₁₀ Bq.m⁻³. Am measured activity, Ac computed activity) for northern Europe

TABLE IV: FRANCE (6°W,7°E,43°N,51°N)								
	Am<-3	-3≤Am<-2	-2≤Am<-1	-1≤Am<0	0≤Am<1	1≤Am<2	2≤Am<3	
Ac<-3	2	0	4	4	1	0	0	11
-3≤Ac<-2	0	0	0	0	0	0	0	0
-2≤Ac<-1	3	0	1	1	2	0	0	7
-1≤Ac<0	1	0	2	2	17	0	0	22
0≤Ac<1	0	0	7	7	50	0	0	64
1≤Ac<2	0	0	0	0	0	0	0	0
2≤Ac<3	0	0	0	0	0	0	0	0
	6	0	14	14	70	0	0	104

Table IV: Comparison between model results and measurements of daily ¹³⁷Cs air activity averages (log₁₀ Bq.m⁻³. Am measured activity, Ac computed activity) for France

Daily ¹³⁷Cs air activity average Am= log of measured activity, Ac= log of computed activity Bq/m³.)

4-3 Local estimations (fig.5)

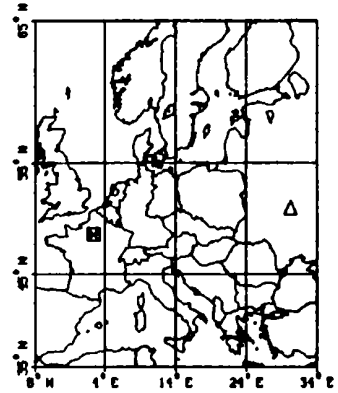
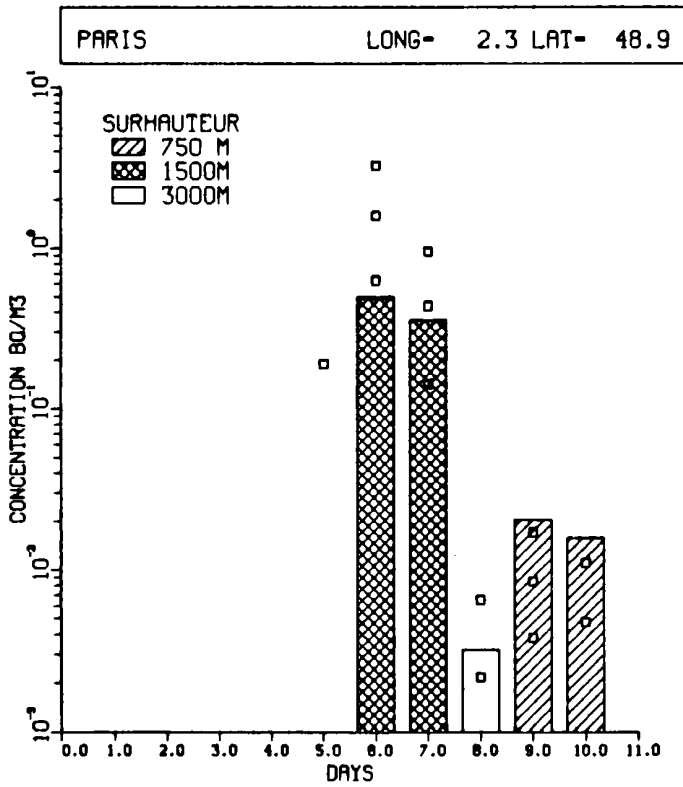
For all measurement sites, the chronological evolutions of computed values (vertical bars) and measured data (squares) are plotted. Values smaller than 10⁻³ Bq.m⁻³ are not considered here. When more than three values are given for the same day and for a 0.5°x0.5° area around the site location, only mean, maximum and minimum are plotted. For model output, the daily average is derived from 8 x 3 hours computed values from midnight to 9 pm. In the measurement of actual data, the precise time of filter change is unknown.

There is a good agreement between the computed evolution and the measured data recorded in Paris and Rome (see figures 5a and 5b).

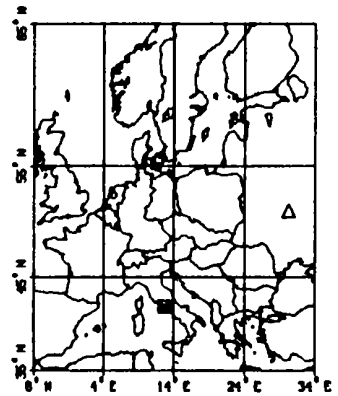
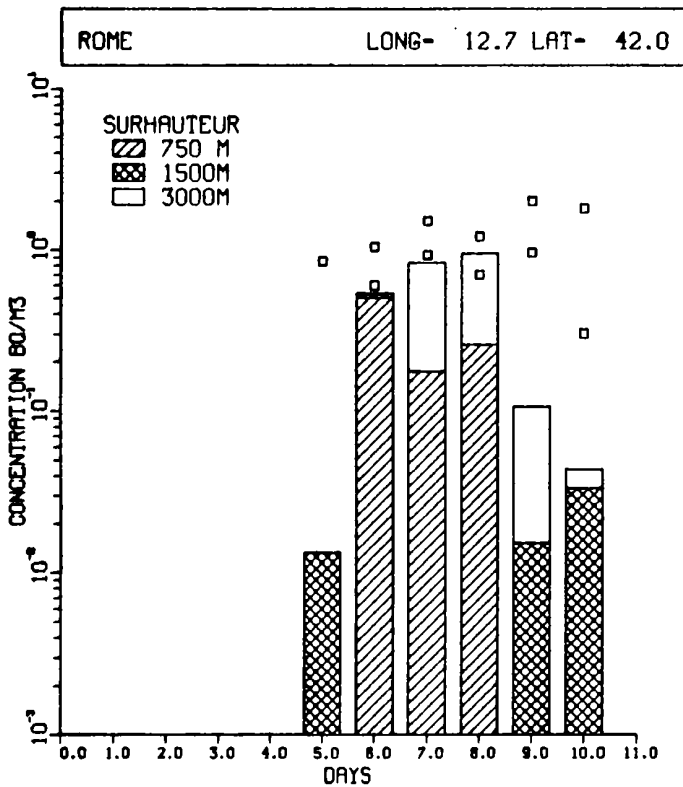
In Northern Europe, the agreement is correct for the first 4-5 days (cloud arrival and high values) but in the following days no pollution is predicted and several measurements can not be explained: see, for instance, Helsinki figure 5d. It is not yet known whether or not the measured activity is due to local pollutant circulation or due to some significant trajectories that have not been computed.

The determination of initial plume rise is very important. Many measured data can be explained only by a trajectory beginning at 925, 850 or 700 mb (see Paris figure 5a), other are explained as the result of several trajectories of different departure altitude (see Rome and Munich figures 5b, 5c).

.ADSO. EAA/METE

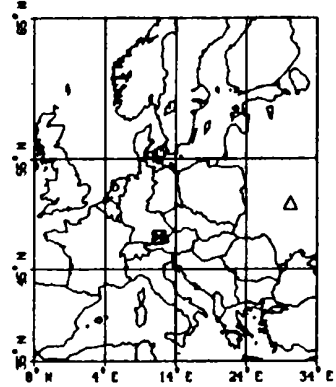
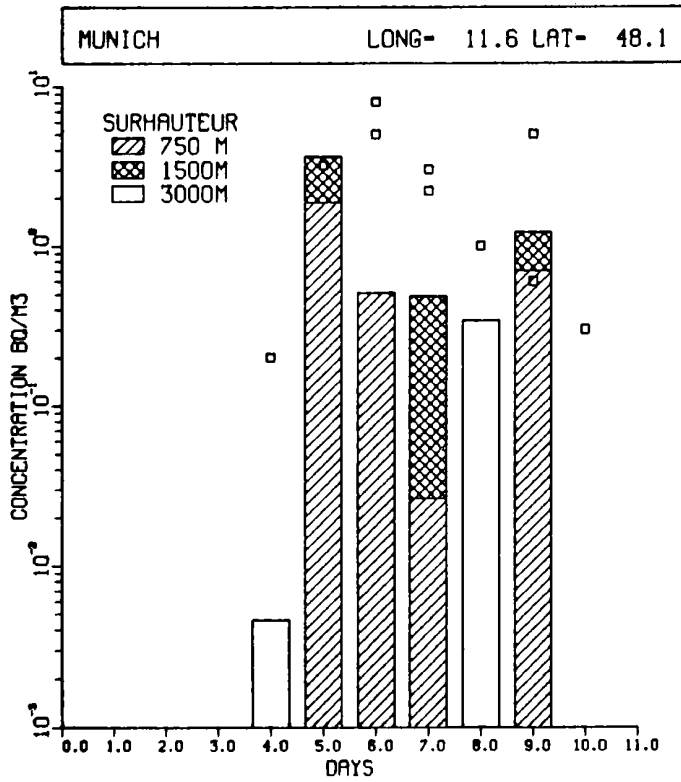


COMPARAISON MODEL/MESURES
 TCHERNOBYL
 ELEMENT - CS.137
 JOUR 1 - 26 AVRIL 1986
 ▲ EMISSION
 □ MESURE



.ADSO. EAA/METE
 COMPARAISON MODEL/MESURES
 TCHERNOBYL
 ELEMENT - CS.137
 JOUR 1 - 26 AVRIL 1986
 ▲ EMISSION
 □ MESURE

.ADSO. EAA/METE



COMPARAISON MODEL/MESURES

TCHERNOBYL

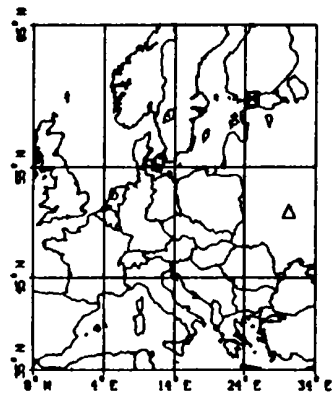
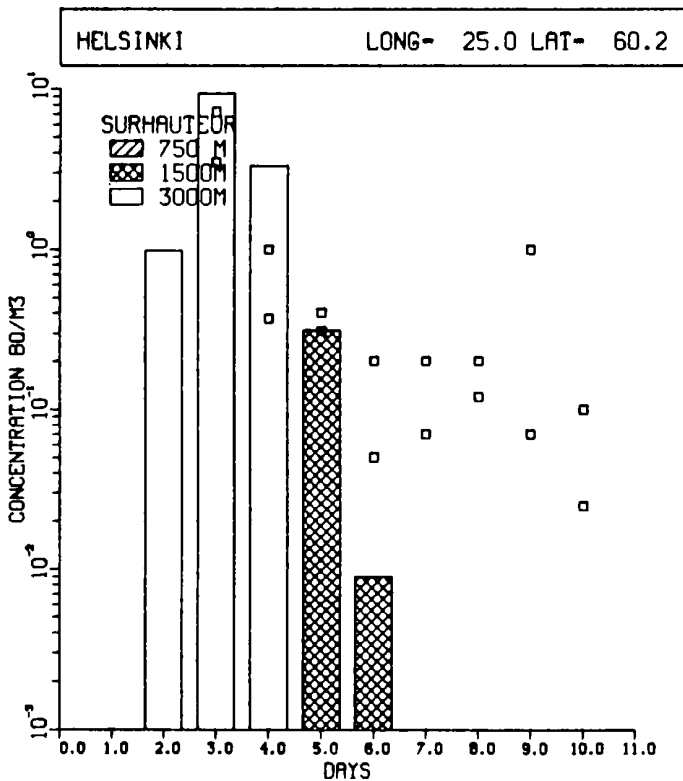
ELEMENT - CS.137

JOUR 1 - 26 AVRIL 1986

△ EMISSION

□ MESURE

.ADSO. EAA/METE



COMPARAISON MODEL/MESURES

TCHERNOBYL

ELEMENT - CS.137

JOUR 1 - 26 AVRIL 1986

△ EMISSION

□ MESURE

5- CONCLUSION

This study shows the validity of the model for the 3D trajectories (taking into account vertical wind component) and the diffusion and removal processes formulation.

Trajectories are fully representative of the main locations reached by the Chernobyl emission. This is also an illustration of the quality of E.C.M.W.F. wind fields analyses. The computed cloud progression agrees with meteorological analyses (Persson . *et al.* 1986, Smith *et al.* 1986, Smith, 1987). Maps of computed air activity and maps of dry or wet deposition are realistic and agree with published information. Predicted values are often close to measured data. However, a few measurements are yet to be explained.

The sheduled model improvements will mainly be in the vertical structure of the atmosphere modelling (taking into account radiosoundings data over Europe) and in the source plume rise modelling.

REFERENCES

- APSIMON H.M., GODDARD A.J.H. and WRIGLEY J. (1985)
'Long-range atmospheric dispersion of radioisotopes. The MESOS model.'
Atmos. Environ., Vol 19 Nr.1 pp 113-125
- APSIMON H.M., Mac DONALD H.F. and WILSON J.J.N. (1986)
'An initial assessment of the Chernobyl-4 reactor accident release source.'
J. Soc. Radiol. Protect., Vol 6 pp 109-119
- BISCAY P. and MOUSSAFIR J. (1987)
'Computer codes developed by Electricité de France for the estimation of atmospheric transfer in emergency situations.' Technical Committee Meeting on Computer Codes for the Probabilistic Assessment of Accident Consequences. I.A.E.A. June 22-26 1987 Vienna
- De LEEUW F., Van AALST R. and Van DOP H. (1987)
'Modelling of transport and deposition over Europe of radionuclides from the Chernobyl accident' 16th International Technical Meeting on Air Pollution and its applications. April 1987 Lindau F.R.G.
- ELLIASSEN A. (1978)
'The OCDE study of long range transport of air pollutants long-range transport modelling.'
Atmos. Environ., vol 12, pp 479-487
- ELLIASSEN A. and SALTBOES J. (1983)
'Modelling of long-range transport of sulphur over Europe: a two-year model run and some model experiments.' Atmos. Environ., vol 17 Nr.8, pp 1457-1473
- MARTIN D., GRANIER J.P., IMBARD M. and STRAUSS B. (1984)
'Application of long range transport model to a mount ETNA plume'
Bull. Volcanol., vol 47-4 (2-1984) pp1097-1106
- MARTIN D., MITHIEUX C. and STRAUSS B. (1987)
'On the use of the synoptic vertical wind component in a transport trajectory model'
Atmos. Environ., Vol.21 Nr.1 pp 45-52
- PERSSON Ch., RODHE H. and De GEER L.E. (1986)
'The Chernobyl accident : a meteorological analysis of how radionuclides reached Sweden'
S.M.H.I. R.M.K. report Nr 55 Dec 1986
- ROBEAU D. and WARTENBERG I. (1987)
'Measurements of radioactivity in Europe during and following the accident of the Chernobyl Nuclear Power Plant' Post Chernobyl Workshop 3rd-5th February 1987 BRUSSELS
- SAVALAINEN A.L., HOPAKOSKI T., KILPINEN J., KUKKONEN P., KUMALA A. and VALKAMA I. (1986)
'Dispersion of radioactive releases following the Chernobyl nuclear power plant accident'
Ilmatieten Laitos, Finnish Meteorological Institute Interim report Nr 1986/2 ISSN 0782-6079
- SMITH F.B. and CLARK M.J. (1986)
'Deposition of radionuclides from the Chernobyl cloud' Nature vol. 322, p. 690
- SMITH F.B. (1987)
'Chernobyl: the radioactive plume and its consequence'
16th International Technical Meeting on Air Pollution and its applications. April 6-10 1987 Lindau
- STRAUSS B. and GROS J.M.(1987)
'Information sur l'accident de TCHERNOBYL' La Météorologie N°15 pp14-15
- THOMAS A.J. and MARTIM J.M. (1986)
'First assesment of Chernobyl radioactive plume over Paris' Nature, vol 321 pp. 817-822
- W.H.O. (1986)
'Chernobyl reactor accident' Report of consultation 6 May 1986 ICP/CEH 129

D I S C U S S I O N

QUESTION: Vergeiner: Has the Chernobyl catastrophe changed the rather negligent attitude of French officials towards other possible nuclear disasters, e.g. in their own country? Do they realize that such a disaster would make parts of France or even of Europe uninhabitable?

ANSWER: EdF is not being asked and not responsible

ASSESSMENT OF SOURCE TERMS IN A NUCLEAR ACCIDENT SITUATION

J. J. N. Wilson and H. M. ApSimon

Air Pollution Group, Department of Mechanical Engineering,
Imperial College of Science, Technology and Medicine, London SW7 2BZ, U.K.

Summary.

The availability of monitoring data, from which the source terms of a nuclear accident may be derived, is considered. The use of multiple linear regression to estimate the fractions of ^{137}Cs , ^{103}Ru and ^{131}I released from Chernobyl and transported over extended distances is illustrated. Potential causes of error in the method and means of avoiding such errors are discussed.

1. Introduction.

In the event of a nuclear accident, both the composition of the resulting release and the temporal variation in the dynamics of the release are likely to be highly uncertain. However such information is vital when assessing potential consequences in the early phase of an accident and also highly pertinent to post-accident analyses. Potential accident scenarios vary widely in character. The duration of releases can range from short puff releases to releases over several days, while the release may be purely non-depositing inert gases such as Xe and Kr, or it may include a large fraction of depositing nuclides such as ^{131}I and $^{134/137}\text{Cs}$. Past accidents such as Windscale, Three Mile Island and most recently, that at Chernobyl have each been quite different in character. It is therefore important to allow for a wide range of possible scenarios when considering methods for source term assessment in nuclear accidents.

This paper will examine how estimates of the source terms can be obtained by optimising the agreement between numerical modelling predictions of the dispersion and transport of an accidental release and observations. For example, calculated atmospheric concentrations of ^{131}I may be compared with measured values at monitoring points over corresponding measurement periods for different prescriptions of the release of ^{131}I as a function of time. Before enlarging on this, and illustrating the techniques by application to the Chernobyl release, the availability of information on which to base such assessments will be addressed.

2. Availability of Monitoring Data

Ideally, on site monitoring equipment would provide direct measurements of the scale of a release and its composition and deposition characteristics, making source term assessments unnecessary. Where a release occurs through a stack then stack monitors may be able to provide this information, if the equipment caters for a sufficient range of concentrations. However, in severe accidents and accidents where the release is disruptive, on site equipment may be destroyed or unable to function. Monitoring equipment placed round the installation can also provide early information on an accidental release and most UK reactor sites are equipped with a circle of sensitive γ detectors within a few hundred metres. The detectors are shielded from ground-shine and can indicate both the variation in time and the direction of the plume. In other countries detectors may be placed in a similar manner at somewhat larger distances out to a few kilometres or more.

Where the release is of a short duration and is hot or explosive, it is likely to be very difficult to prescribe the effective span of the release height accurately. With a more prolonged release, observations with γ -sondes or airborne monitoring can provide direct information. Thus the helicopter flights after Chernobyl indicated that the plume height on 27th April exceeded 1200m, with the maximum radiation level near the power plant recorded at a height of 600m, while on subsequent days the plume height ranged between 200 and 400m.

Information on individual nuclides can be obtained from large volume samplers, but these are limited in their time resolution according to the frequency with which filters are changed and the filters also have to be analysed. Simple indicators like the variation in γ dose with height above the ground, can immediately indicate the presence of depositing nuclides. The radionuclide composition may well be correlated with particle size distribution in a major accident, the more refractory nuclides tending to be associated with particles of fuel. Thus at Chernobyl, it was mainly the volatile nuclides like ^{131}I and ^{137}Cs with radii of the order of a micron which penetrated across Europe and coarser material of different composition which dominated deposition in the close in region. In the very early phase of an accident, or in any warning phase, before a release actually starts, provisional estimates of the radionuclide composition of the release may be based on the reactor inventory, or fuel element inventory and release fractions appropriate to the release scenario (as in probabilistic risk assessment).

Deduction of source terms from such a variety of data may involve the application of short range dispersion models. Such an analysis was undertaken by Israel et al. (1987), yielding very good agreement between the model calculations and the observed fall out in the close in region. Such studies require information on source height, radionuclide composition of the release, particle size spectrum of the release and local meteorological conditions. The latter is normally available from sites with nuclear installations, for example from an instrumented tower. Some nuclear stations now operate SODAR which can give wind and turbulence profiles and indicate where there are any variations above the surface layers which may significantly affect dispersion.

The use of models in the close in region to assess source terms and optimise estimated contamination is fraught with difficulties. The idealised concept of a Gaussian plume or puff dispersing along a simple trajectory is often far from reality (ApSimon, 1986). Changes in wind direction with time and wind shear both complicate the issue. The fitting of such models to tracer releases, even over flat terrain, has been well illustrated at Mol in Belgium (Govaerts, 1985) and the subject of optimising other model parameters, as well as source strength has been discussed by several workers (Govaerts, 1988).

Unlike the close in data, the availability of data for assessments of source fractions transported over extended distances is dependent upon the response of organisations undertaking monitoring in several countries, in addition to the country in which the accident occurred. As a consequence, a variety of different forms of monitoring data are likely to be available, as was the case after Chernobyl. In particular, measurements of ^{131}I in air from Chernobyl were highly variable, depending on the type of filter used; many measurements only referred to the aerosol fraction, whereas as much as 75% of the ^{131}I was in gaseous phase. This has been a major complication in interpreting the data, since little information was provided on the kind of equipment used. Ratios between ^{131}I and other nuclides sometimes helped to assess which data related to just the aerosol form.

However the emphasis of this paper is on the assessment of the effective source terms for the fraction of the release transported over longer distances and across national frontiers. This excludes the coarser material which is deposited close to the source and quite different difficulties arise to those experienced in assessments based on the close in data. The subject is of interest not just as an exercise in independent post accident assessment, but to indicate the overall uncertainties of long range modelling with respect to emissions.

3. Assessment of effective source terms for the fraction of the release from Chernobyl transported over longer distances

3.1 Early analysis

Soon after the Chernobyl accident became known, a version of the numerical long range transport model MESOS was used to simulate the dispersion and transport across Europe, of the release of activity. Results from this Lagrangian trajectory model, treating the release on each day as eight sequential three hour releases, have been described elsewhere. (ApSimon and Wilson 1988).

At the time, little was known about the accident except that there had been a severe breach of the containment. Initial assessments were therefore based on the assumption of a large release on the first day, followed by a gradual decline over subsequent days. The estimated total releases, of $5.6 - 7.5 \times 10^{17}$ Bq ^{131}I and $3.7 - 5.6 \times 10^{16}$ Bq ^{137}Cs , turned out to be in good agreement with figures presented by Soviet scientists in Vienna in 1986. (IAEA 1986). However we presented our results with several caveats, partly because it was very difficult to estimate the initial release and partly, because we had no measurement data available against which to judge how much material had travelled eastwards. In addition it was evident from the areas affected that there had been a prolonged release into the early days of May, but we knew nothing of the nature of this extension of the release.

3.2 Subsequent analyses

After the presentation by Soviet scientists in Vienna in August 1986 and as more suitable measurements became available, further more detailed analyses were undertaken. Daily air concentrations observed at 65 sites were used to estimate daily releases of three nuclides with rather different characteristics; ^{131}I , ^{137}Cs and ^{103}Ru . Air concentrations rather than deposition data were used, in order to study the variation over time, rather than just the total quantities released. Additionally, deposition measurements vary over a much smaller spatial scale than the model and this together with uncertainties in the efficiency of the deposition processes, make identification of representative deposition measurements very difficult. Deposition measurements were also influenced by the methods of sampling and analysis, and few included corrections for pre-existing Cs-137.

3.3 Method

As an initial approximation, the daily release rates of each nuclide were estimated by assuming that they followed the same temporal pattern as the total release specified in the Soviet report. Thus, the Soviet estimate of each nuclide released on 26th April was decayed to 6th May to determine its fractional contribution to the total release. Each nuclide was assumed to contribute this same fraction of the successive daily releases remaining on 6th May. The amounts of each nuclide remaining on 6th May were then ante-decayed to the relevant release day to determine the release rate for that day (Table 1).

Day	^{137}Cs Released		^{131}I Released	
	MCl.day ⁻¹	Bq.day ⁻¹	MCl.day ⁻¹	Bq.day ⁻¹
21.00 25.04 - 21.0026.04	0.30	1.1x10 ¹⁶	4.5	1.7x10 ¹⁷
21.00 26.04 - 21.0027.04	0.10	3.7x10 ¹⁵	1.4	5.2x10 ¹⁶
21.00 27.04 - 21.0028.04	0.085	3.1x10 ¹⁵	1.1	4.1x10 ¹⁶
21.00 28.04 - 21.0029.04	0.065	2.4x10 ¹⁵	0.8	3.0x10 ¹⁶
21.00 29.04 - 21.0030.04	0.05	1.9x10 ¹⁵	0.52	1.9x10 ¹⁶
21.00 30.04 - 21.0001.05	0.05	1.9x10 ¹⁵	0.48	1.8x10 ¹⁶
21.00 01.05 - 21.0002.05	0.10	3.7x10 ¹⁵	0.89	3.3x10 ¹⁶
21.00 02.05 - 21.0003.05	0.13	4.8x10 ¹⁵	1.0	3.7x10 ¹⁶
21.00 03.05 - 21.0004.05	0.18	6.7x10 ¹⁵	1.3	4.8x10 ¹⁶
21.00 04.05 - 21.0005.05	0.20	7.4x10 ¹⁵	1.4	5.2x10 ¹⁶
21.00 05.05 - 21.0006.05	0.003	1.1x10 ¹⁴	0.02	7.4x10 ¹⁴

Table 1. Daily ^{137}Cs and ^{131}I release rates derived from the Soviet data.

The average daily air concentrations of each nuclide at each of the 65 sites, corresponding to this release scenario were then calculated by MESOS. The calculated daily air concentrations are the sum of the contributions from each of the 11 release days. Each day at each site for which there are observed and calculated air concentrations can then be considered as an independent member of the sample distribution for the particular nuclide. The j th observed mean air concentration of a particular nuclide, $X_{\text{air},j}$ can be equated with the calculated air concentration as follows;

$$X_{\text{air},j} = \sum_{i=1,11} \theta_i \chi_{ij}$$

where θ_i is a modifying factor and χ_{ij} is the calculated contribution to the mean air concentration from release day i . The "best fit" between the observed and calculated air levels can then be determined by multiple linear regression of the calculated air concentration onto the observations, minimising the sum of the squares of the differences between the two data sets.

In practice, difficulties can arise in applying such techniques. If there are few calculated contributions to observations from some sections of the release, then the least squares regression can lead to some distortion and in the extreme, negative θ 's can be obtained which clearly unrealistic. In our analysis each observation was given equal weighting, but there are arguments in favour of differential weighting according to the reliability of the data and to average out the inhomogeneous representation of the different sections of the release. The regions where more confidence can be placed in the model calculations may also deserve greater influence.

Another problem is some uncertainty in the allocation of measured air concentrations to successive 24 hour periods. In practice the measurement periods are determined by the times at which filters are changed. In the data used this has been distributed over 24 hour periods, which may not coincide with the periods from 9.00 hours GMT on one day to the same time the next day, for which air concentrations are calculated. Bearing in mind that even after 7 days travel to the UK, concentrations peaked and fell within a few hours; measurements may well reflect air concentrations on the day before or day after that to which they are attributed. Also the model accuracy is such that estimated times of arrival can easily be a day out too.

To overcome this problem a slightly different scheme was used. Instead of basing points in the sample on observed and measured values over 24 hour periods, corresponding quantities were defined based on half the air concentration on a given day i . Regressing the calculated air concentrations onto these 'observations' gave satisfactorily robust values for the θ 's.

There are other variations on this scheme which could be tried. For example air concentrations could be replaced by logarithmic values of air concentrations; the former gives more emphasis to the highest concentrations which was felt to be preferable. There are also independent questions of data quality and outliers in the distribution. In this context the problem of variability in measurements between total and particulate fractions of ^{131}I has already been mentioned, and ratios with other nuclides measured were used as a cross-check where possible. It is obviously preferable to use as many data points as one can, to reduce noise levels in the data, and the influence of individual points where there may be errors.

Even though air concentrations are used rather than deposition, uncertainties in the depletion processes still enter into the calculations. In the MESOS model a simple wash-out model is used and the dilution due to export of material aloft is not allowed for. Despite the need to consider many points, those points where model uncertainties are large should be excluded or given low weightings. Thus points in areas traversed during and after entry into frontal systems for example, have doubtful validity; similarly for complex orographic regions like the Alps.

3.4 Results

The resulting best estimates for the daily releases are given in Table 2. It should be noted that the estimates for the first three days of the release are all derived from monitoring data relating to only part of each 24 hour period, and hence do not allow for any variation within these periods. Apart from modelling difficulties there were very few quantitative observations available to us from the first few hours of the release including the initial explosion. Consequently the revised source estimates obtained for the last eighteen hours of this day have been combined with the Soviet estimate for the initial release to give an upper limit for the total for the first day.

The revised estimates indicate relatively lower proportions of the more volatile nuclides ^{131}I and ^{137}Cs in the second part of the release than assumed in the initial release pattern in Table 1. It is possible that some of the locally observed concentrations were enhanced by the dust and disturbance caused by work on the damaged reactor, and that only a small proportion survived local fall-out. Also the greater volatility of these nuclides would favour their release at an early stage. ^{103}Ru , which is far less volatile, appears to have followed a constant ratio to ^{137}Cs until core temperatures rose above 1000°C with blanketing of the core. At these high temperatures ruthenium emissions increased, the estimated ratio of ^{103}Ru to ^{137}Cs rising to a maximum of about five and then dropping back as ^{137}Cs emissions increased again too.

This is born out in Figure 1 where the model simulations have been used to pick out radiological measurements associated with different phases of the release. The ratio of ^{103}Ru to ^{137}Cs in air concentration measurements shows a clear trend in time, with the highest values associated with releases on 1-2nd May.

Day	$^{103}\text{Ru}(\text{Bq})$	$^{137}\text{Cs}(\text{Bq})$	$^{131}\text{I}(\text{Bq})$
21.00 25.04 - 21.0026.04	2.9×10^{16}	1.5×10^{16}	1.9×10^{17}
21.00 26.04 - 21.0027.04	1.2×10^{16}	5.6×10^{15}	4.3×10^{16}
21.00 27.04 - 21.0028.04	9.9×10^{15}	4.7×10^{15}	2.5×10^{16}
21.00 28.04 - 21.0029.04	LOW	LOW	LOW
21.00 29.04 - 21.0030.04	7.6×10^{14}	3.8×10^{14}	3.8×10^{15}
21.00 30.04 - 21.0001.05	3.6×10^{15}	7.6×10^{14}	1.1×10^{15}
21.00 01.05 - 21.0002.05	6.3×10^{15}	1.1×10^{15}	4.9×10^{15}
21.00 02.05 - 21.0003.05	3.5×10^{15}	1.9×10^{15}	1.5×10^{16}
21.00 03.05 - 21.0004.05	4.9×10^{15}	2.7×10^{15}	1.9×10^{16}
21.00 04.05 - 21.0005.05	5.9×10^{15}	3.0×10^{15}	2.1×10^{16}
21.00 05.05 - 21.0006.05	LOW	LOW	LOW
TOTALS AT 06.05	6.7×10^{16}	3.5×10^{16}	1.7×10^{17}

LOW = $< 1.0 \times 10^{14}$

Table 2. Daily ^{137}Cs , ^{131}I and ^{103}Ru release rates derived from the regression analysis.

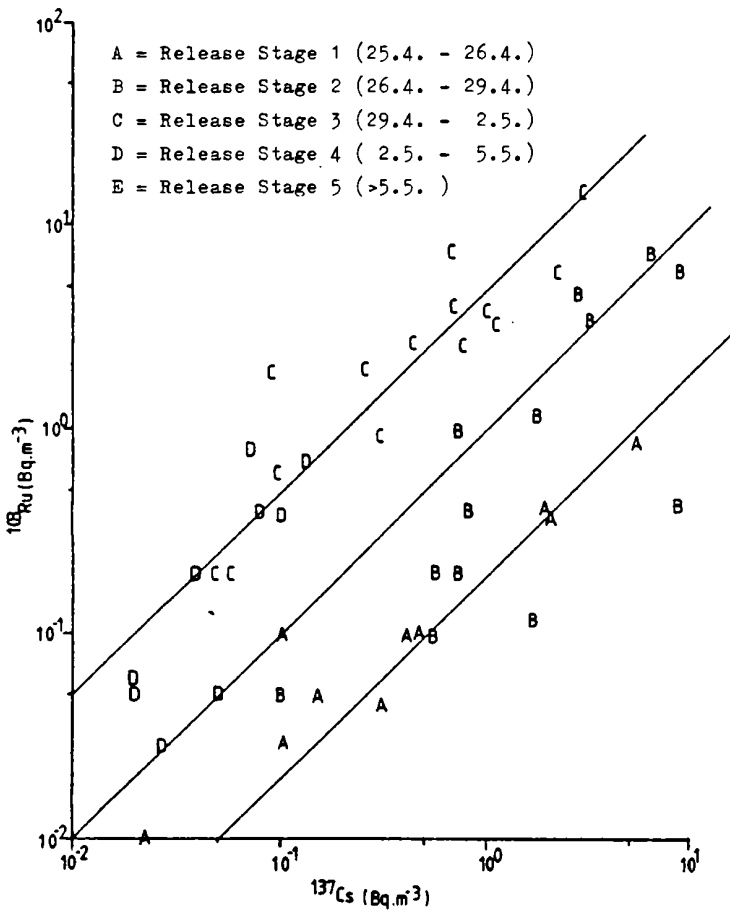


Figure 1. Ratio of $^{103}\text{Ru}/^{137}\text{Cs}$ observed for different sections of the release.

Our estimates for the total amounts of each nuclide released are within a factor of two of the Soviet estimates and somewhat lower. This is consistent since our estimates do not include the coarser material falling out locally. It is also probable that a large proportion of the inert gases including the Xenon and Krypton isotopes in the core were released in the initial phase, though there is almost no monitoring data to prove this. The general picture is that quantities released were somewhat less than figures cited in risk studies for accidents with major breaching of the containment. For example for the most serious accidents considered in safety studies for the Sizewell enquiry with regard to the building of a PWR reactor in the UK, the release postulated was complete release of the inert gases, 50% of the Caesium and 70% of the iodine, and just 2% of the more refractory nuclides like ^{103}Ru , the latter being close to that from Chernobyl including the second phase with heating of the core up to 2000°C .

4. Conclusions

This paper has illustrated how numerical models and measurements at longer distances can be used in combination to determine the quantities of individual nuclides released in gaseous or fine aerosol form and in the event of a prolonged release, an indication of the variation over time. The analysis of the Chernobyl release has indicated release terms in good accord with Soviet estimates and consistent with the pattern of events.

The application of such methods in post accident analysis is dependent on the availability of abundant and reliable measurements of air concentrations of individual nuclides from those countries affected by the release, with clear indications of the time periods to which they refer and the measuring techniques used.

Much of the work reported in this paper was funded by the CEC and their support is gratefully acknowledged.

References:-

- ApSimon, H.M. The use of computers in emergency situations and the choice of dispersion model. Proc. Intl. Symp. on Emergency Planning and Preparedness for Nuclear Facilities, 1985, Rome. IAEA-SM-280/12, 213 - 223, 1986.
- ApSimon, H.M. and Wilson, J.J.N. Numerical Modelling in the event of a nuclear accident. Proceedings of EURASAP meeting on Evaluation of atmospheric dispersion models against the release from Chernobyl, Vienna, 14-16 November 1988.
- Govaerts, P. Input data to real-time computing of consequences of radioactive releases to atmosphere. CEC workshop on real-time assessment of nuclear accidents, Luxembourg, 1985.
- Govaerts, P. and Sohler, A. Feedback of environmental survey data for the optimisation of the input parameters of assessment models during an emergency. Proc. Joint OECD/CEC workshop on Recent Advances in Reactor Accident Consequence Assessment Probabilistic Risk Assessment, Rome. CSNI-145, 2, 299-309, 1988.
- IAEA Summary report on the post-accident review meeting on the Chernobyl accident. Safety Series no 75-INSAG-1, 1986.
- Israel Y A Petrov V N Severov D A Radioactive fall-out in the close-in area of the Chernobyl NPP. Soviet Journal of Meteorology and Hydrology 7, 1987.

DISCUSSION

COMMENT: Dickerson: 24-hr averaged concentration values over Europe transformed into concentration maps would be useful data if it were available.

QUESTION: Kolb: Have you or has anyone else tried an analysis of concentration data other than in time-series for individual sites. If not - is a concentration map not considered to be helpful in model evaluation or are there other difficulties?

ANSWER: We have not done so and do not know of any such work by other groups. I agree that such an analysis could be useful in model evaluation studies.

QUESTION: Maryon. How seriously did you take to weighting exercise: how were weights allocated and how sensitive were the results (allocating weights is not a simple matter).

ANSWER: Weighting the observations was identified as a possible solution to the problems inherent in a simple linear regression. However, because of the complexity of the weighting exercise itself, it was not undertaken.

QUESTION: Pendergast: It would be interesting to try this technique to estimate source strength using the ANATEX data. Are you planning to do this?

ANSWER: I agree that the ANATEX data would be an interesting means of verifying this type of analysis. We have no plans to do such a study with MESOS at present, although we are interested in doing so and intend to investigate the appropriateness of MESOS to the data.

QUESTION: Raes: 1. Did you calculate a source term for Cs-134, and if not would it be easy and worthwhile to it? 2. How sensitive are the results to the manipulation of the data (their time of arrival e.g.)

ANSWER: 1. No. The data sets available to us when the study was carried out did not include sufficient Cs-134 data, although I understand that this is no longer the case in for example the REM data base. It would be interesting to repeat the exercise with the larger data sets now available. 2. The sensitivity studies indicated that it is possible to achieve near optimal agreement (measuring optimal agreement by the sum of the squares of the differences) between observations and concentrations with a wide range of source terms. Manipulating arrival times etc. may have a significant effect on the resulting source term, while remaining a near optimal solution in the above terms.

QUESTION: Seibert: I think it is very good that you analyze observational data, e.g. include ratios. It would be useful to extend that to more nuclides. I have heard that in southern Germany no Ag-110, has been found, which in Austria is being found in the deposition. So it may be possible to check model results and to determine from what day of release a certain material deposited stems.

ANSWER: Thank you - I agree that the consideration of nuclide ratios in radiological monitoring data may be useful in checking model results - in situations where the release dynamics are understood and in giving information on the release dynamics when the transport processes are well understood. However extending such techniques to more nuclides is dependent upon the data being available.

IV

EULERIAN/MONTE CARLO

MODELS

Transport and Deposition of Radionuclides in Europe after the Chernobyl accident studied with the European Acid Deposition Model (EURAD)

A. Ebel¹⁾, H. Geiß²⁾, H. Hass¹⁾, H. J. Jakobs¹⁾, M. Laube¹⁾, M. Memmesheimer¹⁾

¹⁾ Institut für Geophysik und Meteorologie der Universität zu Köln
Außenstelle für atmosphärische Umweltforschung
Salierring 48, 5000 Köln 1

²⁾ Institut für die Chemie der belasteten Atmosphäre
Kernforschungsanlage Jülich GmbH

Summary

The European Acid Deposition Model (EURAD) is used to investigate the long-range transport and deposition of radioactive material in Europe during the first period after the Chernobyl accident. Meteorological fields are predicted with the PSU/NCAR mesoscale model MM4. The multilayer Eulerian model CTM (Chemical Transport Model) is applied to compute transport and deposition of Cs137 using the predicted meteorological fields. The model results are compared with observations.

1. Introduction

On April 26, 1.23 local time (21.23 GMT), the worldwide most serious accident at a nuclear power plant happened in Chernobyl (51°17'N, 30°15'E). About 4% of the core inventory (ca. $2 \cdot 10^{18}$ Bq, [Persson et al., 1986]) were released from April 26 to May 6. During the weeks after the catastrophe the radioactive material could be observed everywhere on the northern hemisphere [Wheeler, 1987]. Of course, the most contaminated areas are found in Europe. However, due to long-range transport, substantial contamination caused by wet deposition of radioactive material, happened more than one week after the accident and thousands of kilometers from Chernobyl (e.g. Finland, the Alps and the northern parts of Greece).

The prediction of the movement of the radioactive material over Europe and its deposition to the ground is an interesting case for testing the capability of numerical models. Recent work on the dispersion of the radioactive plume includes trajectory calculations, Lagrangian models [ApSimon et al., 1987, Albergel et al., 1988] and Eulerian models [Pudykiewicz, 1988]. Most of these investigations are based on the observed meteorological fields. This paper describes a modeling approach with a multilayer three-dimensional Eulerian transport and removal model: the EURAD-model, which is based on the PSU/NCAR mesoscale meteorological model MM4 [Anthes et al., 1987] and the Regional Acid Deposition Model (RADM) [Chang et al., 1987]. It provides a tool for better understanding of the complex chemical and physical processes governing the temporal and spatial development of the distribution of air pollutants and is used within the EUROTRAC subproject EUMAC.

2. Model description

The mesoscale model MM4, which uses topography and landuse data for Europe, provides CTM with hourly meteorological data (wind, humidity, temperature, precipitation rate and surface pressure) for a specific episode. CTM, as MM4, is written in terrain-following σ -coordinates with 15 layers in the vertical. The horizontal resolution is 80 km and a staggered grid is used. The numerical scheme of Smolarkiewicz (1983) is applied to integrate the advection equation for the chemical constituents in time. Diffusive subgrid scale transport is parameterized with the scheme of Louis (1979). Using CTM to model the Chernobyl release the aqueous phase chemistry was shut off and the gas phase chemistry was replaced by a first order conversion process in order to model radioactive decay. The wet removal of radionuclides from the atmosphere is

described by the in-cloud and below-cloud scavenging process, assuming that the effective scavenging rate is given by the accretion rate of small cloud droplets by precipitation. The cloud droplets are assumed to have absorbed most of the aerosol particles during nucleation. The washout coefficient Λ is varied with the rainfall rate J according to *ApSimon et al. (1987)* as

$$\Lambda = 5 \cdot 10^{-5} J^{0.8}$$

where J is in mm/h.

In this first attempt we did calculations for the distribution of Cs137. Scaled SO_4 deposition velocities for Cs137 were assumed. The parameterization used follows the treatment of *Walcek et al. (1986)* and considers variability of dry deposition velocities due to land use categories, radiation, turbulent exchange and wetted surfaces. The values calculated for Cs137 are in the order of some mm/s depending on the local conditions. The period investigated here starts on April 25, 1200 GMT, and lasts till May 3, 1200 GMT. This period is splitted into three episodes (April 25 – April 28, April 28 – May 1, May 1 – May 3). A prediction of the meteorological fields was carried out for each of these episodes by MM4. For initialization and boundary conditions data of the US National Meteorological Center have been used.

In addition to the meteorological input and the parameterization of the deposition processes CTM needs the release function for the radionuclides. The time dependence of the release function is based on the USSR report to the IAEA [e.g.: *Persson et al., 1986*]. The distribution of the radioactive material into different heights during the days after the accident is given in Table 1. Due to temperatures of 3000 – 4000 K the material is assumed to reach heights up to 2000 m in the first time after the explosion (April 25 and April 26). However time dependence and emission heights are uncertain. It may be possible that the Chernobyl release has reached altitudes of 5000 m or even more as it was discussed by *Lange et al. (1988)*.

Table 1: relative distribution of the released radioactive material into the different layers of the EURAD-model

Level	approximate Height (m)	Date				
		April 25/26	April 27	April 28	April 29/30	after May 1
8	2225	10%	—	—	—	—
7	1575	40%	40%	30%	—	—
6	1090	50%	50%	50%	50%	—
5	715	—	10%	20%	50%	100%

3. Results and discussion

The meteorological situation during the first days after the accident was governed by a cyclone over the northern atlantic ocean with its center near Iceland and a high pressure system over the northeastern part of Europe. The main patterns of the large-scale geopotential fields are predicted quite well by MM4. An example is presented in Fig. 1, which shows a comparison of analysis and prediction for the geopotential height at 850 hPa for April 26, 1200 GMT. However, one should notice that some of the small-scale features present in the analysis can not be found in the predicted field (e.g.: the cyclone near the black sea at the border between the USSR and Romania). The predicted geopotential indicates also a more direct atmospheric flow towards Finland at the 850-hPa-level compared to the analysis.

One may get a first information concerning the movement of contaminated air by the calculation of three-dimensional trajectories based on the predicted windfields. An example is shown in Fig. 2 for trajectories started on April 27, 1200 GMT, at different heights (300, 750, 1500 and 3000 m). This case is interesting because trajectories starting at different heights move into different directions. This indicates the necessity to know the release height as exactly as possible to calculate the dispersion of the radioactive cloud with CTM.

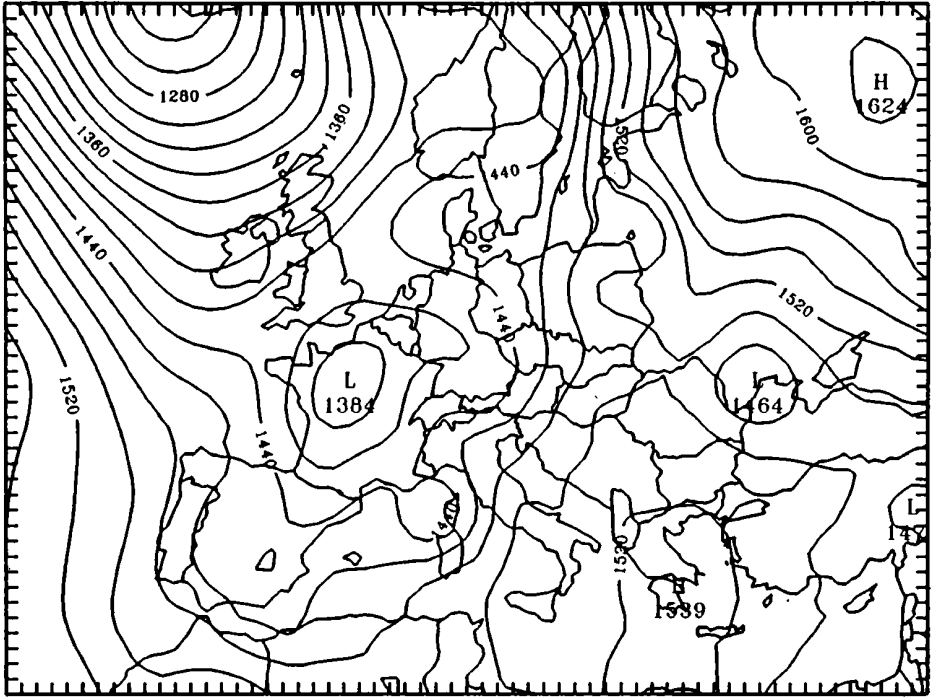


Fig. 1a: Analysis of the geopotential height at the 850-hPa-level for April 26, 1200 GMT

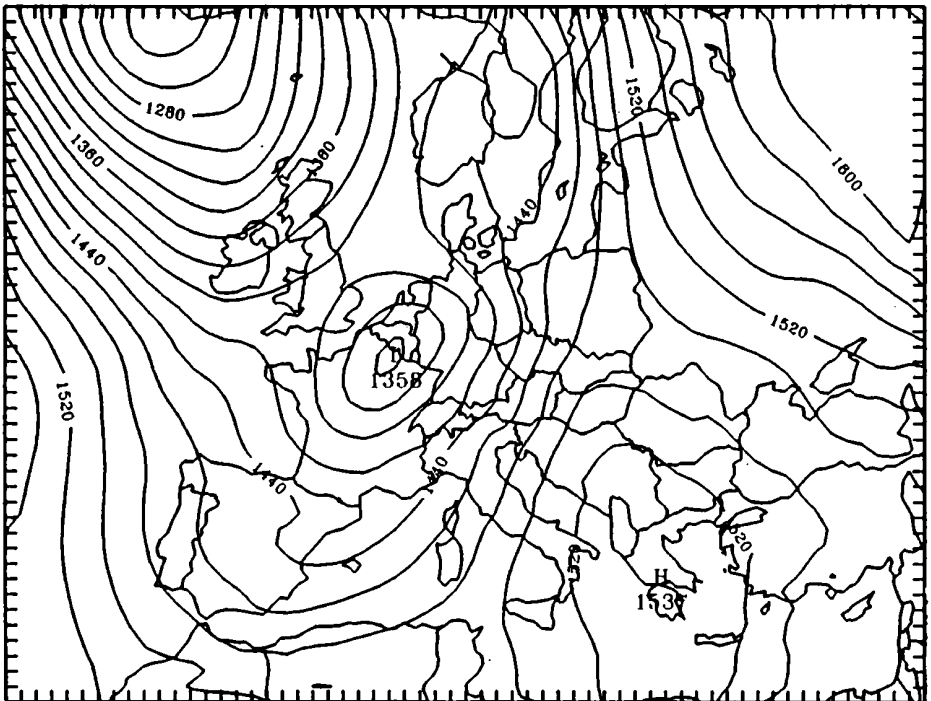


Fig. 1b: As in Fig. 1a, but for the 24-h-prediction of the geopotential height

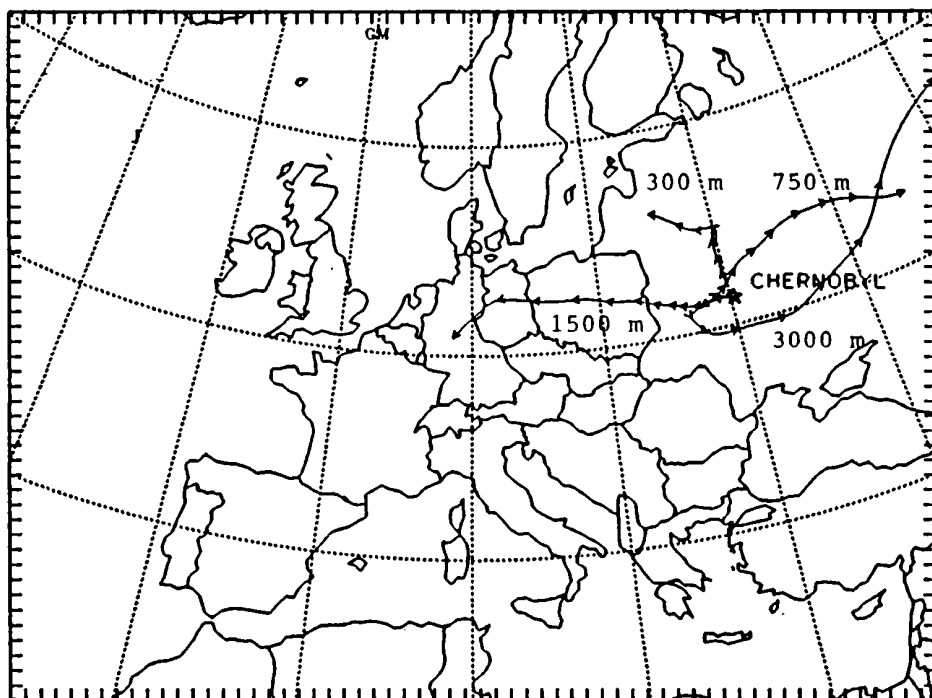


Fig. 2: Forward trajectories calculated with the predicted windfields. The trajectories are started at heights of 300, 750, 1500 and 3000 m on April 27, 1200 GMT. The arrows indicate a time difference of 6 hours.

Results of CTM calculations are presented in Fig. 3 for Cs137-activity in the lowest layer of the model, which reaches from the ground up to about 75 m. On April 28 the center of the radioactive cloud with values of about 5 to 10 Bq/m^3 is located at the border between the USSR and Finland. Two days later (Fig. 3b) the cloud is splitted into three branches: due to changing synoptic conditions the radionuclides are now transported towards the east and the west of Chernobyl reaching the southeastern parts of the Federal Republic of Germany and Austria. The situation for May 2 and May 3 is shown in Fig. 3c and 3d: at that time the radioactive material moved towards the south reaching the western parts of Turkey and Greece. The distribution of the wet deposition of Cs137, which is accumulated from April 26 – May 3 is shown in Fig. 4. It shows maximum values near Chernobyl, in Finland, the Alps and in the northern parts of Greece. These results are in good accordance with observations. However, the maximum of 250 kBq/m^2 in Finland may be to large for Cs137 alone.

A comparison between Cs137 activity observed at Nurmijärvi (Finland) and the the model results for this area is presented in Fig. 5. The maximum value of the activity calculated by the model appears in the afternoon of April 27. Unfortunately there are no data available with an appropriate time resolution before April 28. However, according to the finnish reports [STUK-A56] the arrival time for the radioactive cloud is estimated to be 3 p.m. local time which is in quite good agreement with the model calculations.

4. Further studies

In the future the Chernobyl case will be considered as one of the standard test cases for the transport and deposition part of the EURAD model. Further studies will include sensitivity studies concerning the release function, dry and wet deposition, a so-called nudged version of MM4 for the calculation of the meteorological fields and numerical experiments aiming at for a better description of the wet removal processes.

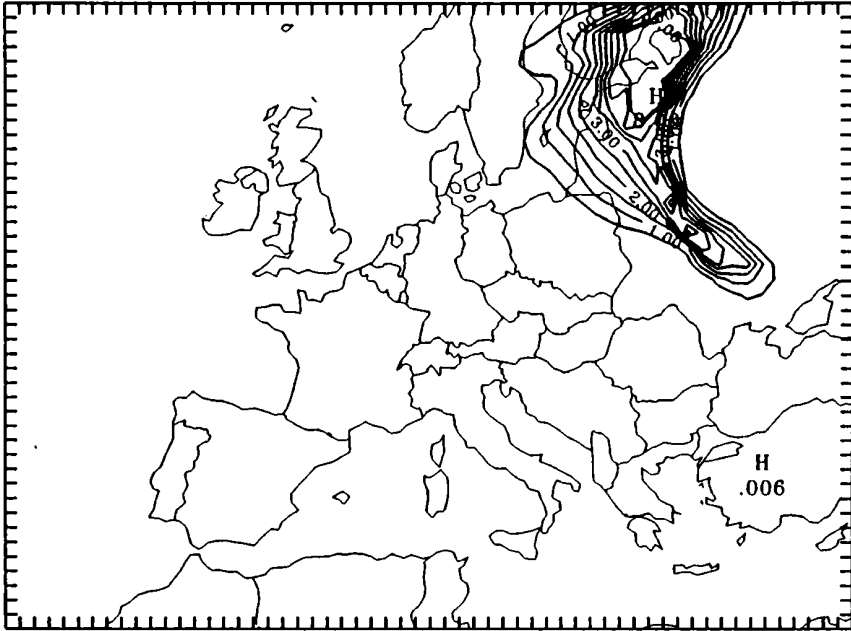


Fig. 3a: Activity [Bq/m^3] due to Cs137 in the lowest model layer (0 bis 75 m) on April 28, 1200 GMT

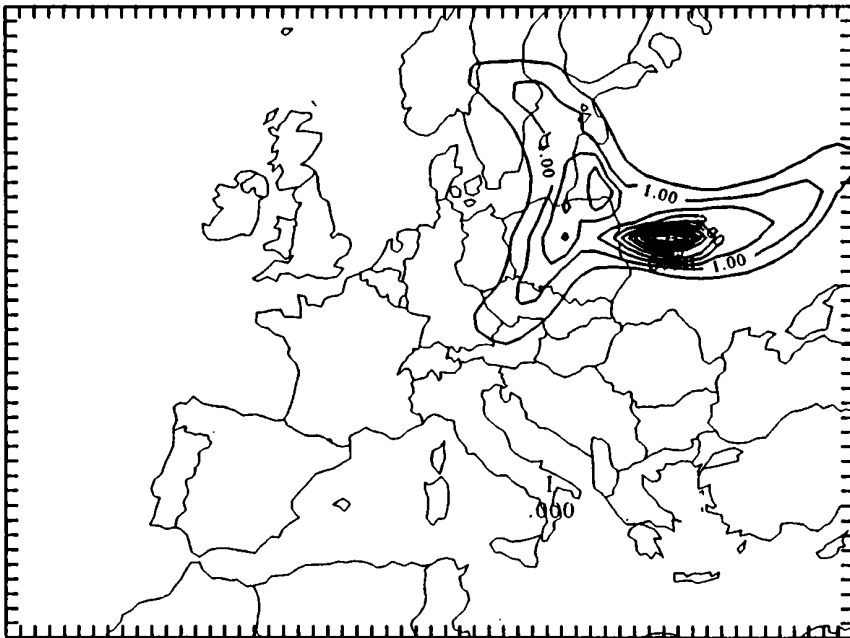


Fig. 3b: as in Fig. 3a, but on April 30, 1200 GMT

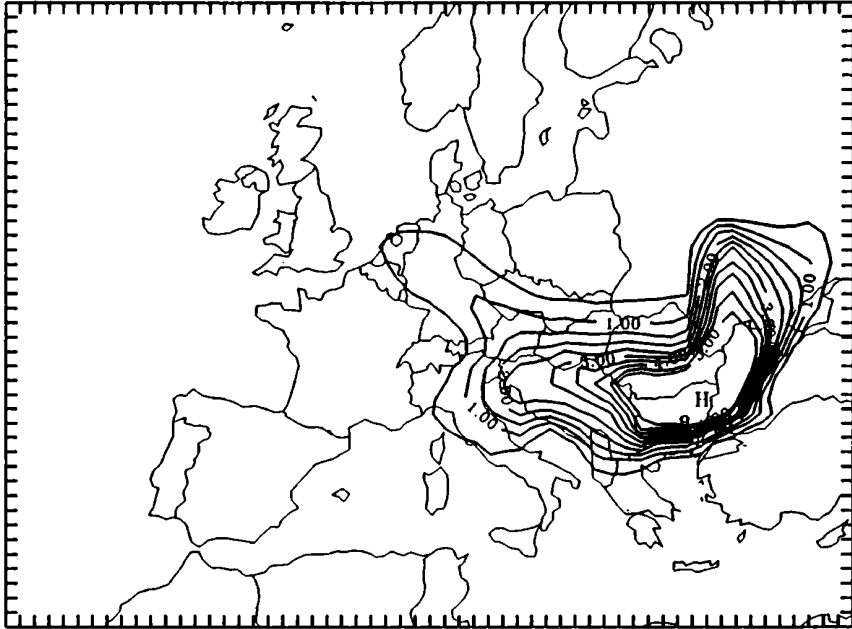


Fig. 3c: as in Fig. 3a, but on May 2, 1200 GMT

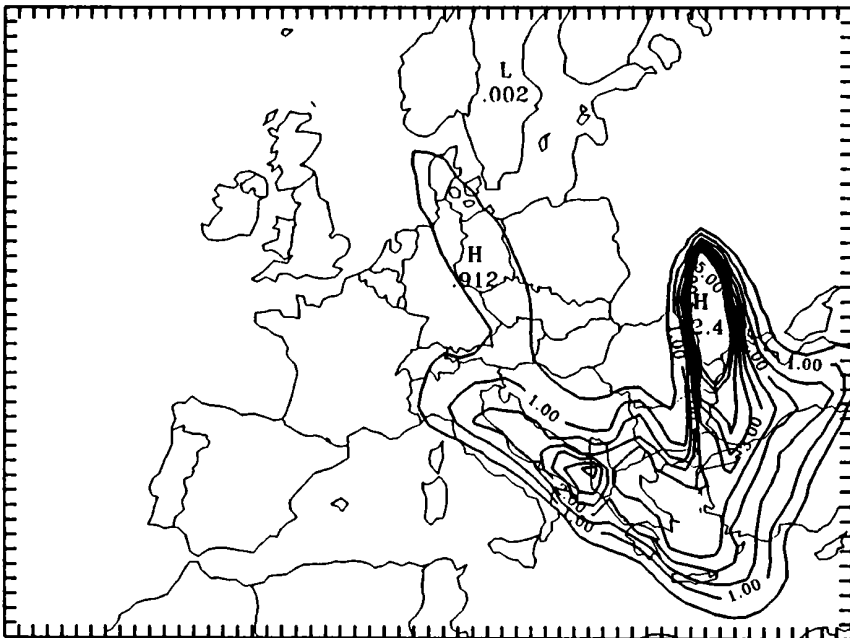


Fig. 3d: as in Fig. 3a, but on May 3, 1200 GMT

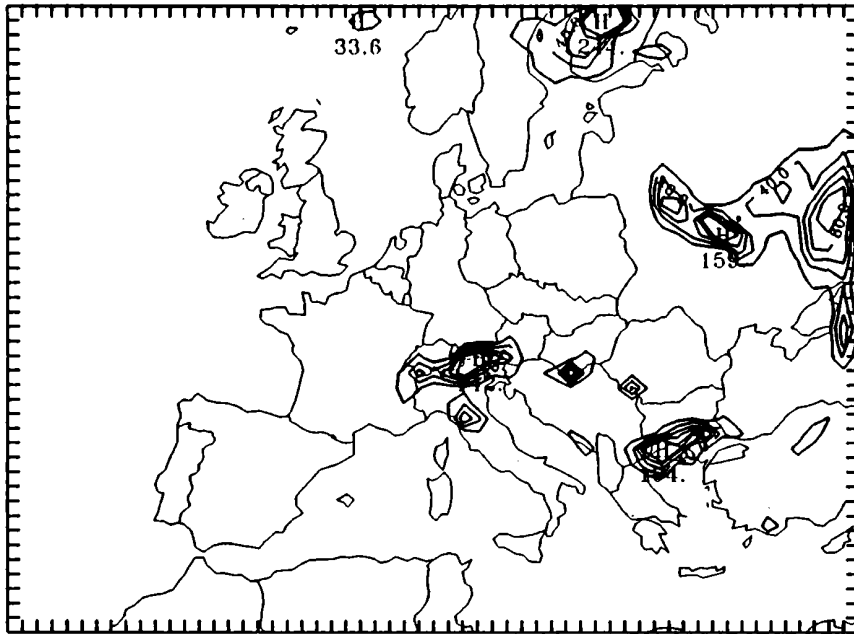


Fig. 4: accumulated wet deposition due to Cs137 [kBq/m^2] on May 3, 1200 GMT

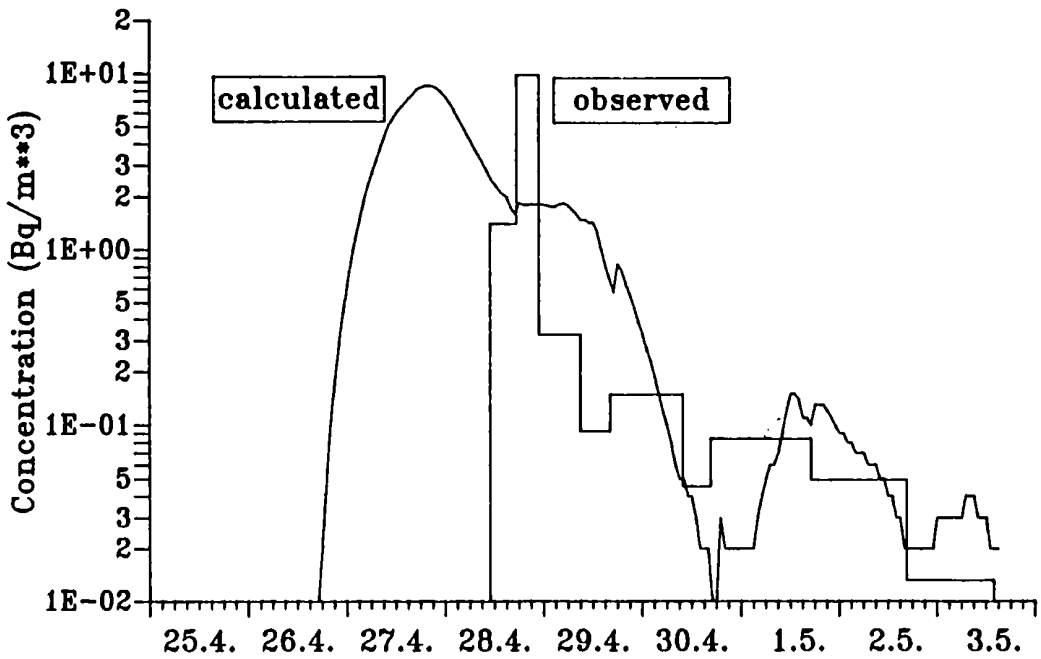


Fig. 5: Comparison of activity due to Cs137 in Nurmijärvi(south finland). The solid line is calculated by the model, the histogram is from observations.

5. References

- Albergel, A., D. Martin, B. Strauss, and J.-M. Gros, The Chernobyl accident: Modelling of Dispersion over Europe of the radioactive plume and comparison with activity measurements, *Atmos. Environm.*, 22, 2431 - 2444, 1988.
- Anthes, R. A., E.-Y. Hsie, and Y.-H. Kuo, Description of the Penn State/NCAR Mesoscale Model Version 4 (MM4), NCAR Technical Note, NCAR/TN-282+STR. 66 pp, 1987.
- ApSimon, H. M. and J. J. N. Wilson, Modeling atmospheric dispersal of the Chernobyl release across Europe, *Boundary Layer Met.*, 41, 123 - 133, 1987.
- Chang, J. S., R. A. Brost, I. S. A. Isaksen, S. Madronich, P. Middleton, W. R. Stockwell, and C. J. Walcek, A threedimensional Eulerian acid deposition model: Physical concepts and formulation, *J. Geophys. Res.*, 92, 14681 - 14700, 1987.
- Lange, R., M. H. Dickerson, and P. H. Gudiksen, Dose estimates from the Chernobyl Accident, *Nuclear Technology*, 82, 311 - 322, 1988.
- Louis, J.-F., A parametric model of the vertical eddy fluxes in the atmosphere, *Bound.-Layer Meteor.*, 17, 187 - 202.
- Persson, Chr. H. Rodhe, and L.-E. De Geer, The Chernobyl Accident, SMHI/RMK Report No. 55, 49 pp, 1986.
- Pudykiewicz, J., Numerical simulation of the transport of radioactive cloud from the Chernobyl nuclear accident, *Tellus*, 40B, 241 - 259, 1988.
- Smolarkiewicz, P. K., A simple positive definit advection scheme with small implicit diffusion, *Mon. Wea. Rev.*, 111, 479 - 486, 1983.
- Walcek, C. J., R. A. Brost, J. S. Chang, M. L. Wesely, SO_2 , sulfate and HNO_3 deposition velocities computed using regional landuse and meteorological data, *Atmos. Environm.*, 20, 949 - 964, 1986.
- Wheeler, D. A., Atmospheric dispersal and deposition of radioactive material from Chernobyl, *Atmos. Environm.*, 22, 853 - 863, 1988.
- STUK-A56, Airborne radioactivity in Finland after the Chernobyl accident in 1986. Finnish Centre for Radiation and Nuclear Safety, 42 pp, 1987.

DISCUSSION

COMMENT: Hehn: We are now in a position that model results are available, which can be compared and validated with detailed evaluations of measurement. For southern Germany the large number of measurements allowed interpolations, so that comparable color graphics have been published in 1987. Presently 2 h-averages are available for J-131 concentration measured in air near ground, giving a unique possibility for model validation.

Fraser: Dry deposition was modelled in a very detailed manner. Bearing in mind the many uncertainties contributing to deposition estimates (in airborne concentrations and precipitation) and the difficulties in validating dry deposition estimates (no standard method of measurement of actual deposition) is the inclusion of such detail in a model of this type likely to be cost-effective?

Memmesheimer: Clearly, the representation of dry deposition requires future experimental and theoretical work for its improvement and validation of the detailed parameterization in the model. On the other hand, it is necessary to provide already now enough detail regarding meteorology, surface characteristics and deposited matter to enable the study of relevant deposition processes and their relative importance under variable conditions. The code used in the model is sufficiently cost-effective in this respect.

Van Ulden: MM4 uses Blackadars turbulent closure scheme while in EURAD the Louis scheme is used. Can this give rise to inconsistencies?

Memmesheimer: There are no inconsistencies regarding the transported properties. The Louis scheme is only applied to chemical species treated in the CTM of EURAD whereas the turbulent transport of meteorological quantities is calculated separately by the MM4 scheme.

Underwood: You indicated a large number of dependencies for the dry deposition velocities. How are these dependencies obtained for the specific case of Cs137?

Memmesheimer: Dry deposition velocity is computed in the model using resistances for its parameterization: $v_D = (r_a + r_b + r_s)^{-1}$. r_a is the aerodynamic resistance, r_b the resistance due to the viscous sublayer and r_s the surface resistance. The aerodynamic resistance depends on the Richardson number, the surface resistance on landuse characteristics, season and solar insolation. Among others, r_s is determined by the physical and chemical properties of the deposited material. The specific case of Cs137 deposition velocity is treated in the same manner as particulate sulfate.

Serrano: What are the advantages and disadvantages of the MM4 model compared with European models (like ECMWF, etc. or LAM's)?

Memmesheimer: The chemical transport modul of the EURAD model is well adjusted to the MM4. The use of other models (like the Europa Model of the DWD) requires special interfaces which have not yet been designed. Yet it is planned to carry out simulations with other meteorological models in the future. One of the great advantages of MM4 is its extreme flexibility regarding its application to different regions, e.g. different parts of Europe, and that its performance has well been tested for a larger number of cases with varying geographical conditions.

Seibert: Some of the speakers were obviously not sure, what release height they should take. I think we should discuss this problem. My opinion is: 1) For models without vertical resolution, the release height is not very important, since the material will soon get mixed vertically. The transport velocity then will be a center-of-mass velocity or maximum wind speed within the mixed layer. 2) For models with good vertical resolution it may be better to prescribe a vertical profile of the source term instead of a single release level.

Memmesheimer: I will only comment on the second statement: our opinion is that it is important to have the correct release function in time and space. Preliminary calculations show that the model results (arrival time, concentrations) are sensitive to the release height. In our base case we have used a vertical profile for the released material.

Geiß: To check the sensitivity we did a second run with keeping the releases in the third layer (150 to 350 m) for the second and the following days. The time variation of the ground level activity changed dramatically at Vienna. The base case calculation gives an activity maximum during the night from May 1 to May 2. The second run shows a first maximum on April 29 and a second higher maximum on April 30 only due to changes in release height.

Labrousse: Which boundary conditions did you use? What do you mean by "using in the future meteorological data from ECMWF and from DWD"?

Memmesheimer: We have used relaxation boundary conditions. This involves the "nudging" of the model-predicted variables toward a large scale analysis. We have used the NMC global analysis as a first guess to perform a Cressman type objective analysis. In the future we intend to use also ECMWF data for initialization and nudging of the mesoscale meteorological model. Instead of MM4 the Europa Model of the DWD could also provide the Chemical Transport Module of the EURAD model with the meteorological data which are needed to perform the dispersion calculations.

Urbancic: What kind of model for wet deposition do you plan to include in the EURAD model?

Laube: Wet deposition is included in the model. It is calculated as a function of precipitation rate and mean liquid water composition during the cloud life time.

Ishikawa: What kind of turbulent model do you use in your model?

Memmesheimer: We use a first order closure scheme: Blackadar is used in MM4, Louis scheme in CTM.

Musson-Genon: What sort of precipitation scheme do you have in your model? Have you realized some comparison between predicted precipitation and observed precipitation?

Laube: The precipitation scheme follows Hsie: condensation, autoconversion, accretion, evaporation and terminal velocity of rain water is considered. Until now we have made no detailed comparison with observed data. This will be done in the near future.

Dickerson: Have you investigated the numerical diffusion in the model?

Memmesheimer: Numerical diffusion in the chemical transport module of the EURAD model is due to the Smolarkiewicz scheme which is used to integrate the advection of species in time. The properties of this scheme were investigated by Smolarkiewicz (1983) and during the development phase of RADM (Chang et al., 1987), especially for the problem of numerical diffusion. However, the extent to which CTM can evaluate source-receptor relationships for different emission sources (point sources, area sources) must be evaluated carefully. This will include further investigations of the numerical diffusion in the advection scheme. Studies concerning this problem are currently underway.

Pinnger: In your Finland example, you showed that your trajectories arrived earlier than the radioactive cloud. Is this a general feature of your model?

Memmesheimer: No. Trajectories starting at other times may arrive at the right time. Dispersion the radioactive cloud as well as trajectory calculations may be sensitive to the predicted meteorological fields. The early arrival time in the Finland example may be caused by a too early initialization of MM4. For the study presented here MM4 is started for April 25, 1200 GMT. Studies which will investigate the influence of initial conditions (e.g. initialization on April 26, 0000 GMT) are underway. However, one should notice, that no detailed information on the time variation of activity before April 28 is available at Nurmijärvi. Therefore we should be careful with statements concerning the validation of model results on April 27.

THE USE OF NUMERICAL WEATHER PREDICTION MODELS OF THE
DEUTSCHER WETTERDIENST IN AIR POLLUTION MODELLING

Ingo Jacobsen and Ulrich Pflüger

Deutscher Wetterdienst, D-6050 Offenbach, FRGermany

Summary : The supply of meteorological input data to air pollution models is discussed and a method to generate these data by numerical weather prediction models presented. The proposed 'nudging method' smoothly connects several short-range prediction runs avoiding discontinuities at the connection points and an unlimited growth of forecast errors. In connection with the Europa-Modell of the DWD it can also supply the liquid water content of clouds and the appropriate micro-physical conversion rates. Results from a 20 day simulation run are presented. Windfields from the ECMWF analyses, short-range predictions and nudged simulations are used to calculate two- and three-dimensional trajectories from Chernobyl and going back from Germany to Chernobyl.

1. Introduction

Results of numerical weather prediction models are becoming increasingly important as input data to air pollution models because:

- Complex Eulerian air pollution models like ADOM/TADAP (see Venkatram and Karamchandani, 1987) or RADM (NCAR, 1985) are used in a diagnostic mode, i.e. they need meteorological input data for periods in the past. The required data, however, cannot be supplied by routine observations alone since the list of input data includes quantities like vertical velocity and cloud-physical quantities such as cloud water content and conversion rates, since the integration area often covers regions with only poor data density (e.g. precipitation data over the North Sea or the Baltic), and since the input is needed at high spatial and temporal densities.
- Prognostic problems as, for instance, the prediction of smog advected from distant sources, and the prediction of the transport, dispersion and deposition of hazardous material from accidental releases obviously need the weather forecast.

Air pollution models designed to study the behaviour of different chemical species within the framework of scenarios or to calculate country by country emitter-receiver matrices can derive their meteorological input data by different methods:

- (a) Short-term predictions are used to interpolate the observations, and the additional variables are computed diagnostically by special subprogrammes.
- (b) The output of the numerical weather prediction models is directly used as input to the air pollution model.
- (c) Short-term predictions are connected by a nudging method.

All three methods have their own merits and drawbacks and depend on the weather prediction model used for this task. Despite the improvement in analysis and data assimilation schemes, actual gradients are smoothed in the analysed fields, and weather prediction models need a spin-up time to generate fields consistent with their resolution and physical content. The resulting differences between the forecast fields and analyses may lead to discontinuities at the connection points of consecutive short-term prediction runs, as well as to physical inconsistencies where different data structures do not match.

If priority is given to observations, meteorological fields needed as input to air pollution models but not obtainable directly from observations have to be computed diagnostically using special subprogrammes. This is especially true for convection and cloud-micro-physical conversion rates. Such subprogrammes, however, are physically restricted when used in a diagnostic computation.

On the other hand, the growth of model errors limits the applicability of weather prediction models as a direct data source to one or two days. As this short period is insufficient for most of the air pollution models, the output of weather prediction models can be used only if the growth of errors can be limited to a tolerable amount over longer periods. This can be achieved by the nudging method described in chapter 2.2.

Models to predict the long-range advection of smog or the transport, dispersion and deposition of hazardous material from accidental releases obviously need the direct output from weather prediction models. But in most cases, they also need meteorological data from the preceding days because the computations have to cover periods longer than the predictability of the weather prediction models. Hence computations have to be updated using the best combination of data from 'analysis' and forecast which is called the mixed mode.

Consequently, the German Weather Service (Deutscher Wetterdienst-DWD) decided to generate input data for air pollution models running in diagnostic, prognostic and mixed mode as well by its numerical weather prediction models.

2. Preparation of meteorological input data for complex air pollution models with the Europa-Modell of the DWD

The decision to generate the meteorological data input to the TADAP model by nudged simulations with the Europa-Modell and to offer the same for the RADM model within the framework of EUMAC was favoured for two reasons:

- (a) The Europa-Modell can supply (after some minor changes) all of the data needed for the TADAP model.
- (b) The nudging method is capable of creating continuous and consistent fields, avoiding an unlimited error growth and discontinuities for any period.

2.1 The Europa-Modell

The Europa-Modell is a limited area weather prediction model for the region North Atlantic - Europe. It is now tested on the Cray XMP at the ECMWF and the new ETA 10 computer of the DWD. After the implementation of a new model suite (1989/90) consisting of a global spectral model and the Europa-Modell, the Europa-Modell will be the central weather prediction model of the DWD. A description of the Europa-Modell is given in Müller et al. (1987).

The reasons for favouring this model for environmental applications are:

- A high vertical resolution of 18 layers with 8 layers between the ground and 2 km height allows a good representation of the atmospheric boundary layer.
- The model predicts the cloud water content q_c and calculates the cloud-microphysical conversion rates including the ice-phase, using a Kessler-type scheme for the parameterization of the stable precipitation.

In order to compute cloud-microphysical conversion rates also for convection, the parameterization of convection normally used in the Europa-Modell has been changed to a Kuo-type scheme including a one-dimensional cloud model with the same microphysical package as used for stable precipitation.

2.2 The nudging method

The nudging method used to generate the meteorological input data for complex air pollution models is schematically depicted in Fig. 1, where the RMS-difference between the simulation runs (A and A_R) and the analysis has been chosen to measure the quality of the simulation. The nudged simulation (thick solid line) is performed by adding relaxation terms $\lambda(A_R - A)$ to the prognostic equations for $A = (u, v, h, q_w, p_s)$, where $h = c_p T + Lq_v$ is the total heat, $q_w = q_v + q_c$ the total water content, and q and q_c the specific contents of water vapour and cloud water, resp.. By performing a forecast with added relaxation terms instead of taking the reference field itself, the corrections are distributed over a longer period of time and the generated fields (except for the influences caused by the relaxation terms) in balance with the nonlinear physical forcing (e.g. advection, turbulence, cloud-microphysics).

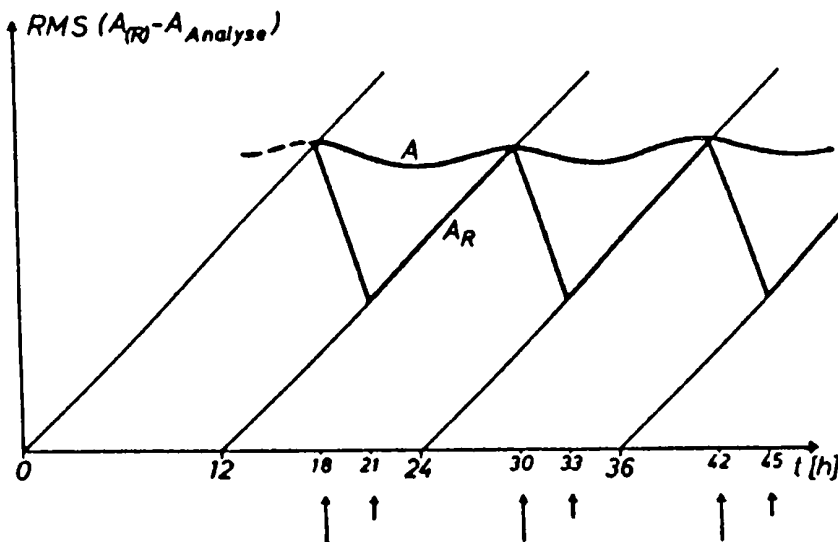


Fig. 1 : Schematic representation of the nudging method. Dashed lines: A_R = reference fields, thick solid line: A = nudged simulation, thin solid lines short prediction runs.

The reference fields A are taken from short term forecasts (thin solid lines) after the spin-up phase has been completed.

The choice of the predicted fields as reference fields A_R instead of the analysed fields is done for two reasons:

1. The analysis does not provide fields of the cloud water content q_c .
2. The forecasted field exhibits in most cases a more detailed and even more realistic picture of the atmosphere.

Fig. 2 and 3 show examples from a 20 day episode simulated using the nudging scheme.

Fig.2 demonstrates in detail how the nudging method works. The predicted moisture field (b) is superior to the analysis (a) with respect to the intensity of the gradient in the frontal region, but inferior with respect to position. This error in position resulting from phase errors is corrected by the nudging mechanism, but the gradient is slightly weakened thereby (c). Another factor contributing to the flattening of sharp gradients and to a slight reduction of convergences is the linear interpolation of the reference fields over 3 hour intervals. These intervals will be reduced to one hour for future operational applications. The correction of phase errors is shown even more clearly in (d) where the thick lines (solid and dashed) mark the maxima of the rising motion of the three different forecasts.

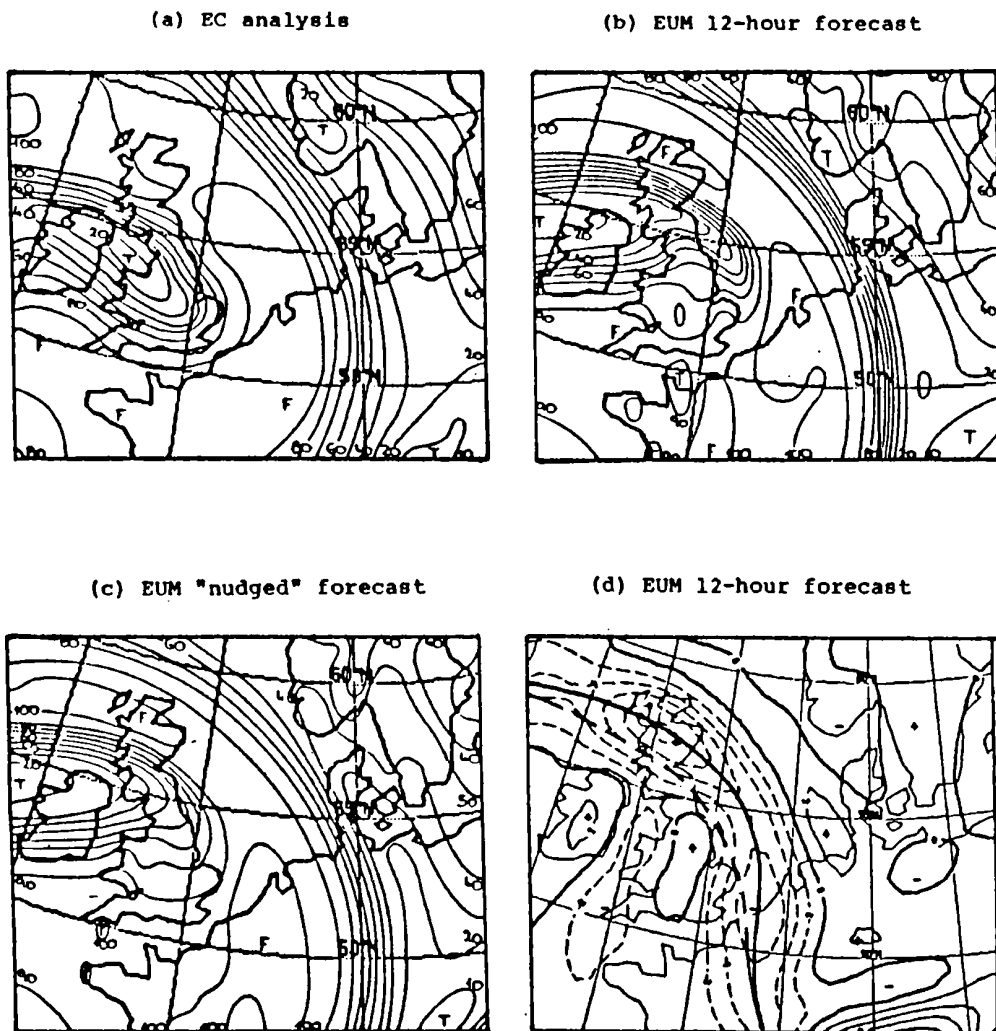


Fig. 2 Relative humidity (%) at 500 hPa (a-c) and vertical velocity (0.1 Pa/s) at 700 hPa (d) valid at 3 March 1982, 00 UTC

Maximum rising motion:
 — EUM 12-hour forecast and "nudged" forecast
 - - EUM 36-hour forecast

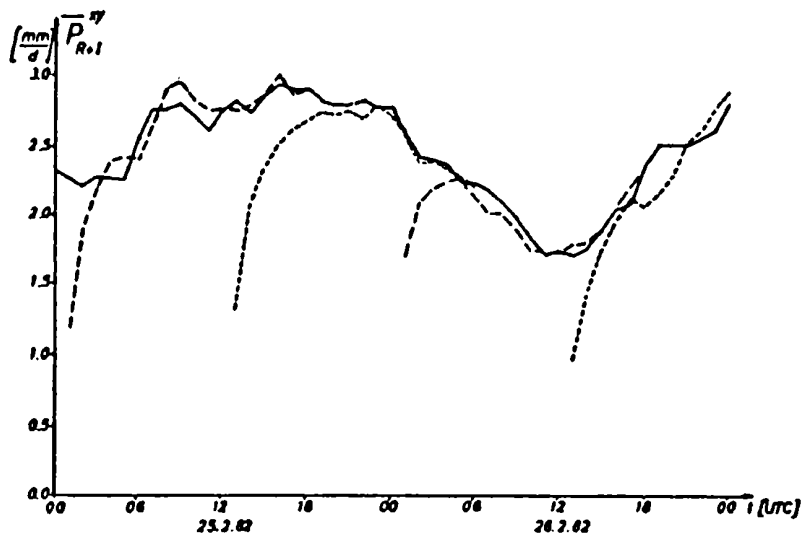


Fig. 3 Area average of the precipitation rate of reference forecast (dashed) and the continuous nudged simulation run (solid line)

Fig. 3 displays the area average of the precipitation rate for day 6 and 7 of the 20 day episode. The solid curve representing the nudged forecast fits very closely the subsequent short term prediction runs (dashed lines) after the individual spin-up phases. Estimated over the whole 20 day period, the nudging mechanism combined with the linear interpolation of the reference fields leads to an overall reduction of the precipitation amount of less than 5% as compared with the short-term predictions.

The RMS-differences between the nudged simulations and the ECMWF analysis remain limited over the whole period. For instance, the RMS-difference for the temperature stays below 1 K except for the lowest layers, where higher values reflect the more detailed orography of the Europa-Modell and the different schemes for parameterizing the atmospheric boundary layer and the soil processes.

2.3 Application to complex Eulerian air pollution models

Nudged simulations with the Europa-Modell have been performed for a 20 day period in February and March 1982 and a 7 day period in August and September 1985. Applications of the data from the first period as input to the TADAP model have been presented by Stern and Scherer (1988 a,b). The overall quality of the data seems to be satisfactory, though there have been some special problems in some places and at some times. This result will be used to improve the method by choosing time dependent relaxation factors and by giving greater weight to those short-term predictions that have a smaller forecast error. Computations with the TADAP model show that the numerical structure of both models, the meteorological model and the air pollution model, should be as similar as possible in order to avoid unnecessary interpolations which may lead to spurious divergences and vertical velocities. The TADAP model will therefore be rewritten to meet the vertical structure of the future operational Europa-Modell.

3. Prediction of long-range advected smog and hazardous material from accidental releases

3.1 Prediction of long-range advected smog

The German Weather Service (DWD) supports a project of the Federal Environmental Agency (Umweltbundesamt - UBA) to predict smog advected over long distances. As a first step in this direction, a version of the MESOS model (ApSimon et al., 1985) as modified by the Nuclear Research Center in Karlsruhe has been implemented on the computers of the DWD. At present this model uses the wind fields predicted by the operational hemispheric model BKF (mesh size 254 km). The first test phase will start in the winter of 1988/89. Future plans are to use the wind fields from the Europa-Modell and a more sophisticated air pollution model.

3.2 Trajectory calculations

At present trajectories are computed based on the wind fields of the current limited area model BKN (mesh size 127 km).

A new trajectory model using different data sets has been tested with data from the Chernobyl period. These data sets are:

- ECMWF analyses interpolated to the mesh size and orography of the Europa-Modell (Majewski, 1985),
- short-term predictions of up to 18 hours by the Europa-Modell,
- a nudged simulation with the Europa-Modell and
- an eight day prediction without nudging by the Europa-Modell.

These data sets are used to calculate three-dimensional forward trajectories starting at Chernobyl, and two- and three-dimensional trajectories going back from Germany to Chernobyl. The forward trajectories were started between 25 April 1986, 21 UTC, and 27 April 1986, 12 UTC, at 25 hPa height increments between 975 and 700 hPa; the backward trajectories at Munich and Aix-la-Chapelle, at times when the measurements indicated that a plume originating from Chernobyl has passed (Fig.4). Back-trajectories were only computed from arrivals in the lowest 200 hPa, and the two-dimensional trajectories were horizontal on the sloping σ -layers of the Europa-Modell.

Fig. 5 shows the areas passed by several trajectories. There are distinctly two sets of trajectories reaching Southern and Western Germany when washout and/or rainout lead to increased radioactivity at the ground between 30 April and 2 May, 1986. Some of the trajectories stayed in the boundary layer whereas the others went up to greater heights and passed Germany at 3 to 5 km height.

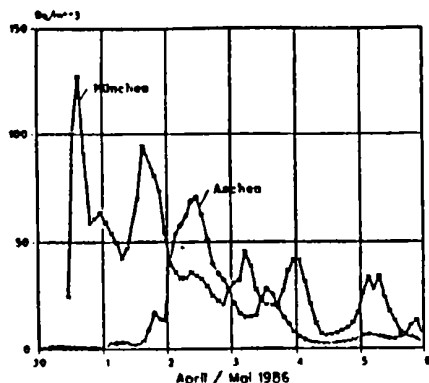


Fig. 4
Measurements of beta-activity at Munich (München) and Aix-la-Chapelle (Aachen)

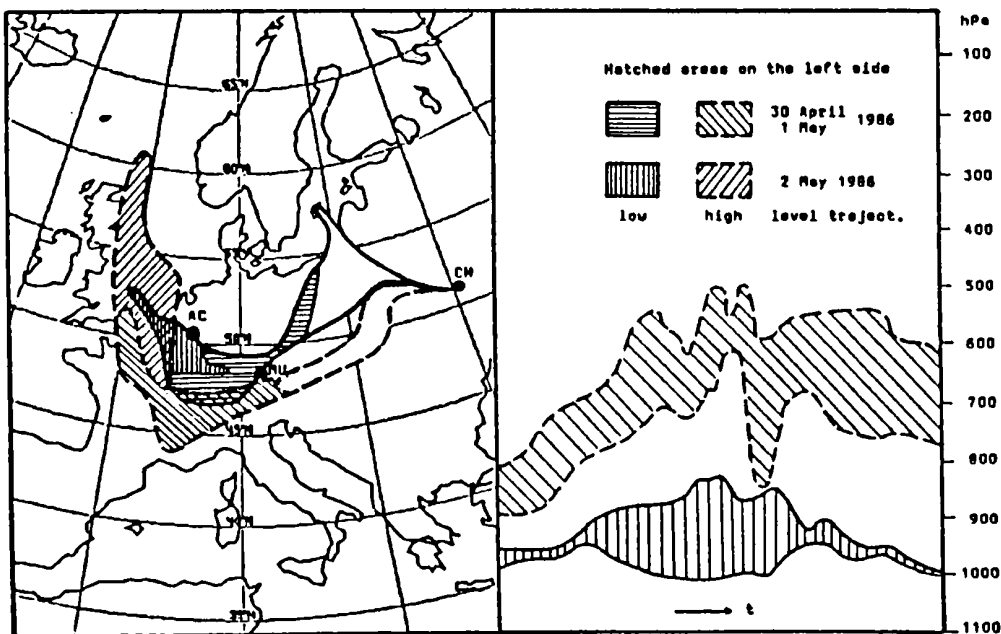


Fig. 5 Horizontal (left) and vertical (right) projections of trajectories from Chernobyl (CH) reaching Southern and Western Germany (MU=Munich, AC=Aix-la-Chapelle). Regions passed during measurements of increased concentrations are hatched.

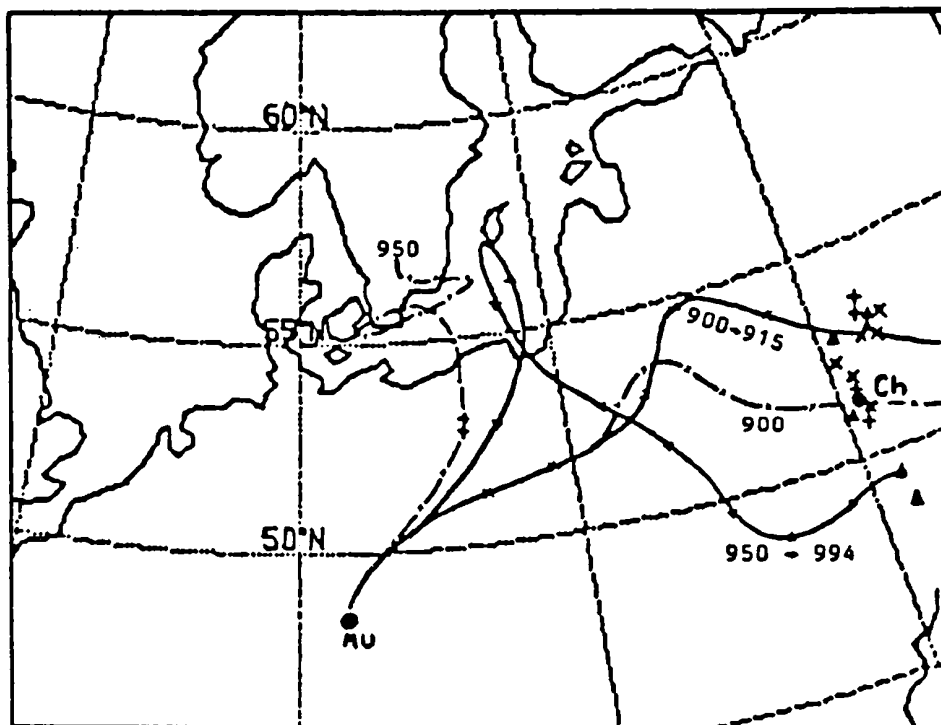


Fig. 6 Back-trajectories started at Munich on 30 April 1986, 15 UTC
 Points nearest to Chernobyl (Ch): + ECMWF-analysis ,
 Δ nudged simulation, x short-range predictions
 Selected trajectories with (——) and without (— — —)
 vertical velocity with departure and/or arrival height in hPa

Because of the great variability of the three-dimensional forward trajectories especially resulting from the interaction of vertical wind shear and vertical motion, a quantitative evaluation of the quality of the data sets used was hampered. As expected, the 8 days forecast proved inadequate. In order to get a quantitative measure, two- and three-dimensional backward trajectories were computed and their minimum distance to Chernobyl calculated. Fig.6 shows selected back-trajectories and the places where the trajectories started at Munich on 30 April 1986, 15 UTC came closest to Chernobyl.

Table 1 : Minimum distance (km) between back-trajectories and Chernobyl. Trajectories which obviously went wrong set in parenthesis and not used to calculate the mean values.

Starting point , height and time		ECMWF-analysis		Short-term prediction		Nudged simulation	
		2-d	3-d	2-d	3-d	2-d	3-d
Munich 30 April 1986 15 UTC	950 hPa	(967)	(969)	275	197	94	69
	900	48	42	9	198	11	173
	850	249	228	213	264	182	249
	800	311	300	313	286	297	289
	800-950	203	190	202	236	104	195
Munich 1 May 1986 15 UTC	950 hPa	190	267	55	(993)	(976)	(1027)
	900	230	212	482	280	455	247
	850	335	13	360	364	339	337
	800	318	226	357	332	352	326
	800-950	268	177	314	325	382	303
Aix-la-Chapelle 2 May 1986 12 UTC	950 hPa	(890)	63	(661)	272	421	359
	900	341	112	335	258	338	322
	850	374	113	346	531	318	325
	800	268	348	361	436	352	286
	800-950	313	159	347	374	357	323
mean value		262	174	282	310	271	271

The Table 1 shows a numerical evaluation of the minimum distances to Chernobyl for the three data sets and the two versions. All data sets yield results of similar quality. This again proves that nudged simulations can be used in the diagnostic mode and in the mixed mode together with forecasts in order to generate continuous data sets.

After the implementation of the new model suite (global spectral model, Europa-Modell) the trajectory model will be used on the whole globe. The program will automatically select the data set containing the most detailed information according the current position of the trajectory.

4. Development of a Lagrangian particle model

The development of a Lagrangian particle model is under way. It will make use of the existing trajectory model and a Lagrangian particle model developed at the Technical University Darmstadt for application on a local scale. First runs to test the coding have been performed. In the first phase, it will only calculate transport and dispersion using the wind and turbulence fields (including the turbulent kinetic energy from the second order closure scheme) of the Europa-Modell. Dry and wet deposition will be included in the second phase.

The Lagrangian particle model will be part of a national early warning system consisting of ground based measuring stations and (in case of a nuclear accident) of measurements by aircraft. It will be the task of the DWD to make predictions of the probable position of a plume to facilitate its localization by aircrafts. As these measurements shall be used to improve the model results, a correction scheme has to be developed in the last phase of model formulation. The model will be tested with data from Chernobyl and tracer experiments like CAPTEX and ANATEX.

The development of the method of nudged simulations and of the trajectory program was sponsored by the Federal Environmental Agency of the Federal Republic of Germany.

References

- ApSimon, H.M., A.J.H. Goddard and J. Wrigley, 1985: Long range atmospheric dispersion of radioisotopes. The MESOS model. Atmos. Envir., 19, 99-111
- Majewski, D., 1985: Balanced initial and boundary values for a limited area model. Beitr. Phys. Atmos., 58, 147-159
- Müller, E., D. Frühwald, I. Jacobsen, A. Link, D. Majewski, J.-U. Schwirner and U. Wacker, 1987: Results and prospects of mesoscale modelling at the Deutscher Wetterdienst J. Meteor. Soc. Japan, Special Vol., 533-546
- NCAR, 1985: The NCAR Eulerian regional acid deposition model. NCAR/TN-256 + STR, NCAR, Boulder, 178 p.
- Scherer, B. and R. Stern, 1988: Simulation of an acid deposition episode over Europe with the TADAP/ADOM Eulerian regional model. NATO/CCMS 17th Internat. Tech. Meeting on Air Pollution Modelling and its Applications, Cambridge, UK
- Stern, R., B. Scherer and J. Pankrath, 1988: Application of a regional model for the transport and deposition of acidifying pollutants to Central Europe. Air Pollution Modeling and its Application VI, ed. H. van Dop, New York and London 1988, 415-430
- Venkatram, A. and P. Karamchandani, 1988: Simulation of an acid deposition episode with a comprehensive long-range transport model. Air Pollution Modeling and its Application VI, ed. H. van Dop, New York and London 1988, 403-413

DISCUSSION

QUESTION: Ishikawa: Do you have a plan to use a kind of dispersion model into your model?

ANSWER: Ten years ago we used an experimental version of our model to simulate the transport, dispersion and deposition of SO₂ and SO₄ in the gas and the water phase. In the last year we prepared the meteorological input to the TADAP model with the Europa-Modell of the DWD and the nudging method. We wrote the full output of our model on an output file every 1 h and additionally the one hour mean values of the convective micro-physical conversion rates and vertical velocities. This has been done for a 20 day and an 8 day episode. We will continue this work within the framework of the EUMAC project. Within the EUMAC project we also want to revitalize our old SO₂/SO₄ model to perform sensitivity studies.

THE DEVELOPMENT OF THE U.K. OPERATIONAL MULTI-PARTICLE TRANSPORT AND DISPERSION MODEL.

R.H.Maryon and F.B.Smith

Meteorological Office, London Road, Bracknell, Berkshire, U.K.

SUMMARY. The National Response Plan initiated by the U.K. Department of the Environment following the accident at Chernobyl required the development of a fast-response numerical model capable of simulating the transport, dispersion and deposition of radionuclides released into the atmosphere from any European installation. A brief account is given of the progress on the model to date, and of an application to the radioactive release from Chernobyl. The model is intended to utilize both meteorological and radiological data, as far as possible in 'real time'. It is a three-dimensional multi-level, multiple particle model simulating sub-grid scale motions by random perturbations and incorporating a realistically evolving boundary layer. Air concentrations, radioactive decay and dry deposition to the surface are computed. Work continues on wet deposition, and there are plans to incorporate adjustments using the observed radiology.

1. INTRODUCTION: PROJECT ORGANIZATION. An outline of the nuclear accident response modelling project is shown schematically in Figure 1. The work is divided into three main parts - (a) the numerical modelling of transport, dispersion and deposition of radionuclides released into the atmosphere, (b) a rainfall package for use in wet deposition estimation and (c) a radiological package to enable observations to be compared with the model output and for use in consequent modification of the model

assumptions and products. The work has developed into a collaborative project under the lead of the Boundary Layer and Atmospheric Chemistry branch of the Met Office with the Safety and Reliability Directorate of the UKAEA (SRD) responsible for the radiological package, while background studies into wet deposition processes will be undertaken by Dr Choularton's group at UMIST and Dr ApSimon's group at Imperial College.

The model is designed for real-time response to an accidental release of radionuclides. Simplified versions can be run in an emergency by the duty weather forecasting staff at the Central Forecasting Office at Bracknell, while more detailed accident analysis can be carried out subsequently by specialized staff. The model can be run in forecast or hindcast mode, with a facility for 'update' runs as fresh data become available.

2. MODEL STRUCTURE. The model is multi-level, the lowest level being the atmospheric boundary layer (BL) and accordingly of variable depth. Otherwise the layers correspond to those of the U.K. Met Office 'fine mesh' operational numerical weather prediction suite (FMM) from which the wind and temperature fields used by the nuclear response model are derived. The horizontal resolution of the model is also based upon that of the FMM, i.e. 0.9375 degrees of longitude, 0.75 degrees of latitude covering an area from 30 - 80 deg. N and from 80 deg W to 40 deg E. Forecast products from the FMM are, of course, available on an operational basis, and a 10-day 'roll-over' archive has been created which contains analyses from the most recent past.

The model is Lagrangian, of the Monte Carlo type. A large number of particles, each 'carrying' a mass of pollutant or quantity of

radioactivity, is released into the model atmosphere from the source, and advected in the 3-dimensional motion fields. The basic forward timestep

$$dx = \underline{u} dt$$

is used, as any more sophisticated integration scheme would prove too expensive computationally, and probably unnecessary, given the random walk formulation. The winds are interpolated from the grid values linearly in space and time. The 'start' distribution of particles among the model levels is prescribed at the outset, as is the allocation of mass among the particles; full emission profiles in space and time can be defined in this way.

Sub-grid scale turbulence is simulated by the addition of a random component - that is, the horizontal position of each particle is assumed to evolve according to the Markov chain

$$x_{i+1} = x_i + \underline{u}(x_i) \Delta t + \underline{A} r.$$

Here, \underline{A} is a constant coefficient vector which if viewed in terms of K-theory can be identified with $(2\Delta t K)^{1/2}$ where Δt is the timestep, K a horizontal diffusivity. r is an independent standard normal variable. The addition of a random velocity component is not considered necessary on these scales. These perturbations are most important in the BL where turbulent mixing is the norm, but they are also applied with a reduced \underline{A} for a limited distance above the inversion (i) to give effect to sub-grid scale motions at these levels, (ii) to improve the statistical reliability of the ensemble of particles released in hourly batches.







The eddy turnover time in a convective BL (CBL) may be approximated z_i/w_* - say about 15 minutes, which was the value adopted for the model

timestep. At each timestep all the particles below the inversion are randomly reassigned in the vertical within the BL. After a few timesteps material may be assumed to be well mixed through the BL, and this reassignment will allow the particles to sample the winds at all levels in the BL (as would occur naturally in convective overturning), thus giving effect to the vertical shear. Above the BL shear can be represented to some extent by 'stacking' the particles in the vertical at the time of release. The magnitude of \underline{A} needs to be larger for 2-dimensional models than for 3-dimensional, which can represent the dispersive effect of shear in this fashion; the 'best' values for both types will be the subject of further study.

RANDOM WALK MODEL - CHERNOBYL RERUN

AIR CONCENTRATION (BQ/M³) x 10

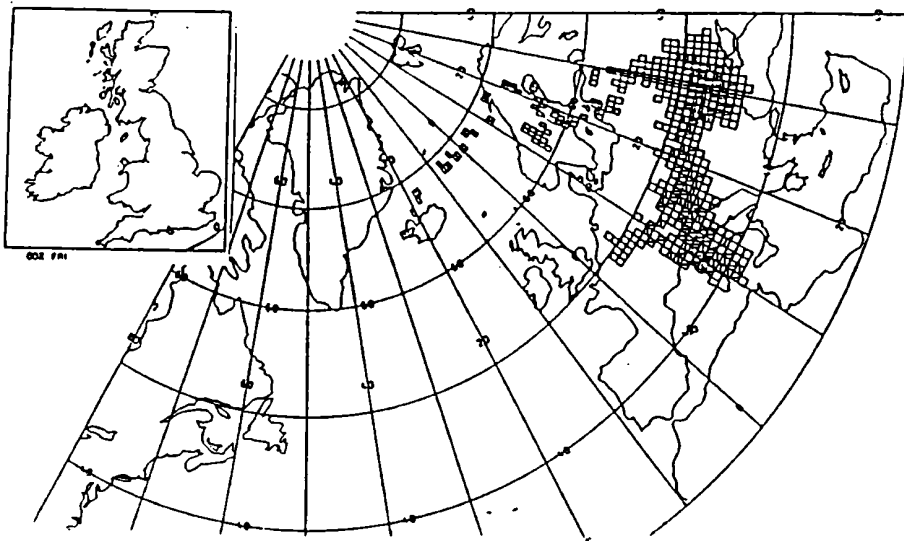
IN BOUNDARY LAYER

	1 - 42		85 - 126		169 - 210
	43 - 84		127 - 168		211 - 252

RELEASE FROM 2123GMT 25/04/1986 - 0000GMT 27/04/1986

AT CHERNOBYL 51 30N 30 30E

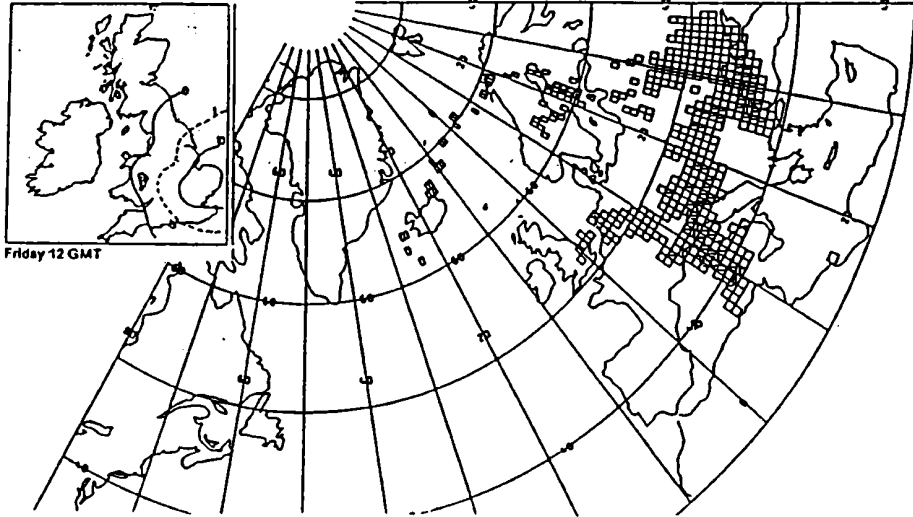
0 Z FRI 2/05/1986



□	1 - 62	▨	125 - 186	■	249 - 310
▨	63 - 124	▨	187 - 248	■	311 - 372

RELEASE FROM 2123GMT 25/04/1986 - 0000GMT 27/04/1986
AT CHERNOBYL 51 30N 30 31E

12 Z FRI 2/05/1986



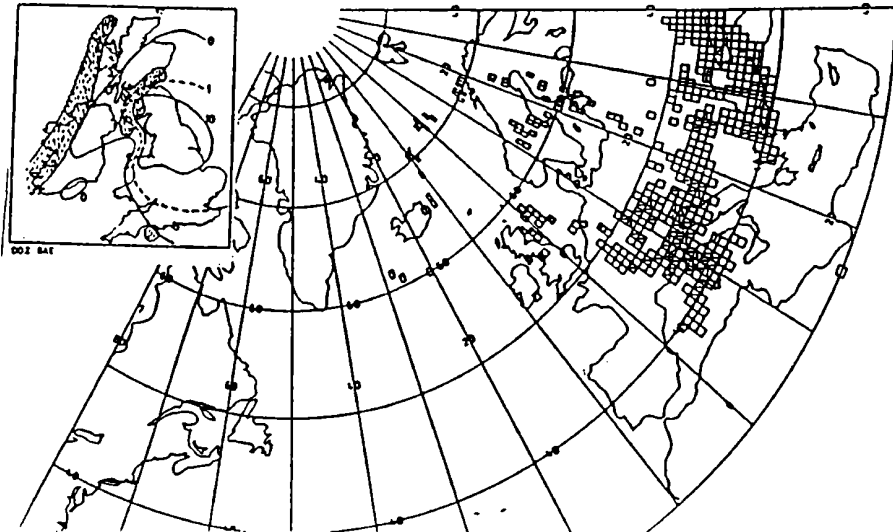
RANDOM WALK MODEL - CHERNOBYL RERUN

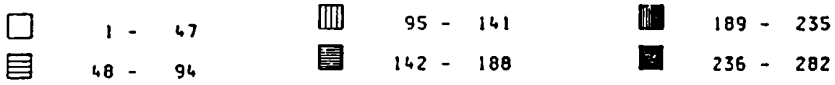
AIR CONCENTRATION (80/M**3) x 10 IN BOUNDARY LAYER

□	1 - 38	▨	77 - 114	▨	153 - 190
▨	39 - 76	▨	115 - 152	■	191 - 228

RELEASE FROM 2123GMT 25/04/1986 - 0000GMT 27/04/1986
AT CHERNOBYL 0 30N 30 30E

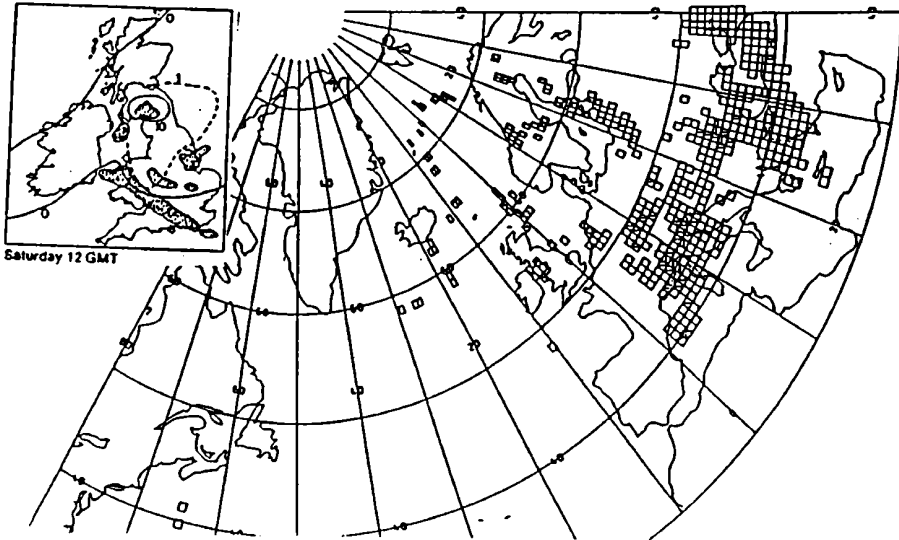
0 Z SAT 3/05/1986





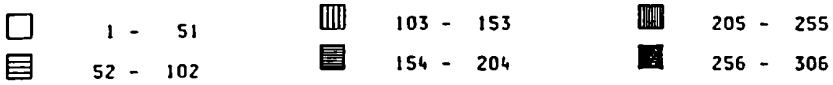
RELEASE FROM 2123GMT 25/04/1986 - 0000GMT 27/04/1986
AT CHERNOBYL 51 30N 30 30E

12 Z SAT 3/05/1986



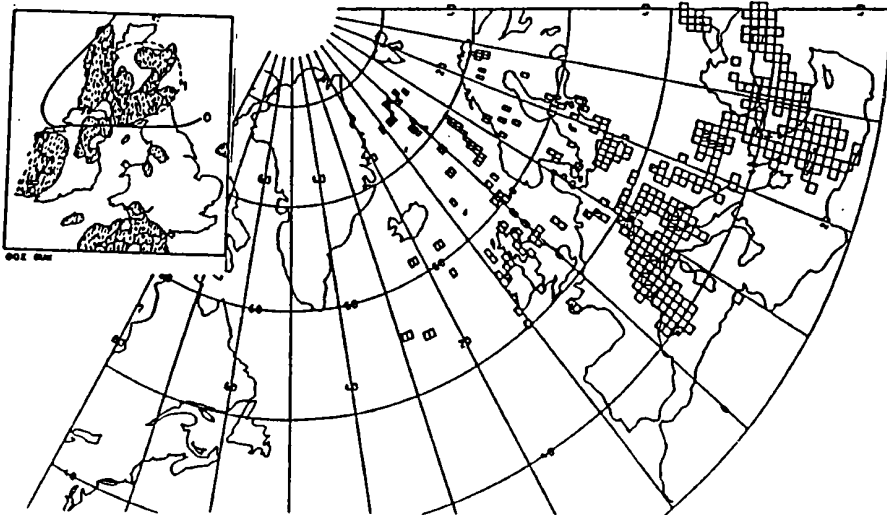
RANDOM WALK MODEL - CHERNOBYL RERUN

AIR CONCENTRATION (BQ/M**3) x 10 IN BOUNDARY LAYER



RELEASE FROM 2123GMT 25/04/1986 - 0000GMT 27/04/1986
AT CHERNOBYL 51 30N 30 30E

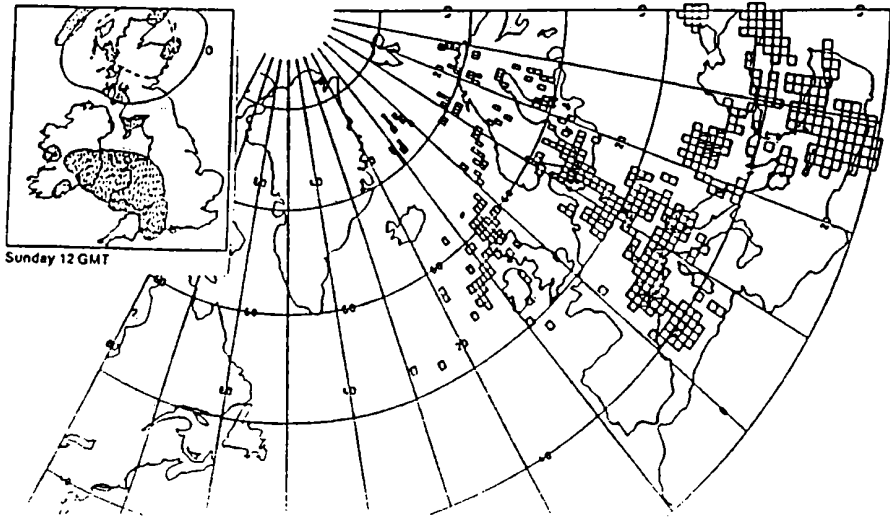
0 Z SUN 4/05/1986



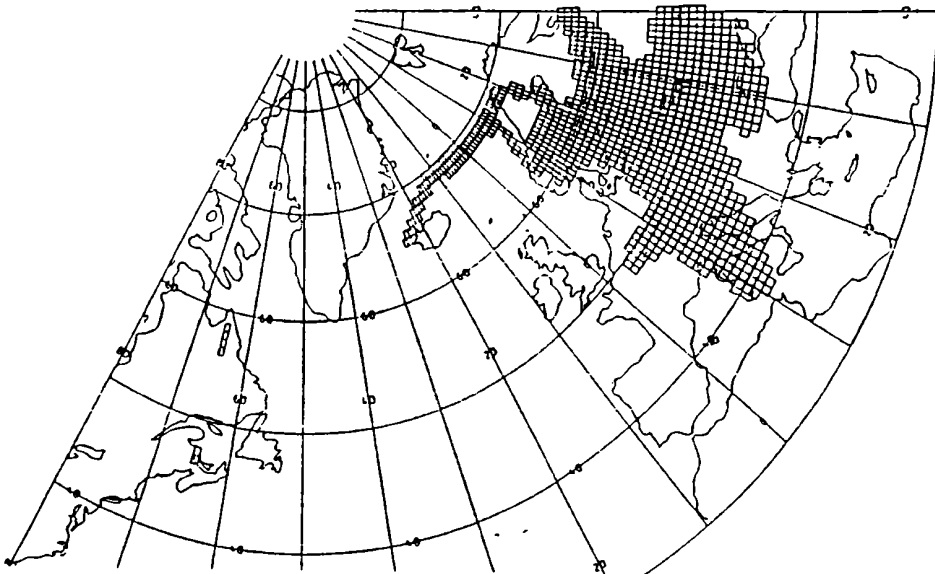
□	1 - 42	▨	85 - 126	■	169 - 210
▨	43 - 84	▨	127 - 168	■	211 - 252

RELEASE FROM 2123GHT 25/04/1986 - 0000GHT 27/04/1986
AT CHERNOBYL 51 30N 30 30E

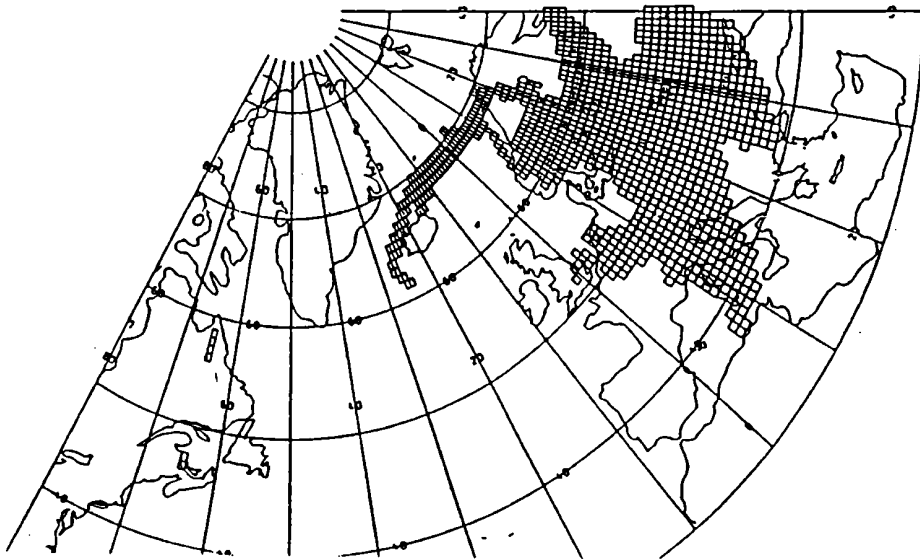
12 Z SUN 4/05/1986



0 Z FRI 2/05/1986



12 Z FRI 2/05/1986



0 Z SAT 3/05/1986



DISCUSSION

QUESTION: Nordlund: 1. When will your model be operative? 2. Is your random walk horizontal diffusivity important in comparison with the dispersion of 15 min trajectories?

ANSWER: 1. In its simple form now! The wet deposition should be working within 6 months, and radiological adjustments in about a year. A further year is required for parametrization and automation. 2. This is yet to be fully investigated. Doubling the diffusivity on one occasion had a relatively limited effect but I can make no categorical comments without further study.

QUESTION: Pendergast: You mentioned that particles are allowed to pass through the boundary layer. Is there a different parameterisation than when particles move within or above the boundary layer?

ANSWER: No, the algorithm is very simple. Boundary layer depth is diagnosed at 3 hr intervals and interpolated to the particle position, where the particle height and vertical velocity are taken into account. This is considered adequate for small scale entrainment/detrainment, but the venting of material from the boundary layer by deep convection is a much more difficult problem.

QUESTION: Van Ulden: In your model - quite rightly - turbulent motion is included in trajectory calculation. In traditional trajectory models only the mean winds are accounted for. I think this is incorrect. Could you comment on this matter?

ANSWER: I agree that a "mean wind" model is inadequate. Random (i.e. sub-gridscale) motions can transfer some particles into aereas of different mean wind, which is a better reflection of reality.

MEDIA : A French Eulerian Operational Model of Pollutant Dispersion in the Atmosphere : Application to the case of Chernobyl release and further developments.

J.P.Piedelievre L.Musson-Genon F.Bompay
Météorologie Nationale SCEM/D/ES
2 avenue Rapp 75007 Paris FRANCE

After the Chernobyl accident, the French Weather Service had few means to answer the questions from political authorities and press concerning the evolution of the toxic cloud. At that time, only a trajectories model was available (Martin 1984). Thanks to an intensive use of this kind of model, combined with Gaussian diffusion schemes, we achieved to locate with a good accuracy the place of the accident and to post-simulate the radioactive falls in quite a good manner (Albergel 1988).

However these experiments, despite many advantages (easily and quickly use, retro-trajectories for source location estimate), pointed out the limitations of the method :

- realistic diffusion including precipitations is difficult to be modeled,
- interpretation in a divergent wind field is uneasy,
- in order to describe a phenomenon as exactly as possible, many trajectories are necessary.

So, though this mean is very useful and sometimes necessary, we have developed an Eulerian Model of Dispersion in the Atmosphere (MEDIA).

This approach can be considered because of many recent improvements in the field of weather numerical forecasting. During the last years, indeed, statistical scores of models have been continually improved (wind field, pressure field, temperature field) and phenomena like rainfalls were better described and will undoubtedly be better taken into account in the future. So, by a judicious choice of numerical schemes that will be presented to you, it is possible to treat the processes of diffusion without being disturbed by numerical effects. The idea of an eulerian diffusion of a pollutant concentration field into a wind, temperature and precipitation field is attractive because it directly profits (and will profit) by improvements already mentioned. This kind of model has already been studied by Pudykiewicz and al (1985) and our purpose here is to apply this method to the Chernobyl accident. We first present the model with equations, parametrizations and the chosen numerical solutions.

I- The equations in the model

The concentration of a passive chemical element in the atmosphere follows the laws of continuous medium, and specially that of mass conservation :

$$\frac{\partial c}{\partial t} + \vec{V} \cdot \vec{\nabla} c = \vec{\nabla} \cdot (\vec{K} \cdot \vec{\nabla} c) + \dot{S} + \dot{P}$$

where c is the pollutant concentration in a point at the time t, \vec{V} the wind vector predicted by a weather numerical model, \vec{K} the REYNOLDS 'tensor, \dot{S} the source terms and \dot{P} the hole terms.

I-1 Advection

The pollutant concentration will be advected in the wind field predicted by the operational coupling model of numerical weather prediction.

I-2 Turbulent diffusion

In a matter of simplicity and to be coherent with the coupling model, the diffusion will be treated by coefficients of exchange. In that case, tensor \vec{K} is diagonal and :

$$\vec{\nabla} \cdot (\vec{K} \cdot \vec{\nabla} c) = \frac{\partial}{\partial x} k_x \frac{\partial c}{\partial x} + \frac{\partial}{\partial y} k_y \frac{\partial c}{\partial y} + \frac{\partial}{\partial z} k_z \frac{\partial c}{\partial z}$$

with $K_x = K_y = 10^5 \text{ m}^2 \text{ s}^{-1}$ (values which are chosen in french operational models EMERAUDE and PERIDOT)

and $K_z = l^2 \frac{\partial |\vec{V}_h|}{\partial z} F(Ri)$ (Louis, 1979)

where \vec{V}_h is the horizontal wind and Ri the Richardson number of gradient

$$Ri = \frac{g}{\theta} \frac{\partial \bar{\theta}}{\partial z} \frac{1}{|\partial \vec{V} / \partial z|^2}$$

with $\bar{\theta}$: potential temperature of the layer

$$l = \frac{kaZ}{1 + kaZ/\lambda} \quad \begin{array}{l} Ka : \text{Karman constant} = 0,4 \\ \lambda = 150 \text{ m} \end{array}$$

The form of the function F(Ri) is taken the same as in EMERAUDE and PERIDOT model (Geleyn, personal communication)

$$F(Ri) = \frac{1}{1 + 3b Ri (1 + d Ri)^{1/2}} \quad \text{in the stable case}$$

$$F(Ri) = \frac{1}{1 + 3bc \frac{\rho^2}{z^2} Ri^{1/2}} \quad \text{in the unstable case}$$

with $b=c=d=5. \frac{1}{z^2 \sqrt{z}}$

I-3 The holes

I-3.1 wet deposition

The wet deposition due to scavenging by precipitation is treated by a global coefficient of air to water transfer which roughly describe dilution or catching. Despite its simplicity, this solution is generally used and well adapted with the accuracy of precipitations predicted by the model. The rate of wet deposition D_w can be written :

$$D_w = C_m \times E \times P_r$$

where C_m is the average concentration of the precipitation layer in Unit of Concentration (UC Bq/m³), E ($=10^4$) the scavenging ratio and P_r the flux of precipitation in Kg m⁻² s⁻¹. The thickness of precipitation layer is arbitrary fixed to 3000 m (the precipitation fluxes are only available at the ground in the coupling model) and we admit that the scavenging is uniformly active in this part of the atmosphere. In the vertical, D_w is dispatched proportionally to the concentration.

I-3.2 dry deposition

The dry deposition describes the catching of the pollutant on the ground by a lot of obstacles. This is modeled by a coefficient which is dimensionally equal to a deposition velocity

$$D_d \text{ sol} = V_d \times C_{\text{sol}}$$

I-3.3 radioactive decay

The well known equation is : $\frac{dC}{dt} = -K C$

where $K = \frac{\ln 2}{T}$ is the splitting constant

with T : the radioactive half lifetime of the pollutant.

I-4 The source

In the source mesh, the diffusion is described at a subgrid scale by a Gaussian distribution :

$$\frac{dC}{dt} = \frac{Q(t)}{2 \pi \sigma_n^2 H} \exp\left(- \frac{d^2}{2 \sigma_n^2} \right)$$

where d is the distance from the source, Q the pollutant flux (UCs⁻¹), H the vertical thickness of the pollutant cloud (m), and σ_n the surface of the mesh which includes the source.

II- Numerical treatment

II-1 the coordinates system

Upon the evolution of data bases of the weather numerical forecasting models we are using (EMERAUDE, PERIDOT, ECMWF), we chose the σ coordinate on a latitude longitude grid. the equation can be written then:

$$\frac{\partial C}{\partial t} + \frac{U_\lambda}{R \cos \phi} \frac{\partial C}{\partial \lambda} + \frac{U_\phi}{R} \frac{\partial C}{\partial \phi} + \sigma \frac{\partial C}{\partial \sigma} = \frac{1}{R^2 \cos^2 \phi} \frac{\partial}{\partial \lambda} (k_x \frac{\partial C}{\partial \lambda}) + \frac{1}{R^2 \cos \phi} \frac{\partial}{\partial \phi} (k_y \cos \phi \frac{\partial C}{\partial \phi}) + \frac{g T}{R a T_v^2} \frac{\partial}{\partial \sigma} (k_z \frac{\partial C}{\partial \sigma})$$

where ϕ is the latitude, λ the longitude, σ the coordinate P/Psol, R the earth radius, $\sigma = \frac{d\sigma}{dt}$, T_v the virtual temperature in K, $g=9.81 \text{ ms}^{-2}$ and $Ra=287.05$ the dry air constant.

II-2 The splitting technique

The linear multi-dimensional operators splitting technique (Marchuk, 1975) was chosen in order to simulate phenomena of different nature (advection, diffusion, physico-chemical evolution...) by different numerical schemes according to the nature of the operator.

The splitting of the operations will follow the scheme :

$$F_1 = (T_O)_D \circ (T_O)_A \circ (T_\sigma)_D \circ (T_\sigma)_A \circ (T_\lambda)_D \circ (T_\lambda)_A \quad \text{on a half time step}$$

$$F_2 = (T_\phi)_A \circ (T_\phi)_D \circ (T_\sigma)_A \circ (T_\sigma)_D \circ (T_\lambda)_A \circ (T_\lambda)_D \quad \text{on the other one.}$$

The computation will then be:

$$C^{t+\delta t} = F_1(t, t+\delta t) \circ T_{ps}(t-\delta t, t+\delta t) \circ F_2(t, t-\delta t) \cdot C^{t-\delta t}$$

II-3 spatial discretization

- The spatial discretization of the advection and the vertical diffusion will be done according to Galerkin's method in finite elements. This technique offers the advantage of respecting the material distributions structure (energy and mass keeping) along the numerical treatment.

- The spatial discretization of the horizontal diffusion will be done, more traditionally, in finite difference. This can be justified by the simplicity of the parametrization we chosed.

II-4 Time integration scheme

For numerical stability, we chosed a Crank-Nicholson implicit scheme for the diffusion, trapezoidal for the advection:

$$C^{t+\delta t} - C^t = \frac{\delta t}{2} [F(C)^{t+\delta t} + F(C)^t]$$

this absolutely stable scheme leads to tri-diagonal linear systems which can be solved by a factorization method (Richtmyer and Morton, 1967).

II-5 Treatment of the boundary conditions

On the six sides of the integration area (4 lateral sides, top of the atmosphere and ground) the boundary conditions are treated in out-going-fluxes according to Orlanski (1976). The concentration C_1 at the boundary can be written then :

$$C_1 = \frac{1-\alpha}{1+\alpha} C_1^t + \frac{2}{1+\alpha} \alpha C_{1-1}^{t+\delta t}$$

$$\alpha = U \frac{\delta t}{\delta x} \quad \text{and } \alpha = 0 \text{ if the flux goes out}$$
$$\alpha = 1 \text{ if } U \frac{\delta t}{\delta x} \geq 1 \text{ (stability)}$$

(U : velocity along the chosen coordinate)

II-6 Negative values treatment

In order to correct the negative values created by the Galerkin method (Gibbs'effect), the suitable material quantity is picked up on one line (row, column or vertical) step by step until the deficit is made up.

Not to introduce a distortion in the wind field due to the use of a non-isotropic method, the way of sweeping is continually alternated which, in a great number, leads to the isotropy.

III - simulation of the chernobyl disaster

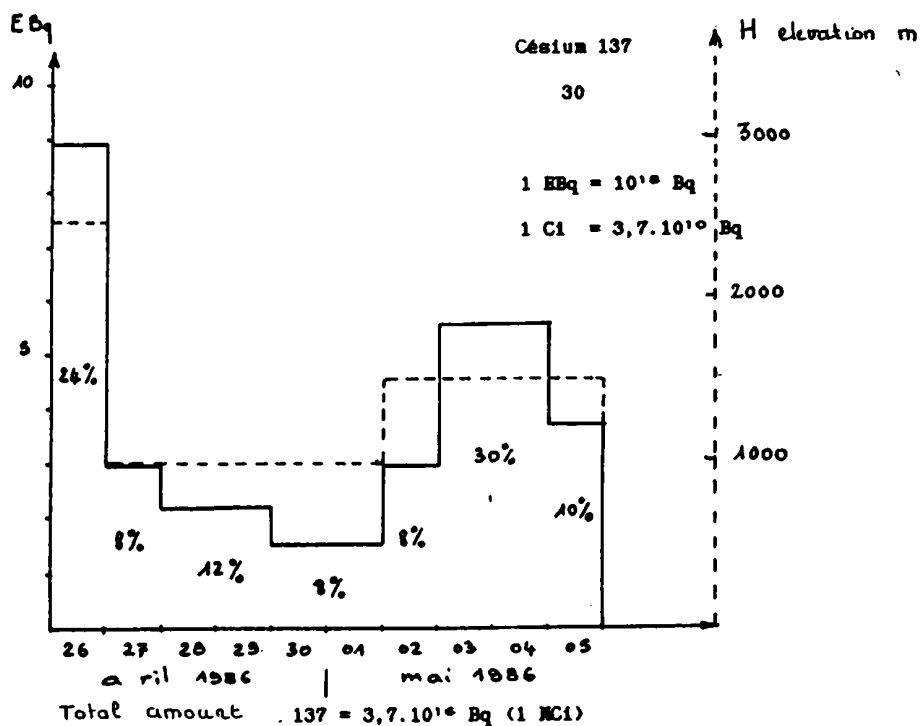
the accident took place around 00 UTC on APRIL 26 1986 in a 1000 MW reactor unit of the RBMK type of the chernobyl nuclear station (51°17 N, 30°15 E)

According to the data given by the soviet authorities at the VIENNA conference, the fire, with radionuclides release, lasted until MAY 5. The simulation results which will be presented concern the $^{137}\text{Cesium}$, one of the most efficiently measured elements. The total release in ^{137}Cs was $3.7 \cdot 10^{16}$ Bq. The release function we are using to simulate the accident is described, in space and time, on the figure 1. The ^{137}Cs half-lifetime is 30 years, that leads us to take for radioactive decay $K = 7.33 \cdot 10^{-10} \text{ s}^{-1}$. The dry deposition velocity is chosen equal to 10^{-3} ms^{-1} which is roughly the sharpness of Cesium nuclides.

III - 1 Meteorological data used in the simulation

Since the french models were not recorded for that situation, we used the data recorded at the European Center for Medium range Weather Forecast (ECMWF). We worked on the initialized data (deduced from observations) every 6 hours from 26-04-86 at 00 UTC to 12-05-86 at 18 UTC, because we did not intend to prove the quality of the weather forecasts. The

precipitations data are not taken into account in the simulation because they are not analysed (the only available information was the precipitations predicted for 12 hours, that was inadequate). This blank should be filled thanks to the work accomplished in the AEIEA. However, this should be kept in mind when interpreting the results.



Daily distribution	mean hourly intensity
1e 26/04/86 : 24 %	Source S ₁ 0,37 EBq/h
1e 27/04/86 : 8 %	Source S ₂ 0,123 EBq/h
1e 28/04/86 : 0,8 %	Source S ₃ 0,093 EBq/h
1e 29/04/86 : 5,2 %	
1e 30/04/86 : 4 %	Source S ₄ 0,062 EBq/h
1e 01/05/86 : 4 %	
1e 02/05/86 : 8 %	Source S ₅ 0,123 EBq/h
1e 03/05/86 : 14 %	Source S ₆ 0,23 EBq/h
1e 04/05/86 : 10 %	
1e 05/05/86 : 10 %	Source S ₇ 0,154 EBq/h

Figure 1 : Source term of Chernobyl Release

III - 2 Weather conditions and results

The weather conditions have been described many times so we will not do it again in that paper, especially since we use the analysed fields of the ECMWF and we did not test the model capability of predicting the meteorological situation. The

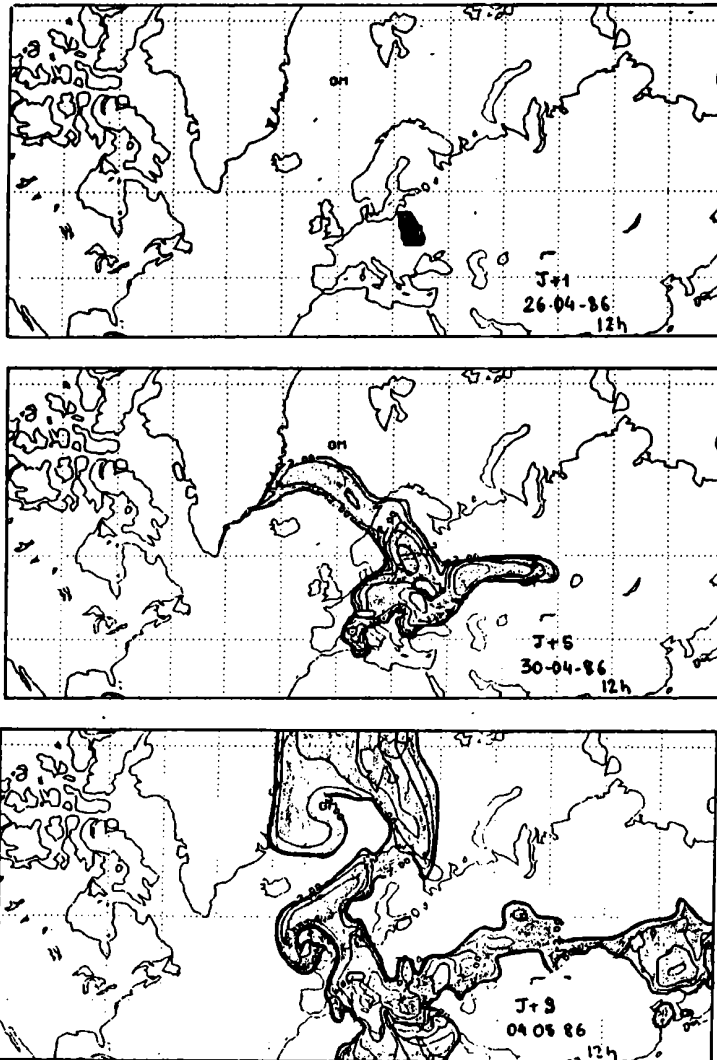


Figure 2a: Time evolution of mean concentration in the lower part of the atmosphere (1000m) in log₁₀

only way to underline the model capability of well describing the evolution of the radioactive cloud (figure 2a) is to compare the values issued from the model to the measurements taken in different towns in western europe. This was computed for measurements of daily average concentration of ¹³⁷Cs given by the "Commissariat à l'Energie Atomique" for PARIS, VERDUN, MARCOULE, CADARACHE, ATHENES, MUNICH, ROME, STOCKHOLM, HELSINKI. These data are compared with the average concentration predicted by the MEDIA model in the lower layers for the nearest grid-point of the town (figure 2 b for PARIS and STOCKHOLM).

Without making any adjustment, since the adjustable parameters of the model have been chosen before the simulation (K_z , source terms, half-lifetime, dry deposition velocity), the

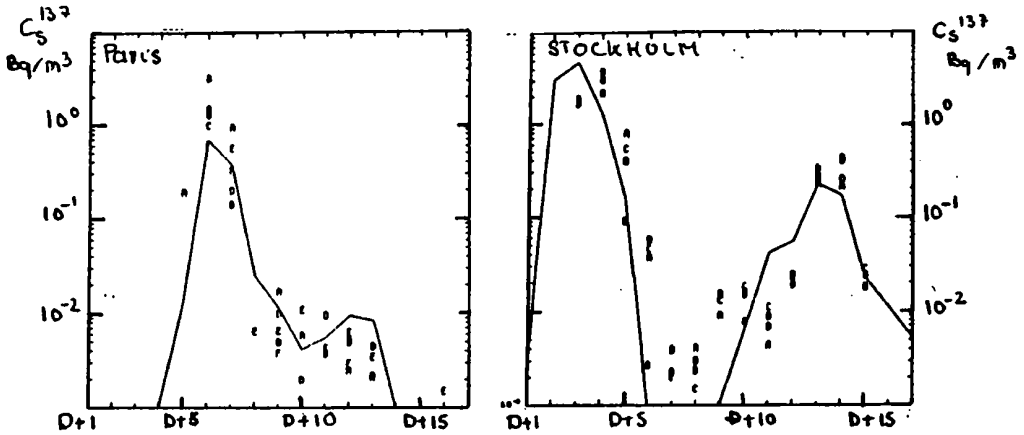


Figure 2b: Time evolution of daily mean concentration at the lowest level compared to observations A, B, C, D, E observations — simulation.

results are very satisfying as well qualitatively as quantitatively for each town except STOCKHOLM where the model predicted a pollution 1 day in advance as regard to the measurements. This problem was pointed out in other simulations. The good quality of the results might look surprising even when the scavenging by precipitations is not taken into account in the model, but the results mentioned there concern the mean concentration of the low layers of the atmosphere and not the values of deposition which should be very sensitive to the scavenging. In addition, considering the amount of pollutant released in the atmosphere, the size of the studied domain, the loss by scavenging in the lowest layers is perhaps negligible in front of the dubiousness on the source term estimate.

The model, with the present parametrizations, is able to describe the evolution of a pollutant concentration cloud as soon as the weather conditions are well predicted by the coupling model.

On the chernobyl simulation, the introduction of measured parametrizations would make the results more credible and we are always fond of these kind of data.

The code is now operational on the global model EMERAUDE (grid $1.5^\circ \times 2^\circ$ in latitude \times longitude) for a movable window (70° to 22° N, 30° W to 50° E) with a finer mesh than the coupling model ($0.75^\circ \times 1^\circ$ latitude \times longitude). Each day of simulation requires 31.5 s on CRAY 2. The data issued from EMERAUDE are available every day at 05 UTC for a 72 hours forecast (step 6 hours) from the 00 UTC. A slipping recording allows us to work on the analysis of the 5 days before the possible accident and then to go on a 3 days forecast.

The code is also operational on the fine mesh model PERIDOT (35 Km x 35 Km) on an area covering the western Europe. The data issued from PERIDOT are available twice a day at 06 UTC for a 48 hours forecast from the 00 UTC (step 3 hours) and at 17 UTC for a 48 hours forecast from the 12 UTC (step 6 hours). The only problem is to be sure that the line between the computer CRAY 2 and the computers of the french weather service is switched on.

CONCLUSION AND FUTURE

This study shows the capability of this kind of model to predict in a good manner the evolution of a radioactive cloud of passive tracer. Nevertheless, a validation alone is not sufficient and we need other data bases (tracers campaigns for example). Besides, the physic developed in the model is rather primary and a better description of the scavenging and the dry deposition must be considered. For the scavenging, it seems an illusion to use only the 6 hours average precipitation flux at the ground predicted by the coupling model. The knowledge at each timestep and each level of the precipitation fluxes predicted by the model is the necessary condition for a better description, though this flux is still unrealistic in the present models.

In operational mode, we are trying to have the PERIDOT model run in any area of the Earth, associated with the code MEDIA. This should be achieved in one year.

In research mode, we are trying to get a model such as PERIDOT but with a finest mesh (5 to 10 km) on a limited area (a quarter of France). This model PERIDOT-MESO is developed in the "Centre National de Recherche Météorologiques" at TOULOUSE and uses the turbulent kinetic energy in order to treat the diffusion. The coupling with the code MEDIA at each timestep of the PERIDOT-MESO model should allow us to study, in a better way, the different physical parametrizations since we could get the whole information of the model.

Anyway, we shall remind you that, in forecasting term, any pollutant transportation model is above all dependent upon the quality of the weather conditions forecasts and especially the precipitations.

REFERENCES

Albergel A., Martin D., Stauss B. and J.M. Gros, 1988: The Chernobyl accident: modelling of dispersion over Europe of the radioactive plume and comparison with air activity measurements. Atmos. Envir., 22, 14pp.

Louis J.F., 1979: A parametric model of vertical eddy fluxes in the atmosphere. Bound. Lay. Meteor., 17, 187-202.

Marchuk G.I., 1976: Methods of numerical mathematics. Springer-Verlag, New-York.

Martin D., Granier J.P., Imbard M. and B. Strauss, 1984: Application of a long range transport model to a mount Etna plume. Bull. Vulcano., vol 47-2.

Orlanski I., 1976: A simple boundary condition for unbounded hyperbolic flows. J. Comput. Phys., 21, 251-269.

Pudykiewicz J., Benoit R. and A. Staniforth, 1985: Preliminary results from a partial long range transport of air pollutants model based on an existing meteorological forecast model. Atmosphere-Ocean, 23, 267-303.

Richtmyer R.D. and K.W. Morton, 1967: Difference methods for initial value problems. Wiley Interscience.

DISCUSSION

QUESTION: Seibert: 1. The first plot of the Chernobyl simulation you showed gave the impression of a rather big horizontal diffusion, and also the numerical value of 10^6 you used seems to me to be very big. You also said that the results are sensitive to horizontal K. So, shouldn't one perhaps use a smaller value for K horizontal? 2. In NWP models large K's are usually used for numerical smoothing of dynamic variables.

ANSWER: You are right for part 2 of your question. But by comparison of concentration at different towns between model and observation, the best results are obtained with this value (10^6). If we do other comparison with other data (ANATEX or CAPTEX) perhaps we change this value!

V

MESOSCALE ASSESSMENTS
WITHIN A COUNTRY
AND DEPOSITION

A MODEL FOR RADIOACTIVE GROUND CONTAMINATION ANALYSIS

Jelko Urbančič and Zvonka Jeran
Jožef Stefan Institute
Ljubljana, Yugoslavia

Abstract

A simple model for analysis of ground contamination over a certain area is described. It requires precipitation data and radiological data. The activity of precipitation is expected to be the most relevant radiological data for input to the model.

An analysis of ground contamination by Cs-134 and Cs-137 in SR Slovenia (NW Yugoslavia) based on the model is presented. The results of the model are related to measurements of Cs-134 and Cs-137 activity in epiphytic lichens and soil samples.

Introduction

The radioactive cloud from Chernobyl moved over SR Slovenija in the late evening on April 29, 1986. Its approach was recorded in Gorenja vas (25 km West of Ljubljana) after 9 pm. It was rainy weather that day and also in the following few days when this area received most of its radioactive fallout.

Three different techniques and data sources were used to analyse the ground contamination of cesium in SR Slovenia:

- A simple model for estimation of ground contamination based on measurements of radioactivity of precipitation and its amount in the period from April 30, to May 9, 1986, when this area got most of its radioactive load from Chernobyl.
- measurements of Cs-134 and Cs-137 in epiphytic lichens
- measurements of Cs-134 and Cs-137 in soil samples

Daily amount of precipitation is measured at over 300 locations in SR Slovenia (area about 20000km^2). It gives us an opportunity to obtain an estimate of ground contamination at a great number of locations. The results of such a model were found useful for finding where samples of soil and lichens should be taken. The complete analysis is not yet finished, but preliminary results are presented.

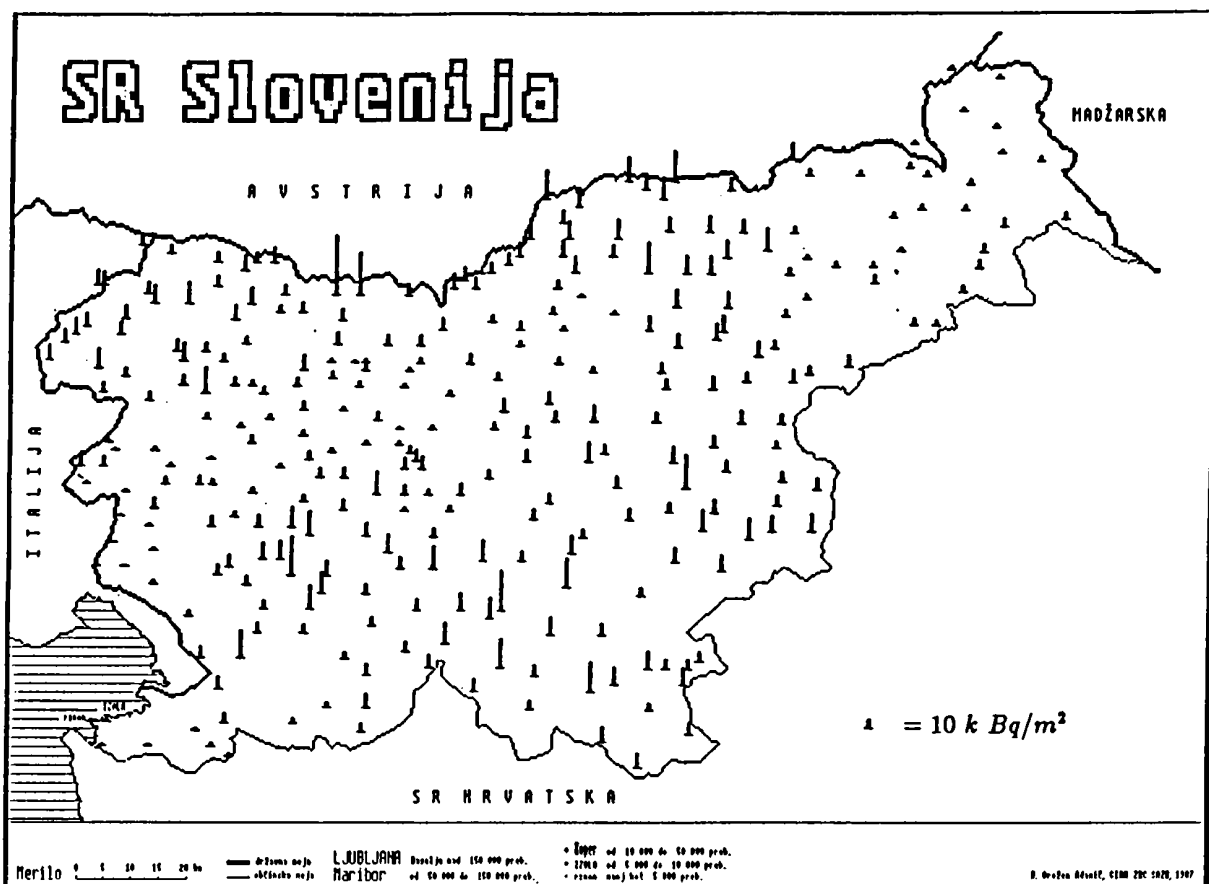


Figure 1: The model prediction for Cs-137 deposition at 301 locations in SR Slovenia

The model

When constructing the model the amount and reliability of the available data were taken into account. Unfortunately, the radioactive cloud came unexpectedly and measurements were not made systematically. The data for the concentration of radioactive pollutants in precipitation can be used only from measurements in Ljubljana (Brajnik, 1986). Measurements in other locations were mostly incomplete and therefore we constructed the model with the following assumptions:

- The air concentration of radioactive pollutants was homogeneous above the total area of Slovenia
- Ground contamination was mostly the result of wet deposition, as estimated by measurement of radioactivity in collected precipitation. Dry deposition was neglected. It was assumed to be less important because after the polluted air moved over Slovenia, precipitation was recorded at all meteorological stations.

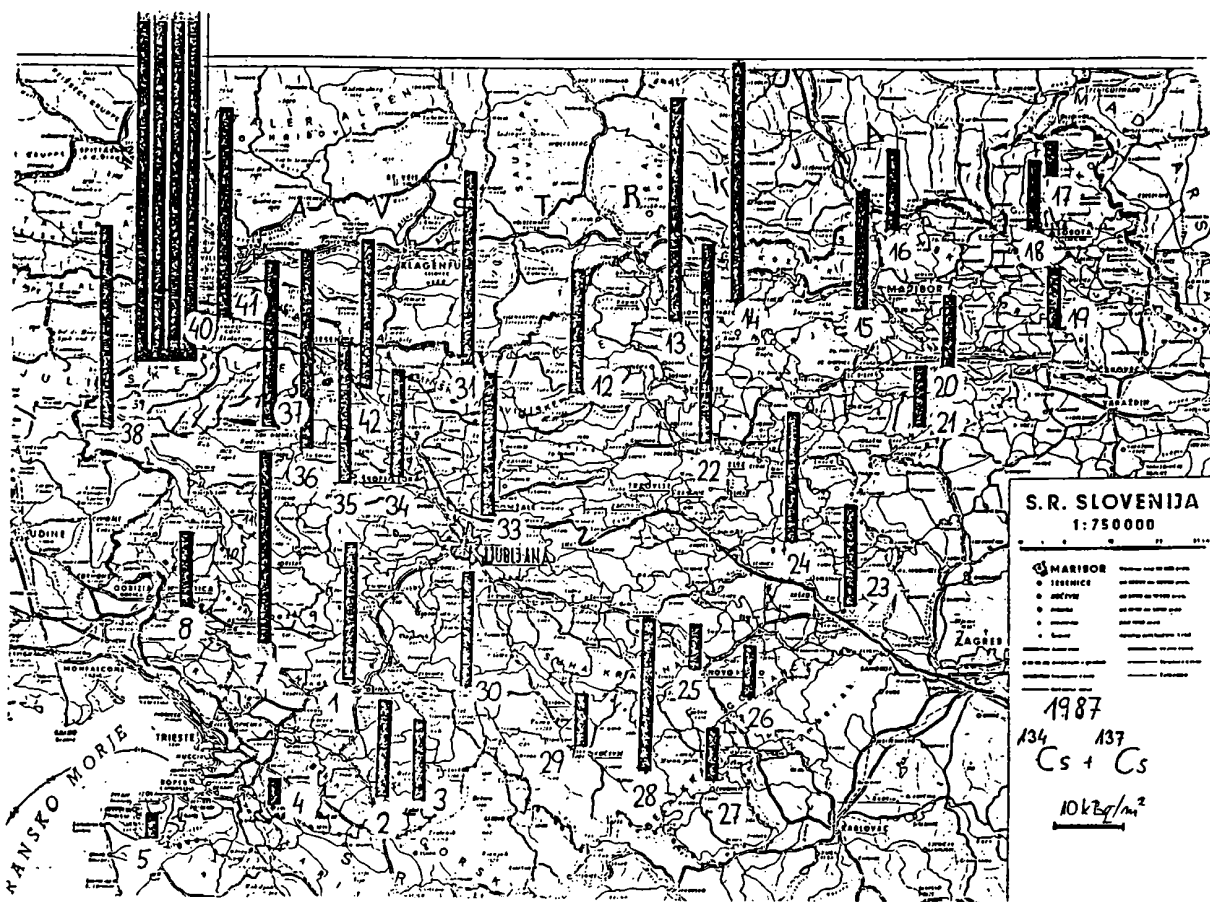


Figure 2: The measured values of Cs-134 and Cs-137 activity in soil samples by Brajnik (1987)

Ground contamination is defined by the model as:

$$G = RR * C_L \quad (1)$$

where G is the ground contamination [Bq/m^2], RR the amount of precipitation [mm] and C_L the concentration of radioactive pollutant in precipitation water [Bq/l] measured at the reference location in Ljubljana.

Precipitation data for 301 meteorological stations in the period from April 30, to May 9, 1986 are available. There were only two days in this period when no precipitation was recorded at any meteorological station. The reference location (Ljubljana) recorded precipitation on all other days. The model was applied to analysis of Cs-134 and Cs-137 contamination only. The results for calculated contamination are presented in Fig. 1.

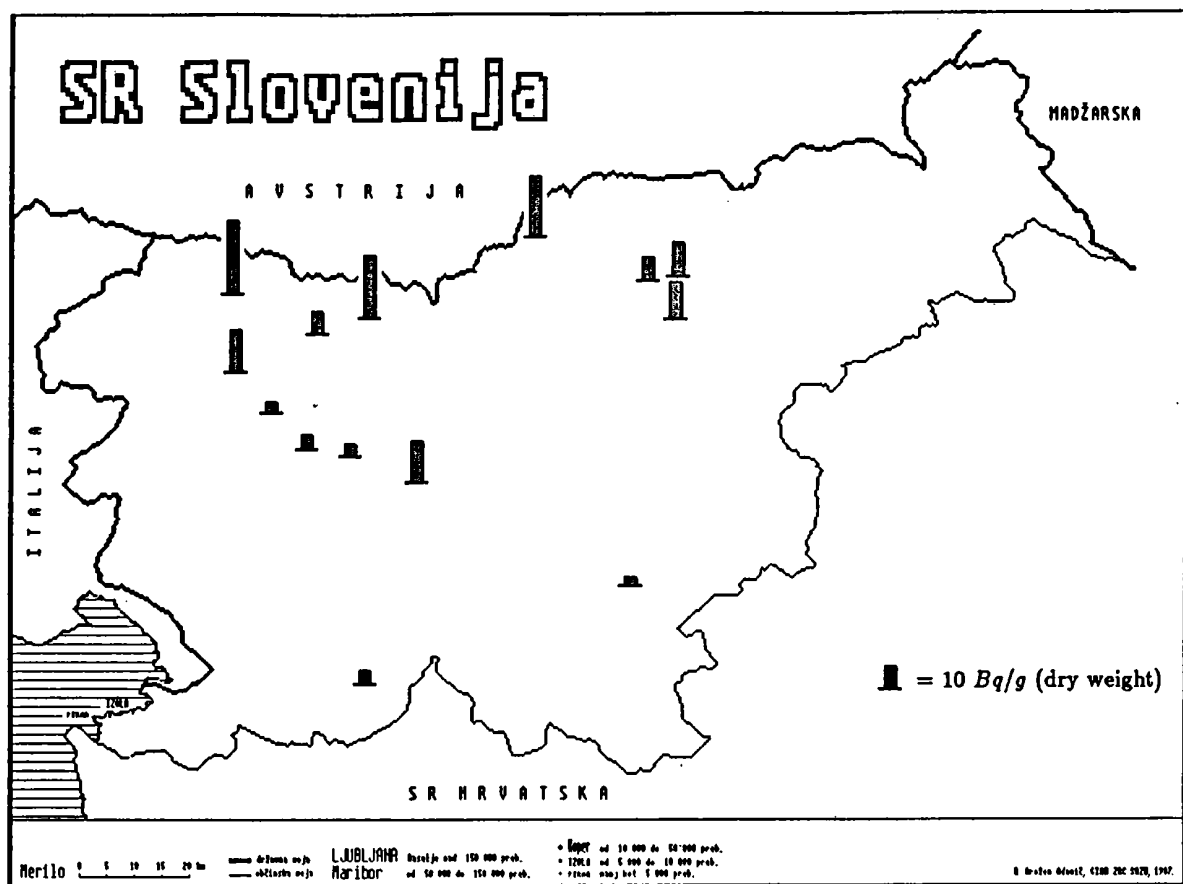


Figure 3: The measured values of Cs-134 and Cs-137 activity in lichens

Lichens as bioindicators for radioactive pollution

Lichens have been reported to accumulate natural and man-made radionuclides. Because of their high absorption efficiencies and high retention capacities for radionuclides, some authors have suggested that lichens and also mosses can be used as natural integrating meters for fallout nuclides, such as Cs-137 (Hoffman, 1972, Svensson, 1965). In 1987 and 1988 we began to determine Cs levels (Cs-134 and Cs-137) in some of the most abundant epiphytic lichen species in Slovenia (*Hypogymnia physodes*, *Parmelia saxatilis*, *Pseudevernia furfuracea* and *Parmelia caperata*) in order to estimate the degree of Cs-contamination after the Chernobyl accident. *Hypogymnia physodes* is known as a tolerant specie for chemical pollution and *P.caperata* as the most sensitive one.

Samples of epiphytic lichens were collected at different locations in Slovenia (in the central and north-western parts of the region). The lichens were carefully separated from the substrate (different trees; beech, scots pine, apple), adhering particles were removed in the laboratory, and then crushed and ground after addition of liquid nitrogen and dried at 105°C for 24 hours. The Cs-134 and Cs-137 activities of these

Location	Lichen Species	Substrate	Cs-134	Cs-137	Cs-137/134
Žirovski vrh	H.physodes	beech (2)	1.12 ± 0.35	3.95 ± 1.25	3.5
		apple (3)	2.47 ± 0.57	8.50 ± 1.49	3.4
		scots pine (3)	0.84 ± 0.64	2.94 ± 2	3.5
	P.saxatilis	beech (8)	1.36 ± 0.24	4.94 ± 0.92	3.6
		apple	-	-	-
		scots pine (1)	0.44	1.36	3.1
	P.caperata	beech (3)	1.35 ± 0.30	5.01 ± 0.91	3.7
		apple (1)	2.50	9.0	3.6
		scots pine	-	-	-
	Ps. furfuracea	beech	-	-	-
		apple (2)	3.52	12.33	3.5
		scots pine	-	-	-
Bukovščica	P.saxatilis	apple	1.02	3.56	3.5
Črni vrh	Ps.furfuracea	scots pine	1.11	3.86	3.5
Ljubljana	H.physodes	apple	3.16	13.17	4.2
Ljubljana	P.saxatilis	apple	3.85	17.20	4.5
Polje pri Bohinju	H.physodes	apple	4.01	14.20	3.5
Mali Slatnik	P.saxatilis		0.72	3.34	3.6
Peca	Ps.furfuracea	scots pine	5.70	20.10	3.5
Velika Kopa, Pohorje	H.physodes	beech	2.18	8.80	4.0
Tolsti vrh, Pohorje	H.physodes	apple	3.70	15.59	4.2
Tolsti vrh, Pohorje	Ps.furfuracea	apple	2.29	9.50	4.1
Mislinjski j., Pohorje	H.physodes	scots pine	3.02	12.49	4.1
Mislinjski j., Pohorje	Ps.furfuracea	scots pine	2.77	11.71	4.2
Paški Kozjek	H.physodes	beech	2.96	12.90	4.4
Kofce	Ps.furfuracea	scots pine	5.46	22.07	4.0
Dobrča	Ps.furfuracea	scots pine	1.89	7.74	4.1
Mojstrana	Ps.furfuracea	scots pine	6.39	26.18	4.1
Trenta	H.physodes		5.05	21.10	4.2

Table 1: The Cs-134 and Cs-137 concentrations (in Bq/g dry weight) and the Cs-137 to Cs-134 activity ratio in some epiphytic lichens collected in 1987 and 1988 in Slovenia.

analyser.

Preliminary results are presented in Table 1. and in Fig 3. As expected, the Cs values in lichens collected at different locations of Slovenia differ from each other, but the values of various lichen species from the same location lie within a very narrow range. The highest activity of both Cs-isotopes were found in samples from the west and north-west (alpine) parts of Slovenia, which are known to receive the highest amounts of precipitation. The Cs-137 to Cs-134 activity ratio in the lichens analysed was the same as the ratio of these isotopes in the radioactive cloud from Chernobyl.

Discussion

Brajnik (1987) made measurements of Cs-134 and Cs-137 in soil samples in various locations in SR Slovenia (Fig. 2.). In this work they were used for comparative purposes with the model results. The results obtained by the three different approaches show quite good agreement. The higher contamination predicted by the model for certain areas is mostly confirmed by the measurements. The topography of this district is mostly very uneven, resulting in a nonuniform space distribution of precipitation. The differences of the model results obtained at various neighbouring locations are mainly the consequence of nonhomogeneous spatial precipitation distribution.

We can conclude that all three analysis techniques should be used in estimation of contamination in hilly terrain. The model described above shows a very inhomogeneous distribution of ground contamination, requiring special care in selection of appropriate sampling sites to avoid sampling errors. Further investigations could supply enough data to make a statistical model that could better fit the measured data.

References

- Brajnik D. et al, 1986 , Early Monitoring of Radioactivity in NW Yugoslavia After the Chernobyl Accident, 32th Conference on Bioasai, NBS Gaithersbury.
- Brajnik D. et al, 1987 , Migration of Cs-134 and Cs-137 in Soil and to Food in One Year after the Chernobyl Accident, 33th Conference on Bioasai, Berkeley.
- Hoffman G.R., 1972 , The accumulation of Cs-137 by cryptogams in Liriodendron tulipifera forest. Bot. Gaz. 133(2): 107-119.
- Svensson, G.K., and K.Linden, 1965, The transport of Cs-137 from lichen to animal to man. Health Physics 11: 1393-1400.

DISCUSSION

QUESTION: ApSimon: Did you look at orographic enhancement - that is the variation on a single mountain with height for example?

ANSWER: We made one example (two samples - one at the foot and one at the top of Dobca mountain). Unfortunately we have not precipitation support at this location. Measurements at lee side locations show no significant difference, and low measured values.

QUESTION: Seibert: 1. What was the resolution in time for the measurements of activity in precipitation samples? 2. Did you compute correlations between lichen or soil activity data and precipitation data?

ANSWER: 1. The resolution time 24 h is used. If more frequent measurements exist, they are averaged on 24 h. 2. We will do it when we will have enough measurements (at least 30) for statistical significance.

DOSE RATE PATTERNS IN AUSTRIA AFTER THE CHERNOBYL ACCIDENT AND THEIR RELATIONS TO PRECIPITATION

P. Seibert, H. Kolb
Institute of Meteorology and Geophysics, University of Vienna,
Hohe Warte 38, A-1190 Wien, Austria

O. Svabik, V. Zwatz-Meise
Central Institute of Meteorology and Geodynamics,
Hohe Warte 38, A-1190 Wien, Austria

Summary: An on-line radiation monitoring system yielding dose rate data at 336 sites covering the whole of Austria gave unique information about the radiation situation during and after the Chernobyl accident. Detailed isochrones of the first arrival of contaminated air have been derived. During and after the passage of the radioactive cloud, dose rates are mainly determined by the amount of deposited activity. Time series of dose rate and precipitation are compared for several locations. Correlation between long-lived ground contamination and total precipitation in the critical period is not satisfactory, when computed for all stations together. The deviation of observed dose rate values from the values estimated by the regression formula using the precipitation data has a distinct regional pattern, probably due to corresponding variations of air contamination

1. Introduction, data base

It is a common experience that data sets from large international experiments usually require years for preparation and will always contain some errors. Chernobyl, however, was not a planned experiment but a continental-scale disaster for which nobody really was prepared. Measurements were made mainly for radiation protection purposes and not for scientific ones, and partly by unskilled personnel and in hurry. Therefore, the quality of the data available does not always meet the standard desired for scientific work.

However, there is one high-quality radiological data set in Austria produced from the network of 336 gamma dose rate monitoring stations with real time data transmission (fig. 1).

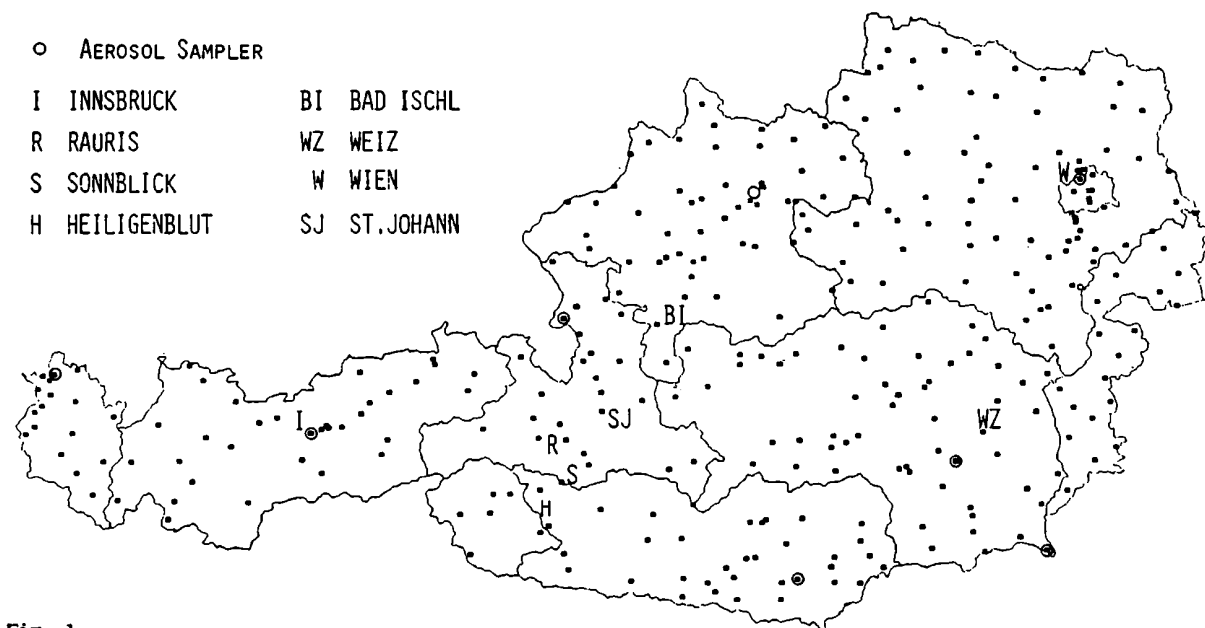


Fig. 1.
Dose rate monitoring stations and aerosol sampler locations in Austria. Stations referred to in the text are indicated.

The average spatial density is one station per 250 km². Two-hourly data from this network have been stored on tape, and allow a detailed analysis of the propagation of contaminated air. From the values recorded after May 8, when the activity in air had dropped to a very low level (resulting from resuspension only), total deposited activity can be estimated.

Aerosol samplers with gamma spectroscopic measurements of the filters are installed at 8 stations (fig. 1), but data suffer from irregular sampling intervals and gaps.

Meteorological measurements (fig. 2) were used from the climatological network (3 observations daily, two precipitation measurements daily) with its 239 stations and the precipitation network of the Hydrological Service (784 stations, daily precipitation totals). Continuous registrations of precipitation are available at several of the climatological stations.

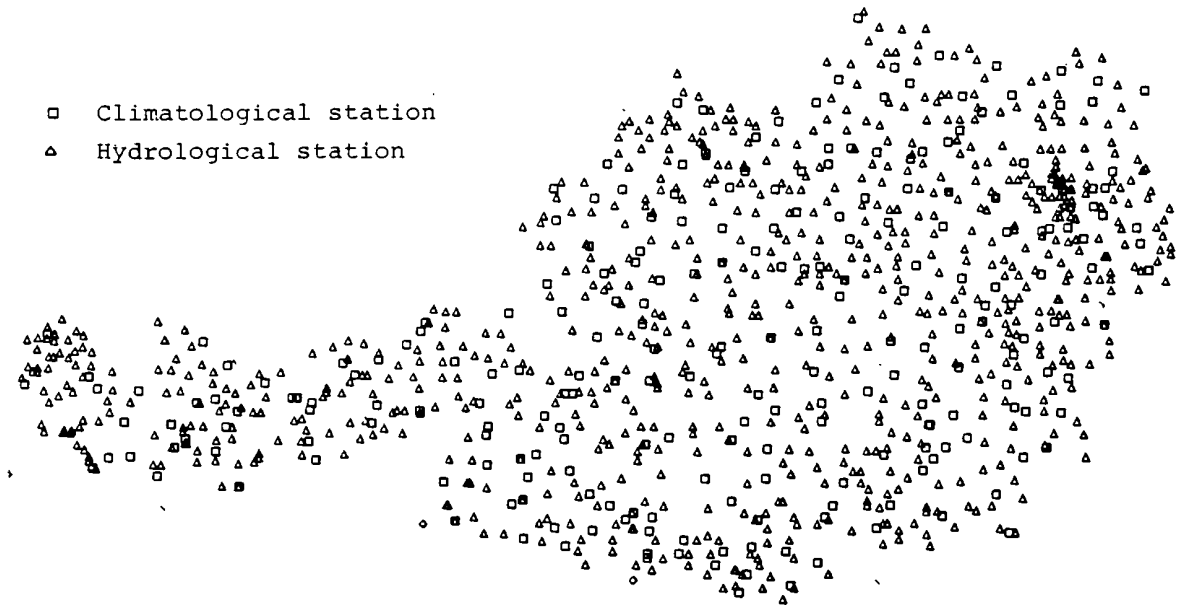


Fig. 2.
Climatological and hydrological networks in Austria.

2. Propagation of contamination

Isochrones of the first significant increase of dose rates have been analyzed and are shown in fig. 3. Generally speaking, the front of contamination crossed Austria from the east to the west (a distance of approx. 600 km) within 24 hours. The front entered Austria at 7 a.m. (LST) on April 29, 1986 in the NE corner of the country and propagated continuously until late afternoon. In the evening hours there is strong retardation of the front north of the Alps, and isolated spots with arrival times of three hours and more later than expected can be seen. From 19 LST on April 29 to 01 LST on April 30, the front made a big jump into the western part of the country, after that moving continuously again.

How is this behaviour to be explained? The propagation of the surface front is determined by three factors: the wind field, the stability and the vertical distribution of activity, and the precipitation. The wind field in the evening of April 29 together with some isochrones is shown in fig. 4. In the SE part, the front propagates with the wind at a rate of 25 km/h, slightly faster than the surface wind speed. In the northern part, the front is slowed down at a pronounced line of convergence, propagating only with the phase speed of this convergence line.

Fig. 5 schematically explains the influence of stability on propagation. During convective conditions, the front is steep and its phase speed is equal to the maximum wind velocity within the mixed layer. This explains why 850 hPa - trajectories performed so well inspite of the fact that the effective release height was considerably lower after the initial phase (IAEA 1986). In stable conditions, activity will soon be removed from the lowest layer by dry deposition while it cannot be replaced by a flux from aloft. Thus, a separation between the surface and the upper front will occur. If in such a situation precipitation starts over a large area, a quasi-simultaneous onset of increased radiation will be observed in this area. This happened over central Austria in the night from April 29 to April 30. Fig. 6 illustrates the event for several stations.

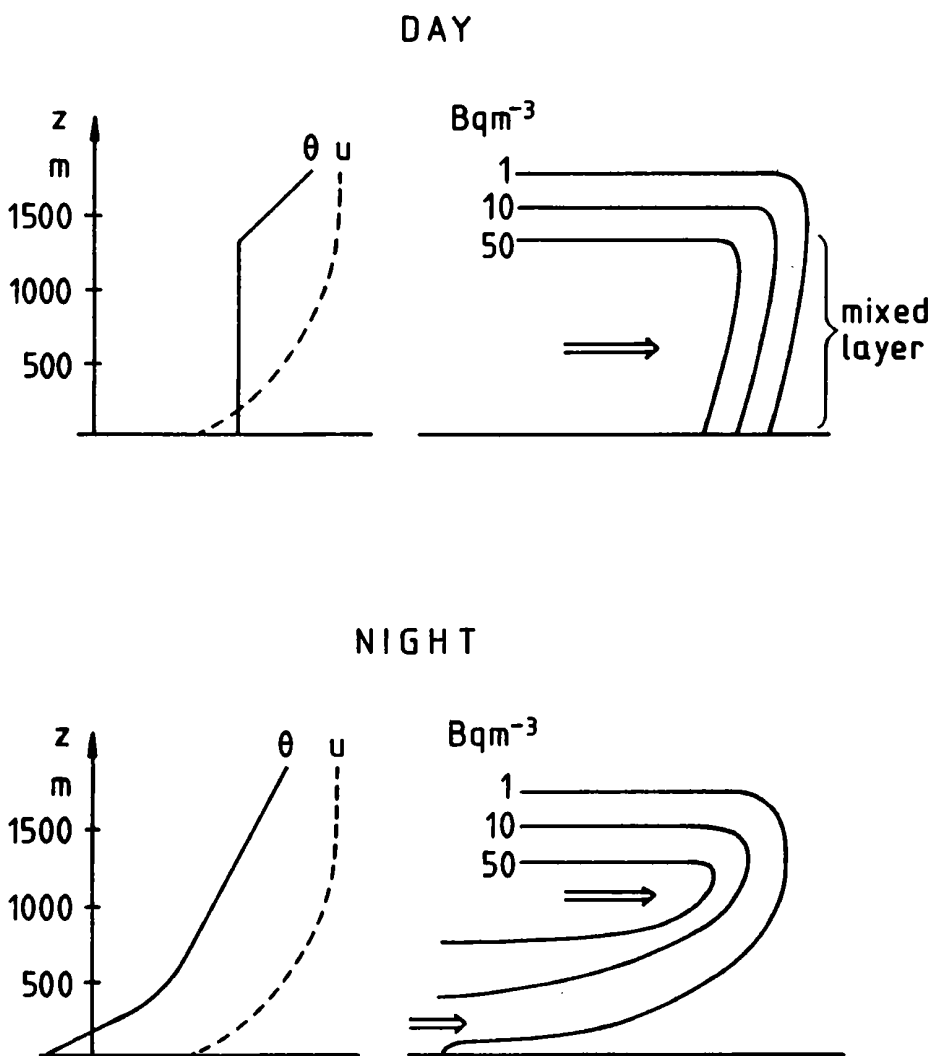


Fig. 5. Schematic cross-section of activity front during unstable (DAY) and stable (NIGHT) conditions.

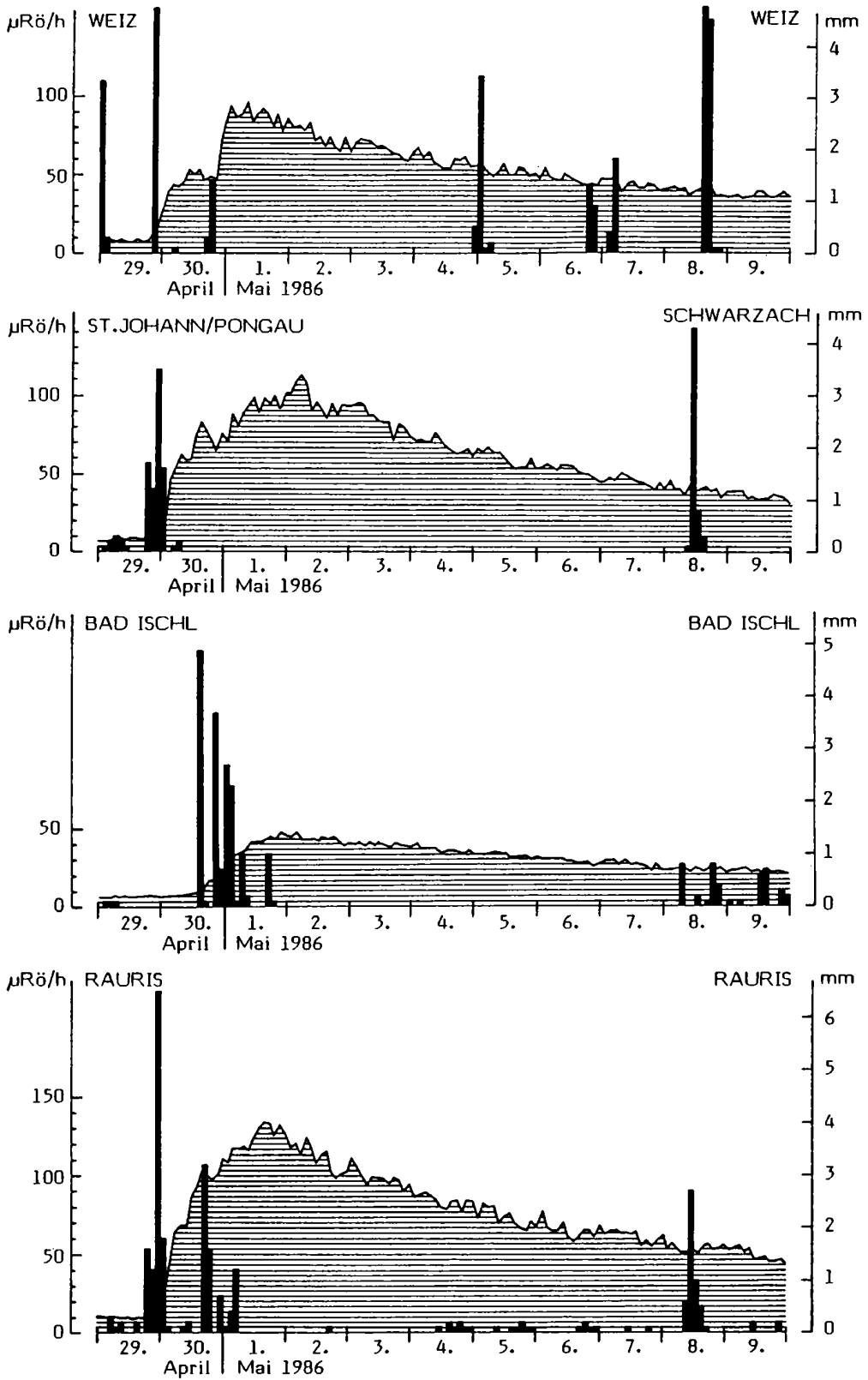


Fig. 6. Time series of gamma dose rate and two-hourly precipitation for several stations. For location of stations, see fig. 1.

3. Precipitation and Deposition

It soon became obvious that, under the prevailing weather conditions during these days, wet deposition was dominating compared with dry deposition, especially for long-lived fission products like cesium; gaseous iodine, which was present with a share of approx. two thirds of total iodine (UBA 1986), is relatively efficiently removed by dry deposition (see, e.g., Kolb et al., 1986). Therefore precipitation data, which are measured in a very dense network, should give a useful first information on the regional distribution of contamination levels in a relatively fine scale. The problem with this approach is the non-homogeneity of activity concentrations in air and the correlation between precipitation events and episodes with contaminated air.

Figures 7 and 8 show the time series of air contamination, measured dose rate and precipitation for the stations Vienna and Innsbruck. In order to separate radiation due to deposited and due to airborne activity, the gamma submersion has been calculated from the results of aerosol filter measurements. In Vienna, two separate maxima of dose rate can be identified and attributed solely to submersion. In the course of May 1, very slight showers deposited enough activity for a 5 $\mu\text{R}/\text{h}$ - rise in the dose rate, which persists after the sharp drop of air activity in the evening of the day. A third major maximum of air activity was observed in the night May 3/4, which again lead to an increase of the dose rate. The frontal precipitation on May 8, accompanied by low air activity, didn't bring a significant increase in radiation levels. In Innsbruck, the first increase in radiation levels coincides with heavy precipitation, as discussed in section 3. Note that the air activity is smaller by a factor of 10 compared to Vienna, while the dose rate levels (over background) are bigger by a factor of 5. Submersion contributed insignificantly to the radiation levels observed in Innsbruck, though the lack of time resolution until May 3 may obscure some peaks. The high airborne concentration on May 7 cannot be explained well; it could be due to resuspension during gusty foehn winds.

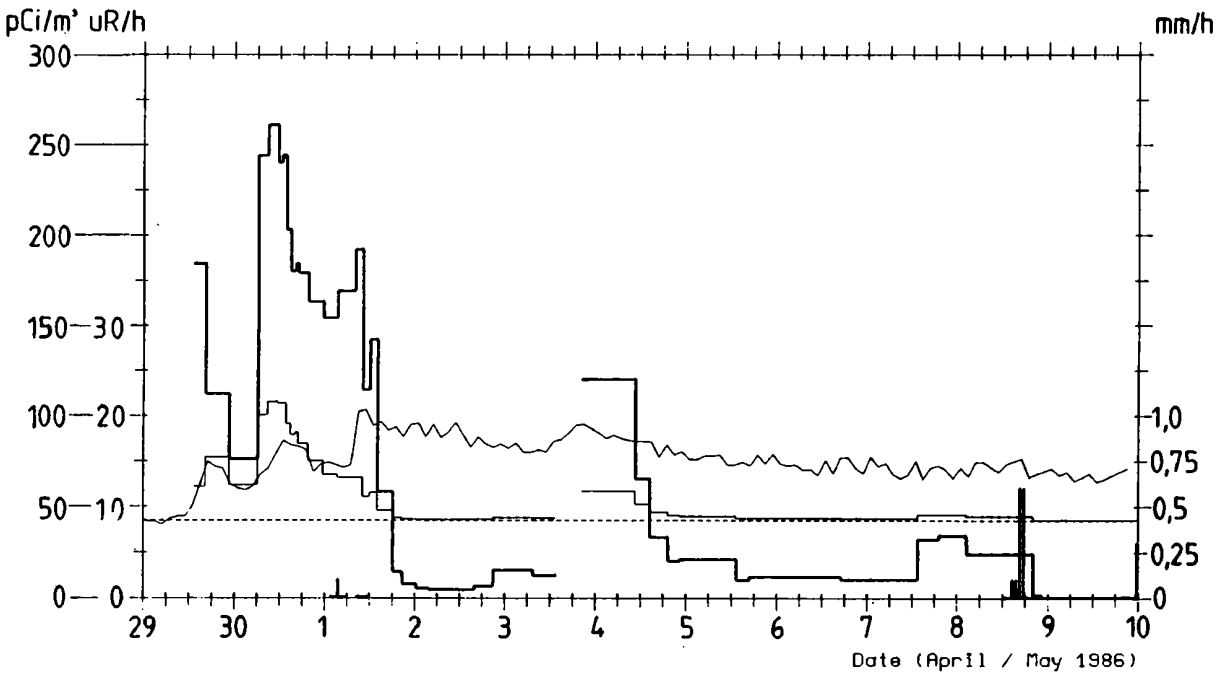


Fig. 7. Time series of gamma dose rate (medium solid line), natural background (thin broken line), calculated submersion dose rate above background (thin solid line), all in $\mu\text{R}/\text{h}$; Cs-137 activity concentration of aerosol in pCi/m^3 ; hourly precipitation values in mm; for Vienna (Wien-Hohe Warte / Grinzing)

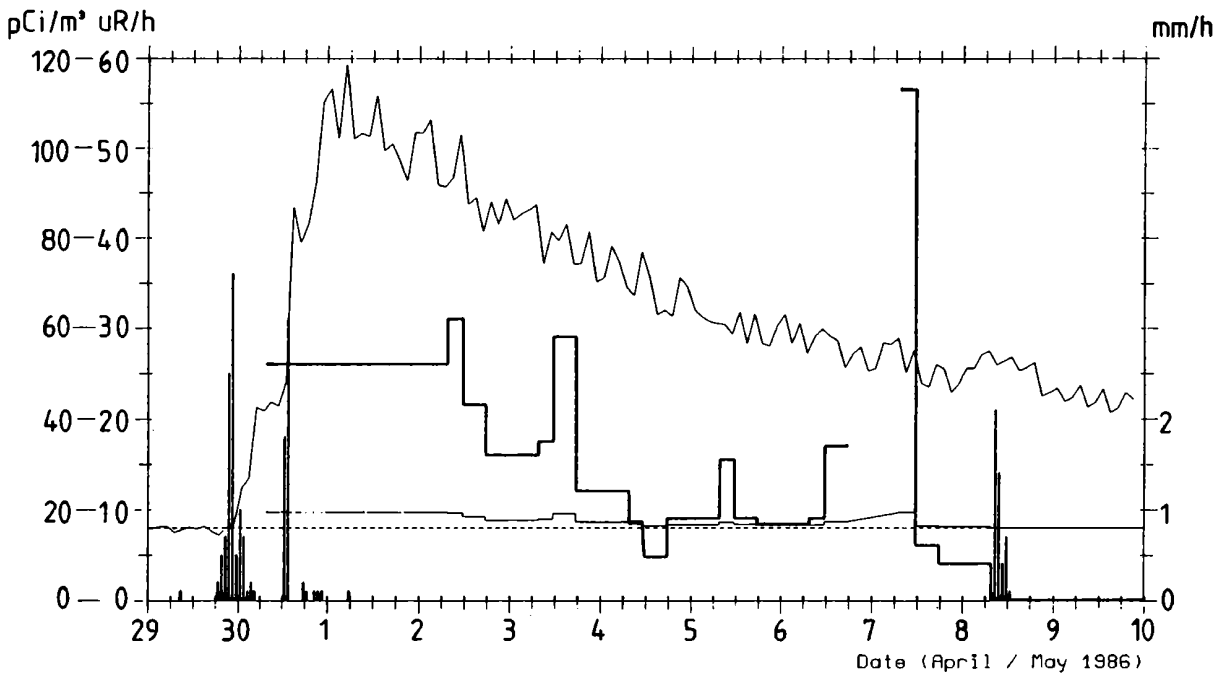


Fig. 8.
Same as fig. 7, but for Innsbruck.

The correlation between maximum observed dose rates (the residual dose rate at end of May gave the same results) and precipitation at nearby weather stations (total over the period April 29, 19 LST until May 3, 07 LST), which includes 240 locations in all the country, yields a correlation coefficient of only 0.5 (fig. 9). However, if the residuals are plotted on a map and analyzed (fig. 10), distinct geographical patterns can be recognized. Contamination levels are underpredicted in the eastern and northern part of the country, where the higher air concentrations were found, and overpredicted in the west, where the air concentrations were low. A portion of the scatter can be attributed to local-scale variations of the precipitation and to the inhomogeneities in siting of the radiation sensors. Unfortunately, data available to us do not allow an analysis like the one by Clark and Smith (1988).

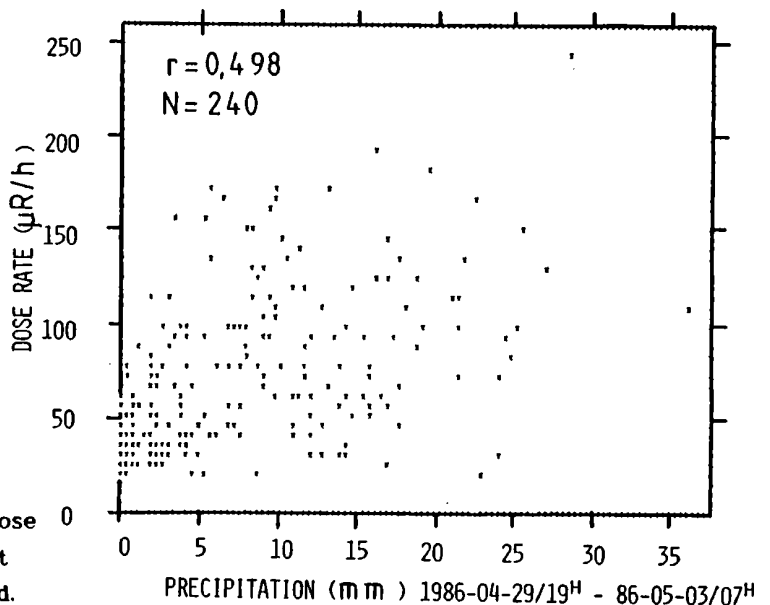


Fig. 9.
Scatter plot of maximum observed dose rate (background subtracted) against precipitation during indicated period.

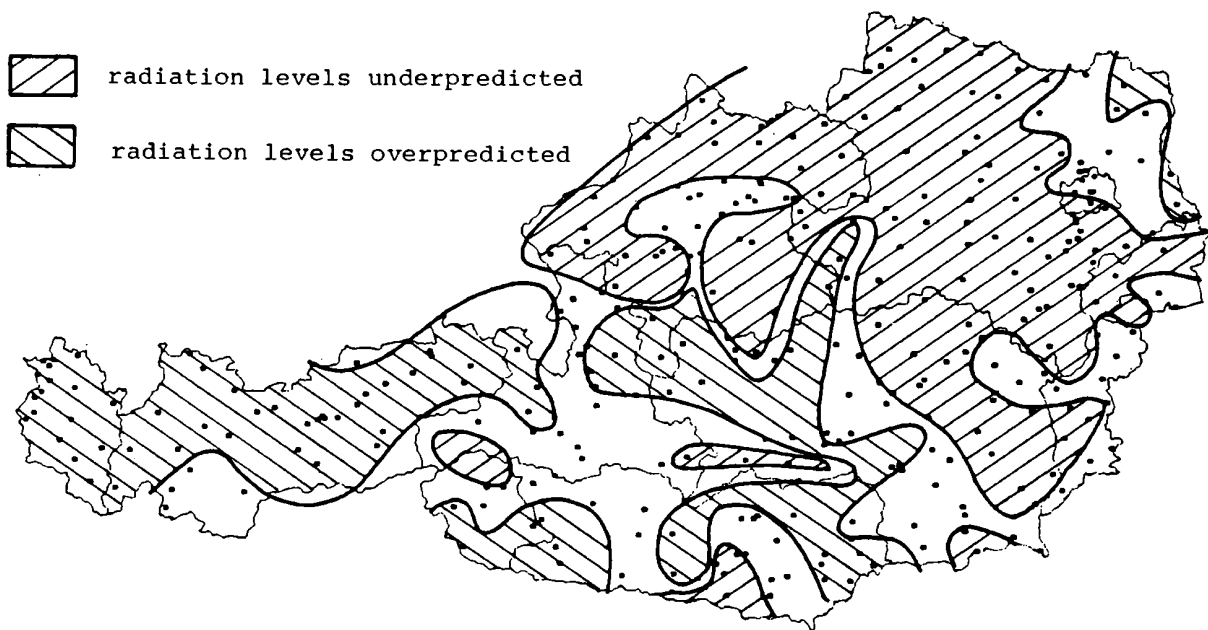


Fig. 10.
Residuals from a regression which estimates dose rates from precipitation according to fig. 9.
Areas with significant under- and overprediction are hatched.

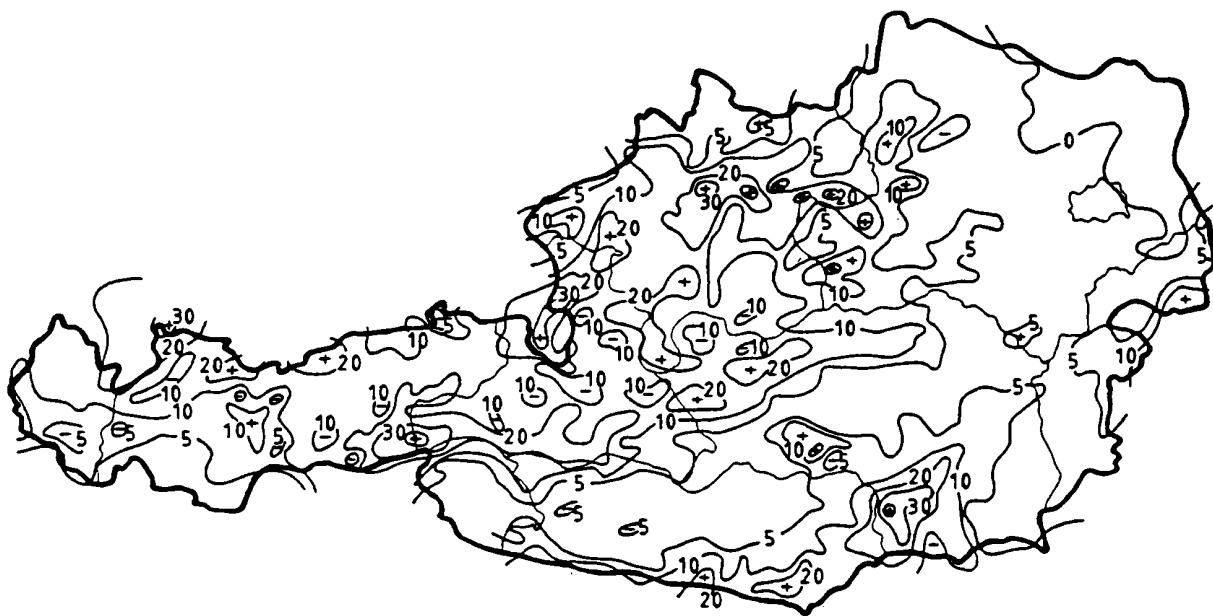


Fig. 11.
Analysis of total precipitation in the period 29 April 1986, 19 LST until 3 May 1986, 7 LST,
based on about 1000 stations.

A careful analysis of all the precipitation data is shown in fig. 11. It is obvious that such a detailed structure of the precipitation field, which is due to convective processes and orographic effects of the Alps, cannot be expected to be simulated by a prognostic model. A dense observation network is the only chance for monitoring, since estimations by radar are unreliable in mountainous areas. The precipitation map has been compared with the results from small-scale contamination investigations for limited areas, e.g. in Styria; the result was that the general coincidence of maxima and minima is quite good, though the contamination showed an even more detailed structure than could be resolved by precipitation network.

5. Situation in high mountain areas

In Austria, only one radiation monitoring station on a mountain top exists, namely the Sonnblick observatory in 3105 m. Fig. 12 shows the variation of the dose rate at Sonnblick and two near-by valley stations. They show a simultaneous first rise at midnight between April 29 and 30 which was due to precipitation. In Italy, however, a time lag up to 48 h has been observed between the arrival times at mountain and low stations (Dietrich et al., 1988). The striking feature is the pronounced peak at Sonnblick on May 3, which does not occur at either of the other stations. The sudden drop ending this episode makes clear that the peak must be due to an activity cloud passing at higher levels. The approximate height of this peak is 60 $\mu\text{R}/\text{h}$; if one assumes that the isotopic composition of the air during the maximum of air concentrations observed 12 h later in Vienna is representative also for Sonnblick, the specific activities in the air at Sonnblick can be reconstructed. The following values result from a computation which assumes a 2π solid angle for the incoming radiation and neglects the effect of reduced air density (thus being somewhat too high):

Te-132	450 Bq/m ³
I-131	370 Bq/m ³
Ru-103	220 Bq/m ³
Cs-137	90 Bq/m ³
Cs-134	45 Bq/m ³

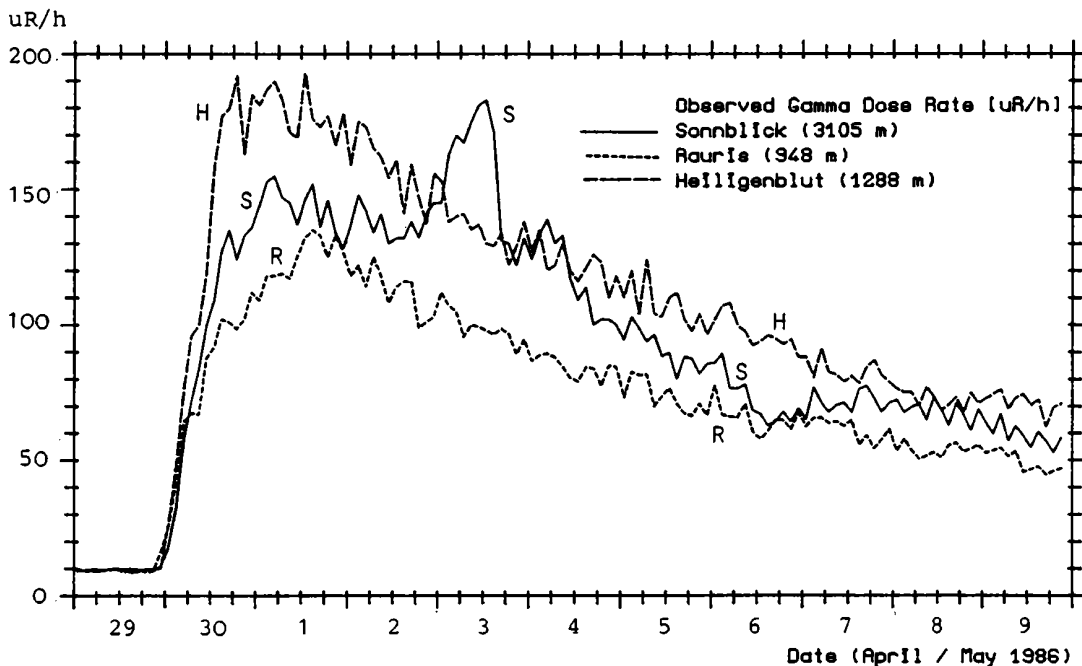


Fig. 12. Time series of gamma dose rate at Sonnblick and two near-by valley stations.

These values exceed the highest ones observed in the plains by a factor of 5. Fig. 11 shows also a higher rate of decrease between May 4 and 6 at Sonnblick, compared with the valley stations. This is due to the "visual field" of the detector, which is mounted on the roof of the building and "sees" near-by ground only in a small solid angle.

It can be assumed that the share of submersion in the first peak is also much higher at Sonnblick than in the valleys, corresponding to a higher activity concentration in air. Together with the increase of precipitation amounts with height, this should lead to a considerable vertical gradient of ground contamination. The few measurements that are available (UBA, 1986; Ambach et al., 1987; Böhm et al., 1988; Hofbauer and Steinhauser, pers. comm.; Wenisch and Bossew, pers. comm.) generally support this conclusion, though a maximum at middle altitudes is suggested by some of the data; systematic investigations of vertical profiles would be desirable.

6. Conclusions for emergency situations and model verification

From the results of this study the following conclusion can be drawn:

1. Information on the vertical distribution of activity is important. It can be collected by aircraft or helicopter soundings, radiosondes with radiation equipment, at mountain stations or - especially in flat countries - on high towers (e.g. TV towers).
2. During stable conditions (strong vertical gradients), one should be careful to adjust models with poor resolution in the vertical by means of surface observations.
3. Monitoring of both air contamination (aerosol activity) and dose rate is important. Sampling intervals should be standardized, e.g. according to synoptic observations. Dose rate measurements and their sites should be standardized like meteorological observations.
4. Convective precipitations cause small-scale variations of contamination and thus render model verification and preparing of countermeasures difficult. A meteorological radar may help in flat terrain, but in high mountain areas near-real-time data transmission from all the precipitation networks is the only solution. In Austria this is now being considered a possibility in emergency situations.

References

- Ambach, W. (1987): Strahlenbelastung im Hochgebirge nach dem Reaktorunfall in Tschernobyl. *Wetter und Leben*, 39, 121-124.
- Böhm, R. et al. (1988): Massenhaushalt Wurtenkees, Jahresbilanz 1985/86. *Wetter und Leben*, 40, 43-57.
- Clark, M.J. and F.B. Smith (1988): Wet and dry deposition of Cernobyl releases. *Nature*, 332, 245-249.
- Dietrich, E. et al. (1988): Le stazioni di montagna per il rilevamento precoce di inquinamento radioattivo dell'atmosfera. 20th Int. Conf. on Alpine Meteor., Sestola, Italy.
- IAEA (1986): The accident at the Chernobyl nuclear power plant and its consequences, Annex 5. Working document IAEA Experts' Meeting Vienna 1986.
- Kolb, H. et al. (1986): Diskussion meteorologischer Aspekte der radioaktiven Belastung in Österreich durch den Reaktorunfall in Tschernobyl. *Arbeiten aus der Zentralanst. f. Meteor. u. Geodyn. (Wien)*, Heft 69.
- UBA (1986): Tschernobyl und die Folgen für Österreich. Vorläufiger Bericht des Umweltbundesamtes.

The radiological data have been measured and made available by the radiation protection departments of the Bundeskanzleramt, the Bundesanstalt für Lebensmitteluntersuchung und -forschung (Wien), and the Bundesanstalt für Lebensmitteluntersuchung (Linz).

DISCUSSION

QUESTION: Dickerson: Have you been able to study the ratios in wet deposition for I-131 and Cs-137?

ANSWER: There are not many radiological measurements of precipitation samples: most of them refer to monthly samples. In addition, the quality of the data is not always satisfying. For the precipitation in Vienna (30/4-1/5) the values are 2410 nCi I-131/l to 45 nCi Cs-137/l.

ASSESSING THE WET DEPOSITION OF RADIONUCLIDES

H. M. ApSimon and P. A. Stott
Air Pollution Group
Imperial College, London, SW7 2AZ.

INTRODUCTION

The correlation between deposition of $\text{Cs}^{137/134}$ from Chernobyl and precipitation intercepting the airborne radioactive material has suggested that numerical simulations can provide estimated maps of deposition which can be of use in guiding monitoring teams to the most severely affected areas. This is dependent on detailed rainfall data being rapidly available such as weather radar, enabling "nowcasting" of the effects as airborne radionuclides pass over a country.

ApSimon and Simms (1988) have illustrated this approach using data from the weather radar networks of the UK Meteorological Office over England and Wales to deduce a pattern of deposition of $\text{Cs}^{137/134}$ from Chernobyl, which effectively picks out the areas of higher contamination as deduced from grass sampling undertaken by the Institute of Terrestrial Ecology. This paper uses more detailed numerical models of different types of storm system to examine the validity of this approach, and how the efficiency of wet deposition depends on the characteristics of the precipitation system and varies with the amount of rainfall scavenging the radionuclides.

1. Wet deposition of pollutants is commonly estimated in numerical models using a wash-out coefficient or wash-out ratio. Both these approaches envisage a rather constant spectrum of raindrops uniformly scavenging a passive pollutant plume as they descend. The wash-out coefficient can thus be expressed as an integral over the raindrop spectrum

$$\Lambda = \int N(a) E(a) \pi a^2 V(a) da$$

where $N(a)$ is the number density of raindrops of radius a ,
 $E(a)$ is their collection efficiency for the pollutant
and $V(a)$ is their terminal velocity.

It is commonly expressed as a simple power law of the rainfall rate J in mm/hr; $\Lambda = \Lambda^* J^p$ where p is in the range 0.75 to 1.0. The wash-out ratio is the ratio of pollutant concentration in precipitation to that in air, usually based on near-surface concentrations and introducing uncertainties about pollutant profiles, but a readily observed parameter. In practice precipitation is caused by the vertical ascent of moist air and often involves highly dynamic transport of polluted air through the system. This paper presents a study on how the efficiency of removal of radionuclides depends on the characteristics of different types of storm. It is based on a computer model, DROPS (Deposition of Radionuclides and Other Pollutants from Storm-systems), which incorporates the dynamical behaviour of precipitating systems and the microphysical and chemical processes affecting pollutants circulating through them.

To illustrate the application of the models, 3 case-studies are described in this paper. Measurements after Chernobyl revealed a very wide spread in values of the wash-out ratio for the important Caesium isotopes (e.g. Persson et al(1987) quote values varying from 0.3 to 5×10^6 over Sweden and Smith(1987) gives values a factor 2 higher). The deposition from Chernobyl was spatially very inhomogeneous and often concentrated on upland areas with enhanced orographic precipitation. The first case study therefore applies to deposition of radioactive caesium aerosols when air is forced above the condensation level over a ridge. Over central Europe however much of the caesium from Chernobyl was deposited in convective storms in the unstable air-mass. These act like giant vacuum cleaners processing large volumes of air and depositing material beneath the core; this provides the basis for our second case-study. It was such a storm that led to the partial evacuation of Gomel, about 100 km away from Chernobyl.

Over the UK the precipitation fell from a particular type of front involving a very steep ascent of air at the frontal surface, and still amenable to 2-D simulations with our current model. This is our third case study.

THE DROPS MODEL

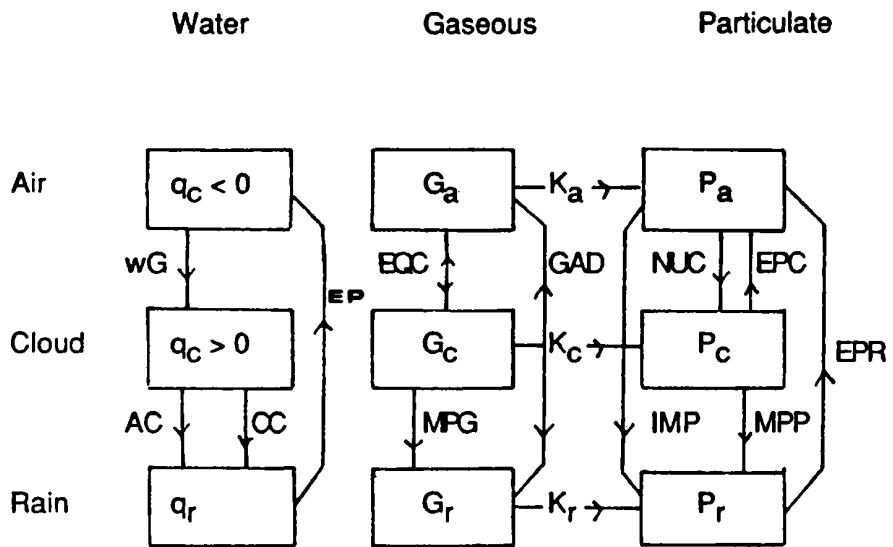
In a full mesoscale atmospheric model the full set of equations governing conservation of mass, heat, momentum, water and other gaseous and aerosol materials is integrated, and the air motion is derived as part of the solution. However such models are very demanding on computer resources. In the DROPS model the dynamics of the system, which could be obtained as output from such a model or from direct observations, are predetermined and provided as input. Provided these air motions satisfy the continuity equation, the transport of water and pollutant material passing through the system, and their transfer between air, cloud droplets, and raindrops, can be simulated. The model can thus be used as a tool to assess how the overall deposition and export of pollutants depend on the microphysical processes involved.

Currently the DROPS model is limited to simulation of warm clouds with no ice-phase, and some simplifications are introduced. The cloud droplets, formed according to the density of CCN, are assumed, as by Kessler (1969), to be monodisperse, growing or evaporating according to changing equilibrium conditions with the interstitial air and transferred to the rain drops by auto-conversion and accretion. Similarly the spectrum of raindrops is treated as though they all fall with the same terminal velocity appropriate to the median of the size distribution.

Hygroscopic aerosols are assumed to be efficiently incorporated in cloud droplets as CCN, and their removal in precipitation is hence largely determined by autoconversion and accretion of these droplets. Hydrophobic aerosols are removed mainly by impaction with falling raindrops. The transfer of gases is based on equilibrium between interstitial air and the cloud droplets and rain according to Henry's law; oxidation and aqueous phase chemistry within the droplets and rain can also be included. In this case the additional data is required on concentrations of all relevant species including the oxidants. A schematic diagram of the model, showing the microphysical processes included, is given in figure 1.

CASE STUDY 1 - OROGRAPHIC ENHANCEMENT FROM AN UPDRAUGHT

The first illustration of this model applies to the "feeder-seeder" mechanism with flow over a hill of height 675 m assuming the Cs-137 is attached to aerosols of 1 micron in diameter - see figure 2. The velocity of the free flow aloft approaching the hill is 15 m.s^{-1} , with light rain of 1 mm per hour falling from the seeder cloud above the condensation level at an altitude of 1 km. As the air approaches the hill unsaturated air beneath the seeder cloud is forced to rise and condenses, with a high proportion (90%) of the Cs-137 aerosol assumed incorporated as CCN in the newly formed cloud droplets. The raindrops from the seeder cloud accrete moisture from



AC - coalescence

CC - accretion

EP - evaporation of rain

wG - condensation

EQC - gas in air and cloud in equilibrium

MPG - transfer of gas from cloud to rain by conversion of cloud water to rain water

GAD - absorption/desorption of gas between air and rain

K_a, K_c, K_r - oxidation in air, cloud and rain

IMP - impaction

NUC - nucleation

EPR - transfer of particulate from rain to air due to evaporation of rain

EPC - transfer of particulate from cloud to air due to evaporation of cloud

MPP - transfer of particulate from cloud to rain by conversion of cloud water to rain water

Figure 1 DROPS model : schematic diagram

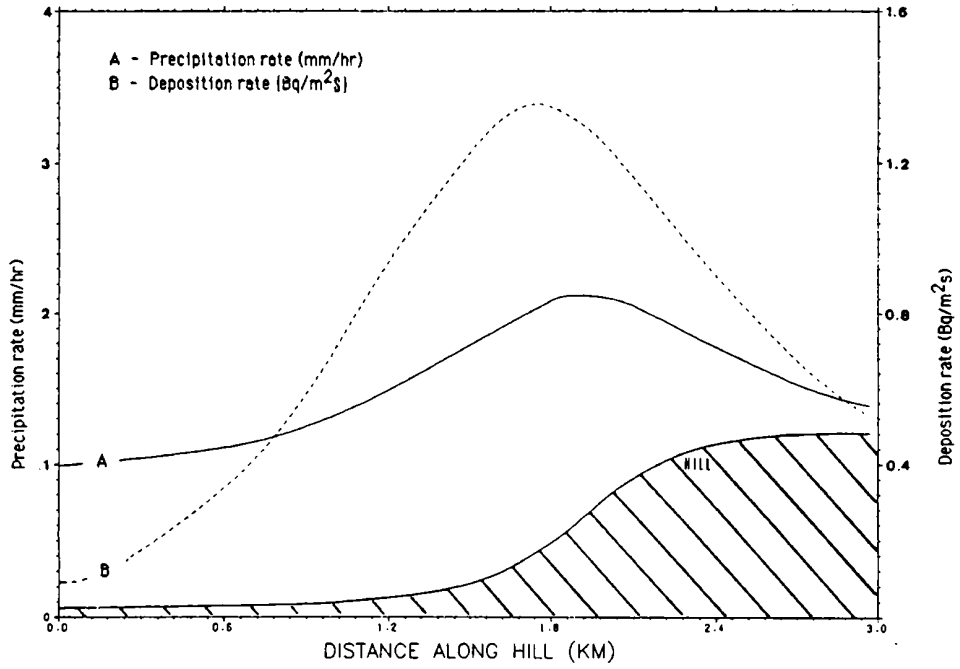


Figure 2 Orographic enhancement to deposition and precipitation over hill of height 675m.

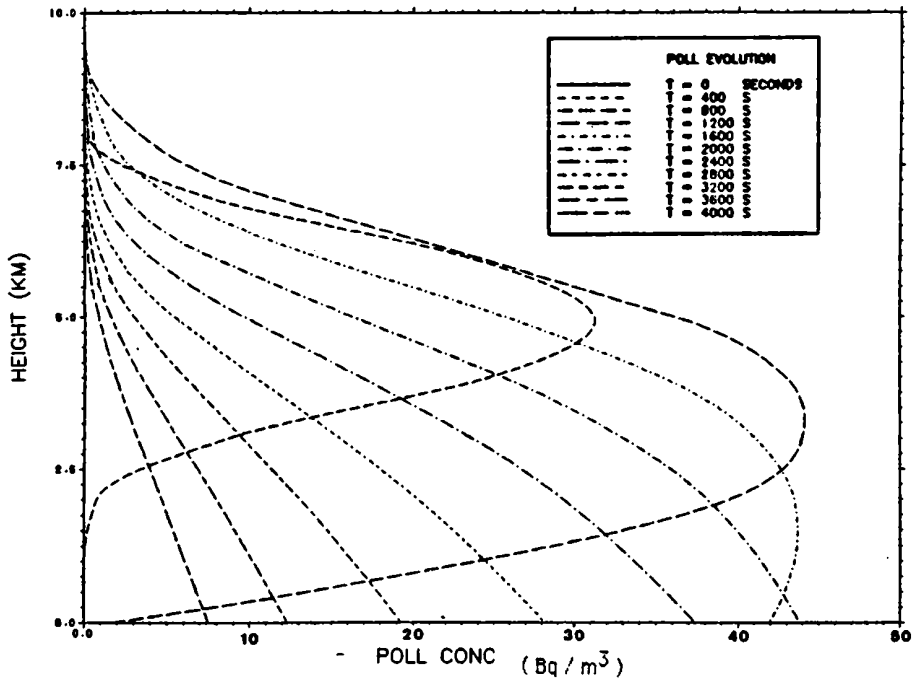


Figure 3 Concentration profiles of pollutant in rain at different stages during evolution of shower

these cloud droplets enhancing the rainfall as indicated in curve a. However because of the greater capture efficiency of the droplets than for the bare dry aerosol by impaction, the deposition of Cs-137 at the ground increases far more than the rainfall (curve b). Thus the effective wash-out coefficient, Λ , increases from $4.6 \cdot 10^{-5}$ to a maximum of $6.3 \cdot 10^{-4}$ slightly downwind of the maximum updraught crossing the condensation level. The wash-out ratio varies proportionately ($0.2 \cdot 10^6$ to $3 \cdot 10^6$). Sensitivity studies have been undertaken varying hill height, nucleation efficiency, aerosol size, and wind-speed on approach. The results are summarised in table 1.

TABLE 1

Parameter varied		Maximum wash-out coeff. s^{-1}
Height of hill,	H = 400 m	$5.6 \cdot 10^{-4}$
Aerosol diameter,	2a = 4μ	$6.2 \cdot 10^{-4}$
Windspeed,	U = 10 m/s	$6.7 \cdot 10^{-4}$
Nucleation efficiency,	$E_{nuc} = 0.6$	$4.3 \cdot 10^{-4}$

As well as nucleation efficiency overall CCN density was changed to see what difference a clean or dirty air-mass could have on the deposition, but this had little overall effect. Whether this is true in all cases remains to be seen.

The conclusion to be drawn from this is that deposition can be very much enhanced wherever there are updraughts taking new air with fresh Cs-137 aerosol above the condensation level and up into the cloud. In hilly terrain such updraughts can easily be initiated systematically by topographic features and hence a very patchy distribution is likely to result over quite small distance scales.

CASE STUDY 2 - CONVECTIVE STORMS AND SHOWERS.

The dynamics within a strong convective storm are extremely complex and 3-dimensional, with rain evaporating below cloud base leading to a downdraught of cooled air. However our initial studies on this followed Fisher (1982) with a 1-D model which we extended to faster updraught speeds, and evolving shower systems. In this model a radially symmetric updraught is assumed at the core of the evolving shower with a maximum speed of 5 m/s. Figure 3 shows concentration profiles of the pollutant in rain at different stages for this fairly typical case. Initially material is distributed within the boundary layer. As the updraught starts carrying material aloft condensation occurs at a height of about 2 km, and the caesium aerosol is transferred to the cloud droplets leaving low concentrations in the interstitial air. After 800s of the simulation rain is beginning to fall through the cloud but has not yet fallen beneath the cloud. After 1200 seconds the first rain has removed a good deal of the material in the lower layers of cloud and this is just beginning to reach the ground. The maximum rate of deposition occurs after about 20 minutes to 1/2 hour and declines thereafter, the peak value of the wash-out ratio being $4.3 \cdot 10^6$. In practice most shower systems would cease after such times as moisture is removed from the column, and rain evaporates cooling and slowing the updraught.

The overall efficiency of removal in convective showers depends on the strength of the shower and the updraught velocity. As well as depositing material on the ground, there is also export at the top of the system to the free troposphere - an important topic in relation to background concentrations of long-range pollutants like SO₄ aerosols. The efficiency of removal and fraction exported assuming a 2000 second duration for the storm is illustrated as a function of updraught speed in table 2. It shows how the fraction exported increases considerably with faster updraughts allowing shorter residence times for scavenging in the column, albeit that the rainfall is heavier with the greater rate of supply of moisture.

TABLE 2

Updraught speed (m/s)	Fraction removed	Fraction exported
2	0.74	0.26
4	0.69	0.31
6	0.59	0.41
8	0.42	0.58
10	0.24	0.76

Persistent convective storms really require at least a 2-dimensional simulation to be realistic, involving both updraught and downdraught. Although we have undertaken such studies the 2-D applications of the DROPS model will be illustrated in this paper for the rather different application of a frontal system.

CASE STUDY 3: 2-D APPLICATION TO AN ANA FRONT

Figure 4 illustrates the motion of air at a steep frontal surface of the type that passed over the UK after Chernobyl. In addition to the motion indicated there would be a component of flow perpendicular to the plane of the diagram introducing a shear across the frontal surface, which is ignored in the 2-D simulation. The velocities at the frontal surface are almost vertical, giving a band with intense rain close to the front, depending on the rate of convergence between the two air masses. With such a steep ascent material is deposited within a short distance of the position at which it starts its ascent from the boundary layer. This allowed ApSimon and Simms(1988) to obtain a good picture of deposition over England and Wales by combining weather radar data on precipitation with the observed time of passage of the Chernobyl cloud.

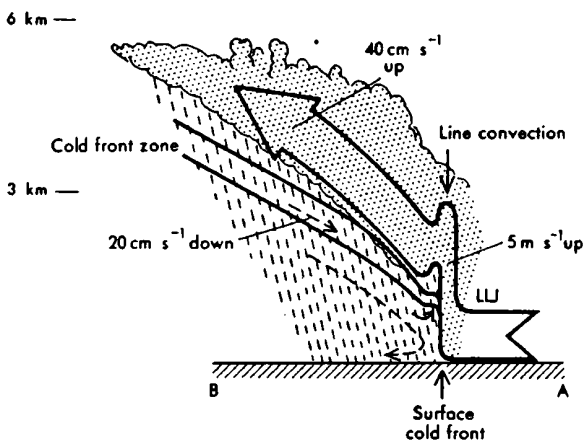


Figure 4 Motion of air at steep cold frontal surface (from Browning, 1985)

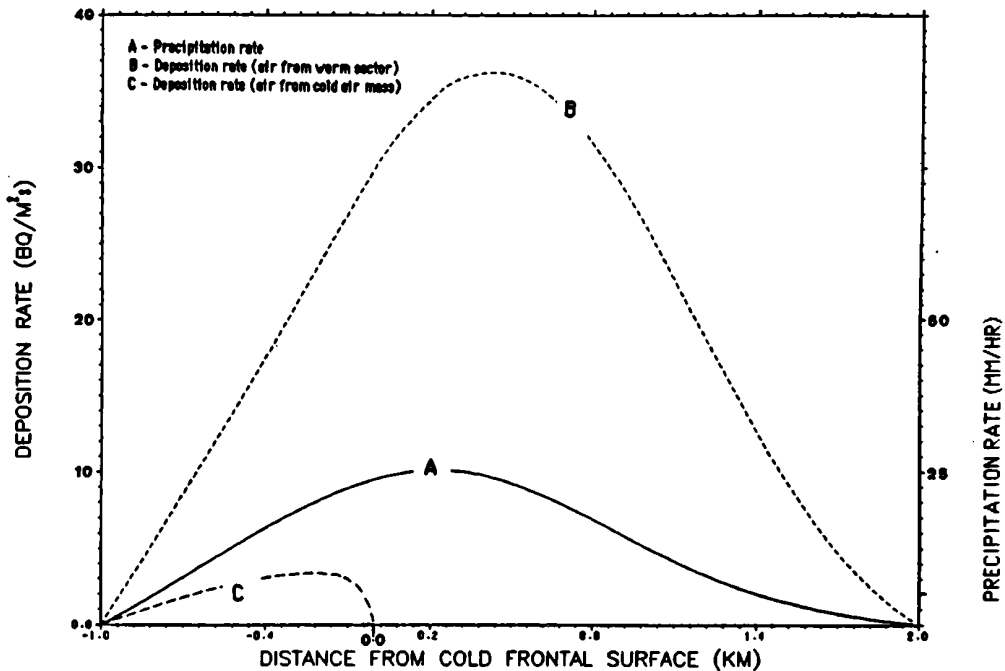


Figure 5 Deposition and precipitation rates in cold frontal circulation

The results of the more detailed simulation with the DROPS model of the circulation and deposition of caesium aerosols through such a system are given in figure 5. This shows the rate of deposition at different distances on either side of the front. Curve(a) shows the rate of rainfall. Curve(b) is the calculated deposition rate assuming 4Bq/m^3 of 1μ diameter aerosol feeding into the frontal ascent from the warm sector (this is consistent with the observations of peak concentrations over the UK in the warm sector); the deposition in this situation is dominated by rain-out processes within the cloud giving wash-out ratios up to 2.10^6 . Curve (c) shows the corresponding calculated deposition rate assuming instead that the contaminated air is in the cold air-mass behind the frontal surface, when removal is dominated by wash-out by precipitation falling from above. Wash-out ratios are obviously very much smaller being up to $0.2.10^6$. The same kind of sensitivity studies can be applied to this case as to the shower analysis. However the order of magnitude difference between the removal efficiencies indicates how important it is to identify where radioactive material is relative to the frontal surfaces.

More commonly, fronts are of the kata type with less steep frontal surfaces, which are much more difficult to simulate with a 2-D model. However there are many other factors to be considered with the 2-D model before progressing to 3-D simulations; these include simulation of cold clouds with ice-phase processes, and various sensitivity studies are planned on the deposition of both hygroscopic and hydrophobic aerosols, and on the fractions exported to the free troposphere.

SUMMARY AND CONCLUSIONS.

The application of a computer model to simulate removal of radioactive aerosols has been illustrated for 3 case studies - orographic effects of a ridge, a convective shower, and an ana-cold-front. These show clearly how the characteristics of the rain-storm affect the efficiency of removal, and the export to the free troposphere. They also indicate how the pattern of deposition is likely to be extremely inhomogeneous, with great variations in wash-out ratio.

Other work is also in progress on acid deposition incorporating simple aqueous chemistry in the DROPS model, and assuming instantaneous chemical equilibrium between the droplets and the air through which they are falling. This provides an interesting insight into the relationship between chemical scales for oxidation and the time-scales for pollutants to cycle through the storm, and on the interaction between ammonia and acidic species. It will be published in due course.

REFERENCES

- ApSimon, H. M. and Simms. K. L., 1988, The use of weather radar in assessing deposition of radioactivity from Chernobyl across England and Wales. In press. Atmospheric Environment, 22.
- Browning, K. A., 1985, Conceptual models of precipitation systems, Meteorological Magazine, 114, 293-319
- Fisher, B. E. A., 1982, The transport and removal of sulphur dioxide in a rain system. Atmospheric Environment, 16, 775 - 783
- Kessler, E., 1969, On the distribution and continuity of water substance in atmospheric circulations, Met Monograph 10 (32), American Meteorological Society
- Persson, C., Rodhe, H., De Geer, L., 1987, The Chernobyl Accident - a meteorological analysis of how radionuclides reached and were deposited in Sweden, Ambio, 16, No 1, 20 - 31
- Smith, F. B., 1987, The environmental consequences of the Chernobyl Nuclear Reactor Accident, Meteorological Office Report, T. D. N. No 189

DISCUSSION

PAPER: ApSimon - wet deposition

COMMENT: Dickerson: We are finding that electrical effects can have an important effect on the scavenging process.

QUESTION: Nordlund: Do you have found any case where there are at the same time and location vertical profiles of nuclide concentration, precipitation amounts and deposition values?

ANSWER: Unfortunately no. It is difficult enough to find locations where surface air and precipitation have been measured simultaneously to give wash-out ratios.

QUESTION: Raes: Can you get all the information together needed to evaluate nucleation efficiency (size, composition, supersaturation)? Can you identify the most critical parameters?

ANSWER: Nucleation efficiency is a very important parameter as I indicated in my talk. We know a little about the Cs-137/134, that it was dissolved in rainwater as hydroxide or in a colloid solution, but if you can supply any more information I shall be grateful.

QUESTION: Urbancic: Do you plan some research on scavenging on the lee side of the mountain crest?

ANSWER: Exactly where the maximum will occur depends on the wind field. The calculations shown have been based on a rather idealised flow field. According to Froude number and the slope and shape of the hill the flow characteristics could vary quite a lot. I think it is impossible to estimate where the maximum on a hill will occur in practice. I merely wanted to illustrate how there can be greatly enhanced areas of deposition, exceeding the enhancement of rainfall, over a hill.

QUESTION: Vychytil: Did you use different modeling approaches for the transport of aerosols (like Caesium) and for the transport of

rare gases like Xenon?

ANSWER: Since we were not considering coarse aerosol deposited locally, we assumed that the Cs on fine aerosols and the rare gases were advected and mixed in the same way. However the rare gases are assumed not to deposit, whereas dry and wet deposition are included for caesium.

VI

FINAL DISCUSSION

Final discussion

The meeting concluded with a general discussion chaired by Dr ApSimon (EURASAP) together with Dr Labrousse(WMO), Dr Asculai(IAEA), and Mr Frazer(CEC). Dr ApSimon began by summarising the topics covered during the meeting. This had opened with the presentation of plans for the joint IAEA/WMO/CEC study to evaluate numerical models for long-range atmospheric transport against data from the Chernobyl accident and the ANATEX tracer releases in North America. Papers had addressed the simulation of the processes involved (advection, horizontal and vertical spreading, and deposition) in the various types of model (plume, Lagrangian puff, Eulerian, and particle models etc) applied over distances from global and continental down to regional and local scales. A very positive feature of the meeting had been the free discussion of the complications and the difficulties of treating the 3-dimensional transport, topographical effects, unresolved sub-grid scale processes, and redistribution and deposition of material by precipitation systems. It was very important to recognise the limitations of models if they were to be used effectively for real-time analysis in accident situations.

Several important aspects of the application of models in emergency situations had been addressed. These included the use of models in forecasting mode, additional data requirements, and the international exchange of radiological measurements as well as meteorological data. The availability of precipitation data, and radiological observations of the spread of the cloud both at ground level and aloft, and concentrations of key nuclides in air and precipitation, had been identified as particularly important. Attention had been drawn to the development of capabilities in modelling assessments, to integrate radiological observations as they became available to check, revise and update calculations. Model evaluation studies might suggest some ideas on how this might be done. The uncertainties involved in model assessments added to the need to consider very carefully how results should be made available.

In the ensuing discussion Dr Dickerson expressed concern that in the event of a future accident there could be a vast number of models applied, quite probably giving conflicting results; this it was agreed would add to the confusion! This raised the subject of the selection of accredited centres, and the conduct of routine international exchange of requisite data and emergency exercises including model assessments. There are two options for accredited centres; these can either be based at existing weather forecasting centres, or at some other location with direct access to forecast windfields and ancillary data.

On the subject of requirements for international exchange of data, the views of member states have been requested both by IAEA and the CEC, and special requirements for modelling applications should be made known to national representatives in this context. Dr Labrousse enlarged on the international exchange of data over the GTS system of the WMO World Weather Watch, and the options for precipitation data in real-time. Apart from raingauge data, weather radar capabilities are still in the development stage and available only in certain countries (although there is collaboration in Europe under a COST scheme, and some arrangements to exchange such data are already operational.)

Dr Labrousse and Dr Pudykiewicz led the discussion on to the improvement of weather prediction models and the problems both of data and parameterisation for better representation of the boundary layer and its processes. The increase in available computing power imposes less of a restriction on modelling capabilities, but points to a relatively few centres equipped and operating large-scale models. There was general agreement that it is desirable to move towards integration of numerical models together with meteorological and radiological data, within overall information systems to assist decision makers in emergency situations. An evaluation of models to help development and improvement, and appreciation of the uncertainties involved, would be a valuable stage towards this long-term objective.

Dr ApSimon concluded the meeting by commending the participants for their frank and open contributions; and thanking the Austrian Academy of Sciences, the Austrian Meteorological Society, and the Institute for Meteorology and Geodynamics for hosting the meeting- particularly Ulrike Pechinger and her colleagues for their impeccable organisation and very hard work.

VII

APPENDIX

L I S T O F P A R T I C I P A N T S

Armand Albergel
EDF Electricité de France
6, Quai Watier
F-78401 Chatou Cedex
France

Helen ApSimon
Imperial College of Science and
Technology
Department of Mechanical Engineering
Exhibition Road, London SW7 2BX
United Kingdom

Ephraim Asculai
International Atomic Energy Agency
Wagramer Str. 5, P.O. Box 100
A-1400 Vienna
Austria

Martin Beniston
Institut d'Hydraulique et d'Énergie
LASEN - Laboratoire de Systèmes
Energetiques
CH-1015 Lausanne
Switzerland

Vladimir A. Borzilov
Institute of Experimental Meteorology
Kaluzksky Distr., St. Geolio, 18
249020 Obninsk
USSR

Roberto Caracciolo
ENEA DISP
Via V. Brancati 48
I-00144 Roma
Italy

Helmut de Witt
Brenk Systemplanung
Ingenieurbüro für wiss. techn.
Umweltschutz
Heinrichsallee 38
D-5100 Aachen
FRG

Marvin H. Dickerson
Lawrence Livermore National
Laboratory
P.O.Box 808, L-262
Livermore, CA 94550, USA

Bruno Favale
Istituto di Fisika dell'Atmosfera CNR
P. de L. Sturzo 31
I-00144 Rome
Italy

George Fraser
CEC DG XI/A/1
Luxembourg, 2920

Fernando Serrano Garcia
Instituto Nacional de Meteorologia
Co. de las Moreras s/n
E-28040 Madrid
Spain

Heiner Geiss
Kernforschungsanlage Jülich
Postfach 1913
D-5170 Jülich
FRG

G. Graziani
Joint Research Centre
I-21020 Ispra (Varese)
Italy

G. Hehn
Universität Stuttgart
Pfaffenwaldring 31
D-7000 Stuttgart 80
FRG

Eberhardt Henrich
Radiation Protection Department
Berggasse 11
A-1090 Vienna
Austria

Hanspeter Isaak
Swiss Nuclear Safety Inspectorate
CH-5303 Würenlingen
Switzerland

Hirohiko Ishikawa
Environmental Research Lab.1
Japan Atomic Energy Research Inst.
Tokai-Mura, Naka-gun,
Ibaraki-ken 319-11, Japan

Ingo Jacobsen
Deutscher Wetterdienst
Frankfurter Str. 135
D-6050 Offenbach
FRG

Zvonka Jeran
Institut "Jozef Stefan"
Jamova 39
YU-6111 Ljubljana
Yugoslavia

J. A. Jones
National Radiological Protection
Board
Chilton Didcot
Oxon OX11 0R9, United Kingdom

August Kaiser
Zentralanstalt für Meteorologie
und Geodynamik
Hohe Warte 38
A-1190 Vienna
Austria

Helga Kolb
Institut für Meteorologie und
Geophysik d. Universität Wien
Hohe Warte 38
A-1190 Vienna
Austria

Jean Labrousse
Research and Development Department
World Meteorological Organization
Case Postale No. 5
CH-1211 Geneva 20
Switzerland

Manfred Laube
Institute for Geophysics, University
of Cologne
Albertus-Magnus-Platz
D-5000 Köln 41
FRG

R. H. Maryon
U.K. Meteorological Office
London Road, Bracknell
Berkshire RG12 2SZ
United Kingdom

Marino Mazzini
Department of Mechanical and Nuclear
Construction, University of Pisa
Italy, Pisa

Michael Memmesheimer
Institute for Geophysics, University
of Cologne
Albertus-Magnus-Platz
D-5000 Köln 41
FRG

R. E. Munn
IIASA
A-2361 Laxenburg
Austria

Luc Musson-Genon
Direction de la Météorologie
Nationale (SCEM/D/ES)
2, Avenue Rapp
F-75007 Paris
France

Göran Nordlund
Finnish Meteorological Institute
Air Quality Department
Sahaajankatu 22 E
SF-00810 Helsinki
Finland

Ulrike Pechinger
Zentralanstalt für Meteorologie
und Geodynamik
Hohe Warte 38
A-1190 Vienna
Austria

Malcolm Pendergast
Savannah River Laboratory
Aiken, SC 29801
USA

Martin Piringer
Zentralanstalt für Meteorologie
und Geodynamik
Hohe Warte 38
A-1190 Vienna
Austria

J. Pudykiewicz
Atmospheric Environment Service
of Canada
2121 Trans Canada Highway,
Dorval, Quebec
Canada H9P 1J3

Frank Raes
CEC - Joint Research Centre
I-21020 Ispra (Varese)
Italy

Heinz Reuter
Zentralanstalt für Meteorologie
und Geodynamik
Hohe Warte 38
A-1190 Vienna
Austria

Ingeborg Schwarzl
Zentralanstalt für Meteorologie
und Geodynamik
Hohe Warte 38
A-1190 Vienna
Austria

P. Seibert
Institut für Meteorologie und
Geophysik d. Universität Wien
Hohe Warte 38
A-1190 Vienna
Austria

Roderick Shaw
IIASA
A-2561 Laxenburg
Austria

A.P. van Ulden
Royal Netherlands Meteorological
Institute
P.O. Box 201
NL-3730 AE de Bilt
The Netherlands

Brian Underwood
Safety and Reliability Direction SRD
Wigshore Lane, Culcheth
Warrington WA3 4NE
United Kingdom

Jelko Urbancic
Institut "Jozef Stefan"
Jamova 39
YU-6111 Ljubljana
Yugoslavia

Ludo van der Auwera
Royal Meteorological Institute
Ringlaan 3
B-1180 Brussels
Belgium

Ignaz Vergeiner
Institut für Meteorologie und
Geophysik d. Universität Innsbruck
Innrain 52
A-6020 Innsbruck
Austria

G.H.L. Verner
Royal Netherland Meteorological
Institute (KNMI)
P.O. Box 201
NL-3730 AE DE BILT
Netherland

Peter Vychytil
Bundeskanzleramt
Abteilung VII/7
Radetzkystr. 2
A-1030 Vienna
Austria

Julian J. N. Wilson
Imperial College of Science and
Technology
Department of Mechanical Engineering
Exhibition Road, London SW7 2BX
United Kingdom

Georg Zapletal
Zentralanstalt für Meteorologie
und Geodynamik
Hohe Warte 38
A-1190 Vienna
Austria

N. Zarimpas
Joint Research Centre
I-21020 Ispra (Varese)
Italy

Johann Züger
Österr. Forschungszentrum Seibersdorf
A-2444 Seibersdorf, Austria

PROTOCOL OF THE WMO/IAEA/CEC ATMOSPHERIC TRANSPORT
MODEL EVALUATION STUDY (ATMES)
DRAFT

Participation in ATMES is contingent on abiding by the following protocols:

1. Participants are to be officially nominated by members of the sponsoring organizations - IAEA, WMO, CEC.
2. Results will be submitted for evaluation according to the schedule specified by the Steering Committee and there will be a representative for each participant at the Model Evaluation Workshop.
3. The information supplied by the project, specifically the data sets on source terms, meteorological and measurements or tracer data will not be transferred in any form to any other person or organization outside the joint project.

4. Reports will be submitted on the study to the Steering Committee for inclusion in the final project report(s). No intercomparison of results relating to this study is to be published prior to dates established by the Steering Committee for the Workshop. Reports on exercises using the data provided may be published freely thereafter.
5. However, whenever results are published utilizing data provided by the sponsors of ATMES, appropriate credits are to be included. Copies of these publications and any others relating to the ATMES study are to be sent to each sponsoring organization.
6. All participants must produce results over a minimum specified map area for the Chernobyl study in the required format. The results which are required pertain to the two radionuclides CS^{137} and I^{131} , as detailed in an Annex, together with additional operational results which are recommended.
7. The results for the Chernobyl study are to be based on the source terms specified, and on meteorological information (data, analysis and forecasts) which would normally be available within 24 hours in an accident situation or from data sets provided for the study (although additional results may be submitted).
8. The use of the available ANATEX data sets , in addition to the Chernobyl case study, is strongly encouraged but is not mandatory.
9. The costs of supplying data sets (transcription onto magnetic tapes/disks in a standard format and postage) will be paid by the participants.
10. A model description will be provided by the participants describing the salient features as specified by the Evaluation Team.
11. The Steering Committee retains the right to extend the schedule under extreme circumstances.

TO BE SIGNED BY PARTICIPANTS:

We, the undersigned, have read the above terms for participation in the study and agree to fulfill the obligations therein.

.....

.....

.....

Bisher erschienene Hefte der
 "ARBEITEN AUS DER ZENTRALANSTALT FÜR METEOROLOGIE UND GEODYNAMIK"

Heft	Publ. Nr.	Fachgebiet	Autor	Titel und Umfang	Preis Ö. S.
1	184	Geophysik	ECKEL, O.:	Über die vertikale Temperaturverteilung im Traunsee. Wien 1967, 42 Seiten, 4 Tabellen, 24 Abbildungen.	80.-
2	186	Meteorologie	STEINHAUSER, F.:	Ergebnisse von Pilotballon-Höhenwindmessungen in Österreich. Wien 1967, 44 Seiten, 16 Seiten Tabellen und 28 Abbildungen.	70.-
3	187	Geophysik	TOPERCZER, M.:	Die Verteilung der erdmagnetischen Elemente in Österreich zur Epoche 1960.0. Wien 1968, 18 Seiten, 3 Tabellen, 10 Kartenbeilagen.	vergriffen
4	190	Geophysik	BRÜCKL, E., G. GANGL und P. STEINHAUSER:	Die Ergebnisse der seismischen Gletschermessungen am Dachstein im Jahre 1967. Wien 1969, 24 Seiten, 11 Abbildungen.	50.-
5	191	Meteorologie	HADER, F.:	Durchschnittliche extreme Niederschlagshöhen in Österreich. Wien 1969, 19 Seiten, 6 Tabellen, 1 Kartenbeilage.	50.-
6	192	Meteorologie	STEINHAUSER, F.:	Der Tagesgang der Bewölkung und Nebelhäufigkeit in Österreich. Wien 1969, 22 Seiten, 4 Tabellen, 16 Abbildungen.	50.-
7	193	Geophysik	GANGL, G.:	Die Erdbeben-tätigkeit in Österreich 1901-1968. Wien 1970, 36 Seiten, 11 Abbildungen, 1 Kartenbeilage.	vergriffen
8	195	Meteorologie	STEINHAUSER, F.:	Die Windverhältnisse im Stadtgebiet von Wien. Wien 1970, 17 Seiten Text, 52 Tabellen, 47 Abbildg.	120.-
9	196	Geophysik	BRÜCKL, E., G. GANGL und P. STEINHAUSER:	Die Ergebnisse der seismischen Gletschermessungen am Dachstein im Jahre 1968. Wien 1971, 31 Seiten, 7 Tabellen, 13 Abbildg.	vergriffen
10	198	Geophysik	BRÜCKL, E., G. GANGL:	Die Ergebnisse der seismischen Gletschermessungen am Gefronne Wand Kees im Jahre 1969. Wien 1972, 13 Seiten, 8 Abbildungen, 3 Karten.	50.-
11	201	Geophysik	BITTMANN, O., E. BRÜCKL, G. GANGL und F.J. WALLNER:	Die Ergebnisse der seismischen Gletschermessungen am Obersten Pasterzenboden (Glocknergruppe) im Jahre 1970. Wien 1973, 21 Seiten, 9 Abbildungen, 3 Karten.	60.-
12	202	Meteorologie	STEINHAUSER, F.:	Tages- und Jahresgang der Sonnenscheindauer in Österreich (1929-1968). Wien 1973, 12 Seiten Text, 98 Tabellen, 5 Abbildungen.	110.-
13	203	Meteorologie		Klimadaten des Neusiedlerseegebietes, I. Teil. Tabellen der Stundenwerte der Lufttemperaturen, 1966 - 1970, 105 Tabellen.	90.-
14	205	Geophysik	PÜHRINGER, A., W. SEIBERL, E. TRAPP und F. PAUSWEG:	Die Verteilung der erdmagnetischen Elemente in Österreich zur Epoche 1970.0. Wien 1975, 18 Seiten, 3 Tabellen, 9 Kartenbeilagen.	140.-
15	206	Meteorologie		Klimadaten des Neusiedlerseegebietes, II. Teil. Tabellen der Stundenwerte der Relativen Feuchte, 1966 - 1970, 105 Tabellen.	100.-

Heft	Publ. Nr.	Fachgebiet	Autor	Titel und Umfang	Preis Ö.S
16	207	Meteorologie		Hundert Jahre Meteorologische Weltorganisation und die Entwicklung der Meteorologie in Österreich. Wien 1975, 50 Seiten.	100,-
17	208	Geophysik	TOPERCZER, M.:	Die Geschichte der Geophysik an der Zentralanstalt für Meteorologie und Geodynamik. Wien 1975, 24 Seiten.	50,-
18	209	Meteorologie	CHALUPA, K.:	Ergebnisse der Registrierung der Schwefeldioxid - Immission in Wien, Hohe Warte, Okt. 1967 - Dez. 1974. Wien 1976, 62 Seiten, mit 19 Tabellen u. 24 Abbildungen	80,-
19	210	Geophysik	GUTDEUTSCH, R. und K. ARIC:	Erdbeben im ostalpinen Raum. Wien 1976, 23 Seiten, 3 Karten.	80,-
20	211	Meteorologie	TOLLNER, H., W. MAHRINGER und F. SÖBERL:	Klima und Witterung der Stadt Salzburg. Wien 1976, 176 Seiten, 29 Abbildungen.	220,-
21	214	Geophysik	SEIBERL, W.:	Das Restfeld der erdmagnetischen Totalintensität in Österreich zur Epoche 1970.0. Wien 1977, 8 Seiten, 1 Kartenbeilage.	vergriffen
22	216	Meteorologie	SABO, P.:	Ein Vergleich deutscher und amerikanischer Höhenvorhersagekarten für den Alpenraum. Wien 1977, 34 Seiten, 11 Tabellen, 5 Abbildungen.	60,-
23	217	Meteorologie	CEHAK, K.:	Die Zahl der Tage mit Tau und Reif in Österreich. Wien 1977, 17 Seiten, 6 Tabellen, 1 Abbildung, 6 Karten.	80,-
24	218	Meteorologie	CHALUPA, K.:	Ergebnisse der Registrierung der Schwefeldioxid- und Summenkohlenwasserstoff-Immission in Wien, Hohe Warte 1975. Wien 1977, 40 Seiten, 13 Tabellen, 12 Abbildg.	70,-
25	219	Geophysik	BRÜCKL, E. und O. BITTMANN:	Die Ergebnisse der seismischen Gletschermessungen im Bereich der Goldberggruppe (Hohe Tauern) in den Jahren 1971 und 1972. Wien 1977, 30 Seiten, 2 Tabellen, 34 Abbildungen, 2 Karten.	80,-
26	222	Geophysik	FIEGWEIL, E.:	Die Nachbebenserien der Friauler Beben vom 6. Mai und 15. September 1976. Wien 1977, 20 Seiten, 7 Tabellen, 5 Abbildungen.	60,-
27	223	Meteorologie	MACHALEK, A.:	Prognosenprüfung im Österreichischen Wetterdienst. Wien 1977, 55 Seiten, 4 Tabellen, 5 Abbildungen.	80,-
28	224	Meteorologie	SKODA, G.:	Kinematisch - Klimatologische Verlagerung von Kaltfronten und Troglinien. Wien 1977, 32 Seiten, 7 Tabellen, 10 Abbildungen.	70,-
29	225	Geophysik	TRAPP, E. und D. ZYCH:	Verteilung der Vertikalintensität im Raum Wien - Salzburg nach Meßergebnissen der Zentralanstalt und der ÖMV - Aktiengesellschaft, Wien 1977, 15 Seiten, 3 Tabellen, 1 Karte, 2 Kartenbeilagen.	50,-
30	226	Meteorologie		Klimadaten des Glocknergebietes, I. Teil: Tabellen der Stundenwerte der Lufttemperatur und der relativen Luftfeuchte 1974 - 1976 (Wallack - Haus, Hochtör - Süd, Hochtör - Nord, Fuscher - Lacke). 117 Tabellen.	150,-
31	227	Meteorologie		Bericht über die 14. Internationale Tagung für Alpine Meteorologie vom 15. - 17. September 1976 in Rauris, Salzburg, 1. Teil. Wien 1978, 323 Seiten.	250,-
32	228	Meteorologie		Bericht über die 14. Internationale Tagung für Alpine Meteorologie vom 15. - 17. September 1976 in Rauris, Salzburg, 2. Teil. Wien 1978, 347 Seiten.	250,-

Heft	Publ. Nr.	Fachgebiet	Autor	Titel und Umfang	Preis Ö. S.
33	229	Meteorologie	CHALUPA, K.:	Ergebnisse der Registrierung der Schwefeldioxid-, Summenkohlenwasserstoff- und Ozon - Immission in Wien, Hohe Warte, 1976. Wien 1978, 53 Seiten, 20 Tabellen, 17 Abbildungen.	90.-
34	231	Meteorologie		Klimadaten des Glocknergebietes, II. Teil: Tabellen der Stundenwerte der Lufttemperatur und der relativen Luftfeuchte 1974 - 1976 (Fusch, Ferleiten, Piffkaralm). Wien 1978, 62 Tabellen.	80.-
35	233	Meteorologie		Klimadaten des Glocknergebietes, III. Teil: Tabellen der Stundenwerte der Lufttemperatur und der relativen Luftfeuchte 1974 - 1976 (Guttal, Seppenbauer, Margaritze, Glocknerhaus, Schneetälchen, Polsterpflanzenstufe). Wien 1978, 100 Tabellen.	130.-
36	234	Meteorologie	CHALUPA, K.:	Ergebnisse der Registrierung der Immission von Stickoxiden, Summenkohlenwasserstoffen, Ozon und Schwefeldioxid in Wien - Hohe Warte, 1977. Wien 1979, 74 Seiten, 31 Tabellen, 24 Abbildungen.	115.-
37	235	Meteorologie	MACHALEK, A.:	Analyse von Fehlprognosen im Österreichischen Wetterdienst und Diskussion ihrer potentiellen Entstehungskriterien. Wien 1979, 45 Seiten, 2 Tabellen, 35 Abbildungen.	100.-
38	236	Geophysik	DRIMMEL, J., FIEGWEL, E., G. LUKESCHITZ:	Die Auswirkung der Friauler Beben in Österreich. Makroseismische Bearbeitung der Starkbeben der Jahre 1976/77 samt historischem Rückblick. Wien 1979, 83 Seiten, 47 Abbildungen, 3 Karten.	150.-
39	238	Geophysik	FIEGWEL, E.:	Über das Vorkommen von Wiederholungsbeben in Mitteleuropa. Wien 1979, 20 Seiten, 9 Abbildungen.	50.-
40	239	Meteorologie		Klimadaten des Glocknergebietes, IV. Teil: Tabellen der Stundenwerte der Windgeschwindigkeit und der Windrichtung 1973 - 1976 (Fusch, Wallack-Haus, Guttal, Glocknerhaus, Margaritze, Fuscher-Lacke). Wien 1979, 94 Tabellen.	120.-
41	242	Meteorologie	CHALUPA, K.:	Ergebnisse der Registrierung der Immission von Stickoxiden, Ozon und Schwefeldioxid in Wien - Hohe Warte, 1978. Wien 1980, 58 Seiten, 30 Tabellen, 15 Abbildungen.	130.-
42	241	Meteorologie	CHALUPA, K.:	Ergebnisse der Registrierung der Immission von Stickoxiden, Ozon und Schwefeldioxid in Wien - Hohe Warte, 1979. Wien 1980, 65 Seiten, 32 Tabellen, 20 Abbildungen.	130.-
43	246	Meteorologie	RAGETTE, G.:	Methoden zur Berechnung großräumigen Niederschlages, Wien 1980, 47 Seiten, 1 Tabelle, 2 Abbildungen.	70.-
44	247	Meteorologie		Klimadaten des Glocknergebietes, V. Teil: Tabellen der Stundenwerte der Lufttemperatur und der relativen Luftfeuchte, 1977 - 1979 (Wallack-Haus, Hochtor-Süd, Hochtor-Nord, Fuscher-Lacke). Wien 1980, 135 Tabellen.	vergriffen

Heft	Publ. Nr.	Fachgebiet	Autor	Titel und Umfang	Preis Ö. S.
45	248	Geophysik	BRÜCKL, E., G. GANGL, W. SEIBERL und Chr. GNAM:	Seismische Eisdickenmessungen auf dem Ober- und Untersulzbachkees in den Sommern der Jahre 1973 und 1974. Wien 1980, 23 Seiten, 2 Tabellen, 18 Abbildungen.	50,-
46	249	Meteorologie		Klimadaten des Glocknergebietes, VI. Teil: Tabellen der Stundenwerte der Lufttemperatur und der relativen Luftfeuchte, 1977 - 1979 (Fusch, Piffkaralm, Guttal, Seppenbauer, Margaritze, Glocknerhaus, Schneetälchen, Obere Grasheide, Polsterpflanzenstufe). Wien 1981, 110 Tabellen.	120,-
47	251	Meteorologie	CHALUPA, K.:	Ergebnisse der Registrierung der Schwefeldioxid - Immission in Wien - Stephansplatz, 1975 - 1979. Wien 1981, 50 Seiten, 13 Tabellen, 21 Abbildungen.	vergriffen
48	252	Meteorologie	LAUSCHER, F.:	Säkulare Schwankungen der Dezennienmittel und extreme Jahreswerte der Temperatur in allen Erdteilen. Wien 1981, 42 Seiten, 8 Tabellen.	50,-
49	254	Meteorologie	CHALUPA, K.:	Ergebnisse der Registrierung der Schwefeldioxid - Immission in Wien - Hohe Warte und in Wien - Stephansplatz, 1980. Wien 1981, 46 Seiten, 24 Tabellen, 13 Abbildungen.	100,-
50	255	Geophysik	MELICHAR, P.:	Ergebnisse der vergleichenden geomagnetischen Absolutmessungen an den Observatorien Tihany - Ungarn und Wien - Kobenzl. Wien 1981, 35 Seiten.	50,-
51	256	Geophysik	BRÜCKL, E. und K. ARIC:	Die Ergebnisse der seismischen Gletschermessungen am Hornkees in den Zillertaler Alpen im Jahre 1975. Wien 1981, 20 Seiten, 5 Tabellen, 5 Abbildungen, 1 Karte.	vergriffen
52	257	Meteorologie		Klimadaten des Glocknergebietes, VII. Teil: Tabellen der Stundenwerte der Windgeschwindigkeit und der Windrichtung 1977 - 1979 (Fusch, Füscher Lacke, Wallackhaus, Guttal). Wien 1982, 82 Tabellen.	120,-
53	260	Meteorologie	STEINHAUSER, F.:	Verteilung der Häufigkeiten der Windrichtungen und der Windstärken in Österreich zu verschiedenen Tages- und Jahreszeiten. Wien 1982, 140 Seiten, 131 Tabellen und 4 Kartenbeilagen.	120,-
54	261	Meteorologie	DOBESCH, H. und F. NEUWIRTH:	Wind in Niederösterreich, insbesondere im Wiener Becken und im Donautal. Wien 1982, 212 Seiten, 183 Abbildungen.	vergriffen
55	266	Meteorologie		Klimadaten des Glocknergebietes, VIII. Teil: Tabellen der Stundenwerte der Globalstrahlung 1975 - 1980 (Füscher - Lacke und Wallack - Haus). Wien 1983, 39 Seiten.	50,-
56	268	Geophysik	WEBER, F. und R. WÜSTRICH:	Ergebnisse der refraktionsseismischen Messungen am Hochkönigsgletscher. Wien 1983, 50 Seiten, 3 Tabellen, 7 Abbildungen, 11 Beilagen.	100,-
57	278	Meteorologie		Klimadaten des Glocknergebietes, IX. Teil: Tabellen der Niederschlagsmeßergebnisse 1974 - 1980. 48 Seiten, 41 Tabellen.	70,-

Heft	Publ. Nr.	Fachgebiet	Autor	Titel und Umfang	Preis Ö. S.
59	283	Meteorologie	KAISER, A.:	Inversionen in der bodennahen Atmosphäre über Klagenfurt. Wien 1984, 79 Seiten, 13 Tabellen, 22 Abbildungen.	80.-
60	284	Meteorologie	LAUSCHER, F.:	Ozonbeobachtungen in Wien von 1853 bis 1981. Zusammenhänge zwischen Ozon und Wetterlagen. Wien 1984, 29 Seiten, 13 Tabellen, 3 Abbildungen.	40.-
61	289	Meteorologie		Klimadaten von Österreich Mittelwerte 1971 - 1980. Teil I (Vorarlberg) und Teil II (Tirol). 71 Seiten.	60.-
62	299	Geophysik	DRIMMEL, J.:	Seismische Intensitätsskala 1985 (SIS - 85). Vorschlag einer Neufassung der Intensitätsskala MSK-64. 28 Seiten, 8 Tabellen, 2 Abbildungen.	40.-
63	300	Meteorologie		Klimadaten von Österreich Mittelwerte 1971 - 1980. Teil III (Salzburg) und Teil IV (Oberösterreich). 107 Seiten.	80.-
64	302	Meteorologie	LAUSCHER, F.:	Klimatologische Synoptik Österreichs mittels der ostalpinen Wetterlagenklassifikation. Wien 1985, 65 Seiten, 32 Tabellen, 5 Abbildungen.	90.-
65	303	Geophysik	ZYCH, D.:	Messungen der erdmagnetischen Vertikalintensität und Suszeptibilitätsuntersuchungen durch die ÖMV AG als Beitrag zur Kohlenwasserstoffexploration in Österreich. Wien 1985, 14 Seiten, 2 Tabellen, 2 Abbildungen und 3 Kartenbeilagen.	60.-
66	304	Meteorologie	HOJESKY, H.:	Langjährige Radiosonden- und Höhenwindmessungen über Wien (1952 - 1984). Wien 1985, 219 Seiten, 64 Tabellen und 13 Abbildungen.	120.-
69	309	Meteorologie	KOLB, H., G. MAHRINGER, P. SEIBERT, W. SOBITSCHKA, P. STEINHAUSER und V. ZWATZ - MEISE:	Diskussion meteorologischer Aspekte der radioaktiven Belastung in Österreich durch den Reaktorunfall in Tschernobyl. Wien 1986, 63 Seiten, 4 Tabellen und 20 Abbildungen.	vergriffen
70	312	Geophysik	ARIC, K., E. BRÜCKL:	Ergebnisse der seismischen Eisdickenmessungen im Gebiet der Stubaier Alpen (Daunkogelferner), der Venedigergruppe (Schlatenkees und Untersulzbachkees) und der Silvrettagruppe (Vermunt - Gletscher). Wien 1987, 18 Seiten, 4 Tabellen, 10 Abbildungen u. 4 Kartenbeilagen.	80.-
71	314	Meteorologie	CHALUPA, K.:	Ergebnisse der Registrierung der Schwefeldioxid - Immission in Wien - Hohe Warte und in Wien - Stephansplatz, 1981. Wien 1987, 67 Seiten, 41 Tabellen, 11 Abbildungen.	100.-
72	315	Meteorologie	CHALUPA, K.:	Ergebnisse der Registrierung der Schwefeldioxid - Immission in Wien - Hohe Warte und in Wien - Stephansplatz, 1982 - 1985. Wien 1987, 76 Seiten, 27 Tabellen, 15 Abbildungen.	100.-
73	317	Geophysik	ARIC, K. et al:	Structure of the lithosphere in the Eastern Alps derived from P-residual analysis. Wien 1988, 35 Seiten, 3 Tabellen, 17 Abbildungen.	60.-

BERICHTE ÜBER DEN TIEFBAU DER OSTALPEN

Herausgegeben von H. W. FLÜGEL und P. STEINHAUSER

Heft	Publ. Nr.	Autor	Titel und Umfang	Preis öS
1			Jahresbericht 1973. Verhandlungen der Geologischen Bundesanstalt, Jahrgang 1974, Heft 4, Seite A 138 - A 148.	
2			Jahresbericht 1974. Zentralanstalt für Meteorologie und Geodynamik, 21 Seiten, 5 Abbildungen, Wien 1975.	vergr.
3	212		Jahresbericht 1975. Zentralanstalt für Meteorologie und Geodynamik, 74 Seiten, 14 Abbildungen, Wien 1976.	115.--
4	215	WALACH G.:	Geophysikalische Arbeiten im Gebiet des Nordsporns der Zentralalpen I: Magnetische Traverse 1 (Neun- kirchen - Hochwechsel - Pöllauer Bucht). Zentral- anstalt für Meteorologie und Geodynamik, 22 Seiten, 5 Abbildungen, 4 Beilagen.	40.--
5	221		Jahresbericht 1976. Zentralanstalt für Meteorologie und Geodynamik, 101 Seiten, 21 Abbildungen, Wien 1977.	130.--
6	230		Jahresbericht 1977, Teil 1. Zentralanstalt für Meteorologie und Geodynamik, 54 Seiten, 9 Abbildungen, Wien 1978.	85.--
7	240		Jahresbericht 1977, Teil 2. Zentralanstalt für Meteorologie und Geodynamik, 60 Seiten, 19 Abbildungen, Wien 1979.	90.--
8	244		Tagungsbericht über das 1. Alpengravimetrie Kolloquium - Wien 1977. Herausgegeben von Peter STEINHAUSER, Zentral- anstalt für Meteorologie und Geodynamik, 129 Seiten, 35 Abbildungen, Wien 1980.	90.--
9	245	GÖTZE, H.J., O. ROSEN- BACH und P. STEINHAUSER:	Die Bestimmung der mittleren Geländehöhen im Hochgebirge für die topographische Reduktion von Schweremessungen. Zentralanstalt für Meteorologie und Geodynamik, 16 Seiten, 2 Tabellen, 5 Abbildungen, Wien 1980.	25.--
10-1	264	ROSEN- BACH, O., P. STEINHAUSER, W. EHRISMANN, H.J. GÖTZE, O. LETTAU, D. RUESS und W. SCHÖLER:	Tabellen der mittleren Geländehöhen der Ostalpen und ihrer Umgebung für Rasterelemente = 0,75, = 1,25, 1. Lieferung. Zentralanstalt für Meteorologie und Geodynamik, 23 Seiten, 20 Tabellen, Wien 1982.	100.--
11	273		Tagungsbericht über das 2. Internationale Alpengravi- metrie Kolloquium - Wien 1980. Herausgegeben von B. MEURERS und P. STEINHAUSER, Zentralanstalt für Meteorologie und Geodynamik, 168 Seiten, 85 Abbildungen, Wien 1983	200.--

Heft	Publ. Nr.	Autor	Titel und Umfang	Preis öS
12	288		<p>Tagungsbericht über das 3. Internationale Alpengravimetrie Kolloquium - Leoben 1983.</p> <p>Herausgegeben von B. MEURERS, P. STEINHAUSER und G. WALACH, Zentralanstalt für Meteorologie und Geodynamik, 222 Seiten, Wien 1985.</p>	270.--
13	323		<p>Tagungsbericht über das 4. Internationale Alpengravimetrie Kolloquium - Wien 1986.</p> <p>Herausgegeben von B. MEURERS und P. STEINHAUSER, Zentralanstalt für Meteorologie und Geodynamik, 200 Seiten, 77 Abbildungen, Wien 1988.</p>	250.--

"Österreichische Beiträge zu Meteorologie und Geophysik"

Heft	Publ. Nr.	Fachgebiet	Autor	Titel und Umfang	Preis
1	329	Meteorologie		Tagungsbericht EURASAP, Wien, 14-16 Nov, 1988 "Evaluation of Atmospheric Dispersion Models Applied to the Release from Chernobyl", 20 Beiträge, 198 Seiten, 100 Abbildungen, 17 Tabellen, Wien 1989	200.-



XX GENERAL ASSEMBLY

IUGG VIENNA

11 - 24 AUGUST 1991

International Union of Geodesy
and Geophysics

Geodesy * Seismology * Physics
of the Earth's Interior * Geo-
magnetism * Meteorology
Aeronomy * Atmospheric
Physics * Physical Sci-
ences of the Ocean
Hydrological Sci-
ences * Vulcanology
Chemistry of the
Earth's Interior
Interunion
Programs;
STEP * ILP
IDNDR
IGBP

Contact address:

Local Organizing Committee - IUGG'91

Prof. Peter Steinhauser
ZAMG, Hehe Warte 38
A-1190 Vienna, Austria

Telephone: +43-222-364353 ext. 2001
Telex: 131837 metfor
Teletex: +43-222-3691239

Telephone: +43-222-364353
Telex: 131837 metfor
Teletex: +43-222-3691239

